Effects of histone 3.3K27M-mutation on CREB binding protein (CBP/p300)- and bromodomain and extra terminal domain (BET) protein- mediated gene regulation in diffuse intrinsic pontine gliomas (DIPG)

Dissertation

for the award of the degree

"Doctor of Philosophy" Ph.D. Division of Mathematics and Natural Science

of the Georg-August-Universität Göttingen

within the doctoral program Molecular Medicine

of the Georg-August University School of Science (GAUSS)

submitted by

Klaudia Kubiak

from Biskupiec, Poland

Göttingen, 2023

Thesis Committee

Prof. Dr. med. Jutta Gärtner
Department of Pediatrics and Adolescent Medicine
University Medical Center Göttingen

Prof. Dr. med. Matthias Dobbelstein
Molecular Oncology
University Medical Center Göttingen

Prof. Dr. rer. nat. Holger Bastians
Molecular Oncology
University Medical Center Göttingen

Members of the Examination Board

Reviewer: **Prof. Dr. med. Jutta Gärtner**
Department of Pediatrics and Adolescent Medicine
University Medical Center Göttingen

Second Reviewer: **Prof. Dr. med. Matthias Dobbelstein**
Molecular Oncology
University Medical Center Göttingen

Additional Reviewer (if applicable):
.....
(Name of Department / Research Group, Institution)

Further members of the Examination Board

Prof. Dr. rer. nat. Holger Bastians
Molecular Oncology
University Medical Center Göttingen
Prof. Dr. med. Christof Kramm
Department of Pediatric Hematology and Oncology
University Medical Center Göttingen
Prof. Dr. rer. nat. Günter Schneider
Clinic for General, Visceral and Pediatric Surgery
University Medical Center Göttingen
Prof. Dr. Argyris Papantonis
Institute of Pathology
University Medical Center Göttingen

Date of the oral examiniation: **09.03.2023**

Promovierenden-Erklärung
der Georg-August-Universität Göttingen

Name: **Kubiak Klaudia**

Anschrift: **Hagenweg 65, 37081, Göttingen**

Ich beabsichtige, eine Dissertation zum Thema **Effects of histone 3.3K27M-mutation on CREB binding protein (CBP/p300)- and bromodomain and extra terminal domain (BET) protein- mediated gene regulation in diffuse intrinsic pontine gliomas (DIPG**) an der Georg-August-Universität Göttingen anzufertigen. Dabei werde ich von **Prof. Dr. med. Jutta Gärtner** betreut.

Ich gebe folgende Erklärung ab:

1. Die Gelegenheit zum vorliegenden Promotionsvorhaben ist mir nicht kommerziell vermittelt worden. Insbesondere habe ich keine Organisation eingeschaltet, die gegen Entgelt Betreuerinnen und Betreuer für die Anfertigung von Dissertationen sucht oder die mir obliegenden Pflichten hinsichtlich der Prüfungsleistungen für mich ganz oder teilweise erledigt.

2. Hilfe Dritter wurde bis jetzt und wird auch künftig nur in wissenschaftlich vertretbarem und prüfungsrechtlich zulässigem Ausmaß in Anspruch genommen. Insbesondere werden alle Teile der Dissertation selbst angefertigt; unzulässige fremde Hilfe habe ich dazu weder unentgeltlich noch entgeltlich entgegengenommen und werde dies auch zukünftig so halten.

3. Die Ordnung zur Sicherung der guten wissenschaftlichen Praxis an der Universität Göttingen wird von mir beachtet.

4. Eine entsprechende Promotion wurde an keiner anderen Hochschule im In- oder Ausland beantragt; die eingereichte Dissertation oder Teile von ihr wurden/werden nicht für ein anderes Promotionsvorhaben verwendet.

Mir ist bekannt, dass unrichtige Angaben die Zulassung zur Promotion ausschließen bzw. später zum Verfahrensabbruch oder zur Rücknahme des erlangten Grades führen können.

Göttingen, 31.01.2023 (Klaudia Kubiak)

Table of contents

Acknowledgements

First and foremost I would like to thank my supervisors, Dr. Maria Wiese and Prof. Christof Kramm for their invaluable advice, continuous support, and patience during my PhD study. They always let this thesis to be my work, but steered me in the right direction whenever I needed it. Their vast knowledge and experience have encouraged me in all the time of my academic research and daily life.

Additionally, I would like to express my gratitude to the members of the Thesis Advisory Committee, Prof. Jutta Gärtner, Prof. Matthias Dobbelstein and Prof. Holger Bastians for their continuous support throughout my PhD work and all the interesting discussions.

I would also like to thank all the labmates of the Department of Pediatrics and Adolescent Medicine. Special thanks go to Effrosyni Kapsali and Dr. Kristin Wendland for constant advice, consistent encouragement and on- and off-topic discussions. Our lunch dates on the balcony helped me stayed sane.

Special thanks go to former medical students, especially Hanna. I really appreciated our mutual support in scientific research and beyond.

Last but not least, I must express my very profound gratitude to my parents and siblings for providing me with support and continuous encouragement throughout my years of studies. Without your tremendous understanding and encouragement in the past few years, it would be impossible for me to be where I am today.

Thank you!

Abstract

Diffuse intrinsic pontine gliomas (DIPG) are incurable pediatric high-grade tumors. The majority of all DIPG carries a mutation in one of the histone 3 genes leading to a substitution of lysine 27 to methionine (H3 K27M) characterized by malfunction of the histone methyltransferase enhancer of zeste homolog 2 (EZH2) that mediates H3K27 trimethylation (H3K27me3). Presence of H3.3K27M-mutation results in an epigenetic imbalance characterized by global loss of H3K27me3 and gain of H3K27 acetylation (H3K27ac) mediated by CREB binding protein (CBP/p300). Therefore it could be hypothesized that the histone acetyltransferase (HAT) CBP/p300 and readers recognizing H3K27ac like bromodomain and extra-terminal domain (BET) proteins might play a dominant role in H3.3K27M-mutated DIPG cells.

Thus, this project aims to identify the probable distinct genetic and resulting tumor-biological effects in DIPG cells caused by presence of H3.3K27M-mutation within the same cellular and genetic background, as well as to determine the H3.3K27M-dependent functions of H3-writers (CBP/p300) and readers (BET proteins) in DIPG cells with H3-wildtype and H3.3K27M-mutation.

In order to study the impact of H3.3K27M-mutation in DIPG cells, isogenic cell lines with and without H3.3K27M-mutation were generated using CRISPR/Cas9 system and compared with each other to investigate H3.3K27M-dependent eigenome, transcriptome and consequent expression tumor-associated characteristics.

Introduction of H3.3K27M-mutation resulted in loss of H3K27me3 and gain of H3K27ac, while removal of H3.3K27M-mutation led to reduction of H3K27ac and restored H3K27me3 level. Moreover, presence of H3.3K27M-mutation caused elevated cell proliferation, clonogenicity and migration/invasion ability of isoDIPG cells. Furthermore, H3.3K27M-mutation influenced the expression of several different histone marks as well as epigenetic key players in DIPG cells.

To investigate and dissect the function of BET family members and CBP/p300 in isoDIPG cells, small molecules were used to inhibit specific functions of the writer/reader proteins. Subsequently, siRNA-mediated knockdown of the proteins of interest was performed to dissect specific functions of BRD2, 3 and 4 or CBP and p300.

Indeed CBP and p300 as well as BET family members BRD2 and BRD4 had a more profound impact on reduction of tumor associated characteristics in isoDIPG-H3.3K27M compared to isoDIPG-H3WT cells. Interestingly, western blot analyses revealed that CBP catalyzed H3K27ac in isoDIPG-H3.3K27M cells, while p300 was responsible for H3K27ac isoDIPG-H3WT cells. Moreover, the study pointed out to a specific function of CBP in regulation of apoptosis, while

p300 turned out to mediate MAPK cascades in isoDIPG-H3.3K27M cells. Within BET proteins family, BRD2 and BRD4 played a more profound role than BRD3 in isoDIPG-H3.3K27M cells, regulating biological processes including cell cycle and Wnt signaling.

In summary, the present study reveals that presence of H3.3K27M-mutation in isoDIPG cells is a leading cause for the malignant phenotype observed in DIPG cells. Moreover, H3.3K27M-mutation modulates the function of H3K27-associated CBP writer and BRD2 and BRD4 readers in isoDIPG cells *in vitro* and *in vivo*, playing important roles in H3.3K27M-DIPG cells.

List of figures

List of tables

List of appendixes

Abbreviations

µ	Micro
AA	Anaplastic astrocytoma
aa	Aminio acid
ac	Acetylation
ACTB	ß-actin (gene)
APS	Ammonium persulfate
BCA	Bicinchoninic acid
BET	Bromo- and extra-terminal domain
BRD2	Bromodomain-containing protein 2
BRD3	Bromodomain-containing protein 3
BRD4	Bromodomain-containing protein 4
BGH-polyA	Bovine growth hormone polyadenylation
BMP	Bone morphogenic protein
bp	Base pairs
BrdU	Bromodeoxyuridine
BSA	Albumin bovine Fraction V
CAM	Chorioallantoic membrane
CBP	CREB-binding protein
CCND1	CyclinD1 gene/mRNA
CD133	Prominin-1
cDNA	Complementary DNA
CE	Cellular extract
CNS	Central nervous system
CREB	cAMP responsive element binding protein 1
CTNNB1	ß-catenin gene/mRNA
CRISPR/Cas	Clustered Regularly-Interspaced Short Palindromic Repeats
Da	Dalton
DAPI	4',6-diamidino-2-phenylindole
DIPG	Diffuse intrinsic pontine glioma
DMEM	Dulbecco’s modified eagle medium
DMG	Diffuse midline glioma
DMSO	Dimetylsulfoxide
DNA	Desoxyribonucleic acid

dNTP	Desoxyribonucleotide triphosphate
DTT	DL-Dithiothreitol
ECL	Enhanced chemiluminescence
EDTA	Ethylenediaminetetraacetate
EGF	Epidermal growth factor
ESC	Embryonic stem-cell
EtBr	Ethidium bromide
EtOH	Ethyl alcohol
EZH2	Enhancer of zeste (Drosophila) homolog 2
FACS	Fluorescence activated cell sorting
FCS	Fetal calf serum
FDR	Fold discovery rate
FGF	Fibroblast growth factor
for	(primer) forward
FZ	Frizzled
g	Gram
GBM	Glioblastoma multiforme
h	hours or human
H&E	Hematoxylin & Eosin
H_2O_2	Peroxygen
H3	Histone 3
H3.1	Histone 3.1
H3.3	Histone 3.3
H3 K27M	Mutation in lysine 27 of histone 3
HAT	Histone acetyltransferases
HCl	Hydrochloric acid
HGG	High-grade glioma
HDAC	Histone deacetylases
HEPES	4-(2-hydroxyethyl)-1-piperazineethanesulfonic acid
HMT	Histone methyltransferases
HRP	Horse radish peroxidase
IgG	Immunoglobulin G
IHC	Immunohistochemistry
K	Lysine
K27	Lysine on position 27

KCl	Potassium chloride
kDa	Kilo Dalton
KDM	Lysine demethylases
KLF	Krüppel-like Factor
KLF4	Gut-enriched Krüppel-like factor 4
KRAS	V-Ki-ras2 Kirsten rat sarcoma viral oncogene homolog
L	Liter
LPP	Laemmli probe buffer
LUC	*Luciferase*
LT	Separating buffer
M	Molare (mol/liter) / Methionine
me	Methylation
MEM NEAA	Minimum essential medium non-essential amino acids
mg	Milligram
$MgCl_2$	Magnesium chloride
$MgSO_4$	Magnesium sulfate
min	Minute
miRNA	Micro RNA
mRNA	Messenger RNA
MTT	Methyl Thiazolyl Diphenyl-tetrazolium Bromide
MUC2	Mucin 2
MYC	Proto-oncogene
Na_2SO_4	Sodium sulfate
NaCl	Sodium chloride
$NaHCO_3$	Sodium hydrogen carbonate
NaOH	Sodium hydroxide
NE	Nuclear extract
NFκB	Nuclear factor 'kappa-light-chain-enhancer' of activated B-cells
ng	Nano gram
nmol	Nano mol
NP40	Nonidet-P40
OCT4	POU domain transcription factor 4
PBS	Phosphate Buffered Saline
PCR	Polymerase chain reaction
PDGF-AA	Platelet-derived growth factor-AA

PDGF-BB	Platelet-derived growth factor-BB
pedHGG	Pediatric high grade glioma
PFA	Paraformaldehyde
pH	Negative decadal logarithm of the hydrogen ion concentration
PMSF	Phenylmethylsulfonyl fluoride
Pol II	RNA-Polymerase II
PRC2	Polycomb repressive complex 2
PVDF	Polyvinylidene fluoride
qPCR	quantitative real-time PCR
rev	(primer) reverse
RNA	Ribonucleic acid
rpm	Rounds per minute
RT	Reverse transcriptase or room temperature
S	Serine
s	Seconds
SDS	Sodium Dodecyl Sulfate
SDS-PAGE	SDS polyacrylamide gel electrophoresis
siRNA	Short interfering RNA
SMAD	Sisters and mothers against decapentaplegic
SNAIL1	Snail
SNAIL2	Slug
SOX	SRY-related HMG-box gene
SOX2	SRY (sex determining region Y)-box 2
TAL	"Transkritomanalyselabor”
TBST	Tris-Buffered Saline Tween-20
TEMED	N,N,N’,N’-Tetramethylethan-1,2-diamin
TF	Transcription factor
TFIID	Transcription factor II D
TGFß	Transforming growth factor
TSM	Tumor stem media
ub	ubiquitination
UT	Stacking buffer
V	Volt
VEGF	Vascular endothelial growth factor
VIM	Vimentin

WHO	World Health Organization
WT	Wildtype
ZEB	Zinc finger E-box binding homeobox

°	Degree
°C	Centigrade
Ø	Untreated
%	Percent

Prefixes are in conformity with the International system of Units (Systeme international d'unites, SI).

Amino acid one letter code was used to abbreviate amino acids.

1 Introduction

1.1 Pediatric high grade gliomas (pedHGG)

Tumors of the central nervous system (CNS) are, after leukemia, the most common pediatric malignancies accounting for 20-25% of all pediatric cancers (Bueren et al. 2017). There are several different types of CNS tumors, including malignant high grade tumors that are very likely to grow and spread, and low grade, less aggressive tumors. Approximately 10-15% of all CNS tumors in children are pediatric high-grade gliomas (pedHGG) (Stupp et al. 2014). They most likely arise from transformed glial progenitor cells of the brain or spinal cord (Canoll and Goldman 2008). HGG in children are very rare, with only 60-70 new cases in Germany per year, but show a malignant behavior growing very fast and diffusely migrating within the CNS (Hayward et al. 2008).

Despite major therapeutic improvements in pediatric oncology, pedHGG still have extremely poor prognosis with a median overall survival rate of 14-15 months (Hatoum et al. 2022). Conventional therapy resembles the one used for adult patients, consisting of irradiation with temozolomide (Stupp et al. 2005) which usually provides only temporary improvement (Cohen et al. 2011). This unfavorable prognosis is also due to the fact that migrating tumor cells evade radiochemotherapy since they acquire stem cell-like characteristics with marked chemo- and radioresistance (Stupp et al. 2005). Additionally, molecular mechanisms such as DNA repair by O-6-methylguanine-DNA-methyltransferase (MGMT) or tumor protein (TP53) mutation leads to aversion to standard treatment (Satoru and van Meir 2017; Messaoudi et al. 2015). Moreover, hypoxic environment of the tumor often results in insufficient transport of therapeutic drugs to the designated area (Haar et al. 2012; Messaoudi et al. 2015). Another limitation of therapy options for pedHGG patients is the inability of many applied therapeutic agents to efficiently cross the blood-brain barrier.

Interestingly, HGG in children differ strongly from HGG in adult patients, showing distinct epigenetic pattern and a different frequency of common somatic mutations (Paugh et al. 2010). For instance, isocitrate dehydrogenase 1 or 2 (*IDH1* or *IDH2*) mutations are present in adult glioblastomas, while very rare in pedHGG (Sturm et al. 2012). Contrastingly, mutations in histone 3 (either lysine 27 substitution to methionine – H3K27M, or glycine 34 to arginine/valine – H3G34R/V) are predominantly observed in pediatric patients (Sturm et al. 2012). In conclusion, pedHGG patients are indeed in need for specific therapeutic options.

1.1.2 Diffuse intrinsic pontine gliomas (DIPG)

According to the World Health Organization (WHO) classification from 2016, pedHGG include anaplastic astrocytoma (AA, Grade III), glioblastoma (GMB, WHO Grade IV), diffuse intrinsic pontine glioma (DIPG, WHO Grade IV) and diffuse midline glioma with histone H3K27M-mutation (DMG, WHO Grade IV) (Louis et al. 2016). DIPG are located in the pons of the brain stem and grow diffusely (**Figure 1**). According to the Central Brain Tumor Registry of the United States, approximately 8-12% of all reported brain tumors in children are HGG and nearly half of those are DIPG (Fangusaro 2012). DIPG can rapidly spread to other areas of the brain including midbrain, medulla or cerebellar peduncles (Grigsby et al. 1989) and are thought to be the most aggressive kind of brain tumors with an overall survival rate less than 12 months after diagnosis (**Figure 2A**) (Cohen et al. 2011). Complete or even subtotal tumor resection is not possible in DIPG since they occur in the pons close to critical for regulation of respiratory and circulatory functions and grow amidst cranial nerves and other essential neuronal tracts (Bailey et al. 2018).

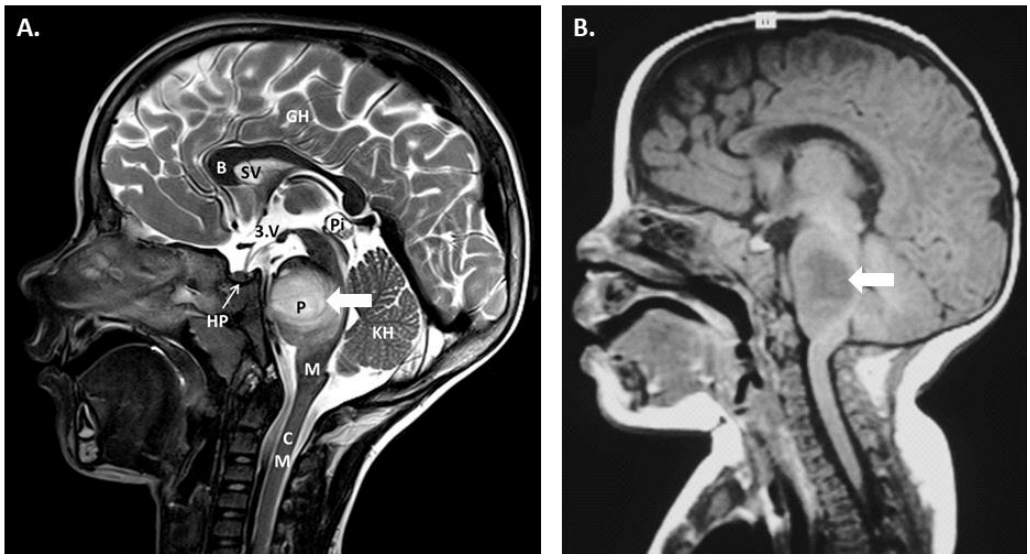

Figure 1 | **Magnetic resonance imaging illustrates diffuse intrinsic pontine gliomas (DIPG).** (A) P (brainstem pons), B (bar), CM (cervical cord), GH (cerebrum), HP (pituitary gland), KH (cerebellum), M (medulla oblongata), SV (lateral ventricle), 3rd V (third ventricle), Pi (pineal nerve with cyst) (adapted from Karremann et al. 2021). (B) Arrow indicates tumor mass in the pons (adapted from Perwein et al. 2021).

DIPG are almost exclusively childhood tumors and about 85% of them carry a heterozygous point mutation in one histone 3 (H3) gene variant, either in H3.3 (encoded by *H3F3A*) or less frequently in H3.1 (encoded by *HIST1H3B/C*), which both result in a lysine (K) to methionine (M) substitution (H3K27M) (Schwartzentruber et al. 2012; Hoffman et al. 2018). Presence of H3K27M-mutation leads to an altered function of histone-lysine N-methyltransferase (HMT) enhancer of zeste homolog 2 (EZH2) which results in global loss of H3K27-trimethylation

(H3K27me3) and H3K27-hyperacetylation (H3K27ac) (Schwartzentruber et al. 2012; Khuong-Quang et al. 2012). Balanced function of histone acetyltransferase (HAT) and HMT is disturbed, and loss of H3K27me3 leads to increased H3K27ac levels (Krug et al. 2019; Piunti et al. 2017). Interestingly, survival rate of DIPG patients does not significantly correlate with the H3-mutation status, but with the subtype of mutated H3 (**Figure 2B**) (Castel et al. 2018; Hoffman et al. 2018).

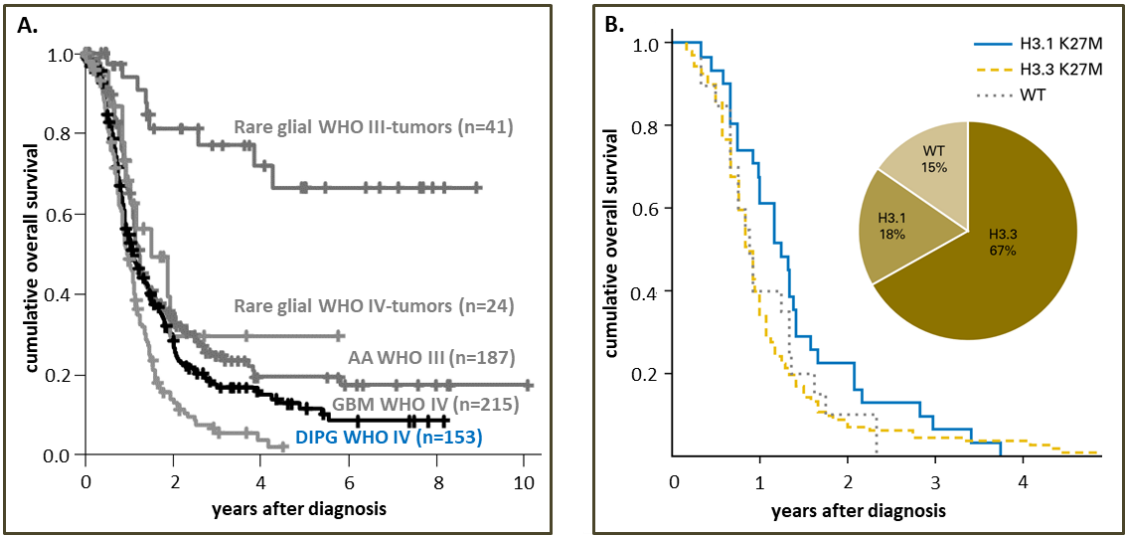

Figure 2 | Kaplan-Meier curves represent overall survival rate based on histone H3-status.
(A) Diffuse intrinsic pontine gliomas (DIPG) represent the lowest survival rate among other pediatric high grade gliomas including glioblastoma (GBM), anaplastic astrocytoma (AA) and rare glial tumors grade III and IV. (B) H3.3K27M-mutation does not change the survival rate for DIPG patients compared to H3-WT (adapted from Hoffman et al. 2018).

The malignant phenotype of CNS tumors is graded by World Health Organization (WHO) from I to IV and classified according to histological and molecular criteria under special consideration of the clinical course (Wang et al. 2013). In 2021, a new edition of the WHO classification was released with an extension and renaming of the superordinate brain tumor diagnosis of diffuse midline glioma, H3K27M mutant which had been introduced in 2016 including DIPG. The renamed diagnosis is now diffuse midline glioma (DMG), H3K27-altered. It is still characterized by midline location, diffuse growth pattern and molecular changes that result in reduced/lost H3K27me3, but now comprises 4 subtypes. Besides the previously DMG with H3.3 or H3.1K27M mutation, there are now two new subtypes either characterized by overexpression of EZH inhibitory protein (EZHIP) or the presence of epidermal growth factor receptor (EGFR) alteration in combination with H3K27M mutations or EZHIP overexpression (Gielen et al. 2022). Therefore, for the purpose of this study DIPG cells which harbor H3.3K27M-mutation and reflect DMG cells according to the latest WHO classification will be referred to as H3.3K27M-DIPG. Whereas, DIPG cells with H3K27-wildtype (WT) are herein referred to as H3WT-DIPG.

1.2 Epigenetic regulatory mechanisms

Epigenetics is the study of heritable changes in gene expression that does not influence changes in the DNA sequence (Berger 2007). Disruption of epigenetic regulatory mechanisms can cause malignant changes on cellular level which are usually associated with cancer initiation (Sharma et al. 2010). Therefore, understanding of epigenetic regulatory mechanisms is essential for discovering new therapeutic options for cancer patients.

Chromatin is formed by nucleosomes consisting of two super-helical turns of DNA, wrapped around an octamer consisting of two molecules each of the four core histone (H) proteins: H2A, H2B, H3 and H4 (Luger et al. 1997). In order to be able to change accessibility of DNA to regulatory proteins, chromatin is folded into higher level structures. Epigenetic modifications at the N-terminal residues of histone tails thereby define accessibility of DNA to transcription factors.

Histone modifications, DNA methylation and non-coding RNAs are three crucial epigenetic mechanisms that modify chromatin structure and accessibility, therefore regulating gene expression without affecting DNA sequence (Sharma et al. 2010).

1.2.1 Epigenetic gene regulation by histone modifications

Characterization of histone modifications and their functions has highlighted potential mechanisms of altered epigenetic regulation in brain cancer (Kundaje 2015). These specific epigenetic modifications are mediated by so called epigenetic writers, readers and erasers (**Figure 3**) (Boland et al. 2014).

H3K27ac is associated with transcriptional activation (Bedford et al. 2010; Zheng et al. 2004), whereas H3K27me3 leads to repression of gene transcription (Hashizume 2017). HAT such as CREB-binding protein (CBP/p300) and HMT such as EZH2 act as epigenetic writers and catalyze acetylation and trimethylation at H3K27, respectively (Zheng et al. 2004).

Histone deacetylases (HDAC) and lysine demethylases (KDM) are epigenetic erasers which remove the respective histone marks (Hashizume 2017; Wang et al. 2009; Caslini et al. 2019; Kania et al. 2022).

Additionally, epigenetic readers such as bromodomain and extra-terminal domain (BET) proteins, as well as CBP/p300 and chromobox (CBX) proteins, recognize acetylation and trimethylation groups, respectively, and mediate transcriptional activation or repression (Filippakopoulos and Knapp 2014; Hashizume 2017).

H3K27me3 confers to ubiquitination of lysine 119 at histone H2A (H2AK119ub), which is thought to have tumor-suppressor function (Lecona et al. 2015), and is catalyzed by ring finger protein 1 (Ring1) as a part of the polycomb repressive complex 1 (PRC1), while ubiquitination is removed by deubiquitinases (DUB) (Li and Reverter 2021).

While histone acetylation is primarily associated with transcriptional activation, trimethylation can be an activating or repressive mark. Trimethylation of lysine 4 at histone H3 (H3K4me3) is associated with transcriptionally active chromatin (Beacon et al. 2021; Facompre et al. 2017). In contrast, trimethylation of lysine 9 at histone H3 (H3K9me3) is linked to closed chromatin state and repression of transcription (Ren et al. 2020).

Acetylation of H4 (H4ac) and lysine 16 at histone H4 (H4K16ac) are associated with transcriptional activation (Taylor et al. 2013; Dhar et al. 2017).

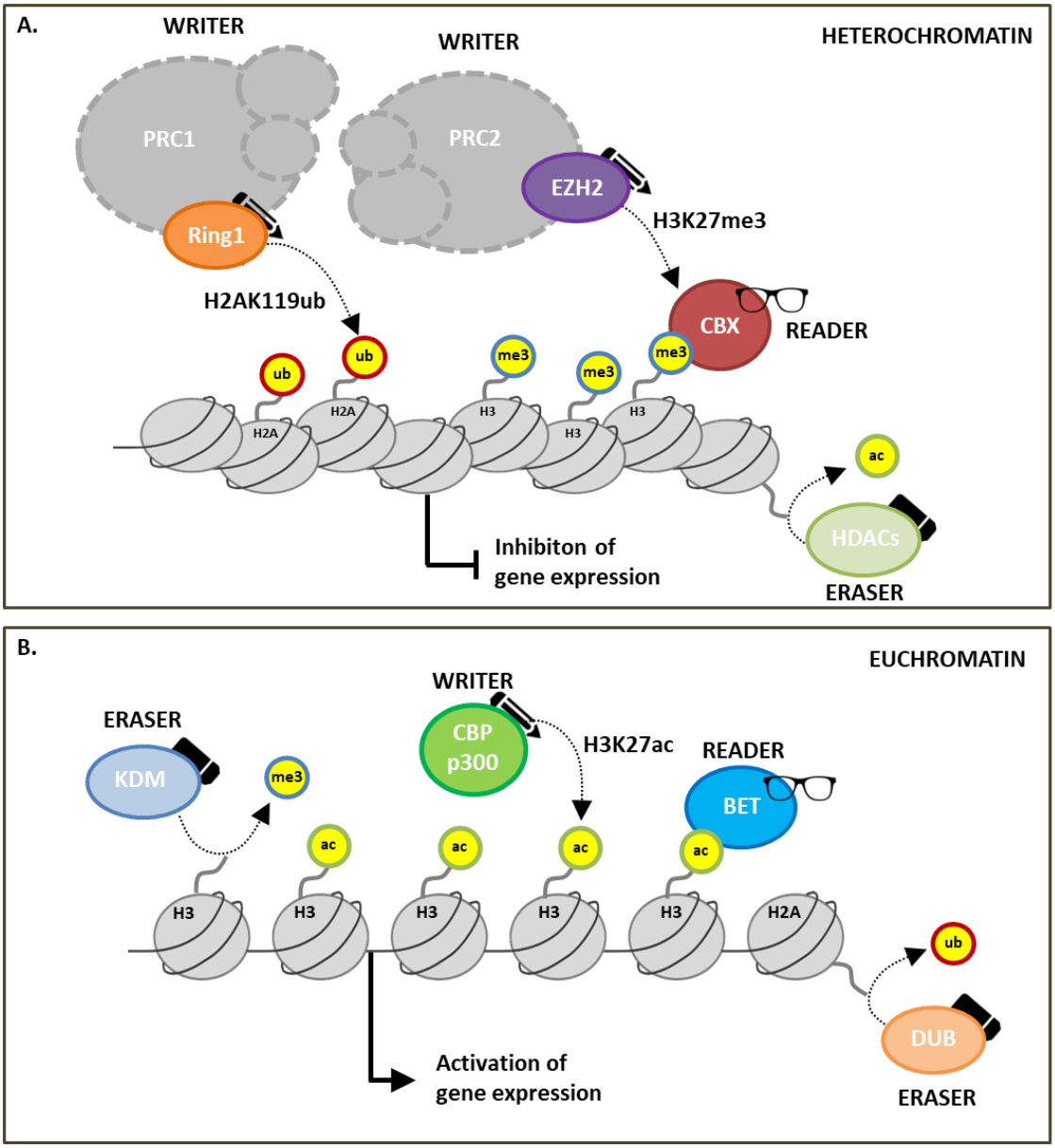

Figure 3 | Schematic representation of epigenetic gene regulation network.
(A) Heterochromatin state: writers such as EZH2 mediate H3K27me3 which can be read by CBX proteins. Ring1 ubiquitinates H2AK119ub. HDAC are responsible for removing acetylation marks from the histones. (B) Euchromatin state: epigenetic writer CBP/p300 mediates H3K27ac and readers, such as BET proteins, recognize acetylated residues. KDM and DUB remove H3K27me3 and H2AK119ub marks, respectively (adapted from Wiese et al. unpublished); (abbreviations explained in the text).

It has been shown that some histone marks are likely to occur in combination while others are mutually exclusive having different effect on gene expression. These observations suggest a crosstalk between different histone marks and emphasize complexity of epigenetic gene regulation (Zhang et al. 2015).

1.2.2 Epigenetic gene regulation by DNA methylation and non-coding RNAs

Apart from histone modifications, DNA methylation appears to play an important role in gene regulation. Gene silencing is established by methylation of cytosine residues in CpG islands of promotor regions (Sharma et al. 2010; Zheng et al. 2021). As a result, methylation prevents binding of transcription factors to their target sites and represses gene activation (Watt and Molloy 1988). This observation also suggests that different epigenetic mechanisms act together to determine definite gene expression pattern.

Additionally, non-coding RNAs are also involved in epigenetic gene regulation. Small non-coding RNAs, for example, silence enzymes which are responsible for DNA methylation and histone modifications, and subsequently impact epigenetic regulation. Interestingly, long non-coding RNAs were also shown to direct chromatin remodeling complexes to specific regions in order to alter DNA methylation and histone modifications (Chen and Xue 2016).

Thus, DNA methylation occurs in parallel with other epigenetic modifications and regulation mediated by non-coding RNAs, indicating the complexity of epigenetic gene regulation to determine definite gene expression pattern.

1.3 Epigenetic impact of H3.3K27M-mutation in DIPG cells

H3.3K27M-mutation is a heterozygous point mutation in histone H3 and is found in approximately 65% of DIPG, resulting in a lysine (K) to methionine (M) substitution (Hoffman et al. 2018). Presence of this mutation causes an impaired function of polycomb repressive complex 2 (PRC2) and is responsible for reprogramming the epigenetic landscape (Bender et al. 2013). H3.3K27M-mutation alters function of EZH2 which results in chromatin remodeling and following changes in gene expression (**Figure 4**) (Harutyunyan et al. 2019). This interference leads to global loss of H3K27me3 with focally increased expression of this histone mark, and

global gain of H3K27ac (Schwartzentruber et al. 2012; Khuong-Quang et al. 2012). Dysregulation of the epigenetic landscape has been described in different types of cancers (Kim and Roberts 2016); for instance EZH2 is found to be overexpressed in many different tumors including adult high-grade gliomas (Helin and Dhanak 2013; Zhang et al. 2015). Since its increased activity is associated with poor prognosis, EZH2 is thought to have tumor driving function. Besides overexpression of EZH2 mutations, loss of function mutations in myeloid neoplasm and T-cell acute lymphoblastic leukemia were also reported (Ernst et al. 2010; Ntziachristos et al. 2012). These findings suggest that EZH2 may display both, tumor driver and tumor suppressor functions in dependence on the respective cell context and might therefore play a dual role in tumorigenesis (Greer and Shi 2012).

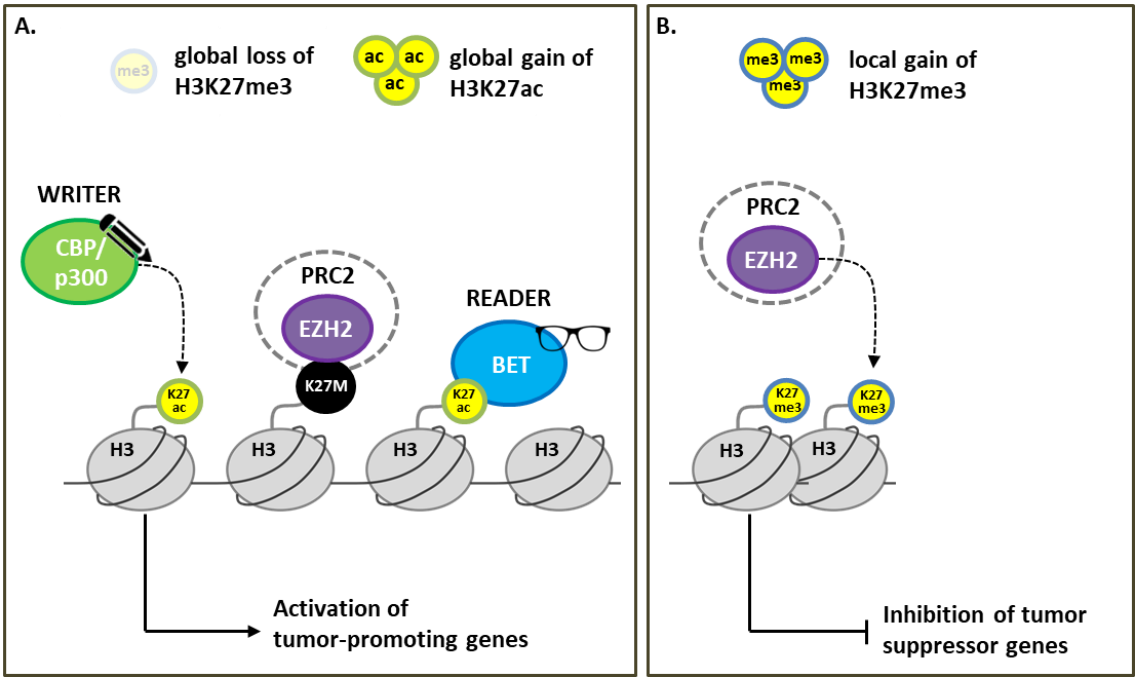

Figure 4 | H3.3K27M-mutation impacts epigenetic regulatory mechanisms.
Presence of H3.3K27M-mutation impairs function of EZH2, which results in global loss of H3K27me3 with local gain of the methylation mark. To compensate the epigenetic imbalance, H3K27ac is elevated through histone acetyltransferases such as CBP/p300. Hyperacetylation potentially results in stronger binding of BET proteins (adapted from Wiese et al. unpublished); (abbreviations explained in the text).

Despite global hypomethylation, H3K27me3 is preferentially maintained at unmethylated CpG islands, resulting in inhibition of crucial tumor suppressive genes in H3.3K27M-DIPG (Zheng et al. 2021). This phenomenon is thought to be due to lower affinity and recruitment of EZH2 to lysine (K) in comparison to methionine (M) in H3.3K27M-DIPG, not allowing PRC2 complex to spread (Lewis et al. 2013). In line with these findings, it was shown that residual PRC2 activity can still be detected in H3.3K27M-DIPG cells, which activity is essential for DIPG cell proliferation (Mohammad et al. 2017).

Since histone methylation and acetylation are well-balanced, H3.3K27M-induced hypomethylation (H3K27me3) inevitably leads to compensatory hyperacetylation of H3 (H3K27ac) (Lewis et al. 2013). Hyperacetylated genes, such as proto-oncogene *MYC* or cyclin-dependent kinases, at H3K27 are involved in regulation of cell cycle and other tumor-promoting mechanisms (Weinberg et al. 2017).

In this regard, Wiese *et al.* found that H3.3K27M-mutation is associated with enhanced cell proliferation and stem cell-like characteristics with increased sphere formation ability and stemness-associated markers compared to H3WT pedHGG (Wiese et al. 2020).

1.4 Function of selected epigenetic writers and readers

Epigenetic modifications represent one of cancer hallmarks and together with genetic changes are involved in tumor initiation and progression. In consequence, any interference of regular epigenetic landscape favors notably altered gene expression and tumorigenesis.

H3.3K27M-mutation results in decrease of H3K27me3 and subsequently elevated levels of H3K27ac (Piunti et al. 2017). Accordingly, acetylation-dependent epigenetic writers and readers might be crucial for the aggressive tumor phenotype observed in H.3.3K27M-DIPG cells.

1.4.1 Function of cAMP response element binding protein (CREB) binding protein (CBP/p300)

cAMP response element binding protein (CBP) and its paralog E1A-binding protein (p300) belong to the family of histone acetyltransferases (HAT) (Wang et al. 2013). They are transcriptional coactivators and interact with more than 400 different proteins (Bedford et al. 2010). CBP/p300 consist of the bromodomain (BD) which recognizes and interacts with acetylated histones (reader function) and the acetyltransferase domain that acetylates histones (especially H3K27) (writer function) (**Figure 5**) (Xu et al. 2006; Spiegelman and Heinrich 2004; Stauffer et al. 2007). Essentially, CBP and p300 are considered to possess identical function. They share a high percentage of sequence identity within their domains (Zeng et al. 2008; Liu et al. 2008). However, they exhibit much lower homology outside of their domains and have been described to interact with distinct partners (Dancy and Cole 2015).

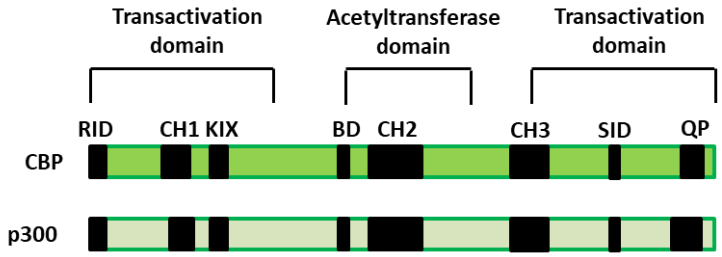

Figure 5 | **Schematic representation of CBP and p300 domains and homologous regions.** Receptor-interacting domain (RID); cysteine and histidine-rich regions 1-3 (CH1-3); binding site of CREB (KIX); bromodomain (BD); steroid receptor co-activator-1 interaction domain (SID); glutamine- and proline-rich domain (QP) (adapted from Karamouzis et al. 2007).

CBP/p300 regulate many different biological processes in the cell. They are thought to act as a "bridge" between different transcription factors and basal transcriptional machinery (BTM) components (Goodman and Smolik 2000). CBP/p300 were reported to function as scaffold proteins in formation of transcriptional complexes, including assembly of ß-interferon gene promoter (Merika et al. 1998). CBP/p300-HAT activity is also responsible for acetylation of some transcription factors (such as p53 or p73), therefore modulating the function of key transcriptional regulators (Wang et al. 2013). Furthermore, CBP/p300 bind additional acetyl-transferase factors and recruit other epigenetic key players, such as histone methyltransferases (HMT) (Vandel and Trouche 2001; Ogryzko et al. 1998).

CBP and p300, just like other proteins that control cell growth, are also regulated by phosphorylation. It was shown that p300 is negatively regulated by cyclin E/CDK2, a checkpoint kinase that regulates G1/S cell cycle transition (Perkins et al. 1997). Previous studies reported that function of CBP could be regulated by calcium/calmodulin (CaM)-dependent protein kinase IV (CaMK4) (Chawla et al. 1998; Hardingham et al. 1999). Moreover, other study has shown that phosphorylation of CBP is carried out by mitogen-activated protein kinase (MAPK), which regulates cell proliferation, cell cycle and apoptosis (Janknecht and Nordheim 1996; Pearson et al. 2001).

CBP and p300 were also reported to have an essential function in several developmental processes (Chrivia et al. 1993; Yao et al. 1998; Ramos et al. 2010; Kasper et al. 2014; Fang et al. 2014). Several investigations demonstrated that mice carrying CBP and p300 mutations showed deficiency in learning and memory (Tanaka et al. 1997; Oike et al. 1999) although no association of CBP/p300 with synaptic functions have been shown yet in human. However, studies in *Xenopus* model revealed a particular function of CBP/p300 in neural determination, suggesting an important role in suppressing neural fate (Izumi et al. 2003). Moreover, p300, but not CBP, was also reported to play a role in myogenesis especially of skeletal muscles, thereby being involved in myoblast determination protein 1 (myo-D) signaling (Fauquier et al. 2018; Eckner et

al. 1996; Sartorelli et al. 1997). Another study reported involvement of p300 in very early B lymphopoiesis, however, both, CBP and p300, seem to control mature B cells (Xu et al. 2006).

Despite clear differences between function of CBP and p300, their individual roles in establishing functional chromatin state at a genome-wide level have not been yet addressed.

1.4.1.1 Function of CBP/p300 in cancer

Since protein acetylation is linked to tumorigenesis (Zheng et al. 2004), CBP and p300 certainly play a crucial role in cancer. Dysregulation of the transcriptional and epigenetic functions of CBP/p300 is commonly associated with different types of cancer, such as colon, ovarian or lung cancer (Ionov et al. 2004; Ward et al. 2005; Ansari et al. 2023).

CBP and p300 seem to contribute to the opposite cellular processes, participating in many tumor-suppressor pathways and at the same time are important for the function of many oncogenes (Goodman and Smolik 2000).

Function of CBP and p300 in reduction of cell proliferation seems to be mediated via interaction with tumor suppressor p53, which contributes to transcriptional activation of mouse double minute 2 homolog (MDM2), cyclin-dependent kinase inhibitor 1 (p21) and Bcl-2-associated X protein (BAX) promoters (Avantaggiati et al. 1997; Gu et al. 1997; Lill et al. 1997). p53-CBP/p300 interaction was also shown to be involved in p53 transcriptional activation and in p53-mediated apoptosis (Shikama et al. 1999; Grossman et al. 1998). CBP/p300 also interacts with a variety of other tumor suppressors, such as breast cancer type 1 susceptibility protein (BRCA-1) (Pao et al. 2000).

CBP was reported to be the mediator of many oncogenes, such as activator protein 1 (AP-1) which controls cell proliferation and apoptosis (Ramos et al. 2010; Ameyar et al. 2003). Although mechanism of this interaction is still poorly understood, relation between CBP and another proto-oncogene, c-myb, has been explored in more details. This interaction leads to activation of c-myb and CBP target genes, such as mitochondrial import protein (MIM-1) (Oelgeschlaeger et al. 1996). Interestingly, c-myb has been shown to have an antagonistic function to (GATA Binding Protein 1) GATA-1, which also interacts with CBP, and block erythroid differentiation (Takahashi et al. 2000). Additionally, it has been reported that CBP/p300 elevate E2F transcription factor 1 (E2F1)-mediated transcriptional activation which is involved in cell cycle regulation (Trouche et al. 1996).

Overall, the capacity of CBP and p300 to bind several transcriptional regulators are mediated by different mechanisms, contributing to transcriptional specificity.

1.4.1.2 Targeting CBP/p300 using small molecules in cancer

As CBP and p300 are crucial for cell maintenance and play a major role in tumorigenesis (Wang et al. 2013; Pastori et al. 2014), small molecules that selectively bind to certain domains of these proteins, subsequently blocking their function, have been developed. Several studies have already tried to investigate the effect of inhibiting CBP/p300 in different carcinomas.

C646 and A-485 are two novel histone acetyltransferase inhibitors of CBP/p300. Inhibition of histone acetylation as well as cell proliferation by C646 suggests its suitability for anticancer treatment (Bowers et al. 2010). Treatment with C646 led to cell cycle arrest in pancreatic cancer (Ono et al. 2021) and in acute myeloid leukemia (Gao et al. 2013). It also sensitized lung cancer cells to radiotherapy (Oike et al. 2014). A-485 was shown to increase cell death and inhibit long-term cell proliferation in non-small-cell lung carcinoma (Zhang et al. 2020). It also displayed antitumor effects in growth hormone pituitary adenoma (Ji et al. 2022). Another study showed that A-485 treatment of small lung cancer promoted tumor growth arrest via autophagy (Ansari et al. 2023).

Inhibition of BD function of CBP/p300 by CBP112 impaired aberrant self-renewal of leukemic cells and increased cytotoxic activity of BET inhibitor, JQ1 (Picaud et al. 2015), providing new opportunity for combinatory treatment in tumor studies. CBP112 also sensitized cells to chemotherapy in various types of cancer (Strachowska et al. 2021). Another study demonstrated that the combination of CBP112 and HAT inhibitor, A-485, led to synergistic inhibition of prostate cancer cell proliferation (Zucconi et al. 2019). Clinical trials in prostate cancer showed that inhibition of CBP/p300 BD as a single treatment or in combination with BET proteins inhibitors could have beneficial effects (Welti et al. 2021; Yan et al. 2019). Furthermore, it was shown that inhibition of BD by GNE-049 and HAT by A-485 of CBP/p300 effectively blocked estrogen receptor function and consequently inhibited cell proliferation in luminal breast cancer (Waddel et al. 2021).

CBP30, which also inhibits BD of CBP/p300, has already been studied as anticancer agent, thereby showing significantly less side effects compared to other epigenetic inhibitors currently used in clinical trials (Hammitzsch et al. 2015). Treatment with CBP30 reduced *MYC* expression and cell proliferation in prostate cancer (Garcia-Carpizo et al. 2018).

Wiese *et al.* showed that treatment with Wnt/ß-catenin inhibitor (ICG-001) led to antitumor effects in pedHGG (Wiese et al. 2017; Wiese et al. 2020). Additionally, ICG-001 was reported to suppress cell proliferation and reduce chemoresistance in gastric cancer (Liu et al. 2017), and to

induce apoptosis in colon cancer (Emami et al. 2004). Treatment with ICG-001 also showed strong antiproliferative effect, leading to cell cycle arrest and programmed cell death in uveal melanoma (Kaochar et al. 2018). Surprisingly, in osteosarcoma it was revealed that, although ICG-001 inhibited cell proliferation *in vitro*, *in vivo* it had a pro-migratory effect (Danieau et al. 2021).

Since most of the clinical investigations of small molecules inhibiting CBP/p300 stop at I or II phase of clinical trials due to their severe side effects or lack of tumor repression, there is an urgent need for different therapeutic approaches.

1.4.2 Function of bromodomain and extra-terminal domain (BET) proteins

Proteins of the bromodomain and extra-terminal domain (BET) family include four bromodomain-containing (BRD) members: BRD2, BRD3, BRD4 and BRDT, and contain two N-terminal acetyl-lysine (Kac) binding bromodomains (BD1 and BD2) followed by an ET domain (Zaware and Zhou 2019). BRD4, but not BRD2 or BRD3, possesses an additional carboxyterminal domain (CTD) (**Figure 6**). The most important function of BET proteins is regulation of gene transcription, including recruitment and regulation of different transcription factors which can either increase partners binding or lead to their degradation (Cheung et al. 2021). Moreover, BET proteins were also reported to interact with chromatin remodeling proteins such as nuclear receptor binding SET domain protein 3 (NSD3) or jumonji domain containing 6, arginine demethylase and lysine hydroxylase (JMJD6) through their ET domain (Rahman et al. 2011), thereby actively organizing chromatin structure for gene transcription (Hsu et al. 2017). Apart from controlling transcription, BET proteins have a crucial function in DNA double-strand break (DSB) repair during S phase (Barrows et al. 2022).

Although BET proteins share similar functional domains (**Figure 6**), they display non-redundant functions, emphasizing the importance to understand distinct and overlapping functions of BET proteins (Cheung et al. 2007).

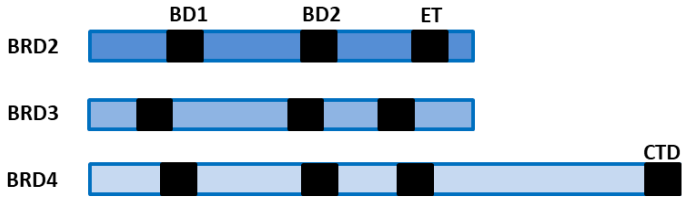

Figure 6 | Schematic representation of domain organization of BET proteins.
Bromodomains (BD1 and BD2); extra-terminal domain (ET); carboxyterminal domain (CTD) (adapted from Hajmirza et al. 2018).

BRD2 plays a main role in chromatin organization. It has been shown that BRD2, but not BRD4, is recruited by chromatin architectural/insulator protein (CTCF), suggesting function of BRD2 in boundary activities (Hsu et al. 2017). Furthermore, BRD2 is known to recruit E2F-1 and E2F-2 transcription factors mediating transcription in hyperacetylated chromatin (Denis et al. 2006; LeRoy et al. 2008). BRD2 promotes variety of cell cycle regulators, such as cyclin A or cyclin E (Sinha et al. 2005). BRD2 and BRD4 are reported to share similar functions. They were shown to promote DNA repair, replication and regulation of replication stress response signaling (Li et al. 2018; Sansam et al. 2018). Moreover, in mouse embryonic stem cells (mESC), BRD2 and BRD4 were demonstrated to control pluripotency, recruiting GLTSCR1/like-containing BAF complex-glioma tumor suppressor candidate region gene 1 (GBAF-GLTSCR1) to form BAF complex (Gatchalian et al. 2018).

Generally, BRD3 is thought to have mostly overlapping cellular functions with BRD2 (Stonestrom et al. 2015). Nevertheless some studies showed more distinct function of BRD3, for instance in nucleosome remodeling in the context of transcription (LeRoy et al. 2008) or its interactions with RNA molecules (Daneshvar et al. 2020). BRD3 was also reported to bind to several chromatin remodeling complexes, such as nucleosome remodeling deacetylase (NuRD) or BRG1/BRM-associated factor (BAF) complexes (Wai et al. 2018) and transcription factors, such as erythroid transcription factor (GATA1), facilitating stable connection with chromatin (Lamonica et al. 2011; Stonestrom et al. 2015).

BRD4 is probably the most studied member of BET proteins family. Elongation of transcription is coupled with splicing and genome stability, therefore BRD4 regulates alternative splicing by mediating interactions with heat shock factor 1 (HSF1) (Hussong et al. 2017). Recently it has been shown that interactions of BRD4 with RNA/DNA may have a crucial function in BRD4 chromatin binding (Miller et al. 2016; Rahnamoun et al. 2018). Furthermore, it was also demonstrated that BRD4 is able to recognize a combination of histone marks, such as phosphorylation and acetylation, and not just a single mark (Filippakopoulos et al. 2012). BRD4 is known to interact with a variety of transcription factors either enhancing binding partner stability, for example in prostate cancer where p300 acetylates JMJD1A at K421 that recruits BRD4 to block JMJD1A from degradation (Xu et al. 2020), or inducing degradation, for instance c-myc phosphorylation by BRD4 which leads to its degradation (Devaiah et al. 2020). It was also reported that BRD4 forms a complex with CBP/p300 through its bromodomain which results in elevation of HAT activity, and thus, modifies chromatin structure (Wu et al. 2018).

1.4.2.1 Function of BET proteins in cancer

BET proteins, especially BRD4, were implicated in cancer. BRD3 and BRD4 gene translocations were shown to cause aggressive human squamous carcinoma (Lee et al. 2017). Moreover, elevated expression of BRD4 was reported in a variety of cancers, leading to dysregulation of of tumor-promoting genes expression (Delmore et al. 2011; Mertz et al. 2011). BRD4 was also shown to form a complex with positive transcription elongation factor b (P-TEFb) which results in a P-TEF-b-dependent stimulation of RNA polymerase II (Jang et al. 2005). This interaction demonstrates translation from H3K27ac mark to active transcription which is required for the expression of tumor driving oncogenes (such as c-myc) (Da Costa et al. 2013) and its aberration commonly appears in midline carcinomas (French 2010). Additionally, many studies suggested that overexpression of BRD4 observed in many types of cancer is likely due to enhanced transcription and translation (Bhattacharyya et al. 2017; Tonouchi et al. 2018; Shi et al. 2019; Choe et al. 2018). Since it was shown that phosphorylation of BRD4 is often linked to its upregulated oncogenic function (Wang et al. 2017; Wu et al. 2013), new therapeutic strategies targeting BRD4 phosphorylation may be beneficial.

Potential role of BRD2 was also implicated in cancer (Belkina and Denis 2012). BRD2 was shown to regulate transcription of cyclin D1 (CCND1) (Cheung et al. 2017) which overexpression correlates with early cancer onset and tumor progression (Diehl 2002) and may lead to increased chemotherapeutic resistance as well as protection from apoptosis (Shintani et al. 2002). Whereas BRD3 was shown to play a prominent role in repression of tumor cell differentiation (Roberts et al. 2017).

1.4.2.2 Targeting BET proteins using small molecules in cancer

Pharmacological inhibition of BET proteins has emerged as a new therapeutic strategy targeting transcriptional expression of c-myc-dependent target genes. The best known BD inhibitor, JQ1, inhibits BET proteins interaction with acetylated histones (Filippakopoulos et al. 2010). *In vivo* efficacy of JQ1 in inhibition of cancer cell growth was proven in several different types of cancers including multiple myeloma (Delmore et al. 2011), acute myeloid leukemia (AML) (Zuber et al. 2011), breast cancer (Shu et al. 2016), pedHGG (Wiese et al. 2020) and melanoma (Fontanals-Cirera et al. 2017).

Another BET proteins inhibitor, OTX-015, has been shown to reduce cell growth, promote cell cycle arrest and apoptosis, reducing c-myc expression in diffuse large B-cell lymphoma (DLBCL) cells (Boi et al. 2015). Moreover, OTX-015 was reported to be able to penetrate the blood-brain-

barrier (Berthon et al. 2016). However, in phase I of clinical trials in lymphoma and multiple myeloma, OTX-015 failed to display any significant antitumor activity (Amorim et al. 2016).

TEN-010, structurally similar to JQ1, is currently being explored in clinical trials in solid tumors. Preliminary data revealed disease progression upon treatment with TEN-010 (Shapiro et al. 2015). GSK525762 is another BET proteins inhibitor being investigated in hematologic malignancies. Preliminary data showed many adverse effects including thrombocytopenia, anemia, and fatigue (O'Dwyer et al. 2016).

Since none of the reported BET proteins inhibitors showed effectiveness in clinical trials, combinatory therapy approach or advances in the development of next-generation compounds might be necessary to overcome the resistance that could develop to BET proteins inhibition.

2 Aim of study

Diffuse intrinsic pontine gliomas (DIPG) represent the pediatric tumor type with the worst prognosis. Many attempts to change the fatal clinical situations have failed, neither DIPG-specific nor novel treatment approaches could be established. Thus, standard treatment options still resemble those used in adult glioblastoma patients with radiotherapy and temozolomide chemotherapy. Up to 85% of DIPG carry a heterozygous point mutation resulting in lysine to methionine substitution (H3K27M) either in histone 3.3 (encoded by *H3F3A*) or less frequently in histone 3.1 (encoded by *HIST1H3B/C*) which both result in hyperacetylation and hypotrimethylation at H3K27. Since H3K27 hyperacetylation obviously appears to represent a kind of a hallmark of H3.3K27M DIPG, it may be hypothesized that epigenetic writers such as H3K27 histone acetyltransferase cAMP response element binding protein (CREB) binding protein (CBP/p300) and epigenetic readers recognizing acetylated histones such as bromodomain and extra-terminal domain (BET) proteins (and also CBP/p300) may play a more significant role in H3.3K27M-DIPG when compared to H3WT-DIPG cells. Thus, the present project aimed to identify H3.3K27M-mutation-associated epigenetic and tumor-biological effects in H3.3K27M-mutated DIPG cells and to investigate how CBP/p300 and BET proteins may be involved.

To be able to identify distinct epigenetic and tumor-biological effects in DIPG cells associated with H3.3K27M-mutation, isogenic CRISPR/Cas cell lines were generated by introducing H3.3K27M-mutation into originally H3-wildtype DIPG cells (VUMC-DIPG-010) and by removing H3.3K27M-mutation from originally H3.3K27M-mutated DIPG cell line (HSJD-DIPG-012). Thus, each resulting pair of DIPG cell lines differed only in the H3-mutation status, but otherwise had the same cellular and genetic background. Isogenic DIPG cell lines pairs were analyzed with regard to their tumor phenotype characteristics, nucleosome and transcriptome.

In order to investigate potential functions of CBP/p300 and BET proteins in dependence on H3-mutation status in isogenic DIPG cells, small molecules were employed inhibiting distinct functions of their respective targets: CBP30 and OTX-015 inhibiting reader functions of CBP/p300 and BET proteins, respectively, and A-485 inhibiting histone acetyltransferase writer activity of CBP/p300. To dissect the role of CBP and p300 and different BET proteins members, siRNA was used to specifically knock down the respective proteins of interest. After inhibition and knockdown of CBP, p300 and BET proteins in isogenic DIPG cells with different H3-mutation status, functions of the proteins of interest were investigated regarding tumor biology as well as H3K27ac-associated gene regulatory processes.

In summary, the present project aimed to determine H3.3K27M-dependent tumor-biological effects and the particular function of CBP/p300 and BET proteins in isogenic H3.3K27M-DIPG and H3WT-DIPG cell lines.

3 Materials and Methods

3.1 Materials

3.1.1 Cell lines, culture media and inhibitors

For CRISPR/Cas9 transfection, two different patients-derived cell lines were used (**Table 1**). VUMC-DIPG-010 was kindly provided by Dr Esther Hulleman (VU University Medical Center, Amsterdam, the Netherlands) and HSJD-DIPG-012 by Dr Angel Montero Carcaboso (Sant Joan de Deu Hospital, Barcelona, Spain).

Table 1 | Cell lines used in the present study

Cell line	H3-status	Origin
VUMC-DIPG-010	H3WT	VU University Medical Center Amsterdam, the Netherlands
HSJD-DIPG-012	H3.3K27M	Hospital Sant Joan de Deu, Barcelona, Spain

Isogenic cell lines used for further experiments can be found in **Table 2**.

Table 2 | Isogenic cell lines used in the present study

Original cell line	Isogenic cell line	H3-status	Clone number
VUMC-DIPG-010	isoDIPG-010	H3WT	#1, #2, #3
		H3.3K27M	#1, #2, #3
HSJD-DIPG-012	isoDIPG-012	H3WT	#1, #2, #3
		H3.3K27M	#1, #2, #3

Cells were cultured under spheroid conditions in TSM work. Composition of media can be found in **Table 3**.

Table 3 | Media used for cell culture in the present study

Medium	Composition
TSM base	1:1 Neurobasal®-A Medium: DMEM/F-12, 1% HEPES buffer, 1mM Sodium pyruvate, 1x MEM NEAA, 1x GlutaMAX, 1% Penicillin-Streptomycin
TSM diff	TSM base, 10% FCS
TSM work	TSM base, 0.5X B27® Supplement, 20 ng/mL EGF, 20 ng/mL FGF, 10 ng/mL PDGF-AA, 10 ng/mL PDGF-BB, 2 µg/mL Heparin

Ingredients used for supplementing media are listed in **Table 4**.

Table 4 | Supplements used for cell culture in the present study

Additional supplements	Manufacturer	Place of origin
B27 Supplement (50x)	Gibco® by life technologies™	Waltham, USA
DMEM/F-12 (1:1) (1x)	Gibco® by life technologies™	Waltham, USA
Fetal calf serum (FCS)	Biochrom	Cambridge, UK
GlutaMAX™-I (100x)	Gibco® by life technologies™	Waltham, USA
Heparin sodium salt from porcine intestinal mucosa	Sigma-Aldrich	St. Louis, USA
HEPES Buffer (1x)	Gibco® by life technologies™	Waltham, USA
MEM NEAA (100x) Minimum Essential Medium Non-Essential Amino Acids	Gibco® by life technologies™	Waltham, USA
Neurobasal R-A Medium (1x)	Gibco® by life technologies™	Waltham, USA
OptiMEM® I	Gibco® by life technologies™	Waltham, USA
PDGF-AA	PeproTech	Waltham, USA
PDGF-BB	PeproTech	Waltham, USA
Penicillin-streptomycin	Gibco® by life technologies™	Waltham, USA
Recombinant human EGF	PeproTech	Waltham, USA
Recombinant human FGF	PeproTech	Waltham, USA
Sodium Pyruvate 100mM (100x)	Gibco® by life technologies™	Waltham, USA

Inhibitors with their working concentrations used for this study are presented in the **Table 5** below.

Table 5 | Inhibitors used in the present study

Inhibitor	Working concentration	Manufacturer	Place of origin
A-485	50 nM	Tocris	Bristol, UK
BAY-876	500 nM	Selleckchem	Houston, USA
Birabresib (OTX-015)	50 nM	Selleckchem	Houston, USA
C646	-	Selleckchem	Houston, USA
CBP112	-	Selleckchem	Houston, USA
CBP30	1 µM	Selleckchem	Houston, USA
ICG-001	-	MedChemExpress	Monmouth Junction, USA
ISOX-DUAL	-	Tocris	Bristol, UK
JQ1	-	Tocris	Bristol, UK
MS346	-	LKT Labs	St. Paul, USA
Tazemetostat (EPZ-6438)	3 µM	Selleckchem	Houston, USA
Temozolomide (TMZ)	10 µM or 100 µM	Selleckchem	Houston, USA

3.1.2 *In vivo* model

In order to perform chorioallantoic membrane (CAM) assay, specific pathogen free (SPF) chicken eggs were used, which had been obtained from VALO BioMedia, Osterholz-Scharmbeck. Eggs used for CAM are specific pathogen free from flocks that have been confirmed to be free of specific disease pathogens.

3.1.3 Instruments

Instruments used in the present study are listed in **Table 6**.

Table 6 | Instruments used in the present study

Instrument	Manufacturer	Place of origin
7900HT Fast Real-Time PCR System	Applied Biosystems	Waltham, USA
Blotting system	Biometra	Göttingen, Germany
Cell culture incubator	Heraeus, Thermo Scientific	Waltham, USA
Cell culture sterile bench	Labotect, The Baker Company inc.	Rosdorf, Germany
Cell culture centrifuge	Eppendorf	Hamburg, Germany
ChemoCam Imager	Intas	Göttingen, Germany
Electrophoresis power supply	Peqlab	Erlangen, Germany
Electrophoresis system for agarose gels	Peqlab	Erlangen, Germany
Freezer (-20 °C)	Bosch	Gerlingen, Germany
Freezer (-80 °C)	PHCbi	Etten-Leur, the Netherlands
Fridge (+4 °C)	Liebherr	Moringen, Germany
Gel documentation	Intas	Göttingen, Germany
Genetic Analyzer 3500	Thermo Scientific	Waltham, USA
Heating block – Thermostat plus	Eppendorf	Hamburg, Germany
Ice machine EF103	Scotsman	Vernon Hills, USA
Incubator	Rostfrei	Netphen-Deuz, Germany
Incubator 8204 BSS 300 MP GTFS	ProCon & Grumbach automatic systems GmbH & Co.KG	Mücke, Germany
Infinite F50 absorbance plate reader	Tecan	Wiesbaden, Germany
Lamp KLI500	Leica Microsystems GmbH	Nußloch, Germany

LSRII FACS instrument	Becton Dickinson	Heilderberg, Germany
Luminescent image analyzer LAS-4000 mini	Fujifilm	Düsseldorf, Germany
Microcentrifuge	Eppendorf	Hamburg, Germany
Micropipettes (1, 2, 10, 20, 100, 200, 1000 µl)	Eppendorf	Hamburg, Germany
Microscope	Zeiss	Oberkochen, Germany
Microtome RM2165	Leica Microsystems GmbH	Nußloch, Germany
Microwave oven	Brother	Berlin, Germany
Mini-PROTEAN Tetra Cell electrophoresis system	BioRad	Feldkirchen, Germany
Multipette	Eppendorf	Hamburg, Germany
Neubauer cell counting chamber	Brand	Wertheim, Germany
Paraffin Embedding Station EC 350	Thomas Medical Systems	Mitterhofen, Austria
Paraffin Stretching Bath GFL 1052	GFL Lab Unlimited	Dublin, Ireland
Power supplier EV231	Peqlab	Erlangen, Germany
Printer	Mitsubishi	Berlin, Germany
Pump VDE0530	Adam.Baumüller GmbH	Helmstedt, Germany
Rotator	GLW	Petersberg, Germany
RS 225 X-Ray Research System	Gulmay Medical Systems	Camberley, UK
Shaker MTS4	W.Krannich GmbH+Co.KG	Göttingen, Germany
Shaker for bacteria	Sartorius	Göttingen, Germany
Sonifier	Dr. Hielscher GmbH	Teltow, Germany
Spectrophotometer NanoDrop® ND-1000	Thermo Scientific	Waltham, USA
SynergyMx microplate reader	BioTek®	Bad Friedrichshall, Germany
Thermocycler	Biometra®	Göttingen, Germany
Thermomixer 5436	Eppendorf	Hamburg, Germany

Transferpette-8 (1-20 µl)	BRAND	Wertheim, Germany
Vortex	W.Krannich GmbH+Co.KG	Göttingen, Germany
Water bath GFL 1003	W.Krannich GmbH+Co.KG	Göttingen, Germany
Water purification system	Sartorius	Göttingen, Germany

Consumables used in this study are presented in **Table 7**.

Table 7 | Consumables used in the present study

Consumable	**Manufacturer**	**Place of origin**
Boyden chamber	Merck	Darmstadt, Germany
Cryovials	Nunc	Waltham, USA
Cell scraper	Sarstedt	Nümbrecht, Germany
Combitips	Eppendorf	Hamburg, Germany
Cuvettes	Roth	Karlsruhe, Germany
Falcon tubes (15 mL)	Sarstedt	Nümbrecht, Germany
Falcon tubes (50 mL)	Sarstedt	Nümbrecht, Germany
Filters for solutions (0.2 µm and 0.45 µm)	Sartorius	Göttingen, Germany
Flasks for cell culture (75 cm^2 and 175 cm^2)	Sarstedt	Nümbrecht, Germany
Gloves (nitrile)	LABSOLUTE	Renningen, Germany
Low Protein Binding Collection Tubes (1.5 mL)	Thermo Scientific	Waltham, USA
Microscope slides	Epredia	Waltham, USA
Microplates (384-well)	Greiner-bio-one	Kremsmünster, Austria
Nunclon Delta Surface cell culture plates (6-well, 12-well and 96-well)	Thermo Scientific	Waltham, USA
Parafilm	Pechiney Plastic Packaging	Akron, USA
Pasteur pipettes	Brand	Wertheim, Germany
PCR tubes (0.2 mL)	Sarstedt	Nümbrecht, Germany
Petri dishes	Falcon	Falkensee, Germany
Pipette filter tips (10, 100, 200, 1000 µL)	Starlab	Hamburg, Germany

Pipette tips (10, 200, 1000 µL)	Sarstedt	Nümbrecht, Germany
Pipettes (5, 10 and 25 ml)	Sarstedt	Nümbrecht, Germany
PVDF membrane (pore size 0.45 µm)	Merck	Darmstadt, Germany
Reaction tubes (1.5 mL and 2 mL)	Sarstedt	Nümbrecht, Germany
Scalpels	Technic cut	Berlin, Germany
Tissue cassettes M491-4	Simport	Saint-Mathieu-de-Beloeil, Canada
Whatman paper	Sartorius	Göttingen, Germany

3.1.4 Basic chemicals, reagents and solutions

Basic chemicals and reagents used for this study are listed in **Table 8**.

Table 8 | Chemicals and reagents used in the present study

Chemical/Reagent	Manufacturer	Place of origin
6x DNA Loading Dye	Thermo Scientific	Waltham, USA
10x DNase I Buffer	Ambion®	Kaufungen, Germany
β-Mercaptoethanol	Sigma-Aldrich	St. Louis, USA
Acetic acid	Merck	Darmstadt, Germany
Acetic acid glacial	Merck	Darmstadt, Germany
Agarose	Canvax	Valladolid, Spain
Albumin bovine Fraction V (BSA)	Serva	Halle, Germany
Albumin Standard	Thermo Scientific	Waltham, USA
Ammonium persulfate (APS)	Roth	Karlsruhe, Germany
Ampicillin	Roth	Karlsruhe, Germany
A-Sepharose	Invitrogen	Waltham, USA
Bacto tryptone	Becton Dickinson	Kelberg, Germany
Bacto Yeast extract	Becton Dickinson	Kelberg, Germany
BC Assay Reagent A	Interchim	Mannheim, Germany
BC Assay Reagent B	Interchim	Mannheim, Germany
BlueStar Prestained Protein Marker	Genetics	Waltham, USA
BrdU (Bromdesoxyuridin)	Roche	Basel, Switzerland

Bromphenolblue	Sigma-Aldrich	St. Louis, USA
Calcium chloride ($CaCl_2$)	Sigma	St. Louis, USA
Collagen	Sigma	St. Louis, USA
Coomassie Brilliant Blue	BioRad	Hercules, USA
Crystal violet solution	Sigma-Aldrich	St. Louis, USA
DAB Chromogen	Zytomed	Berlin, Germany
DAB Substrate Buffer	Zytomed	Berlin, Germany
DEPC (diethyl pyrocarbonate)	Roth	Karlsruhe, Germany
Dimethyl sulfoxide (DMSO)	Roth	Karlsruhe, Germany
DirectPCR Lysis Reagent (Cell)	Viagen	Hilden, Germany
dNTP mix	Thermo Scientific	Waltham, USA
Eosin	Roth	Karlsruhe, Germany
Ethanol	Roth	Karlsruhe, Germany
Ethidium bromide	Roth	Karlsruhe, Germany
Ethylenediaminetetraacetic acid (EDTA)	Sigma-Aldrich	St. Louis, USA
Formaldehyde solution min. 37%	Merck	Darmstadt, Germany
Formamid	Merck	Darmstadt, Germany
Formic acid 98-100%	AppliChem	Darmstadt, Germany
Glycerin	Merck	Darmstadt, Germany
Glycerol	Sigma	St. Louis, USA
Glycin	Roth	Karlsruhe, Germany
Glycoblue	Thermo Scientific	Waltham, USA
Goat Serum	Merck	Darmstadt, Germany
G-Sepharose	GE Healthcare	Chicago, USA
Hematoxylin	Merck	Darmstadt, Germany
Hydrochloric acid (HCl) fuming 37%	Roth	Karlsruhe, Germany
Immu-Mount	ThermoScientific	Waltham, USA
Isopropanol	Roth	Karlsruhe, Germany
L-glutamine	Invitrogen	Waltham, USA
Lipofectamine RNAiMAX	Thermo Fischer Scientific	Waltham, USA

Luminol	Sigma-Aldrich	St. Louis, USA
Magnesium chloride ($MgCl_2$)	Roth	Karlsruhe, Germany
Matrigel® Matrix	Corning	Wiesbaden, Germany
Methanol	Chemsolute	Renningen, Germany
N,N,N',N'-Tetramethylethylenediamine (TEMED)	Roth	Karlsruhe, Germany
Nonidet-P40 (NP40)	Fluka	Buchs, Switherland
Paraformaldehyde (PFA)	Merck	Darmstadt, Germany
p-coumaric acid	Sigma-Aldrich	St. Louis, USA
Peroxygen (H_2O_2)	Merck	Darmstadt, Germany
Phenol/chloroform/isoamylalcohol	Roth	Karlsruhe, Germany
Phenylmethylsulfonyl fluoride (PMSF)	Roth	Karlsruhe, Germany
Potassium chloride (KCl)	Roth	Karlsruhe, Germany
Potassium dihydrogen phosphate (KH_2PO_4)	Roth	Karlsruhe, Germany
Powdered milk	Roth	Karlsruhe, Germany
Propidium iodide	Sigma	St. Louis, USA
Protease Inhibitor Cocktail Tablets	Roche	Basel, Switzerland
Protein A - Sepharose™ 4B	Invitrogen	Waltham, USA
Protein G Sepharose High Performance	GE Healthcare	Chicago, USA
Quick-Load Purple 1 kb DNA Ladder	New England BioLabs	Ipswich, USA
Roti® - Histokit	Roth	Karlsruhe, Germany
Rotiphorese® Gel 40 (29:1)	Roth	Karlsruhe, Germany
SeaKem® LE Agarose	Biozym	Oldendorf, Germany
Sodium acetate	Roth	Karlsruhe, Germany
Sodium citrate	Roth	Karlsruhe, Germany
Sodium chloride (NaCl)	Roth	Karlsruhe, Germany
Sodium dodecyl sulfate (SDS), ultra pure	Roth	Karlsruhe, Germany
di- Sodium hydrogen phosphate (Na_2HPO_4)	Roth	Karlsruhe, Germany
sparQ PureMag Beads	Quantabio	Beverly, USA
Thiazolyl Blue tetrazolium bromide (MTT)	Alfa Aesar	Ward Hill, USA

Thymidine	Roth	Karlsruhe, Germany
Tris	Roth	Karlsruhe, Germany
Triton X-100	Sigma	St. Louis, USA
Trypan Blue Stain (0.4%)	Gibco® by life technologies™	Waltham, USA
Tween 20	Sigma-Aldrich	St. Louis, USA
Xylol	Roth	Karlsruhe, Germany

Self-made solutions can be found in **Table 9**.

Table 9 | Self-made solutions used in the present study

Name	Composition
10x Crystal violet staining solution	5% crystal violet solution, 27% formaldehyde (min. 37%), 10% methanol, 10% 10x PBS, 48% H_2O
4x Laemmli probe buffer (LPP)	240 mM Tris-HCl (pH 6.8), 40% glycerin, 8% SDS, 20% β-mercaptoethanol, 0.04% bromphenolblue
4x separating (LT) buffer (pH 8.8)	1.5 M Tris-HCl (pH 8.8), 0.4% SDS
4x stacking (UT) buffer (pH 6.8)	0.5 M Tris-HCl (pH 6.8), 0.4% SDS
Antigen retrieval buffer	0.01 M sodium citrate, 0.01 M citric acid (pH 6.0)
Blocking solution	5% powdered milk/BSA in TBS-T
Blotting buffer	25 mM Tris, 192 mM glycine, 10% methanol
Cytoplasmic extract (CE) buffer	10 mM HEPES, 60 mM KCl, 1 mM EDTA, 1mM DTT, 1 mM PMSF, 0.075% NP40, 1x Protease Inhibitor (pH 7.6)
Coomassie destaining solution	40% ethanol, 10% acetic acid glacial
Coomassie staining solution	0.2% Coomassie Brilliant Blue, 30% isopropanol, 10% acetic acid
Crystal violet staining solution	0.5% crystal violet, 1% formaldehyde, 1% methanol, 1x PBS
ECL solution A	2.5 mM luminol, 0.36 mM p-coumaric acid, 0.1 M Tris-HCl (pH 8.5)
ECL solution B	0.0182% H_2O_2, 0.1 M Tris-HCl (pH 8.5)
Laemmli running buffer	25 mM Tris, 192 mM glycin, 0.01% SDS

LB Medium	5 g Yeast extract, 10 g NaCl, 10 g Tryptone in 1 L ddH_2O
MTT solution	5 mg/ml MTT in PBS
MTT lysis buffer	33% DMSO, 5% formic acid, 62% isopropanol
Nuclear extract (NE) buffer	20 mM Tris Cl, 420 mM NaCl, 1.5 mM $MgCl_2$, 0.2 mM EDTA, 1 mM PMSF, 25% glycerol, 1x Protease Inhibitor (pH 8.0)
Permeabilization buffer	0.1% Trition in PBS
PBS	5.48 mM NaCl, 0.108 mM KCl, 0.08 mM KH_2PO_4, 0.4 mM Na_2HPO_4
TBS-T (pH 7.4)	20 mM Tris-HCl, 150 mM NaCl, 0.1% Tween
TE Buffer (pH 8)	10 mM Tris, 0.1 mM EDTA (pH 8)

Commercial kits can be found in **Table 10**.

Table 10|**Commercial kits used in the present study**

Kit	REF number	Manufacturer	Place of origin
BigDye® Terminator v1.1 Cycle Sequencing Kit	4337450	Applied Biosystems	Waltham, USA
Blue S'Green qPCR Kit Separate ROX	331416XL	Biozym	Oldendorf, Germany
Cell Proliferation ELISA, BrdU (colorimetric)	11 647 229 001	Roche	Basel, Switzerland
CloneJET PCR Cloning Kit	K1232	Thermo Fischer Scientific	Waltham, USA
NucleoSpin Gel and PCR Clean-up Kit	740609.50	Macherey-Nagel	Düren, Germany
ReliaPrep RNA Cell Miniprep System	Z6012	Promega	Madison, USA
RevertAid First Strand cDNA Synthesis Kit	K1621	Thermo Scientific	Waltham, USA
SignalFire Elite ECL Reagent	12757S	Cell Signaling Technology	Danvers, USA
ZR Plasmid Miniprep	D4016	Zymo Research	Irvine, USA

3.1.5 Enzymes and antibodies

The enzymes used in this study are listed in **Table 11**.

Table 11 | Enzymes used in the present study

Enzyme	Manufacturer	Place of origin
DNA Blunting Enzyme	Thermo Fisher	Waltham, USA
DNase I (RNase-free)	Ambion	Kaufungen, Germany
HOT FIREPol DNA Polymerase	Solis BioDyne	Tartu, Estonia
Proteinase K	Roche	Basel, Switzerland
RiboLock RNase Inhibitor	Thermo Scientific	Waltham, USA
RNase A	Roche	Basel, Switzerland
T4 DNA Ligase	Thermo Fisher	Waltham, USA
TrypLE™ Express	Gibco® by life technologies™	Waltham, USA

Antibodies used for western blots are presented in **Table 12**.

Table 12 | Antibodies used for western blots in the present study

Antibody	Origin	Dilution	REF number	Manufacturer	Place of origin
Anti-β-actin HRP	mouse	1:10000	A3854	Sigma-Aldrich	St. Louis, USA
Anti-Atg7	rabbit	1:1000	8558S	Cell Signaling	Danvers, USA
Anti-Bax	rabbit	1:1000	ab32503	Abcam	Cambridge, UK
Anti-BRD2	rabbit	1:1000	ab139690	Abcam	Cambridge, UK
Anti-BRD3	rabbit	1:1000	A302-368A	BETHYL	Hamburg, Germany
Anti-BRD4	rabbit	1:1000	ab243862	Abcam	Cambridge, UK
Anti-Caspase 3	rabbit	1:1000	9662S	Cell Signaling	Danvers, USA
Anti-CBP	rabbit	1:500	7389S	Cell Signaling	Danvers, USA
Anti-CD133	rabbit	1:1000	64326S	Cell Signaling	Danvers, USA
Anti-Cdk2	rabbit	1:1000	ab32147	Abcam	Cambridge, UK
Anti-CDKN2A/p16INK4a	rabbit	1:1000	ab108349	Abcam	Cambridge, UK

Anti-cleaved Caspase 3	rabbit	1:1000	9664S	Cell Signaling	Danvers, USA
Anti-cleaved PARP	rabbit	1:1000	5625S	Cell Signaling	Danvers, USA
Anti-c-myc	rabbit	1:1000	ab32072	Abcam	Cambridge, UK
Anti-E-cadherin	rabbit	1:1000	3195S	Cell Signaling	Danvers, USA
Anti-EZH2	rabbit	1:1000	5246S	Cell Signaling	Danvers, USA
Anti-GFAP	rabbit	1:1000	GA52461-2	Dako	Jena, Germany
Anti-Glut1	rabbit	1:1000	ab115730	Abcam	Cambridge, UK
Anti-Histone H2A (ubiquityl K119)	rabbit	1:2000	8240S	Cell Signaling	Danvers, USA
Anti-H3K27M-mutation	rabbit	1:2000	74829S	Cell Signaling	Danvers, USA
Anti-Histone H3.3 (phospho S31)	rabbit	1:1000	ab92628	Abcam	Cambridge, UK
Anti-Histone H3 (tri methyl K4)	rabbit	1:1000	ab213224	Abcam	Cambridge, UK
Anti-Histone H3 (tri methyl K9)	rabbit	1:1000	ab176916	Abcam	Cambridge, UK
Anti-Histone H3 (acetyl Lys27)	rabbit	1:1000	ab177178	Abcam	Cambridge, UK
Anti-Histone H3 (tri methyl K27)	rabbit	1:1000	9733	Cell Signaling	Danvers, USA
Anti-Histone H3 (di methyl K36)	rabbit	1:1000	ab176921	Abcam	Cambridge, UK
Anti-Histone H3 (tri methyl K36)	rabbit	1:1000	ab282572	Abcam	Cambridge, UK
Anti-Histone H4 (acetyl K5 + K8 + K12 + K16)	rabbit	1:1000	ab177790	Abcam	Cambridge, UK
Anti-Histone H4 (acetyl K16)	rabbit	1:1000	ab109463	Abcam	Cambridge, UK
Anti-LC3B	rabbit	1:1000	3868S	Cell Signaling	Danvers, USA
Anti-MMP9	rabbit	1:1000	ab38898	Abcam	Cambridge, UK

Anti-mouse IgG HRP	goat	1:10000	115-035-174	Immuno Research	Cambridge, UK
Anti-Nanog	mouse	1:1000	sc-374103	Santa Cruz Biotechnology	Dallas, USA
Anti-N-cadherin	rabbit	1:1000	13116S	Cell Signaling	Danvers, USA
Anti-Nestin	rabbit	1:1000	ABD69	Merck Millipore	Burlington, USA
Anti-Oct4	rabbit	1:1000	2750S	Cell Signaling	Danvers, USA
Anti-p21	rabbit	1:1000	ab109520	Abcam	Cambridge, UK
Anti-p300	rabbit	1:1000	54062S	Cell Signaling	Danvers, USA
Anti-PARP	rabbit	1:1000	9532S	Cell Signaling	Danvers, USA
Anti-PAX6	rabbit	1:1000	60433S	Cell Signaling	Danvers, USA
Anti-rabbit IgG HRP	goat	1:10000	7074	Cell Signaling	Danvers, USA
Anti-SOX2	rabbit	1:1000	ab97959	Abcam	Cambridge, UK
Anti-SQSTM1/p62	mouse	1:1000	88588S	Cell Signaling	Danvers, USA
Anti-Vimentin	rabbit	1:1000	5741S	Cell Signaling	Danvers, USA
Anti-ZEB1	rabbit	1:1000	3396S	Cell Signaling	Danvers, USA

3.1.6 Oligonucleotides and siRNA

Oligonucleotides were synthesized by metabion international AG (Göttingen, Germany) (**Table 13 and Table 14**). Oligonucleotides for quantitative real-time PCR were designed using NCBI/Primer-BLAST (Ye et al. 2012). Primers were designed to span exon junctions when possible and to target all isoforms of one gene, if possible. Primer specificity was verified using nucleotide BLAST® from NCBI.

Table 13 | Oligonucleotide primers for qPCR with their corresponding sequences used in the present study

Primer	Forward (5'-3')	Reverse (3'-5')
β-ACTIN	CTGGGAGTGGGTGGAGGC	TCAACTGGTCTCAAGTCAGTG
BRD2	GCACCAAGCTCCCCAAAAAG	ATCGTAACTCATGGGCCTGC
BRD3	TTGAACCTGCCGGATTATCATAAAA	GCATACATTCGCTTGCACTCC
BRD4	AACAGCAATGTGAGCAAGAAGG	GCTTGTTGATGTCCAAGCTGAG
CDH1	CCTGCCAATCCCGATGAAAT	ACTCTGAGGAGTTCAGGGAG
CDH2	TGGGAATCCGACGAATGG	TGCAGATCGGACCGGATACT
CDK8	CCAGATAGTAAAGCATTCCACTTGCT	GGTCCTGCATAGCCTGTTCTGA
CDKN2A	CGGTCGGAGGCCGATCCAG	GCGCCGTGGAGCAGCAGCAGCT
c-MYC	GGCCCCCAAGGTAGTTATCCTT	CGTTTCCGCAACAAGTCCTCT
CREBBP	GTGCATAAACTCGTCCAAGCC	CTGCTGTTGGCAGACTCGTA
CTNNB1	GCTGGGACCTTGCATAACCTT	ATTTTCACCAGGGCAGGAATG
DKK1	GAAGGTTCTGTTTGTCTCCGGTC	ACAACACAATCCTGAGGCACAGT
EP300	GCGGCCTAAACTCTCATCTC	TCTGGTAAGTCGTGCTCCAA
EZH2	AAACAGCTCTTCGCCAGTCT	GATGCAACCCGCAAGGGTAA
GATA4	CTTGCAATGCGGAAAGAGG	TGCTGGAGTTGCTGGAAG
GFAP	CTGGAGAGGAAGATTGAGTCGC	ACGTCAAGCTCCACATGGACCT
HPRT	TATGCTGAGGATTTGGAAAGG	CATCTCCTTCATCACATCTCG
IL10	CTTGCTGGAGGACTTTAAGG	CTGGATCATCTCAGACAAGG
JDP2	GCTGAAATACGCTGACATC	CTCACTTTTCACGGGCTGG
MMP2	TGCTGGAGACAAATTCTGGAGATAC	GGATCCATTTTCTTCTTCACCTCAT
NANOG	CTCCAACATCCTGAACCTCAGC	CGTCACACCATTGCTATTCTTCG
NES	ACTTCCCTCAGCTTTCAG	GTGTCTCAAGGGTAGCAG
PROM1	TGGATGCAGAACTTGACAACGT	ATACCTGCTACGACAGTCGTGGT
POU5F1	GAGAACCGAGTGAGAGGCAACC	CATAGTCGCTGCTTGATCGCTTG
SNAI1	CAATCGGAAGCCTAACTACAG	CTGCTGGAAGGTAAACTCTG
SNAI2	TCCAAAAAGCCAAACTACAGCG	TCTCTGGTTGTGGTATGACAGG
SOX2	CCCTGCTGCGAGTAGGACAT	CCCTGCAGTACAACTCCATG
TP53	TTGCAATAGGTGTGCGTCAGA	AGTGCAGGCCAACTTGTTCAG

TWIST1	TCTACCAGGTCCTCCAGAGC	TAGGTCTCCGGCCCTGC
VEGFA	CTGAGGAGTCCAACATCAC	GTCTTGCTCTATCTTTCTTTGG
VIM	CCTTGAACGCAAAGTGGAATC	GACATGCTGTTCCTGAATCTGAG
WNT3	GCATCTACGACGTGCACACCT	CATGAGACTTCGCTGAATCCG
ZEB1	ACAACAAGACACTGCTGTCA	TGGACAGGTGAGTAATTGTGAA
ZEB2	TTCCTGGGCTACGACCATAC	TGTGCTCCATCAAGCAATTC

Table 14 | Oligonucleotide primers for conventional PCR and Sanger sequencing with their corresponding sequences used in the present study

Primer	Forward (5'-3')	Reverse (3'-5')
SeqH3	GGTCTCTGTACCATGGCTCG	AGACCTCCAGGTAAGATTATGGC
pJET1.2	CGACTCACTATAGGGAGAGCGGC	AAGAACATCGATTTTCCATGGCAG

ON-TARGET plus siRNA pools each consisting of four different siRNAs to reduce off target effects were used for siRNA-mediated knockdown of BRD2, BRD3, BRD4, CBP and p300. As control an unspecific siRNA was used. siRNAs were purchased from Dharmacon (Lafayette, Colorado, United States) and their target sequences are listed in **Table 15**.

Table 15 | siRNAs with their corresponding sequences used in the present study

siRNA	ID number	Target sequence (5'-3')
siControl	D-001810-20	UGGUUUACAUGUUUUCCUA
siBRD2	LQ-004935-00-0005	CACGAAAGCUACAGGAUGU GGGCCGAGUUGUGCAUAUA CCUAAGAAGUCCAAGAAAG GUCCUUUCCUGCCUACGUA
siBRD3	LQ-004936-00-0005	AAUUGAACCUGCCGGAUUA CGGCUGAUGUUCUCGAAUU GGAGAGAUAUGUCAAGUCU GCGAAUGUAUGCAGGACUU
siBRD4	LQ-004937-00-0005	AAACCGAGAUCAUGAUAGU CUACACGACUACUGUGACA AAACACAACUCAAGCAUCG CAGCGAAGACUCCGAAACA
siCBP	LQ-003477-00-0005	GCACAGCCGUUUACCAUGA

		UCACCAACGUGCCAAAUAU GGAUGAAGUCACCGGUUUG AAUAGUAACUCUGGCCAUA
sip300	LQ-003486-00-0005	GGACUACCCUAUCAAGUAA GACAAGGGAUAAUGCCUAA GUUCAAUAAUGCCUGGUUA CGACAGGGAUGCAGCAACA

3.1.7 HDR templates and CRISPR/Cas9 target sequences

HDR templates used for CRISPR/Cas9 genetic modification with their corresponding sequences are listed below in **Table 16**.

Table 16 | HDR templates used in the present study. Mutation- (H3.3K27M) and wildtype- (H3WT) specific triplets are highlighted in grey

HDR template	Sequence
HDR-H3.3WT	AGCACCCAGGAAGCAACTGGCTACAAAAGCCGCTCGC*AAG*AGTGC GCCCTCTACTGGAGGGGTGAAGAAACCTCATCGTTACAGGTATTAA AAAACAGGAAAAAAATGGGACAAAGTCTCTCTTGTAT
HDR-H3.3K27	AGCACCCAGGAAGCAACTGGCTACAAAAGCCGCTCGC*ATG*AGTGCG CCCTCTACTGGAGGGGTGAAGAAACCTCATCGTTACAGGTATTAAA AAACAGGAAAAAAATGGGACAAAGTCTCTCTTGTAT

CRISPR/Cas9 target sequences are presented in **Table 17**.

Table 17 | CRISPR/Cas9 target sequences used in the present study

CRISPR/Cas9 target	Strand	PAM	Sequence
CD.Cas9.VFTZ4576.AQ	-	CGG	AGAGGGCGCACTCTTGCGAG
CD.Cas9.VFTZ4576.AN	+	AGG	CGTTACAGGTATTAAAAAAC

3.1.8 Plasmids

For subcloning and consequential Sanger sequencing, pJET1.2 plasmid was used and obtained from Thermo Fisher (Waltham, Massachusetts, United States).

3.1.9 Software

The software used in this study is listed in **Table 18**.

Table 18|Software used in the present study

Software	Company	Place of origin
7900HT Fast Real-Time PCR System	Applied Biosystems	Waltham, USA
Citavi	Swiss Academic Software	Wädenswil, Switzerland
Flowing Software 2.5.1	Turku Bioscience	Turku, Finland
GENtle	University of Cologne, Germany	Cologne, Germany
GraphPad PRISM	GraphPad Software	San Diego, USA
Image J. 1.48	National Institutes of Health	Bethesda, USA
Magellan for F50 7.0SignalFire™ Elite	Tecan Group Ltd.	Männedorf, Switzerland
Microsoft Office 2013	Microsoft	Redmond, USA
Scry	Christian Dullin	Göttingen, Germany

3.2 Methods

3.2.1 Cell culture

Cell lines used in the present study: VUMC-DIPG-010 (herein referred to as isoDIPG-010 after CRISPR/Cas9 transfection) and HSJD-DIPG-012 (herein referred to as isoDIPG-012 after CRISPR/Cas9 transfection) were grown and maintained as gliomaspheres in TSM base (**Table 3**), supplemented with fibroblast- (FGF) and epidermal- (EGF) growth factors, protein B-27, H-PDGF AA-BB and heparin (**Table 4**). Cells were maintained in an incubator at 37°C with a humidity of 5% CO_2. For passaging or seeding cells were collected and centrifuged at 1000 rpm for 5 min. Spheres from the cell pellets were treated with 1x-trypsin-EDTA to obtain single cells, washed with 1x PBS and resuspended in TSM Base. 100 µL of the cell suspension was used for cell counting using a Neubauer counting chamber. The desired quantity of cells was suspended in corresponding media and seeded. The remaining cells were used for cell maintenance and cultured in TSM work.

3.2.1.1 Inhibitor treatment and irradiation

Unless stated otherwise, inhibition of EZH2 methyltransferase activity in isoDIPG-012 and isoDIPG-010 cells was achieved by 3 µM EPZ-6438 treatment. A-485 (50 nM) was used as HAT activity inhibitor of CBP/p300. CBP30 (1 µM) and OTX-015 (50 nM) served as BD inhibitors of CBP/p300 and BET proteins, respectively. For this purpose, 50 000 cells/mL were seeded under spheroid conditions as gliomaspheres before treatment. Approximately 24 h after seeding, cells were treated with corresponding concentrations of used inhibitors diluted in DMSO. Corresponding volume of DMSO was used as control.

To investigate cell viability with regard to their response to irradiation upon treatment with small molecules, cells were seeded in a 96-well plate at a concentration of 50 000 cells/mL and incubated at 37°C overnight. The following day, cells were treated with appropriate amount of corresponding inhibitor and/or 10 or 100 µM TMZ. The next day, cells were irradiated at a dose rate of 1 Gy/min. 24 hours later cells were treated again with the respective inhibitor and/or TMZ and incubated for 72 h at 37°C prior harvesting.

3.2.1.2 3-(4.5-dimethylthiazol-2-yl)-2.5-diphenyltetrazolium bromide (MTT) assay

In order to study cell viability and proliferation of CRISPR/Cas9 clones as well as upon siRNA-mediated knockdown or inhibitor treatment, MTT (3-(4.5-dimethylthiazol-2-yl)-2.5-diphenyltetrazolium bromide) cell viability assay was performed. For this purpose, isoDIPG-010 and isoDIPG-012 cells were seeded at a concentration of 50 000 cells/mL under spheroid conditions in a 96-well plate. Cells were incubated for total amount of 120 h at 37°C. After 0 h, 12 h, 24 h, 48 h, 72 h, 96 h and 120 h cells were harvested by incubation with 10% MTT solution (**Table 9**) at 37°C for 4 h. Medium was aspirated and MTT-lysis buffer (**Table 9**) was added to the cells. Plates were then shaken for 15 min and absorbance was measured using TECAN Infinite F50 absorbance plate reader at 560 nm. Experiments were repeated three times and samples were conducted in triplicates.

3.2.1.3 Crystal violet assay

Another method used to investigate cell viability was crystal violet assay. For this purpose, isoDIPG-010 and isoDIPG-012 cells were seeded at a concentration of 50 000 cells/mL under spheroid conditions in a 96-well plate. Cells were incubated for total amount of 120 h at 37°C. After certain time points (0 h, 12 h, 24 h, 48 h, 72 h, 96 h, 120 h) cells were incubated with crystal violet staining solution (**Table 9**) at RT for another 20 min on a bench rocker with a frequency of 20 oscillations per minute. Medium was aspirated and 200 µL of methanol was added to the cells and plates were shaken for 20 min. Absorbance was measured using TECAN Infinite F50 absorbance plate reader at 570 nm. Experiments were repeated three times and samples were conducted in triplicates.

3.2.1.4 Bromodeoxyuridine (BrdU) assay

BrdU assay was used as another way to study cell proliferation. For this purpose, isoDIPG-010 and isoDIPG-012 cells were seeded at a concentration of 50 000 cells/mL under spheroid conditions in a 96-well plate. Cells were incubated at 37°C. After 0 h, 12 h, 24 h, 48 h, 72 h, 96 h and 120 h cells were incubated with BrdU labeling solution (**Table 10**) at 37°C for 8 h. Medium was aspirated and cells were dried at 60°C overnight. The next day FixDenat (**Table 10**) was added to the cells and incubated at RT for 30 min. After removal of the solution, cells were incubated with anti-BrdU-POD working solution (**Table 10**) at RT for 90 min. Cells were then rinsed three times with 1xPBS and incubated with substrate solution (**Table 10**) at RT for 5 min. Absorbance was measured using TECAN Infinite F50 absorbance plate reader at 450 nm. Experiments were repeated three times and samples were conducted in triplicates.

3.2.1.5 Sphere formation assay

To investigate the effect of H3.3K27M-mutation and siRNA-mediated transfection or inhibitor treatment on stem cell-like properties, isoDIPG-010 and isoDIPG-012 cells were seeded under spheroid conditions (in TSM work) at a concentration of 5000 cells/mL in a 12-well plate. After six days, 10% fetal calf serum (FCS) was added and cells were incubated for another 6 h. After incubation time, 10x crystal violet staining solution (**Table 9**) was added to the cells and incubated for 20 min at RT, gently shaking. Wells were then washed with water and dried at 37°C overnight. Taken photos were analyzed using ImageJ tool "Particle Analyzer" (Schneider et al. 2012). Experiments were repeated three times.

3.2.1.6 Colony formation assay

To study the effect of H3.3K27M-mutation and siRNA-mediated transfection or inhibitor treatment on clonogenicity, isoDIPG-010 and isoDIPG-012 cells were seeded under differentiating conditions (with 10% FCS) at a concentration of 5000 cells/mL in a 12-well plate. After seven days, 10x crystal violet staining solution (**Table 9**) was added to the cells and incubated for 20 min at RT, gently shaking. Wells were then washed with water and dried in the incubator at 37°C overnight. Taken photos were analyzed using ImageJ tool "ColonyArea" (Schneider et al. 2012). Experiments were repeated three times.

3.2.1.7 Migration and invasion assays

To study migration and invasion abilities of isoDIPG-010 and isoDIPG-012 cells, with and without inhibitor treatment or after siRNA-mediated knockdown, migration and invasion assays were performed. To this end, cells were seeded at a density of 500 000 cells/mL in a 6-well plate. After 48 h of preincubation, 100 000 cells/mL were distributed among wells of the adapted Boyden chamber (**Table 7**) using membranes with 8 µm pores, and incubated for 8 h at 37°C. To attract cells to migrate or invade, medium without growth factors (EGF and FGF) was used. For invasion assay, ECM was added to create a matrix for the cells to invade through. After 8 h of incubation, membranes were stained with crystal violet solution (**Table 9**) for 20 min at RT, washed three times with PBS, air-dried and analyzed using ImageJ (Schneider et al. 2012).

3.2.1.8 Fluorescence-Activated Cell Sorting (FACS)

To investigate the effect of CBP/p300 and BET proteins inhibition on cell cycle phase distribution of DIPG cells, fluorescence-activated cell sorting (FACS) analysis was performed. To this end, isoDIPG-010 and isoDIPG-012 cells were seeded at a density of 500 000 cells/mL in 10 cm^3 dishes and treated with 2 mM thymidine to prevent DNA synthesis and S phase progression. After 24 h, cells were distributed to different dishes for the respective treatment and subsequently incubated for another 24 h. Following the treatment cells were collected by centrifugation, lysed (0.1% sodium citrate, 0.1% Triton-X 100 in dH_20) and stained with propidium iodide staining solution (0.1% sodium citrate, 0.1% Triton-X 100, 100 µg/mL PI in dH_20) for 2 h at 4°C. After measurements data was analyzed using flowing software (University of Turku).

3.2.2 Molecular biology

3.2.2.1 CRISPR/Cas9 transfection

In order to introduce H3.3K27M-mutation to VUMC-DIPG-010 (originally H3-wildtype) and to remove it from HSJD-DIPG-012 (originally carrying H3.3K27M-mutation), CRISPR/Cas9 system was used (**Table 19**).

Table 19| **Ingredients used in the present study to perform CRISPR/Cas9 editing**

Ingredient	REF number	Manufactured	Place of origin
Alt-R CRISPR-Cas9 gRNA	1072533	IDT	Coralville, USA
Alt-R S.p. Cas9 D10A Nickase V3	1081062	IDT	Coralville, USA
Alt-R HDR Enhancer	1081072	IDT	Coralville, USA
Lipofectamine RNAiMAX	13778100	Invitrogen	Waltham, USA

Native bacterial CRISPR system in *S. pyogenes* required Alt-R CRISPR-Cas9 gRNA (guide RNA) providing high editing potency (**Figure 7**). 10 µM RNA oligos diluted in nuclease free duplex buffer were stored at -20°C. To form the RNP complex, 10 µL of 10 µM Alt-R CRISPR-Cas9 gRNA, 3.2 µL Alt-R S.p. Cas9 D10A nickase V3 inducing single-stranded breaks in order to reduce off-target effects and promoting homology-directed repair (HDR) were diluted in 88.4 µL PBS and stored at 4°C.

In order to generate isogenic cell lines, reverse transfection of the RNP complex was performed in a 96-well plate. For each well of a 96-well plate 3 µL of each RNP complex, 3 µL of each

enzyme, 1.5 µL of 2 nM HDR template and 11.5 µL of Opti-MEM were mixed and incubated for 5 min at RT. Finally, 25 µL of the incubation mix was mixed with 0.6 µL of lipofectamine RNAiMAX and 24.4 µL of Opti-MEM. Cells at a density of 50 000 cells/mL diluted in a complete medium without antibiotics were then added to the transfection complexes. To enhance homology-directed repair, 20 µM HDR enhancer was added to the mix. The plate was incubated at 37°C for 48 h. 12 h after transfection medium volume was doubled to reduce toxicity of the transfection reagent. After transfection was complete, single cells were isolated and cultured until they grew in colonies.

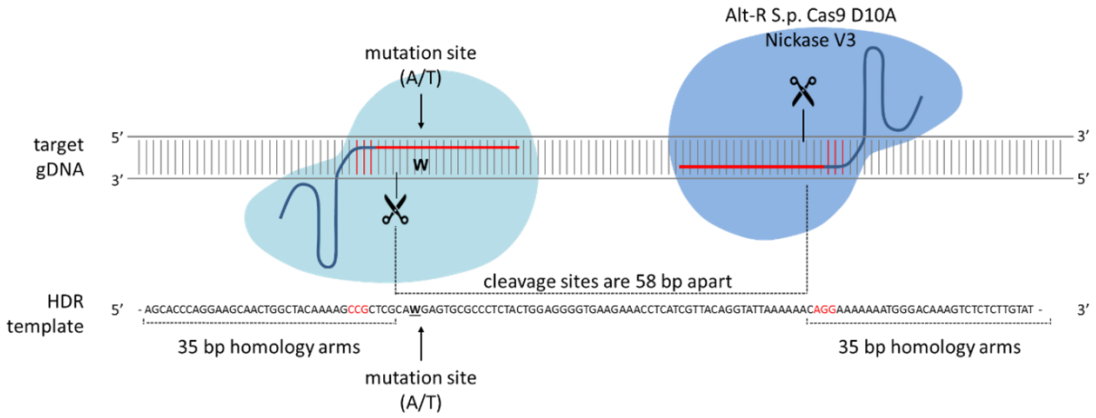

Figure 7 | CRISPR/Cas9 approach to generate isogenic cell lines.
To introduce and remove the H3.3K27M-mutation to VUMC-DIPG-010 and from HSJD-DIPG-012 respectively, the RNP reverse transcription was performed. The RNP complex contained of gRNA, nickase V3 and lipofectamine RNAiMAX diluted in OptiMEM.

3.2.2.2 siRNA-mediated transfection

In order to achieve knockdown of BRD2, BRD3, BRD4, CBP and p300 in isoDIPG-012 and isoDIPG-010 cell lines, spheroid cells were seeded at a density of 50 000 cells/mL using complete medium without antibiotics and immediately transfected with a control siRNA and a pool of four siRNAs targeting BRD2, BRD3, BRD4, CBP or p300, respectively (**Table 16**) at a final concentration of 30 nM. siRNA transfection was performed using Lipofectamine 3000. For each well of a 6-well plate 2.5 µL of each siRNA pool (75 pmol final) and 3.5 µL Lipofectamine 3000 were separately diluted in 250 µL OptiMEM. After 5 min incubation, both solutions were mixed together and incubated for 20 min. The incubation mix (500 µL) was added to the plated cells. To reduce cell toxicity caused by transfection reagent, additional medium was added to double the volume after 12 h. The amount of siRNA, lipofectamine 3000 and OptiMEM were adjusted according to the used tissue culture format.

3.2.2.3 Isolation of nucleic acids

3.2.2.3.1 Isolation of genomic DNA

Genomic DNA isolation was achieved using a DirectPCR-Cell and proteinase K mix (**Table 8**) according to manufacturer's instructions. DNA was dissolved in dH_2O and concentration was measured using nanodrop-spectrophotometer (**Table 6**). DNA was stored at -20 °C.

3.2.2.3.2 Isolation of RNA

RNA isolation was conducted using the RNA isolation kit (**Table 10**) according to manufacturer's instructions. RNA was isolated from frozen cell pellets kept at -80°C. To avoid contamination of RNA with genomic DNA, isolated RNA was digested with DNaseI (**Table 11**) for 30 min. Quality and quantity of RNA were determined using nanodrop-spectrophotometer (**Table 6**) and agarose gel electrophoresis (**Table 6**), respectively.

3.2.2.3.3 Isolation of plasmid DNA from *E.coli*

Plasmid DNA was isolated from overnight *E.coli* bacterial suspensions (**3.2.3.1**). CloneJET PCR cloning kit (**Table 10**) was used for cloning procedures and ZR plasmid miniprep kit (**Table 11**) for isolation of plasmid DNA according to manufacturer's instructions. DNA was dissolved in dH_2O and stored at -20 °C.

3.2.2.4 Purification and extraction of nucleic acids from agarose gels

DNA fragments were extracted and purified from agarose gels using the nucleospin gel and PCR clean-up kit (**Table 10**) according to the manufacturer's instructions.

3.2.2.5 Amplification of nucleic acids

3.2.2.5.1 Detection of transcripts by Polymerase chain reaction (PCR)

For Sanger sequencing, transcript was examined by PCR using specific primers and the following cycling conditions:

95°C	12 min	
95°C	15 s	⎫
58°C	30 s	⎬ 40 x
72°C	30 s	⎭
72°C	10 min	

For analytical proposes a reaction was set up as follows:

1x Taq buffer, 2.5 mM $MgCl_2$, 0.2 µM primer each, 0.2 mM dNTPs each and 0.6 U HotStartTaq DNA polymerase (**Table 11**) in a final volume of 50 µL per reaction. 3 µL of genomic DNA (**3.2.2.3.1**) was used as template. dH_2O, instead of gDNA, served as negative control. Resulting products were analyzed on 1 % agarose gels.

Successful transformation (**3.2.2.6**) was verified by colony PCR using specific primers (**Table 14**) and the following cycling conditions:

95°C	3 min	
94°C	30 s	⎫
60°C	30 s	⎭ 25 x
72°C	10 min	

For analytical proposes a reaction was set up as follows:

1x Taq buffer, 1.5 mM $MgCl_2$, 0.2 µM primer each, 0.2 mM dNTPs each, 0.5 U HotStartTaq DNA polymerase (**Table 11**) and in a final volume of 20 µL per reaction. dH_2O served as a negative control. Resulting products were analyzed on 1 % agarose gel.

3.2.2.5.2 Synthesis of copy DNA (cDNA)

RNA samples were used to synthesize cDNA using the RevertAid first strand cDNA synthesis kit (**Table 10**) according to manufacturer's instructions. Briefly, 2000 ng of single stranded RNA derived from cell cultures was added to 3 pmol random hexamer primer in a total volume of 13 µl. Of these, 1 µL served as minus RT control to ensure lack of genomic DNA contamination. After initial sample incubation at 65°C for 5 min, the following master mix was added to a final volume of 20 µL: 5x reaction buffer, 20 U RiboLock RNase inhibitor, 10 mM dNTPs, 200 U RevertAid M-MuLV RT. Samples were incubated for 5 min at 25°C, followed by 60 min at 42°C and 5 min at 70°C. Resulting cDNA was stored at -20°C.

3.2.2.5.3 Quantitative real-time PCR (qPCR)

Quantitative real-time polymerase chain reaction (qPCR) was used to confirm the siRNA knockdown of BRD2, BRD3, BRD4, CBP and p300, and to investigate transcription of specific mRNAs oligonucleotides. qPCR was performed using Blue S'Green qPCR kit separate ROX (**Table 10**) according to the manufacturer's instructions. In a total volume of 10 µL per sample, 15 ng of cDNA and 0.4 µM of each primer (**Table 13**) were used. Samples were amplified in standard cycling conditions (primer Tm ≥ 60°C). The amount of PCR product per cycle was measured using the Applied Biosystems' 7900HT Fast Real-Time PCR system (**Table 6**). Relative gene expression was calculated using $2^{-\Delta\Delta Ct}$ (Fleige and Pfaffl 2006). β-actin was used as a housekeeping gene.

3.2.2.6 Molecular cloning

Purified DNA transcripts amplified by PCR (**3.2.2.5.1**) for subcloning into pJET2.1 (**3.1.8**) according to manufacturer's instructions. Resulting ligation reaction was used for transformation of competent *E. coli* (**3.2.3.1**). Successfully transformed bacterial colonies were checked using colony PCR (**3.2.2.5.1**) and purified DNA was used for Sanger sequencing (**3.2.2.7.1**).

3.2.2.7 Sequencing

3.2.2.7.1 Sanger sequencing

In order to verify successfully generated CRISPR/Cas9 clones, Sanger sequencing was used. Each clone's isolated DNA (**3.2.2.3.1**) was amplified (**3.2.2.5.1**) using specific primers (**Table 14**). Transcripts had been subcloned (**3.2.2.6**) into pJET2.1 and 400 ng of purified DNA from each *E.coli* clone was used for sequencing reaction as follows: 0.80 µL Ready Reaction PreMix, 2 µL BigDye sequencing buffer, 10 µM primer in a final volume of 10 µL per reaction. Sequencing reaction was performed under following cycling conditions:

96°C	1 min	
96°C	10 s	⎤
60°C	4 min	⎦ 30 x

The PCR product was purified, pellet was resuspended in 10 µL formamide and sequenced using Genetic Analyzer 3500 (**Table 6**).

3.2.2.7.2 mRNA sequencing

To discover differentially regulated genes in isoDIPG-H3WT and isoDIPG-H3.3K27M cells, as well as upon inhibitor treatment or siRNA-mediated knockdown, isoDIPG-010 and isoDIPG-012 cells were seeded at a density of 50 000 cells/mL in a 6-well plate. After 48 h of incubation with inhibitors or knockdown, cells were collected and RNA was isolated from three independent biological replicates using RNA isolation kit (**Table 10**) according to manufacturer's instructions. Library preparation and sequencing analysis were performed by the Transcriptome and Genome Analysis Laboratory (TAL) – Microarray and Deep-Sequencing Facility Göttingen. Statistical evaluation of the sequencing results was carried out according to *Babelova et al.* in cooperation with Dr. Gabriela Salinas-Riester and Dr. Maren Sitte (NIG) (Babelova et al. 2015). The threshold values for the relevance of the corresponding genes were set as follows: for the relative difference in gene expression level (fold change, FC), FC ≤ 0.75 and FC ≥ 1.5 and a false discovery rate (FDR)-corrected p value of ≤ 0.05 was determined.

3.2.3 Microbiology

3.2.3.1 Generation of chemically competent *E.coli*

10 mL LB-medium (**Table 9**) was inoculated with 200 µL of an overnight *E. coli* suspension. Bacterial culture was incubated until an OD_{600} of 0.6 was reached. Bacterial suspension was incubated on ice for 10 min and afterwards centrifuged for 30 min at 4°C with 3000 rpm. Resulting pellets were resolved in 10 mL ice cold 100 mM $CaCl_2$ and incubated on ice for another 30 min. After another centrifugation step for 30 min at 4°C with 3000 rpm, *E. coli* pellets were resolved in 1 mL ice cold 100 mM $CaCl_2$, supplemented with 175 µL 86% glycerin. Aliquots of 100 µL competent bacterial suspensions were snap frozen in liquid nitrogen and stored at -80°C.

3.2.3.2 Transformation of *E.coli*

Plasmid DNA was introduced in *E. coli* bacteria using heat shock. 10 µL of ligation reaction (**3.2.2.6**) was added to 50 µL of chemically competent *E. coli* bacterial solution (**3.2.3.1**). After 30 min incubation on ice, the transformation mix was set to 42°C for 45 s. After the bacteria mix was cooled down on ice, 250 µL LB medium (without antibiotics) was added and incubated at 37°C and 300 rpm for 45 min. The mixture was then plated on LB agar plates and cultivated overnight at 37°C.

3.2.4 Biochemistry

3.2.4.1 Protein isolation and determination of protein concentration

3.2.4.1.1 Isolation of nuclear and cytoplasmic proteins for SDS-PAGE

To separate nuclear and cytoplasmic protein fractions, cell cultures grown in 10cm^3 dishes at a density of 50 000 cells/mL, 72 h after incubation, were centrifuged and cell pellets were either stored at -80°C or used immediately for protein isolation.

In order to isolate proteins, pelleted cells were resuspended in cellular extract (CE) buffer (**Table 9**), supplemented with 1x protease inhibitor cocktail (**Table 8**). Cells were centrifuged for 5 min at 1000 rpm and pellets were then resuspended in nuclear extract (NE) buffer (**Table 9**) supplemented with 1x protease inhibitor cocktail (**Table 8**). Salt concentration was adjusted by adding the corresponding amount of 5 M NaCl. Protein extracts were then sonicated for 15 s and incubated on ice for 30 min. After centrifugation for 5 min at 4°C supernatant was transferred to a new tube. Protein samples were stored at -80°C or immediately used for bicinchoninic acid (BCA) assay.

3.2.4.1.2 Bicinchoninic acid (BCA) assay

To determine concentration of proteins, bicinchoninic acid (BCA) assay (**Table 8**) was performed. Protein extracts were diluted in water (1 µL and 3 µL of protein extract) and added in duplicates onto a 96-well plate. 200 µL of BC assay working reagent (1:50 reagent A and reagent B) was added to each well and incubated for 30 min at 37°C. Formed purple complexes were measured at 563 nm by the BioTek SynergyMx microplate reader (**Table 6**). In order to determine protein concentration, a standard curve with BCA dilutions of known concentrations (0-30 µg) was used.

The appropriate amount of protein samples was diluted in NE buffer and 4x Laemmli-probe buffer (**Table 9**) to obtain a final protein concentration of 1 µg/µL. Proteins were denaturated by cooking for 5 min at 95°C and stored at -20°C or used immediately for SDS-PAGE.

3.2.4.2 Sodium dodecyl sulfate-polyacrylamide gel electrophoresis (SDS-PAGE) and western blot

To detect proteins of interest, protein samples were separated using sodium dodecyl sulfate-polyacrylamide gel electrophoresis (SDS-PAGE). Molecular weight of the proteins was determined with a pre-stained protein ladder (**Table 8**). Proteins were concentrated in the stacking gel (**Table 20**) at 60 V, followed by separation at 100 to 200 V.

Table 20| **Composition of polyacrylamide gels used for SDS-PAGE**

SDS-polyacrylamide gel	Composition
Stacking gel	12.5 % RotiphoreseR Gel 40 (29:1), 1x stacking buffer (UT), 0.1 % APS, 0.1 % TEMED
Separating gel	15 % 37.5 % RotiphoreseR Gel 40 (29:1), 1x separating buffer (LT), 0.1 % APS, 0.1 % TEMED

Separated proteins were transferred onto methanol-activated PVDF membranes by the wet blot system (**Table 6**). Blotting was performed for either 45 min at 500 mA (for smaller proteins) or 2 h at 200 mA (for bigger proteins). Membranes were then blocked with blocking solution (5% BSA or 5% milk) to avoid unspecific binding of the primary antibody and incubated overnight with primary antibody at 4°C with dilution according to the manufacturer's instructions. After membranes were washed 3 times with TBST, the horseradish peroxidase (HRP) coupled secondary antibody diluted in TBST with 5% milk or BSA. Membranes were incubated for 1 h at RT and washed again 3 times with TBST. Proteins bound to antibody-complexes were visualized after incubation with 1:1 (v/v) ECL solution A and B (**Table 9**). The resulting chemo-luminescent signals were detected with ChemoCam Imager (**Table 6**). Finally, membranes were washed with TBST to remove ECL solution residues and air-dried for storage at 4°C.

3.2.5 *In vivo* model systems

In order to investigate the role of H3.3K27M-mutation as well as CBP/p300 and BET proteins in DIPG *in vivo*, chick chorioallantoic membrane (CAM) assay was used.

3.2.5.1 Chick chorioallantoic membrane (CAM) assay

Specified pathogen-free (SPF) eggs defined as hatching eggs, which are derived from chicken flocks free from specified pathogens, were used to study the effect of specific CBP/p300 and BET proteins inhibitors on tumors *in vivo*. Eggs were incubated horizontally for 10 days prior

inoculation at 37 °C in a 60% humidified atmosphere with one hour scheduled rotation. At day 10-post fertilization, a hacksaw blade was used to make an approximate 1 cm^2 square incision on the eggshell under sterile conditions and the eggshell window fragment was removed to access the CAM beneath. Eggs were then further incubated without rotation. After 7 days of incubation, total amount of 3 million 48 h pre-stimulated cells mixed with Matrigel (total volume of 35 µL) was added onto the scored CAM. One tumor was implanted per embryo. Chick embryos were gently placed back into the incubator and maintained at 37°C for further 7 days. Tumors were harvested from CAM and stored in 4% PFA at RT overnight before being embedded in paraffin for subsequent microtome sectioning.

3.2.6 Statistics

Experiments were performed using three independent biological replicates unless stated otherwise. Results obtained from the replicates were summarized as mean ± standard error of the mean (SEM). Data were compared by student's t-test using Microsoft Excel or GraphPad Prism; p values < 0.05 were considered to be statistically significant with the subsequent mode of further semi quantitative description: */# $p < 0.05$; **/## $p < 0.01$; ***/### $p < 0.005$; ****/#### $p < 0.001$.

4 Results

Recent genomic studies have revealed that around 85% of all diffuse intrinsic pediatric gliomas (DIPG) carry a heterozygous point mutation in one histone 3 (H3) variant, either in H3.3 (encoded by *H3F3A*) or, less frequently, in H3.1 (encoded by *HIST1H3B/C*) which both result in a lysine (K) to methionine (M) substitution (H3K27M) (Lewis et al. 2013). H3.3K27M-mutation influences global chromatin changes with hypotrimetylation and hyperacetylation at H3K27 (Castel et al. 2015). Epigenetic disruption is often associated with promoting tumorigenesis (Lu et al. 2020). This imbalance in the epigenetic landscape is thought to be a reason for the observed malignant phenotype of DIPG (Castel et al. 2018). To find out if H3.3K27M-mutation contributes to the malignant phenotype observed in DIPG, isogenic cell lines with and without H3.3K27M-mutation were generated using CRISPR/Cas9 and analyzed with regard to their tumor-biological characteristics, gene expression pattern and epigenetic landscape.

The observed hyperacetylation in H3.3K27M-DIPG cells suggests that acetylation-associated proteins might play a more prominent role compared to H3WT-DIPG cells. Indeed, epigenetic readers that set and writers that recognize acetylation marks at histones, respectively, such as CREB-binding protein (CBP/p300) and epigenetic reader bromodomain and extraterminal domain (BET) proteins, have been proven to play a significant role in tumor malignancy, oncogenesis and tumor development (Wang et al. 2013; Pastori et al. 2014; Wiese et al. 2020). Moreover, treatment with BET proteins inhibitor JQ1 resulted in reduction of different tumor characteristics in DIPG cells (Piunti et al. 2017). These findings indicate that CBP/p300 as well as BET proteins may indeed play an important role in the aggressive tumor phenotype observed in DIPG patients.

In order to investigate the reader function of CBP/p300 and BET proteins in H3WT-DIPG and H3.3K27M-DIPG cells, treatment with CBP30 and OTX-015, respectively, had been carried out. To unravel the writer function of CBP/p300 in dependence on H3-mutation status in DIPG cells, histone acetyltransferase (HAT) inhibitor A-485 was used. Finally, to be able to distinguish different functions of BRD2, BRD3 and BRD4, as well as CBP and p300 from one another, siRNA-mediated knockdown of the proteins of interest was carried out. Obtained results from CBP/p300 and BET proteins inhibition and knockdown were compared with each other with regard to tumor-biological and gene regulatory effects in isoDIPG cells with and without H3.3 K27-mutation.

4.1 Impact of H3.3K27M-mutation in diffuse intrinsic pontine gliomas (DIPG)

The majority of DIPG is characterized by presence of H3.3K27M-mutation (Lewis et al. 2013) which results in global chromatin changes with hypotrimetylation and hyperacetylation at H3K27 (Castel et al. 2015). To be able to identify epigenetic and tumor-biological changes in DIPG cells caused by H3.3K27M-mutation within the same cellular and genetic background, isogenic DIPG cell lines were generated using CRISPR/Cas9 system and were analyzed with regard to the tumor-biological characteristics and gene regulatory effects *in vitro* and *in vivo*.

4.1.1 H3.3K27M-mutation is responsible for decreased H3K27me3 and elevated H3K27ac levels in isoDIPG cells

To investigate if the aggressive phenotype of DIPG indeed depends on the dominant H3.3K27M-mutation within the same cellular and molecular background, DIPG cell clones with and without H3.3K27M-mutation and had been generated using CRISPR/Cas9 technology. To this end, H3.3K27M-mutation was introduced to originally H3-wildtype (H3WT) VUMC-DIPG-010 cells and removed from originally H3.3K27M-mutated (H3.3K27M) HSJD-DIPG-012 cell line (**Figure 8A**).

Out of six examined VUMC-DIPG-010 clones which originally carried an H3WT allele, three clones were successfully genetically edited, exhibiting presence of H3.3K27M-mutation as proven by Sanger sequencing (**Figure 8B**) and corresponsing western blot analyses of histone marks at H3K27 (**Figure 8C; Appendix A**). Introduction of H3.3K27M-mutation resulted in loss of H3K27me3 and gain of H3K27ac as depicted by western blot (**Figure 8C and 8D; Appendix A**).

In opposite, out of six examined originally H3.3K27M-mutated HSJD-DIPG-012 clones, three did not show presence of H3.3K27M-mutation after CRISPR/Cas9 transfection (**Figure 8B and 8C**). Loss of H3.3K27M-mutation was associated with an increase of H3K27me3 and decreased levels of H3K27ac compared to unsuccessfully engineered HSJD-DIPG-012 cells with H3.3K27M-mutation (**Figure 8C and 8D; Appendix A**)**.**

H3.3K27M-mutated isogenic DIPG cells were herein referred to as isoDIPG-H3.3K27M cells (isoDIPG-010-H3.3K27M and isoDIPG-012-H3.3K27M) and H3WT carrying isogenic DIPG cells as isoDIPG-H3WT cells (isoDIPG-012-H3WT and isoDIPG-010-H3WT).

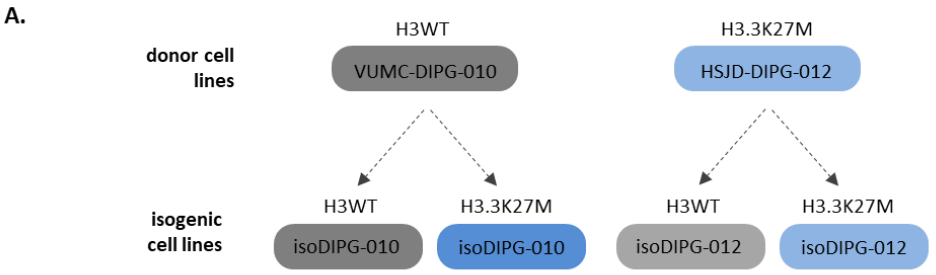
A.
donor cell lines
H3WT
VUMC-DIPG-010
H3.3K27M
HSJD-DIPG-012
isogenic cell lines
H3WT
H3.3K27M
isoDIPG-010
isoDIPG-010
H3WT
H3.3K27M
isoDIPG-012
isoDIPG-012

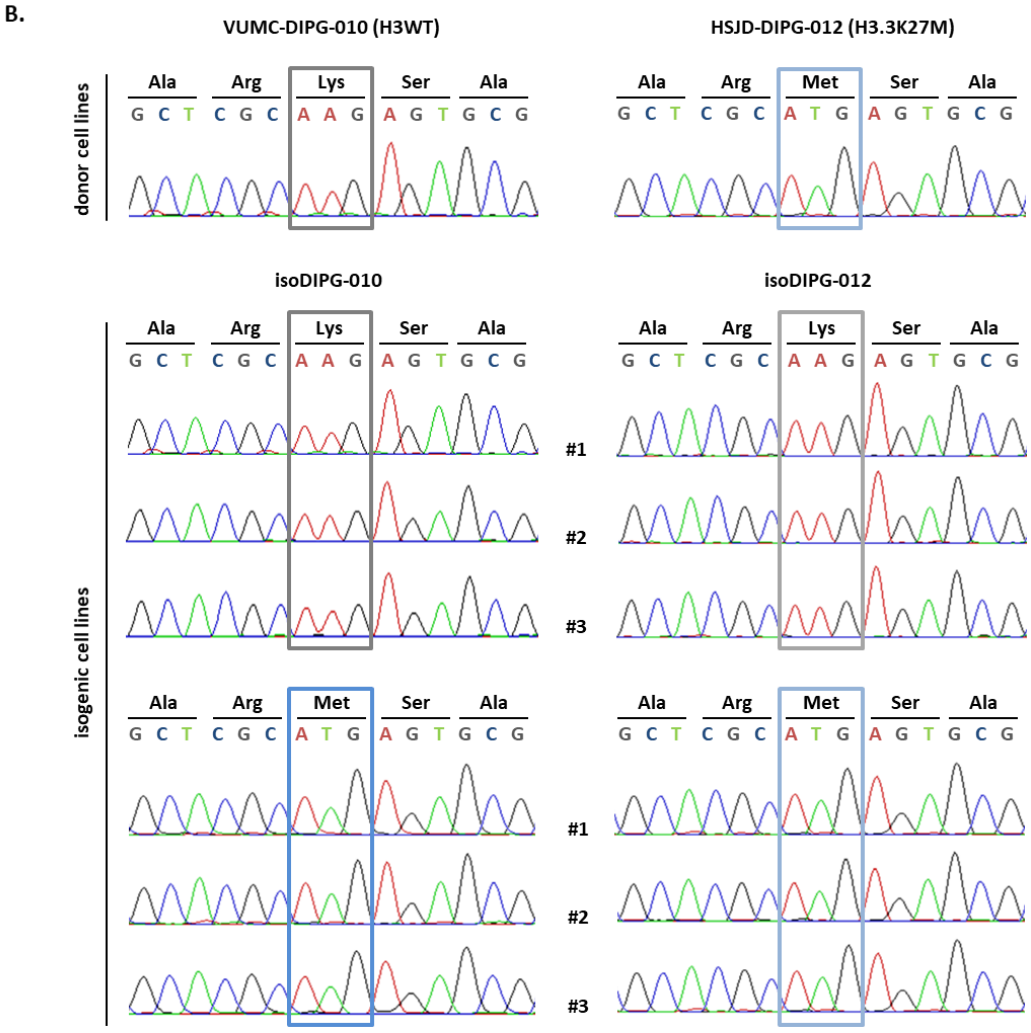
B.
VUMC-DIPG-010 (H3WT)
HSJD-DIPG-012 (H3.3K27M)
donor cell lines
Ala Arg Lys Ser Ala
G C T C G C A A G A G T G C G
Ala Arg Met Ser Ala
G C T C G C A T G A G T G C G
isoDIPG-010
isoDIPG-012
isogenic cell lines
#1
#2
#3
#1
#2
#3

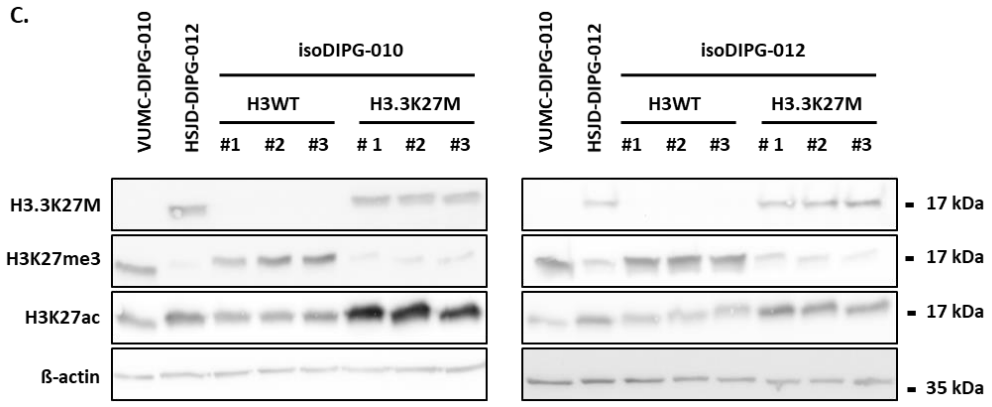
C.
VUMC-DIPG-010
HSJD-DIPG-012
isoDIPG-010
H3WT
H3.3K27M
#1 #2 #3 # 1 #2 #3
VUMC-DIPG-010
HSJD-DIPG-012
isoDIPG-012
H3WT
H3.3K27M
#1 #2 #3 # 1 #2 #3
H3.3K27M
H3K27me3
H3K27ac
ß-actin
17 kDa
17 kDa
17 kDa
35 kDa

Figure 8 | Efficiently generated CRISPR/Cas9 DIPG cells reflect molecular and epigenetic features observed in unmodified H3K27M-DIPG and H3WT-DIPG cells, respectively.
CRISPR/Cas9-mediated gene editing of VUMC-DIPG-010 cells, originally H3WT, and H3.3K27M-mutated HSJD-DIPG-012 cells resulted in four different cell lines used for further studies. (B) Presence of H3.3K27M-mutation and H3WT was evaluated using Sanger sequencing and (C) western blot analyses with specific antibodies against H3K27M-mutation, H3K27me3 and H3K27ac. ß-actin served as a loading control.

In summary, CRISPR/Cas9 technology was used to successfully generate isogenic DIPG cell lines with and without H3.3K27M-mutation. Created isoDIPG-H3.3K27M cells resembled loss of H3K27me3 and gain of H3K27ac commonly observed in non-engineered H3.3K27M-DIPG cells. Removal of H3.3K27M-mutation from originally H3.3K27M-DIPG cells reversed the observed phenotype: restored H3K27me3 and reduced H3K27ac levels.

4.1.2 H3.3K27M-mutation is responsible for enhanced tumor-related biological characteristics in isoDIPG cells

Previous studies showed that H3.3K27M-DIPG cells exhibit increased cell viability, proliferation and clonogenicity under stemness and differentiating conditions (Wiese et al. 2020). H3.3K27M-DIPG cells were also proven to display higher migration and invasion levels compared to H3WT-DIPG cells (Cockle et al. 2015; Kluiver et al. 2020).

To examine if H3.3K27M-mutation leads to increased tumor-associated biological characteristics of the isogenic DIPG cell clones, cell viability and cell proliferation were assessed using 3-(4.5-Dimethylthiazol-2-yl)-2.5-diphenyltetrazolium bromide (MTT) assay (**Figure 9A**), crystal violet (CV) staining (**Figure 9B**) and bromodeoxyuridine (BrdU) assay (**Figure 9C**) after 24 h, 72 h and 120 h after seeding.

Introduction of H3.3K27M-mutation significantly increased cell proliferation and cell viability of isoDIPG-010-H3.3K27M clones to a comparable level of originally H3.3K27M-mutated HSJD-DIPG-012 cells compared to isoDIPG-010-H3WT control cells, while removal of H3.3K27M-mutation from HSJD-DIPG-012 cells caused decrease in cell proliferation and cell viability levels of isoDIPG-012-H3WT clones to a comparable level observed in original H3WT VUMC-DIPG-010 cells (**Figure 9A, 9B and 9C**).

Brightfield (**Figure 9D**) confirmed these results obtained from proliferation assays (**Figure 9A-C**). DIPG cells carrying H3.3K27M-mutation formed larger neurospheres on day 3 and day 5 after seeding compared to their H3WT counterparts.

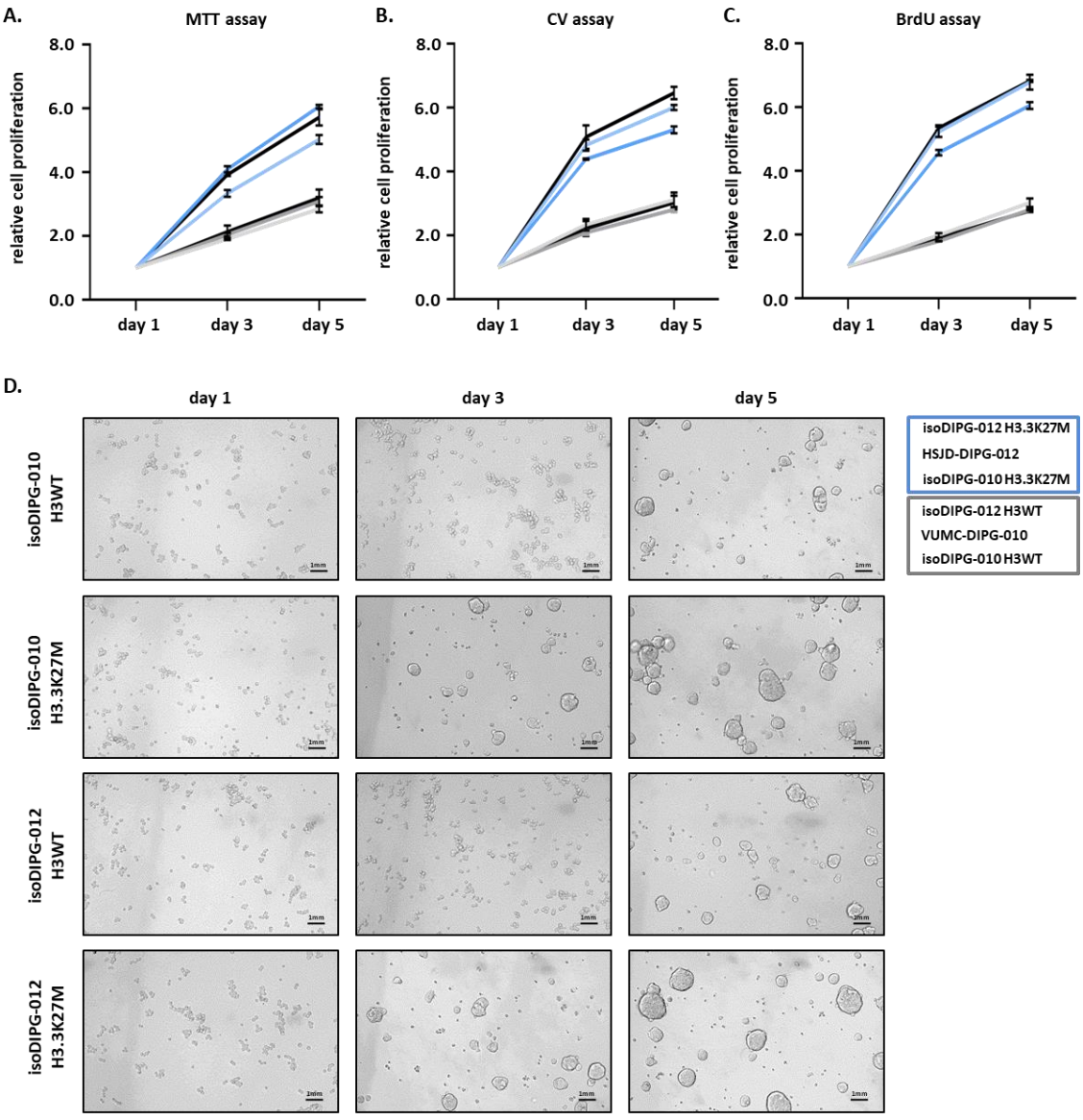

Figure 9 | H3.3K27M-mutation in isoDIPG cells leads to strong cell viability and proliferation potential.
Cell viability and cell proliferation of isoDIPG cells assessed by (A) MTT, (B) CV and (C) BrdU assays were determined after day 1, day 3 and day 5 after seeding and normalized to time point day 1. (D) Representative brightfield microscopy images of proliferating cells were taken at indicated time points. Bar size 1 mm.

To address clonogenicity and stem cell-like properties of isoDIPG cells, sphere formation (**Figure 10A**) and colony formation (**Figure 10B**) abilities were assessed.

Introduction of H3.3K27M-mutation into originally H3-wildtype DIPG cells led to around 4-fold increase of colony and sphere formation ability compared to isoDIPG-H3WT cells. Removal of H3.3K27M-mutation from originally H3.3K27M-mutated DIPG cells resulted in around 4-fold decrease of colony and sphere formation abilities compared to isoDIPG-H3.3K27M cells (**Figure 10A and 10B**). In line with these results, expression of stemness markers OCT4 (*POU5F1*), SOX2 and Nanog was elevated in isoDIPG-H3.3K27M cells compared to isoDIPG-H3WT cells on protein

level determined by western blot analyses (**Figure 10C; Appendix B**), as well as on mRNA level assessed by qPCR (**Figure 10D**).

Interestingly, expression of the stemness markers PAX6 and CD133 was found to be increased on protein level in isoDIPG-H3WT cells compared to isoDIPG-H3.3K27M cells (**Figure 10C; Appendix B**). However, on mRNA level, CD133 (*PROM1*) was found to be elevated in isoDIPG-H3.3K27M cells when the mutation had been introduced and in isoDIPG-H3WT cells when the mutation had been removed (**Figure 10D**). Moreover, expression of Nestin and GFAP was upregulated in isoDIPG-H3.3K27M compared to isoDIPG-H3WT cells on protein (**Figure 10C; Appendix B**) and mRNA (**Figure 10D**) level. Altogether, these results point out to a crucial role of H3.3K27M-mutation in regulation of stemness-associated genes and stem cell-like characteristics in DIPG cells.

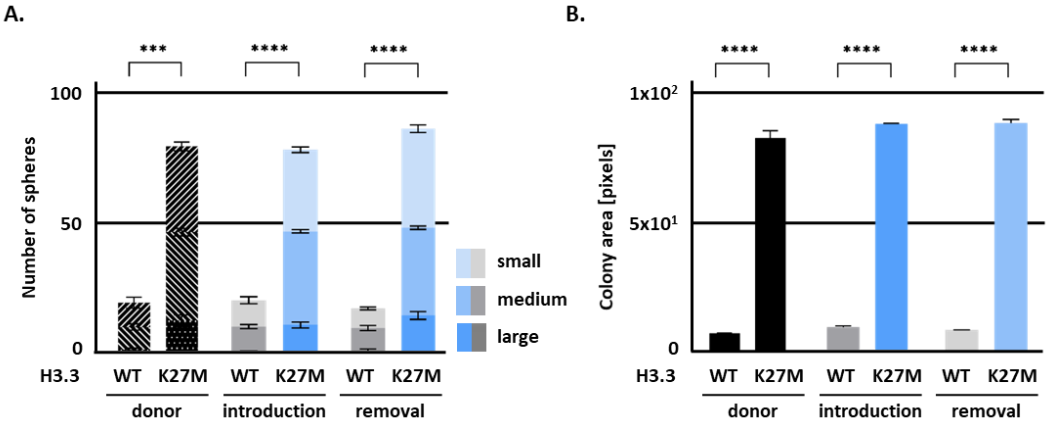

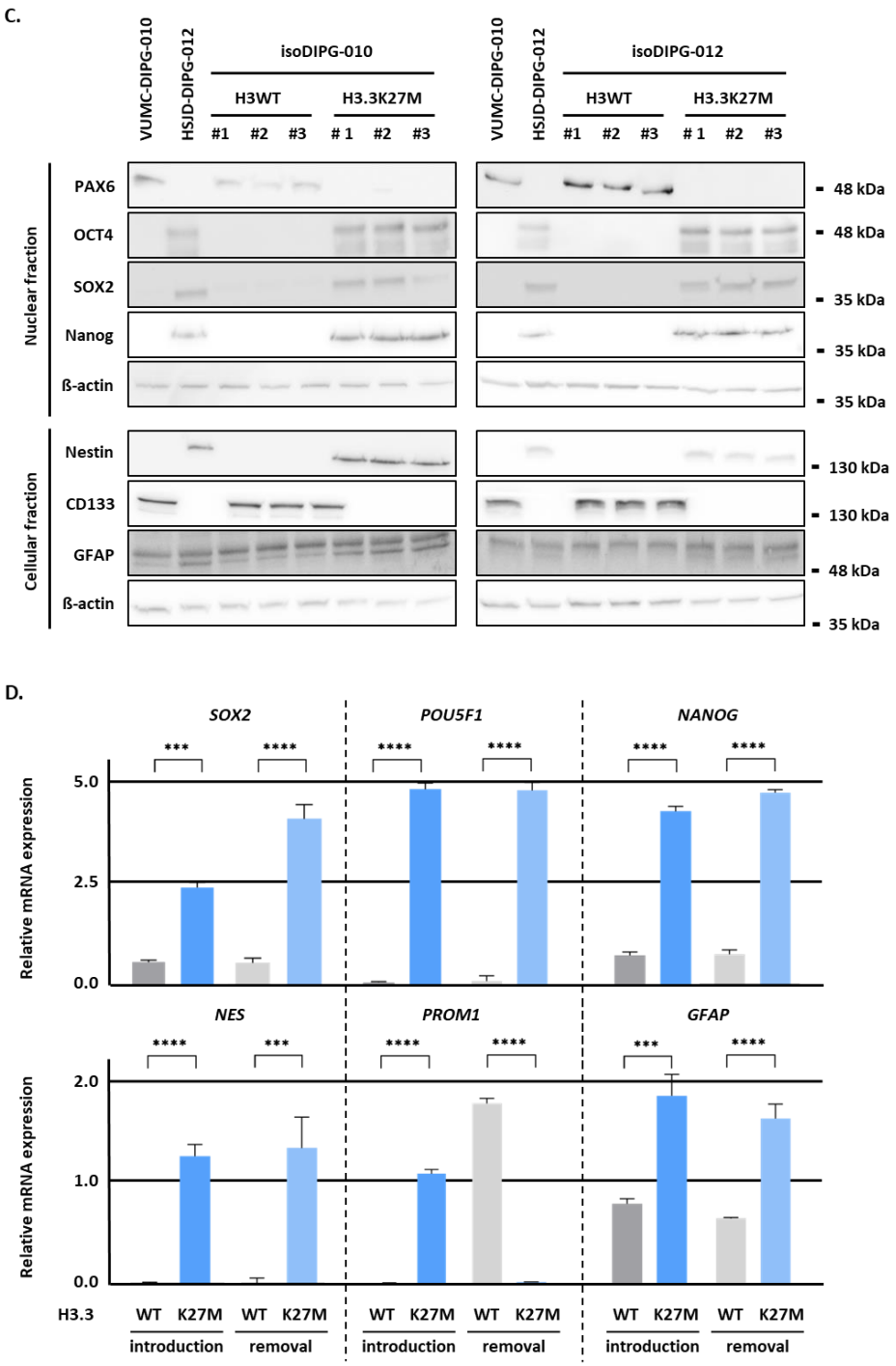

Figure 10 | isoDIPG cells carrying H3.3K27M-mutation show increased stem cell-like properties and elevated levels of selected stemness markers.

Sphere formation ability of isoDIPG cells was evaluated after 6 days of incubation cultured under spheroid conditions. Spheres were distinguished according to their size as small (50 – 100 µm), medium (100 – 300 µm) and large (> 300 µm). (B) Colony formation assay was evaluated after 7 days of incubation under monolayer conditions. (C) Western blot analyses were performed using specific antibodies for stemness markers as indicated. ß-actin served as loading control. (D) Expression of stemness markers on mRNA level was investigated using qPCR and normalized to ß-actin. * $p < 0.05$; ** $p < 0.01$; ***$p < 0.005$; ****$p < 0.001$.

The ability of tumor cells to infiltrate into surrounding tissue is an important characteristic of the aggressive tumor phenotype observed in DIPG. To address migratory and infiltrative properties of isoDIPG-H3WT and isoDIPG-H3.3K27M cells, migration (**Figure 11A**) and invasion (**Figure 11B**) assays were performed.

Introduction of H3.3K27M-mutation into originally H3-wildtype DIPG cells resulted in around 4-fold increase of migration (**Figure 11A**) and invasion (**Figure 11B**) abilities compared to isoDIPG-H3WT cells. While removal of H3.3K27M-mutation from originally H3.3K27M-mutated DIPG cells resulted in around 4-fold decrease in their migratory and infiltrative abilities compared to isoDIPG-H3.3K27M cells (**Figure 11A and 11B**). In line with these results, expression of mesenchymal markers ZEB1, Vimentin and MMP9 was elevated in isoDIPG-H3.3K27M cells compared to isoDIPG-H3WT cells on protein level (**Figure 11C; Appendix C**), as well as on mRNA level (**Figure 11D**). Interestingly, expression of N-cadherin (*CDH2*) was significantly increased on mRNA-level in isoDIPG-H3WT compared to isoDIPG-H3.3K27M cells (**Figure 11D**), while on protein level its expression remained unchanged (**Figure 11C; Appendix C**). Furthermore, the epithelial marker E-cadherin (*CDH1*) was elevated in isoDIPG-H3.3K27M cells compared to isoDIPG-H3WT cells on protein (**Figure 11C; Appendix C**), as well as on mRNA level (**Figure 11D**)**.**

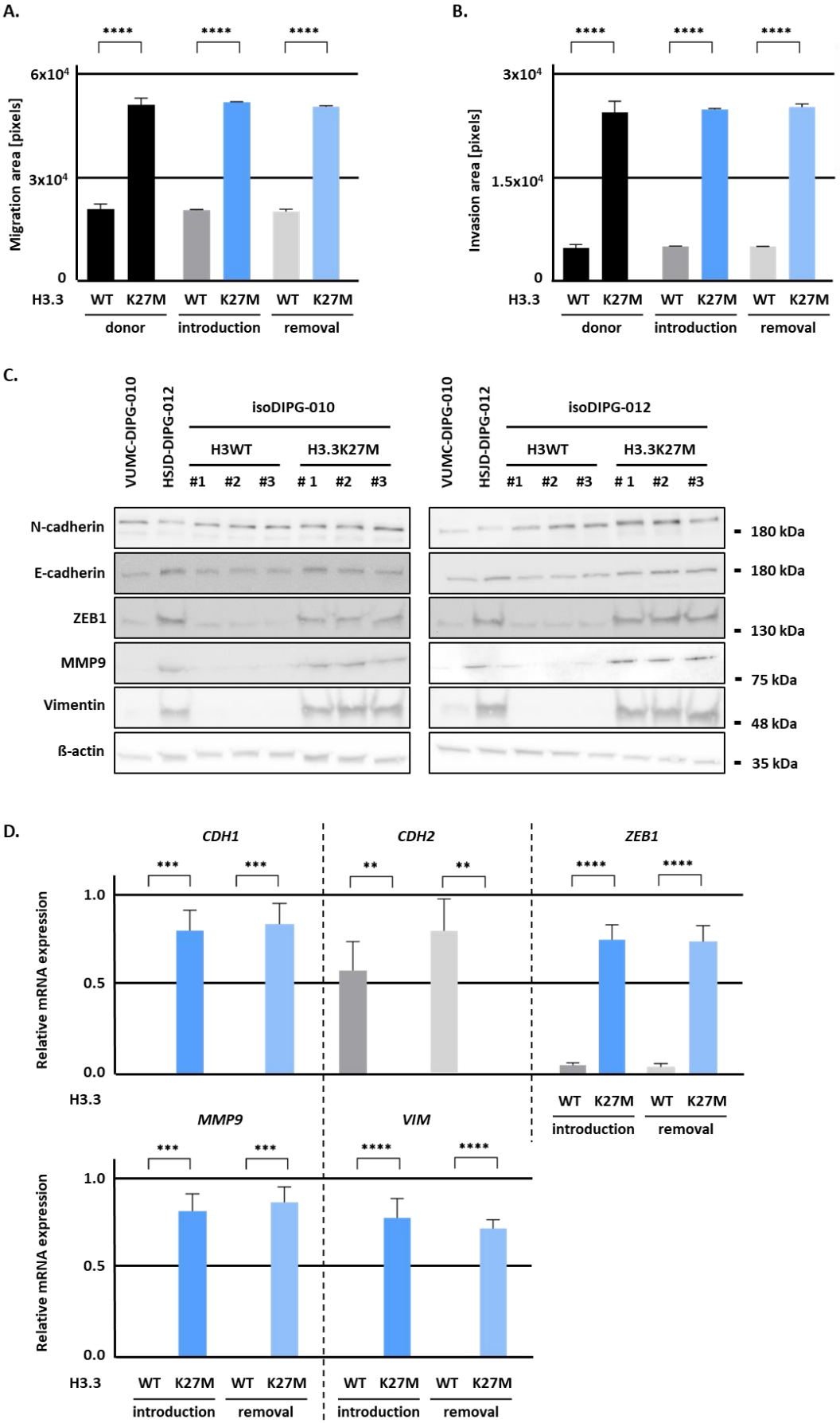
A.
B.
Migration area [pixels]
Invasion area [pixels]
H3.3
WT K27M WT K27M WT K27M
donor
introduction
removal
C.
VUMC-DIPG-010
HSJD-DIPG-012
isoDIPG-010
isoDIPG-012
H3WT
H3.3K27M
#1 #2 #3 # 1 #2 #3
N-cadherin
E-cadherin
ZEB1
MMP9
Vimentin
ß-actin
180 kDa
180 kDa
130 kDa
75 kDa
48 kDa
35 kDa
D.
CDH1
CDH2
ZEB1
MMP9
VIM
Relative mRNA expression

Figure 11 | H3.3K27M-mutation in isoDIPG cells led is associated with increased invasiveness. (A) Migration and (B) invasion assays, as well as (C) western blot analyses using specific antibodies for mesenchymal markers as indicated. ß-actin served as a loading control (D) Expression of mesenchymal markers on mRNA level was investigated using qPCR and normalized to ß-actin. * $p < 0.05$; ** $p < 0.01$; ***$p < 0.005$; ****$p < 0.001$

In summary, introduction of H3.3K27M-mutation to originally H3-wildtype DIPG cells led to a significant increase of cell viability and proliferation as well as the ability to form spheres and colonies with an elevated expression of stemness markers compared to isoDIPG-H3WT cells. isoDIPG-H3.3K27M cells exhibited also significantly higher levels of migration and invasion abilities associated with increased expression of mesenchymal markers. Whereas removal of H3.3K27M-mutation from originally H3.3K27M-mutated DIPG cells led to reduction of cell proliferation, clonogenicity and invasive phenotype compared to isoDIPG-H3.3K27M cells. These findings strongly support the hypothesis that H3.3K27M-mutation may indeed essentially contribute to the aggressive tumor phenotype observed in isoDIPG-H3.3K27M cells.

4.1.3 Presence of H3.3K27M-mutation affects expression of different epigenetic histone modifications in isoDIPG cells

It is well known that H3.3K27M-mutation affects H3K27ac and H3K27me3 levels (Bender et al. 2013; Castel et al. 2015). Recent studies suggested that also other histone modifications that are dependent on presence of H3.3K27M-mutation might be relevant for epigenetic regulation in DIPG (Kumar et al. 2017; Vethantham et al. 2012; Yu et al. 2021; An et al. 2020; Foglizzo et al. 2018; Tamburri et al. 2020). In order to confirm already known or identify new H3.3K27M-mutation-dependent histone marks, western blot analyses were performed (**Figure 12; Appendix D**).

Histone modifications that are mainly associated with transcriptional repression (Benayoun et al. 2014; Tamburri et al. 2020; Martire et al. 2019); were reduced in isoDIPG-H3.3K27M cells compared to their wild type counterparts, including ubiquitination of lysine 119 of histone 2A (H2AK119ub), phosphorylation of serine 31 of histone 3.3 (H3.3S31p) and trimethylation of lysine 9 of histone 3 (H3K9me3).

In opposite, histone marks associated with active chromatin (An et al. 2020; Yu et al. 2021) were found to be elevated in isoDIPG-H3.3K27M cells, including trimethylation of lysine 4 of histone 3 (H3K4me3), dimethylation of lysine 36 of histone 3 (H3K36me2) and acetylation of histone 4 (H4ac) (An et al. 2020; Yu et al. 2021).

Acetylation of lysine 16 of histone 4 (H4K16ac) and trimethylation of lysine 36 of histone 3 (H3K36me3) are histone marks linked to activation and repression of transcription (Taylor et al. 2013; Su et al. 2020). Levels of H4K16ac were found to be decreased in isoDIPG-H3.3K27M cells, while H3K36me3 remained unaffected by presence of H3.3K27M-mutation in isoDIPG cells.

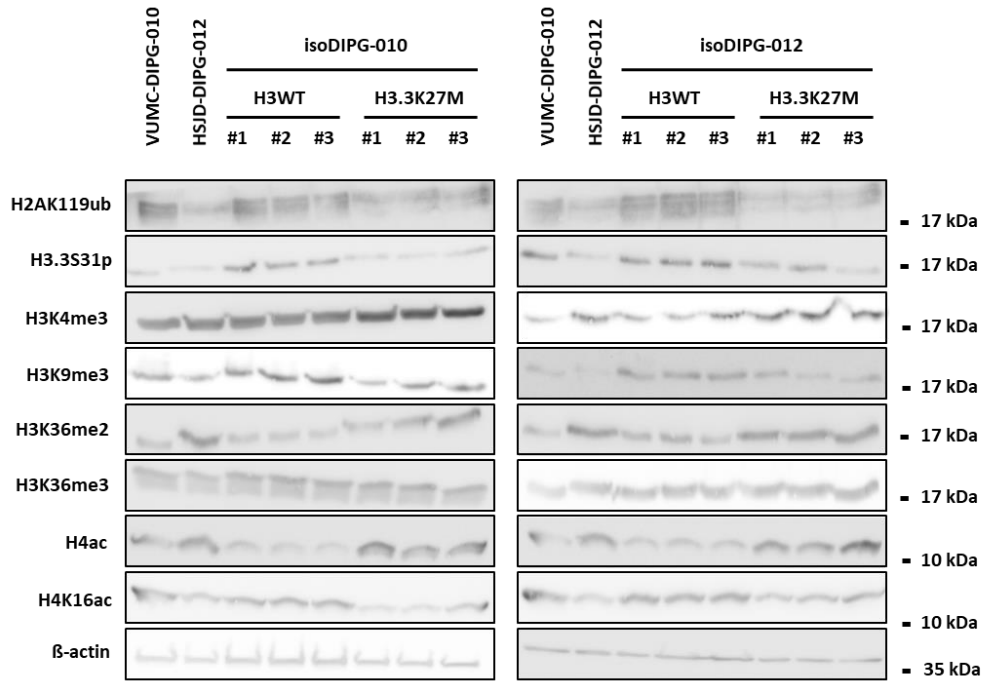

Figure 12 | H3.3K27M-mutation affects expression of different epigenetic histone modifications in isoDIPG cells.
Western blot analyses using specific antibodies for different histone modifications, as indicated. ß-actin served as loading control.

In summary, H3.3K27M-mutation displayed not only well-established effect on histone marks H3K27ac and H3K27me3, but also showed an interaction with several other epigenetic modifications, indicating an even more global epigenetic function of H3.3K27M-mutation in DIPG cells.

4.1.4 Presence of H3.3K27M-mutation affects expression of epigenetic key players in isoDIPG cells

Since presence of H3.3K27M-mutation is associated with hyperacetylation and hypotrimethylation of lysine 27 of histone 3 (Bender et al. 2013; Piunti et al. 2017), it could be assumed that H3.3K27M-mutation may also affect expression of different epigenetic key players involved in H3K27ac and H3K27me3, including histone acetyltransferases CBP and p300, H3K27 methyltransferase EZH2 or BET proteins that function as transcriptional activators. In order to investigate the expression of these epigenetically relevant proteins, western blot (**Figure13A; Appendix E**) and qPCR (**Figure13B**) analyses were performed. Upon introduction of H3.3K27M-

mutation CBP and p300 as well as BRD2, 3 and 4 expression was elevated, while deletion of H3.3K27M-mutation resulted in decreased expression of these proteins on both, mRNA (**Figure13B**) and protein (**Figure13A; Appendix E**) level. In addition, expression of EZH2 on mRNA and protein level (**Figure13A and 13B**) was strongly decreased in presence of H3.3K27M-mutation in isoDIPG cells.

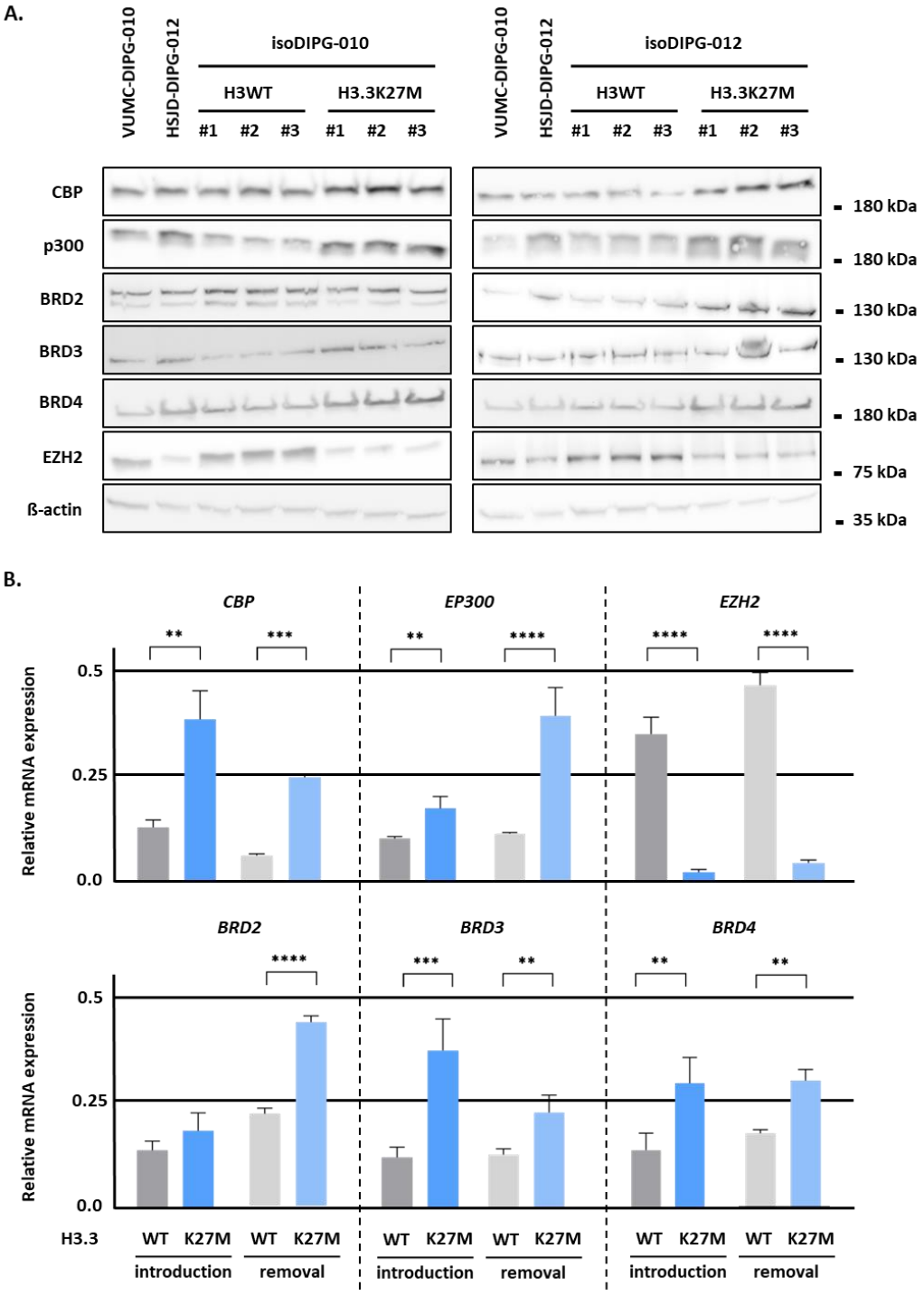

Figure 13 | H3.3K27M-mutation affects the expression of different epigenetic key players involved in H3K27 acetylation and trimethylation in isoDIPG cells.
(A) Western blot analyses using specific antibodies detecting different epigenetic proteins as indicated. ß-actin served as loading control. (B) Expression of epigenetic proteins on mRNA level was investigated using qPCR and normalized to ß-actin. * $p < 0.05$; ** $p < 0.01$; ***$p < 0.005$; ****$p < 0.001$

In summary, H3.3K27M-mutation appears to regulate expression of epigenetic key players involved in H3K27 acetylation and trimethylation in DIPG cells.

4.1.5 Irradiation affects stemness potential of H3.3K27M-mutated DIPG cells

Standard treatment strategy for DIPG patients includes chemotherapy using temozolomide (TMZ) combined with radiotherapy (Stupp et al. 2005). Irradiation is known to cause DNA damage (Fu and Phillips 1991) and is used to prevent tumor progression. However, especially stemness-like DIPG cells evade radiochemotherapy (Stupp et al. 2005).

To investigate the effect of irradiation on stem cell-like characteristics of DIPG cells, sphere formation assay was performed. In addition, western blot analyses were carried out to study the impact of irradiation on apoptosis. Irradiation led to an approximately 2-fold decrease of sphere formation ability in isoDIPG-H3.3K27M cells compared to non-irradiated control cells, while there was no significant difference observed in isoDIPG-H3WT cells (**Figure 14A**). However, irradiation led to elevated levels of the apoptosis marker cleaved Caspase 3 not only in isoDIPG-H3.3K27M, but also in isoDIPG-H3WT cells (**Figure 14B; Appendix F**).

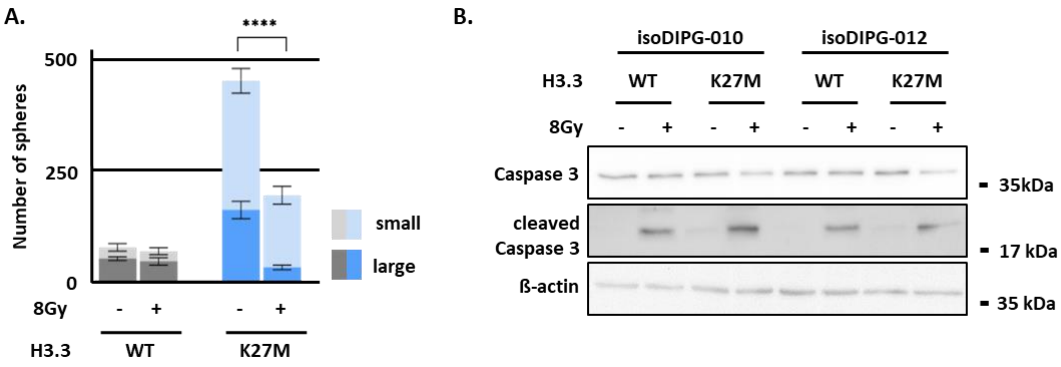

Figure 14 | Irradiation reduces stemness characteristics and induces apoptosis in isoDIPG cells.
Sphere formation assay was evaluated after 5 days after irradiation. Spheres were distinguished according to their size as small (100 – 200 µm) and large (> 200 µm). (B) Western blot analyses were performed using specific as indicated. ß-actin served as loading control. * $p < 0.05$; ** $p < 0.01$; ***$p < 0.005$; ****$p < 0.001$

In conclusion, irradiation significantly decreased stem cell-like properties in isoDIPG-H3.3K27M cells and induced apoptosis in both, isoDIPG-H3WT and isoDIPG-H3.3K27M cells. These findings suggest H3-dependent effects of irradiation in DIPG cells.

4.1.6 Glut1 inhibition decreases cell viability and sensitizes especially isoDIPG-H3.3K27M cells to irradiation and temozolomide

Previous studies showed that glucose transporter 1 (Glut1) suppresses the diffuse phenotype in a DIPG mouse model (Miyai et al. 2021) and Glut1 inhibition sensitizes radioresistant breast cancer cells to irradiation (Zhao et al. 2016) making it a promising therapeutic target for DIPG patients.

To study DIPG cell viability upon Glut1 inhibition, MTT cell viability assay was performed after treatment with increasing concentrations of Glut1 inhibitor, BAY-876. Irrespectively of H3-status isoDIPG cells strongly responded to Glut1 inhibition (**Figure 15**).

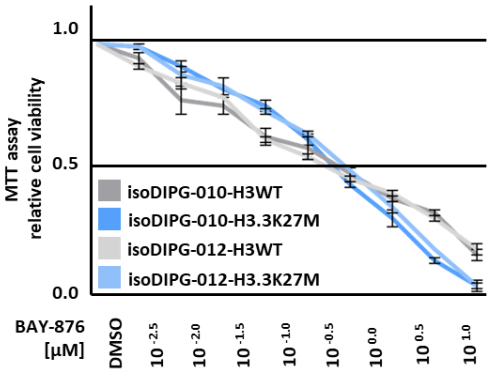

Figure 15 | Glut1 inhibition reduces cell viability in isoDIPG cells independently of H3-mutation status.
MTT assays illustrating viability of isoDIPG-010 and isoDIPG-012 cell lines (isoDIPG-H3WT cells shown in shades of grey, isoDIPG-H3.3K27M cells shown in shades of blue) upon treatment with increasing concentrations of BAY-876 for 72 h.

To study whether Glut1 inhibition sensitizes DIPG cells to standard treatment, combinatory MTT cell viability assay was performed (**Figure 16**). Thus, two different concentrations of temozolomide, 10 and 100 µM, were used in combination with 500 nM BAY-876 treatment and 8 Gy dose of irradiation.

Single treatment with temozolomide reduced cell viability to a significantly higher extent in isoDIPG-H3WT cells, while isoDIPG-H3.3K27M cells reacted stronger to a single dose of irradiation. Single treatment with Glut1 inhibitor resulted in a comparable reduction of cell viability, irrespectively of H3-mutation status. Interestingly, especially isoDIPG-H3.3K27M cells had been susceptible to double treatment with BAY-876 and TMZ or irradiation, respectively. When BAY-876 was used in combination with combined radiochemotherapy, isoDIPG-H3WT and isoDIPG-H3.3K27M cells were both sensitized towards combined temozolomide and irradiation treatment (**Figure 16**).

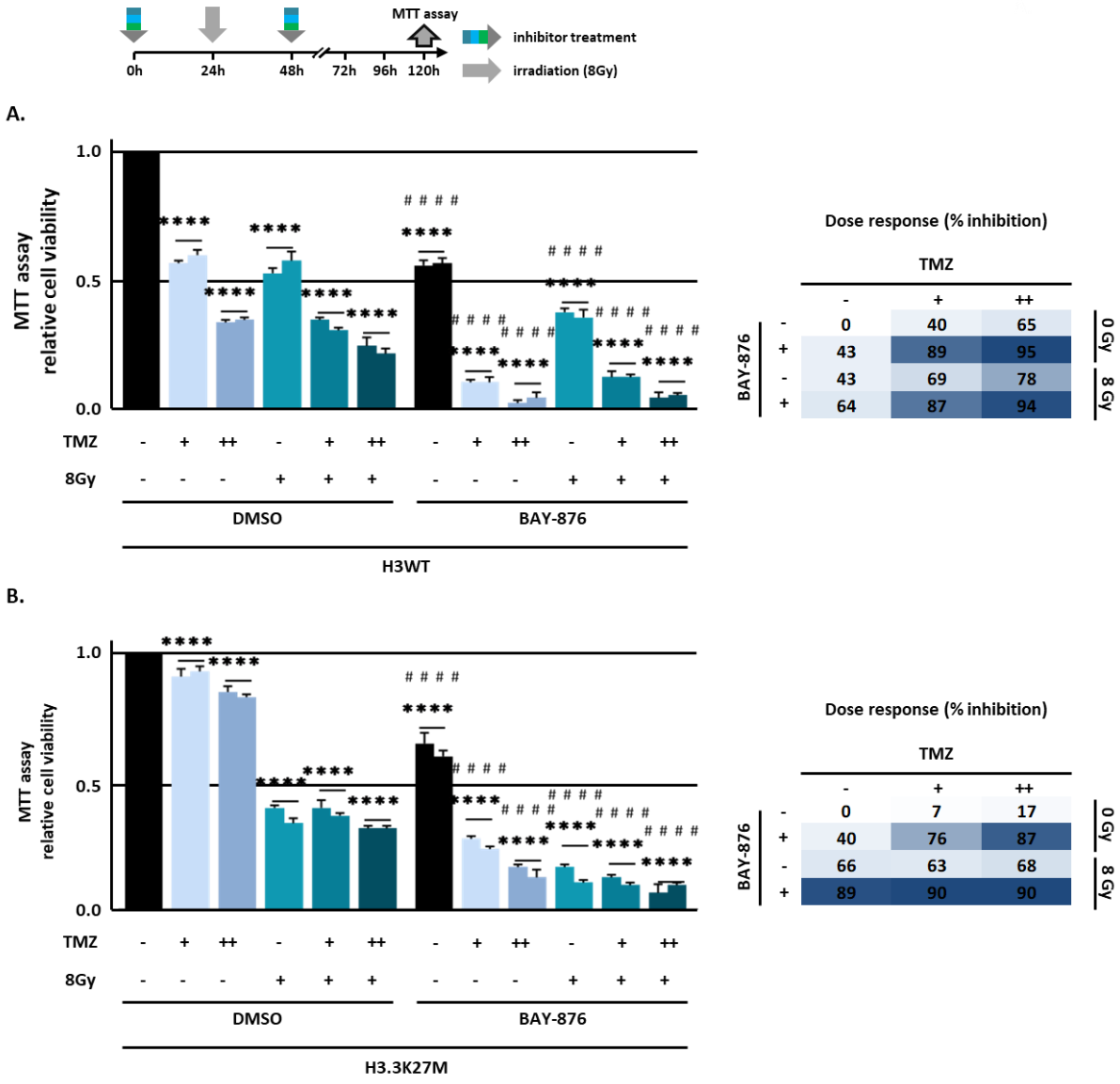

Figure 16 | Glut1 inhibition sensitizes isoDIPG cells to standard therapy. MTT viability assay illustrating viability of (A) isoDIPG-H3WT and (B) isoDIPG-H3.3 K27M cells upon single and combinatory treatment with two different temozolomide concentrations (10 and 100 µM), 500 nM BAY-876 and dose of 8 Gy irradiation. */# $p < 0.05$; **/## $p < 0.01$; ***/### $p < 0.005$; ****/#### $p < 0.001$ # used for comparison between isoDIPG-H3WT and isoDIPG-H3.3K27M cells.

In summary, Glut1 inhibition seemed to sensitize especially isoDIPG-H3.3K27M cells towards standard treatment therapy making it an attractive target for future investigations to identify new therapeutic options for DIPG patients.

4.1.7 mRNA sequencing reveals differently expressed gene sets in isoDIPG-H3WT and isoDIPG-H3.3K27M cells

H3.3K27M-mutation has a very strong effect on the epigenetic landscape of affected DIPG cells which is very much likely associated with a global change of gene expression. To investigate the

impact of H3.3K27M-mutation on global gene expression, the transcriptome of isoDIPG cell lines was determined by whole genome mRNA-sequencing. Dendrogram (**Figure 17A**) and principal component analysis (PCA) plots (**Figure 17B**) revealed that originally H3-wildtype VUMC-DIPG-010 cells after introduction of H3.3K27M-mutation (isoDIPG-010-H3.3K27M) shared a majority of expressed genes with originally H3.3K27M-mutated HSJD-DIPG-012 cells (isoDIPG-012-H3.3K27M) (**Figure 17**). On the other hand, when H3.3K27M-mutation had been removed from originally mutated HSJD-DIPG-012 cells (isoDIPG-012-H3WT), isoDIPG-012-H3WT cells still shared the majority of genes with originally mutated isoDIPG-012-H3.3K27M cells rather than originally H3-wildtype VUMC-DIPG-010 cells (isoDIPG-010-H3WT) (**Figure 17**).

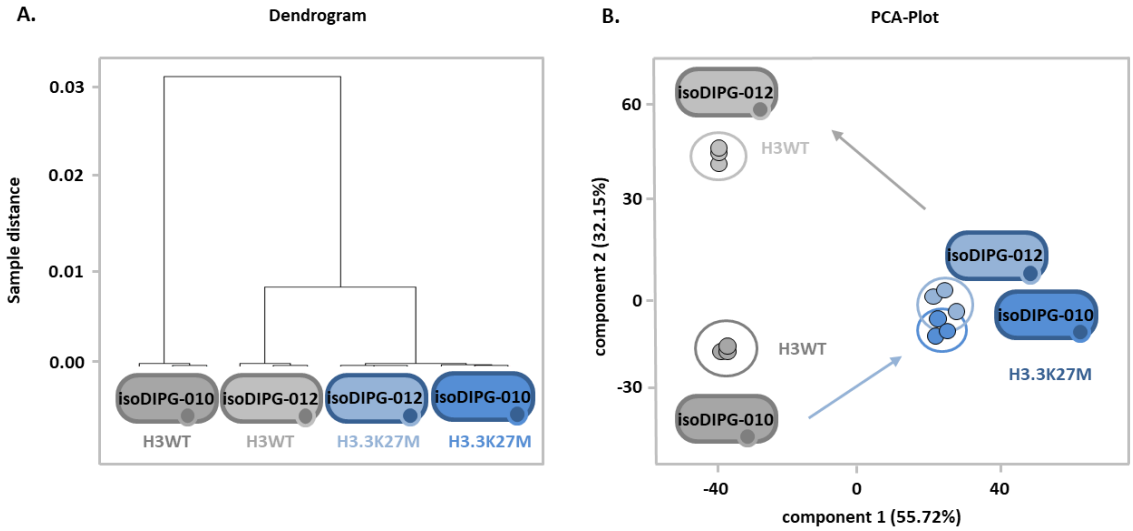

Figure 17 | H3.3K27M-mutation mediates specific gene expression pattern in isoDIPG cells.
(A) Dendrogram and (B) principal component analysis (PCA) plot were used to cluster isogenic cell lines with and without H3.3K27M-mutation based on their similarity in regard to gene expression profiles. Proportion of variance captured is expressed as percentage for both the first and second principal components (component 1 and 2).

In order to investigate the role of H3.3K27M-mutation in gene regulation and to identify commonly regulated subsets of genes after introduction of H3.3K27M-mutation in isoDIPG-010 and genes enriched in isoDIPG-012-H3.3K27M cells compared to their isoDIPG-H3WT counterparts, venn diagram and gene ontology analyses were performed. Venn diagram analysis revealed that more than 40% of genes in isoDIPG-H3.3K27M cells compared to their isoDIPG-H3WT counterparts were commonly enriched in isoDIPG-012 and isoDIPG-010 cells (**Figure 18A**). GO annotation analysis revealed that these genes are involved in biological processes like signal transduction, cell migration and cell motility (**Figure 18B**) and KEGG pathways including P53 signaling, pluripotency of stem cells and metabolic signaling (**Figure 18C**). Analysis of the top 50 commonly upregulated genes in both isoDIPG-H3.3K27M cell lines revealed the overrepresentation of different genes associated with tumor growth and aggressiveness, the HOX genes homeobox B4 (*HOXB4*), homeobox B8 (*HOXB8*) and homeobox B5 (*HOXB5*), but also

DAB adaptor protein 2 (*DAB2*), mesothelin (*MSLN*), fibroblast growth factor binding protein 1 (*FGFBP1*), gap junction protein beta 5 (*GJB5*), FXYD domain containing ion transport regulator 5 (*FXYD5*), caveolin 2 (*CAV2*) and annexin A3 (*ANXA3*) (**Figure 18D**).

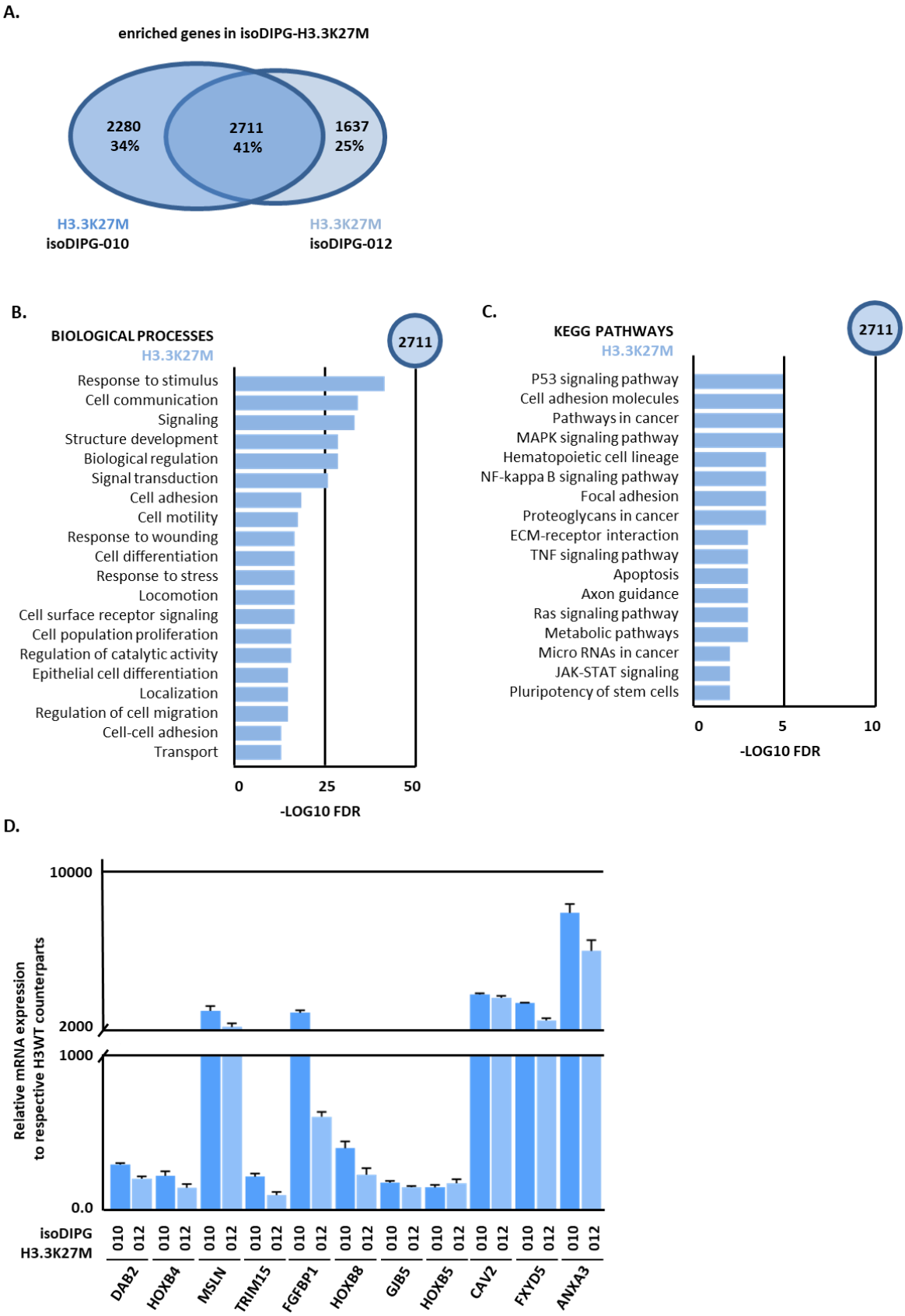

Figure 18 | H3.3K27M-mutation induces similar gene signatures in isoDIPG-010 and isoDIPG-012 cells.
(A) Venn diagram analysis identified commonly enriched genes in isoDIPG-010 and isoDIPG-012 cells in the presence of H3.3K27M-mutation in comparison to their respective isoDIPG-H3WT cell counterparts. (B) Gene ontology and (C) KEGG pathway analyses identified biological processes and KEGG pathways regulated by commonly expressed genes in the presence of H3.3K27M-mutation (log2FC ≤1.0, adjusted p-value ≤0.05). (D) Relative mRNA expression of selected genes from the top50 regulated genes associated with tumor biology in isoDIPG-012-H3.3K27M and isoDIPG-010-H3.3K27M cell lines compared to their respective isoDIPG-H3WT counterparts.

Venn diagram analysis revealed that almost 30% of all genes enriched in isoDIPG-H3WT cells compared to their isoDIPG-H3.3K27M counterparts were commonly enriched in isoDIPG-012 and isoDIPG-010 (**Figure 19A**). GO annotation analysis revealed that these similarly expressed genes were involved in biological processes like nervous system development, angiogenesis and cell differentiation (**Figure 19B**), and KEGG pathways including axon guidance and focal adhesion (**Figure 19C**). Analysis of the top 50 commonly upregulated genes in both isoDIPG-H3WT cell lines revealed the overrepresentation of different genes associated with tumor biology compared to isoDIPG-H3.3K27M cells, including PiggyBac transposable element derived 5 (*PGBD5*), glutathione S-transferase mu 3 (*GSTM3*), cadherin 6 (*CDH6*), cadherin 2 (*CDH2*), frizzled class receptor 8 (*FZD8*), activator of transcription and developmental regulator AUTS2 (*AUTS2*), insulin like growth factor binding protein like 1 (*IGFBPL1*), POU class 4 homeobox 1 (*POU4F1*), secreted frizzled related protein 1 (*SFRP1*), growth arrest specific 1 (*GAS1*) and meis homeobox 1 (*MEIS1*) **Figure 19D**.

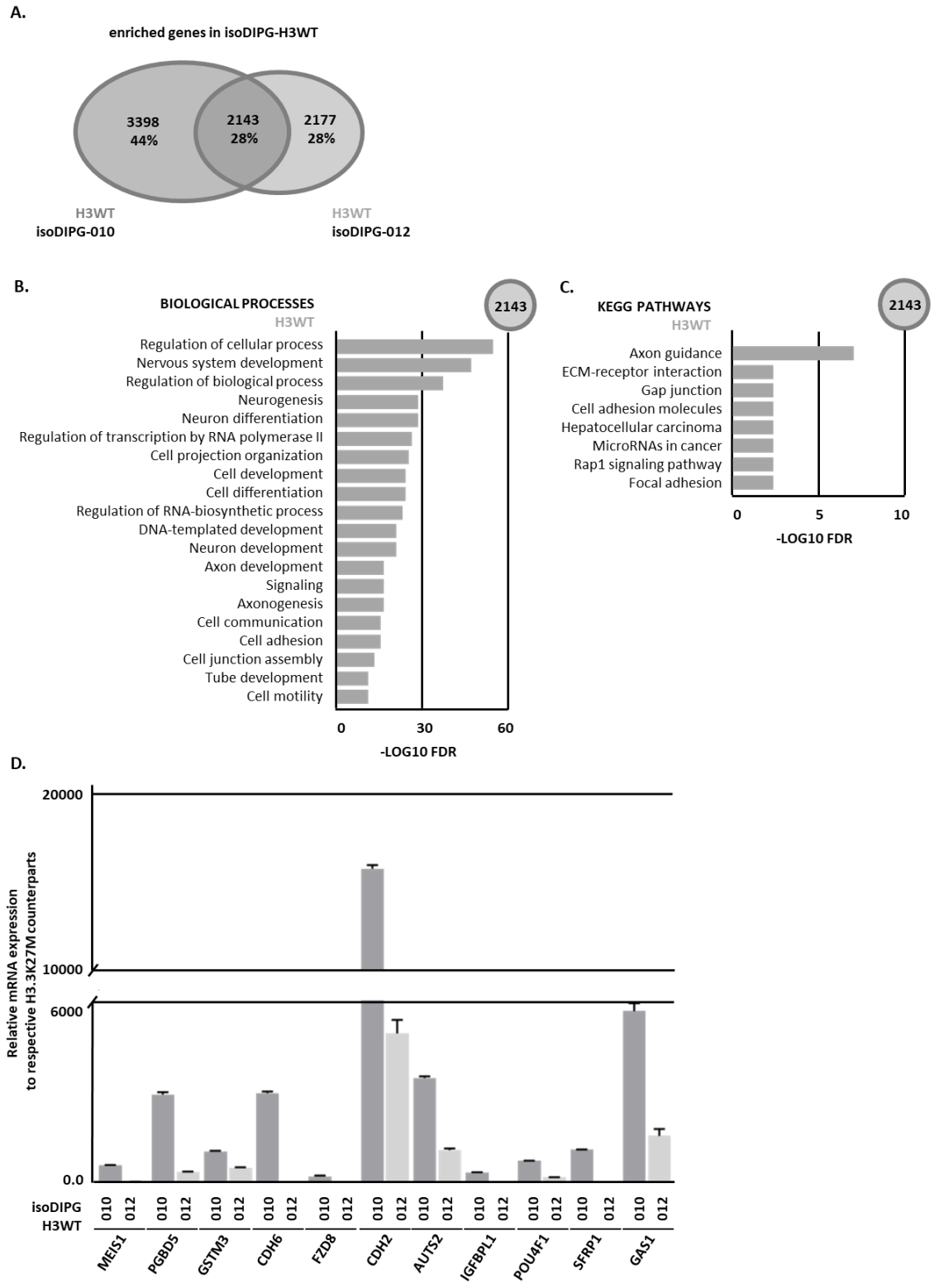

Figure 19 | isoDIPG-H3WT cells share different gene sets associated with differentiation and development compared to isoDIPG-H3.3K27M cells.

(A) Venn diagrams diagram analysis identified commonly enriched genes in isoDIPG-010-H3WT and isoDIPG-012-H3WT cells in comparison to their respective isoDIPG-H3.3K27M cell counterparts. (B) Gene ontology and (C) KEGG pathway analyses identified biological processes and KEGG pathways regulated by commonly expressed genes in the absence of H3.3K27M-mutation (log2FC ≤1.0, adjusted p-value ≤0.05). (D) Relative mRNA expression of selected genes from the top50 regulated genes associated with tumor biology in isoDIPG-012-H3WT and isoDIPG-010-H3WT cell lines compared to their respective isoDIPG-H3.3K27M counterparts.

To study molecular interactions dependent on presence of H3.3K27M-mutation in DIPG cells, KEGG pathway map was generated using ShinyGo (http://bioinformatics.sdstate.edu/go/). Genes that were strongly expressed in isoDIPG-H3.3K27M cells in comparison to isoDIPG-H3WT cells were involved in pathways like Wnt signaling, calcium signaling, p53 signaling as well as cell cycle **(Appendix G)**.

As it has already been shown above, removal of H3.3K27M-mutation resulted in less change in global gene expression than introduction of H3.3K27M-mutation. To investigate the differences between both isoDIPG-10-H3WT and isoDIPG-12-H3WT and between isoDIPG-10-H3.3K27M and isoDIPG-10-H3.3K27M cells, volcano plots and GO annotation analyses were performed. Volcano plots showed less differential regulated genes in isoDIPG-012-H3.3K27M and isoDIPG-010-H3.3K27M cells (**Figure 20A**) when compared to the isoDIPG-H3WT cell lines, where significantly more genes were differentially regulated between isoDIPG-010 and isoDIPG-012 cell lines (**Figure 20B**). Gene ontology analysis was used to discover biological processes exclusively enriched either in isoDIPG-010-H3WT or isoDIPG-012-H3WT cells. In isoDIPG-010-H3WT cells, identified processes were involved in cell differentiation and neuron development (**Figure 20C**), while in isoDIPG-012-H3WT cells, enriched genes were involved in nervous system development processes as well as in cell differentiation, cell migration and cell adhesion (**Figure 20D**). Analysis of the top 50 commonly regulated genes exclusively regulated in isoDIPG-012-H3WT cells revealed the overrepresentation of different genes associated with tumor biology, including glypican 6 (*GPC6*), Wnt family member 5A (*WNT5A*), BMP/retinoic acid inducible neural specific 3 (*BRINP3*), collagen type IV alpha 1 chain (*COL4A1*), proprotein convertase subtilisin/kexin type 2 (*PCSK2*), RAN binding protein 17 (*RANBP17*) and CCDC26 long non-coding RNA (*CCDC26*) (**Figure 20E**).

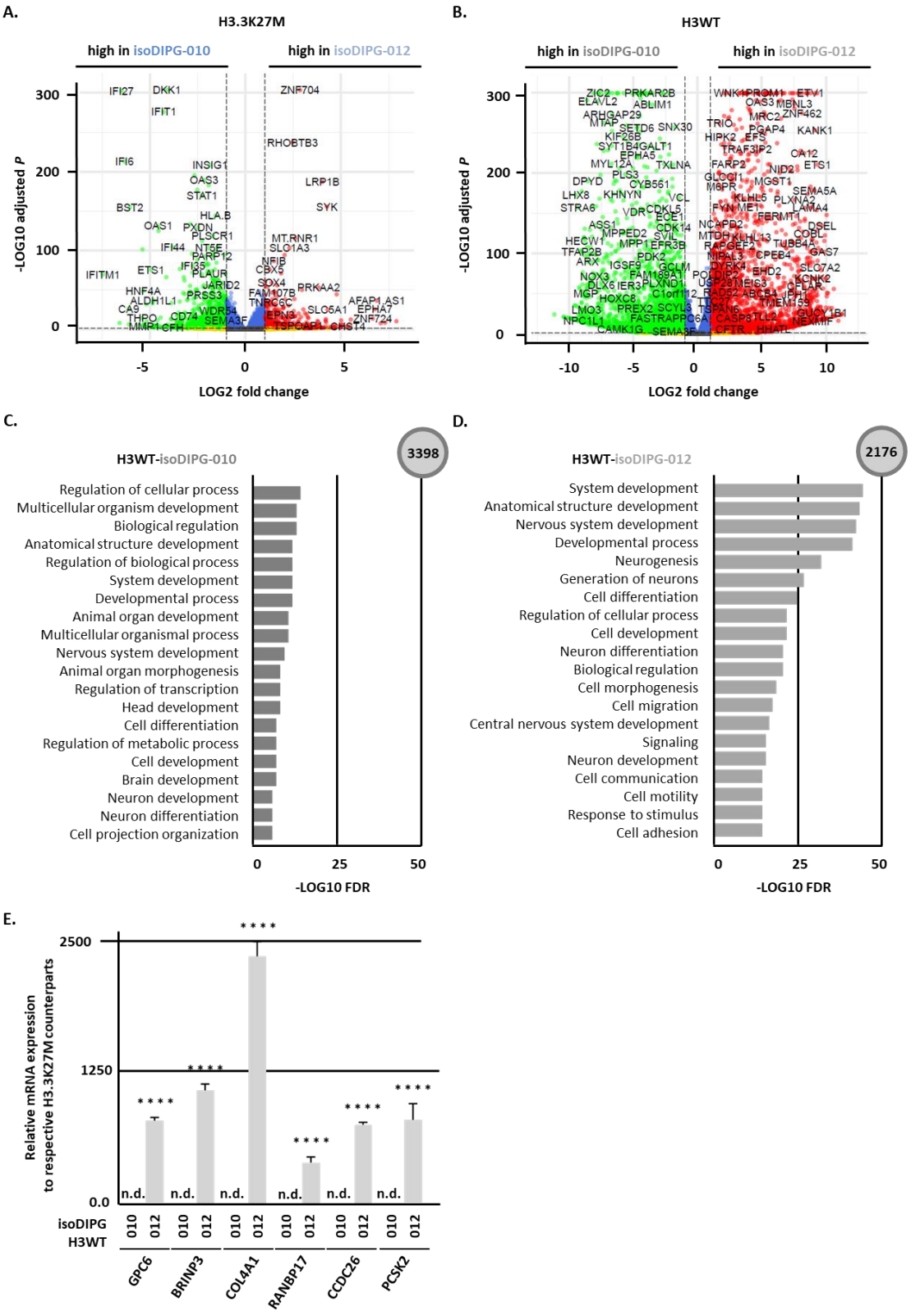

Figure 20 | Removal of H3.3K27M-mutation results in less change in global gene expression than introduction of H3.3K27M-mutation in isoDIPG cells.

Volcano plots identified differently expressed genes in isoDIPG-010 and isoDIPG-012 in the presence (A) and absence (B) of H3.3K27M-mutation. Gene ontology analysis identified biological processes and pathways regulated by exclusively expressed genes in (C) isoDIPG-012-H3WT and (D) isoDIPG-010-H3WT cells (log2FC ≤1.0, adjusted p-value ≤0.05). (E) Relative mRNA expression of top50 genes associated with tumor biology was shown exclusively in isoDIPG-012-H3WT cell line.

In summary, mRNA sequencing data suggested that presence of H3.3K27M-mutation may be crucial, but not the only factor responsible for the malignant phenotype observed in DIPG-H3.3K27M cells. Moreover, DIPG cell lines carrying H3.3K27M-mutation share gene expression profiles associated with commonly regulated biological processes and KEGG pathways, such as cell proliferation, cell motility, cell migration, MAPK signaling pathway, p53 signaling pathway and pluripotency of stem cells, which may explain the effect of presence of H3.3K27M-mutation on proliferation, stem cell-like characteristics and invasiveness in isoDIPG-H3.3K27M cells.

4.1.8 H3.3K27M-mutation impacts tumor growth *in vivo*

In order to study the effect of H3.3K27M-mutation on tumor growth, chicken embryo chorioallantoic membrane (CAM) assay was used, which has already been proven to be a suitable *in vivo* model to study tumor biology and therapeutic options in DIPG (Li et al. 2015; Power et al. 2022).

Introduction of H3.3K27M-mutation resulted in DIPG cells derived tumors to be significantly larger in size (**Figure 21A and 21C**) and volume (**Figure 21B and 21D**) compared to their H3-wildtype equivalent. Accordingly, removal of H3.3K27M-mutation led to significantly smaller isoDIPG-012-H3WT cells derived tumors compared to isoDIPG-012-H3.3K27M cells (**Figure 21**).

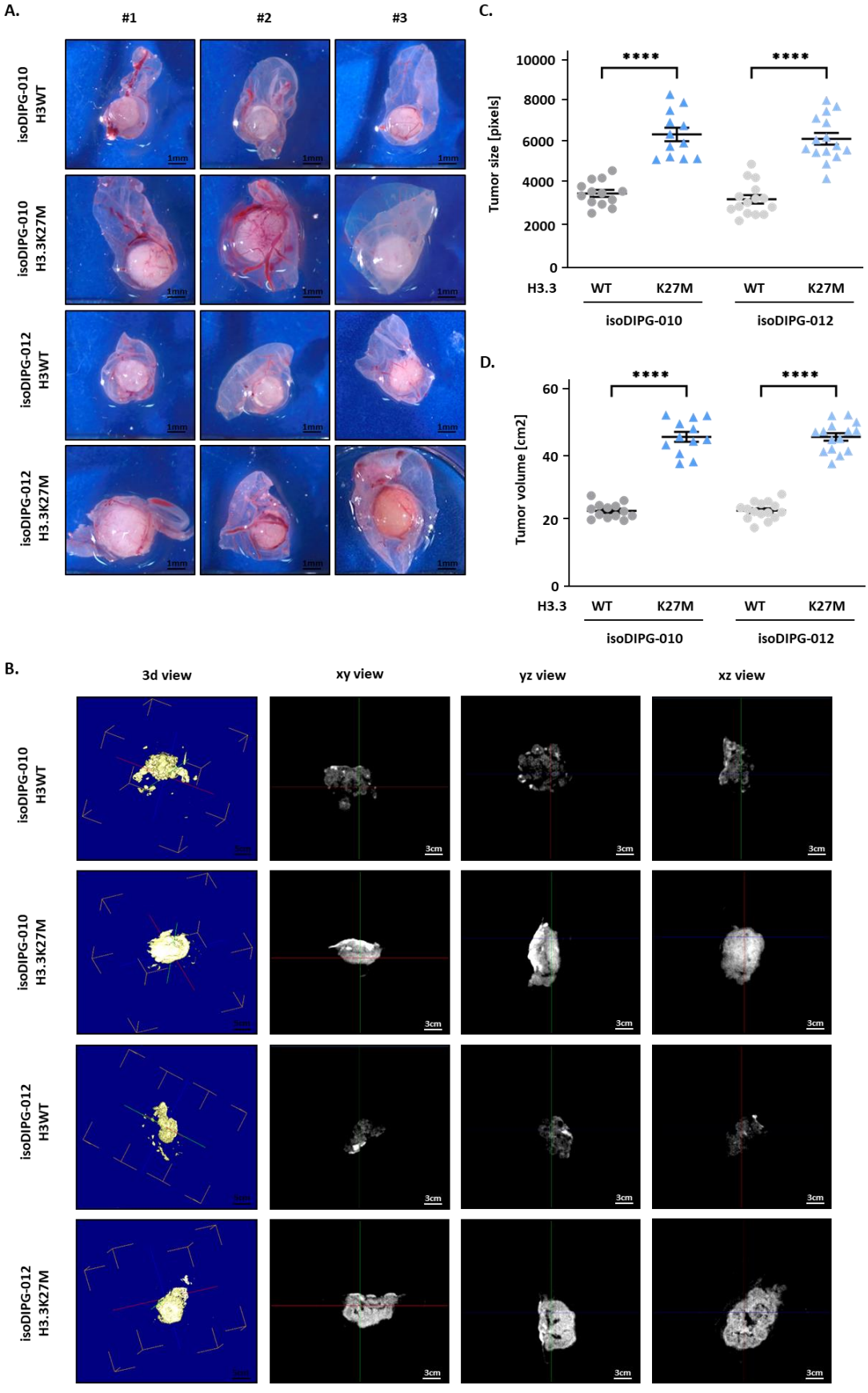

Figure 21 | Presence of H3.3K27M-mutation leads to increased tumor size and volume *in vivo*. DIPG cell derived tumors carrying H3.3K27M-mutation grown in the CAM model were significantly bigger in size (A, C) and volume (B, D) than their H3-wildtype equivalents. * $p < 0.05$; ** $p < 0.01$; *** $p < 0.005$; **** $p < 0.001$.

In conclusion, CAM assay revealed that tumors harboring H3.3K27M-mutation grew significantly bigger in size and volume than their H3-wildtype equivalents.

Overall, presence of H3.3K27M-mutation resulted in an increase of tumor-related characteristics, such as cell proliferation, stemness characteristics and invasive phenotype compared to H3-wildtype equivalent *in vitro* and *in vivo*. In addition, these characteristics were reflected by the expression profile of isoDIPG cells, with isoDIPG-H3.3K27M cells regulating pluripotency of stem cells, p53 signaling pathway, MAPK cascade and cell cycle.

4.2 H3.3K27M-dependent function of CBP/p300 and BET proteins in isoDIPG cells

Our previous studies showed that especially isoDIPG-H3.3K27M cells display very pronounced tumor cell characteristics, including cell proliferation rate, stem cell-like properties and malignant phenotype. These features may be at least partially associated with the higher expression of H3K27ac levels observed in isoDIPG-H3.3K27M cells compared to their H3-wildtype counterparts. In line with previous findings, DIPG cells carrying H3.3K27M-mutation might be more dependent on proteins associated with H3K27ac, such as epigenetic writers and readers CBP/p300 and BET proteins, respectively, which have been shown to play a role in tumor maintenance (Wiese et al. 2017; Piunti et al. 2017; Wiese et al. 2020; Zheng and Jefcoate 2004; Belkina and Denis 2012). Therefore, targeting epigenetically relevant proteins that might be responsible for the observed hyperacetylation at H3K27 or mediate their impact on gene expression may be a promising therapeutic option for DIPG patients.

To this end, nine small molecules (**Table 21**) were used to inhibit CBP/p300 and BET proteins in isogenic DIPG cells. Subsequently, siRNA-mediated knockdown of CBP, p300, BRD2, BRD3 and BRD4 was conducted in two isogenic cell lines – isoDIPG-010 and isoDIPG-012 with and without H3.3K27M-mutation to differentiate distinct functions of CBP and p300 as well as of the three BET proteins: BRD2, BRD3 and BRD4.

Table 21 | Small molecules and their targets used in the present study

Inhibitor	Target protein	Target function
A-485	CBP/p300	HAT domain of CBP/p300
C646	CBP/p300	HAT domain of CBP/p300
CBP112	CBP/p300	BD
CBP30	CBP/p300	BD
ICG-001	CBP/p300	N-terminus of CBP/p300
ISOX-DUAL	CBP/p300 and BRD4	BD of CBP/p300 and BRD4
JQ1	BET proteins	BD of BRD2/3/4
MS346	BRD4	BD of BRD4
OTX-015	BET proteins	BD of BRD2/3/4

4.2.1 Cell viability assay unravels the most potent CBP/p300 and BET proteins inhibitors in isoDIPG cells

To investigate the effectiveness and possible H3-mutation-dependent effects of different CBP/p300 and BET proteins inhibitors on cell viability, MTT cell viability assays were performed. For this purpose, isoDIPG-010 and isoDIPG-012 cells were treated with increasing concentrations of five different exclusive CBP/p300 inhibitors (CBP30, A-485, CBP112, C646, ICG-001), three exclusive BET proteins inhibitors (OTX-015, JQ1, MS346) and one dual inhibitor (ISOX-DUAL) (**Table 22**).

Overall, no cell line depending effect was observed: isoDIPG-10 and isoDIPG-12 cells with the same H3-mutation status responded similarly to each tested CBP/p300 and BET proteins inhibitors (**Figure 22**).

CBP/p300 inhibition

In order to inhibit bromodomain (BD) function of CBP/p300 in isoDIPG cells, CBP112 (Picaud et al. 2015) and CBP30 (Hammitzsch et al. 2015) were used. A-485 (Zhang et al. 2020) and C646 (Shrimp et al. 2015) were chosen to inhibit histone acetyltransferase (HAT) activity of CBP/p300, while ICG-001 was used to inhibit binding of co-factors to the N-terminus of CBP/p300, including ß-catenin as canonical Wnt signaling pathway activator (Gang et al. 2014).

CBP30 and A-485 significantly decreased cell viability, to a higher extent in isoDIPG-H3WT cells when compared to isoDIPG-H3.3 K27M cells, with approximate IC_{80} of 1 µM for CBP30 and 50 nM for A-485 (**Figure 22A and 22B**). Treatment with CBP112 resulted in only slight reduction of

cell viability with approximate IC_{80} of 1 μM for isoDIPG-H3WT cells, whereas in isoDIPG-H3.3K27M cells IC_{80} was not reached (**Figure 22C**). Treatment with C646 and ICG-001 showed effective reduction of cell viability, independently of H3-mutation status with approximate IC_{80} of 1 μM (**Figure 22D and 22E**).

BET inhibition

JQ1 and OTX-015 were used in order to inhibit bromodomains of BRD2, BRD3 and BRD4 in isoDIPG cells (Berthon et al. 2016), whereas MS346 was chosen to exclusively inhibit BRD4 bromodomains (Zhang et al. 2013).

Treatment with OTX-015 resulted in a significant reduction of cell viability, to a higher extent in isoDIPG-H3WT cells, with IC_{80} oscillating around 50 nM for isoDIPG-H3WT cells and 500 nM for isoDIPG-H3.3 K27M cells (**Figure 22G**). MS346 and JQ1 treatment decreased cell viability in a dose dependent manner, independently on H3-mutation status, with approximate IC_{80} of 1 μM for MS346 and 100 nM for JQ1 (**Figure 22H and 22I**).

CBP/p300 and BET inhibition

ISOX-DUAL binds to CBP/p300 and BRD4 bromodomains and inhibits their interaction with chromatin (Chekler et al. 2015). MTT viability assay showed slight reduction in cell viability of isoDIPG cells, independently of H3-mutation status with IC_{80} oscillating around 5 μM (**Figure 22F**).

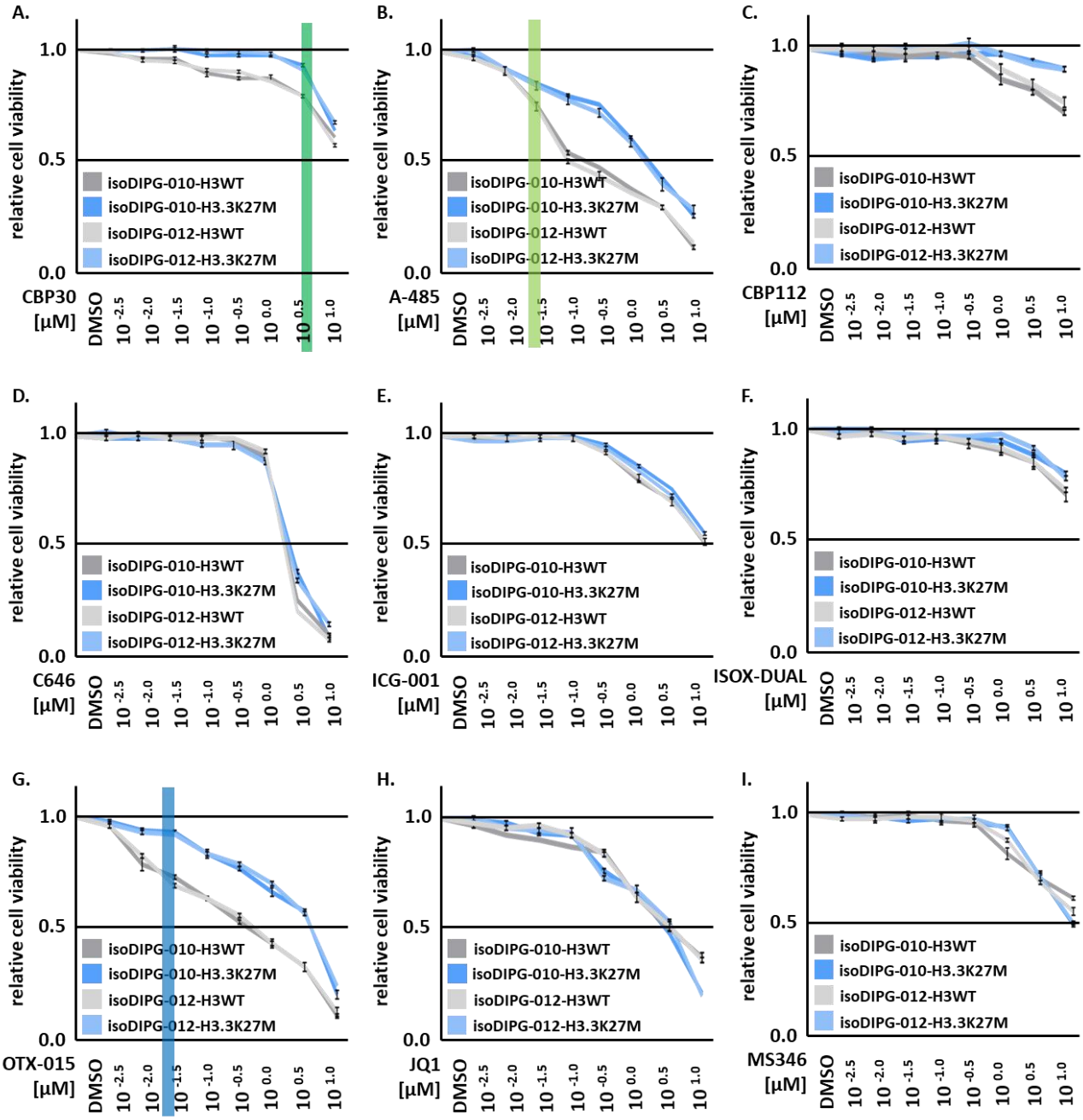

Figure 22 | Selected CBP/p300 and BET proteins inhibitors reduce cell viability in isoDIPG-H3WT and isoDIPG-H3.3K27M cells.
MTT cell viability assays (H3WT shown in shades of grey, H3.3K27M shown in shades of blue) upon treatment with increasing concentrations of studied inhibitors 72 h after seeding. Chosen concentrations for further experiments are depicted by bars in green (1 µM for CBP30), light green (50 nM for A-485), and blue (50 nM for OTX-015).

In summary, every selected CBP/p300 and BET proteins inhibitor affected cell viability in isoDIPG-H3WT and isoDIPG-H3.3 K27M cells to a different extent. Three out of nine tested molecules were chosen for further experiments – 1 µM CBP30, 50 nM A-485 and 50 nM OTX-015, since only those showed differences in cell viability in dependence on H3-mutation status and haven't been investigated closely in DIPG cells.

4.2.2 Verification of successful siRNA-mediated knockdown of CBP, p300, BRD2, BRD3 and BRD4 in isoDIPG cells

To further investigate the role of CBP/p300 and BET proteins in dependence on H3-mutation status in particular and to be able to distinguish between CBP and p300, as well as between BRD2, BRD3 and BRD4 function, siRNA-mediated knockdown of the proteins of interest was performed. To validate the successful knockdown of CBP, p300, BRD2, BRD3 and BRD4, qPCR and western blot analyses were carried out.

Interestingly, absolute expression of CBP, p300, BRD3 and BRD4, but not BRD2, was found to be significantly elevated in isoDIPG-H3.3K27M cells compared to isoDIPG-H3WT cells on mRNA level. These results are also reflected on protein level apart from BRD3, which expression was found not to be affected by presence of H3.3K27M-mutation in isoDIPG cells.

However, qPCR (**Figure 23A**) as well as western blot (**Figure 23B**) analyses showed successful knockdown of CBP, p300, BRD2, BRD3 and BRD4 in isoDIPG-010 and isoDIPG-012 cell lines.

CBP knockdown turned out to be exceptionally efficient in isoDIPG-010 and isoDIPG-012 cell lines. isoDIPG-H3WT cells showed reduction of *CBP* expression on mRNA level of approximately 60% in isoDIPG-010-H3WT and 90% in isoDIPG-012-H3WT, while in isoDIPG-H3.3K27M cells of approximately 65% in isoDIPG-010-H3.3K27M cells and 90% in isoDIPG-012-H3.3K27M cells. Knockdown of p300 resulted in decreased levels of *EP300* on mRNA level of around 70% in isoDIPG-H3WT cells and 75% in isoDIPG-010-H3.3K27M cells, and nearly 100% in isoDIPG-012-H3.3K27M cells. BRD2 knockdown showed reduction of *BRD2* on mRNA level of approximately 65% in isoDIPG-010-H3WT cells and almost 100% in isoDIPG-012-H3WT cells. Whereas in isoDIPG-H3.3K27M cells BRD2 knockdown resulted in decreased *BRD2* expression of around 85% in isoDIPG-010-H3.3K27M cells and 70% in isoDIPG-012-H3.3K27M cells. BRD3 knockdown showed reduction of *BRD3* mRNA level of approximately 75% in isoDIPG-010-H3WT cells and 70% in isoDIPG-012-H3WT cells. While in isoDIPG-H3.3K27M cells, siRNA mediated knockdown of BRD3 resulted in decreased *BRD3* expression of around 80% in isoDIPG-010-H3.3K27M cells and almost 100% in isoDIPG-012-H3.3K27M cells. Knockdown of BRD4 caused reduction of *BRD4* on mRNA level of approximately 55% and 90% in isoDIPG-010-H3WT and isoDIPG-012-H3WT cells, respectively. siRNA-mediated knockdown of BRD4 resulted in reduction of *BRD4* mRNA expression of around 80% and 90% in isoDIPG-010-H3.3K27M and isoDIPG-012-H3.3K27M cells, respectively.

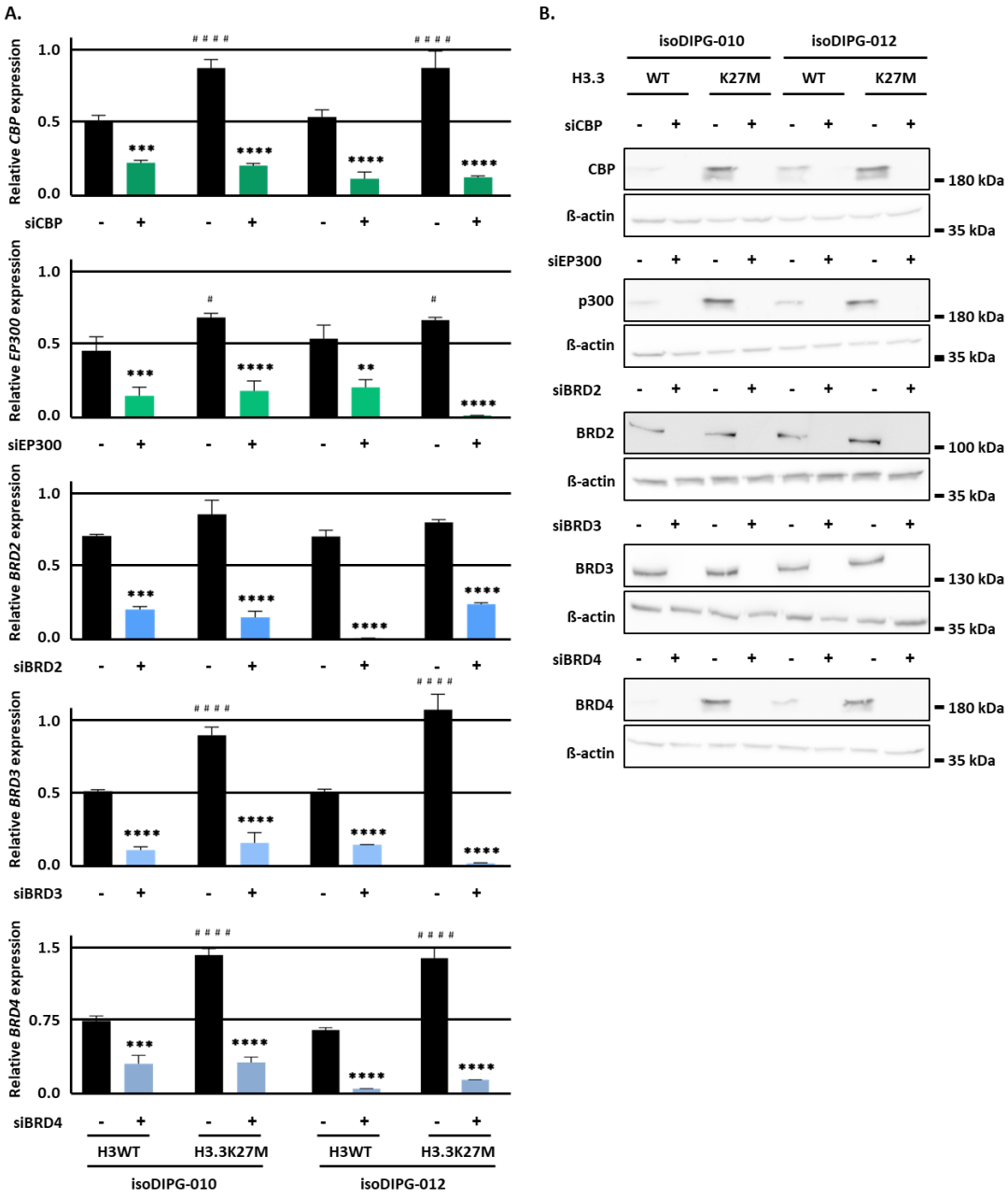

Figure 23 | Verification of successful knockdown of CBP, p300, BRD2, BRD3 and BRD4 on mRNA and protein level in isoDIPG cells.

siRNA-mediated knockdown of CBP, p300, BRD2, BRD3 and BRD4 was validated 48 h after transfection on mRNA level using (A) qPCR relative to ß-actin housekeeping gene expression and 72 h after transfection on protein level using (B) western blot analyses. ß-actin served as loading control. */# $p < 0.05$; **/## $p < 0.01$; ***/### $p < 0.005$; ****/#### $p < 0.001$ # used for comparison between isoDIPG-H3WT and isoDIPG-H3.3K27M cells.

In summary, although slight differences in the effectiveness of siRNA mediated knockdown on mRNA level were observed, protein expression of CBP, p300, BRD2, BRD3 and BRD4 was completely abolished in all tested isoDIPG cell lines.

4.2.3 CBP/p300 and BET proteins regulate expression of H3K27me3 and H3K27ac in isoDIPG cells

Previous findings suggest that hypotrimethylation and hyperacetylation at H3K27 in isoDIPG cells is induced by H3.3K27M-mutation which is associated with elevated expression of tumor-biological characteristics. In consequence, it can be assumed that the aggressive phenotype of isoDIPG-H3.3K27M cells may depend on the observed epigenetic changes. Thus, histone acetylation-associated proteins might be involved in regulation of H3K27 marks. In order to investigate these hypotheses, effects of CBP/p300 and BET proteins inhibition on H3K27me3 and H3K27ac levels were investigated using western blot analyses. To this end, HAT-activity of CBP/p300 was inhibited using A-485. In addition, CBP/p300 and BET protein bromodomains were inhibited by CBP30 and OTX-015, respectively. In addition, to dissect the specific function of CBP and p300, as well as BRD2, BRD3 and BRD4, siRNA-mediated knockdown was performed.

CBP/p300

Levels of H3K27me3 were not very strongly affected by inhibition or knockdown of CBP/p300 in isoDIPG-H3WT cells in comparison to isoDIPG-H3.3K27M cells which show a very profound increase of H3K27me3 levels upon knockdown of CBP, but not p300 (**Figure 24A and 24B; Appendix H**). In contrast, inhibition of BD (CBP30) and HAT activity (A-485) of CBP/p300 resulted in decreased H3K27ac levels, irrespectively of H3-mutation status (**Figure 24A and 24B; Appendix H**). Interestingly, knockdown of p300 strongly reduced H3K27ac expression in isoDIPG-H3WT cells and knockdown of CBP in isoDIPG-H3.3K27M cells (**Figure 24A and 24B; Appendix H**). These data suggest that p300 is responsible for H3K27ac in isoDIPG-H3WT cells, whereas CBP appears to be crucial for H3K27 acetylation in isoDIPG-H3.3K27M cells.

BET proteins

In isoDIPG-H3WT cells, H3K27me3 was restored only upon knockdown of BRD3, while in isoDIPG-H3.3K27M cells upon BRD2 and BRD3 knockdown (**Figure 24A and 24B; Appendix H**). Contrastingly, H3K27ac was found to be elevated upon BET inhibition by OTX-015, as well as BRD2, BRD3 and BRD4 knockdown in isoDIPG-H3WT cells, but downregulated in isoDIPG-H3.3K27M cells (**Figure 24A and 24B; Appendix H**), suggesting a differential role of BET proteins in dependence on H3-mutation status in DIPG cells.

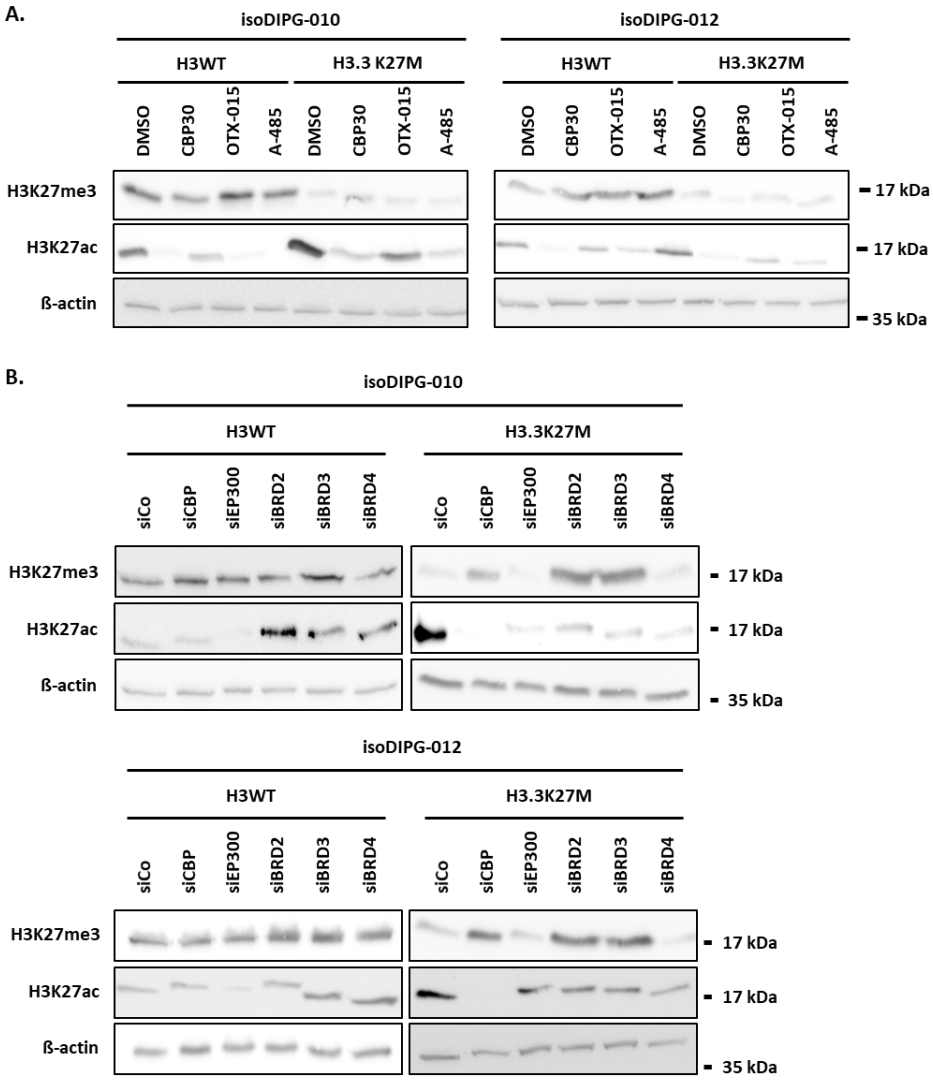

Figure 24 | CBP/p300 and BET proteins regulate expression of H3K27me3 and H3K27ac in isoDIPG cells.

Expression of H3K27me3 and H3K27ac levels was investigated using western blot analysis after (A) CBP/p300 and BET proteins inhibition and (B) siRNA-mediated knockdown of the indicated proteins of interest. ß-actin served as loading control.

In summary, CBP/p300 and BET proteins appear to strongly affect the epigenetic profile of DIPG cells by influencing H3K27ac and H3K27me3 levels. CBP regulates H3K27ac in isoDIPG-H3.3K27M cells, while p300 plays similar role in isoDIPG-H3WT cells. Furthermore, H3K27me3 is being restored after knockdown of CBP, BRD2 and BRD3 in isoDIPG-H3.3K27M cells.

4.2.4 CBP/p300 and BET proteins are important for expression of tumor-related characteristics in isoDIPG cells

Previous studies showed that inhibition of CBP/p300 and BET proteins reduce tumor characteristics (Wiese et al. 2017; Piunti et al. 2017; Wiese et al. 2020; Zheng and Jefcoate 2004; Belkina and Denis 2012). Since isoDIPG-H3.3K27M cells were found to have significantly higher expression of H3K27ac compared to isoDIPG-H3WT cells, acetylation-associated proteins might play a more profound role in DIPG cells carrying H3.3K27M-mutation.

4.2.4.1 CBP/p300 and BET proteins are essential for proliferation of isoDIPG-H3.3K27M cells

To examine the impact of CBP, p300, BRD2, BRD3 and BRD4 on cell proliferation in dependence on H3-mutation status, cell viability and cell proliferation assays were performed using isoDIPG-010 and isoDIPG-012 cell lines after siRNA-mediated knockdown as well as inhibition of CBP/p300 and BET proteins.

CBP/p300

Knockdown of CBP and p300 caused only a slight reduction of cell viability and cell proliferation, independently of H3-mutation status (**Figure 25; Appendix I**). Whereas inhibition of CBP/p300 BD (CBP30) and HAT activity (A-485) resulted in significantly stronger effects in isoDIPG-H3WT cells compared to isoDIPG-H3.3K27M cells (**Figure 25; Appendix I**).

BET proteins

Viability and proliferation of isoDIPG-H3WT cells was reduced only upon inhibition of BET proteins using OTX-015, while knockdown of BRD2, BRD3 and BRD4 caused no changes (**Figure 25; Appendix I**). In opposite, in isoDIPG-H3.3K27M cells, reduction of cell viability and proliferation was observed upon knockdown of BRD2 and BRD4, whereas siBRD3 transfection had only slight, but no significant effect (**Figure 25; Appendix I**).

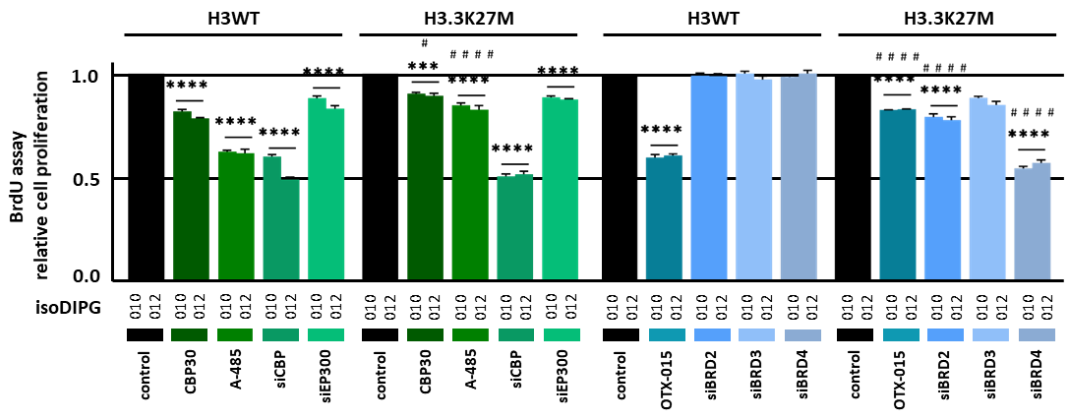

Figure 25 | CBP/p300 and BET proteins are essential for proliferation of isoDIPG cells.
Cell viability and cell proliferation of isoDIPG cells assessed by (A) MTT, (B) CV and (C) BrdU assay were determined after day 1, day 3 and day 5 after seeding and normalized to time point day 1. */# $p < 0.05$; **/## $p < 0.01$; ***/### $p < 0.005$; ****/#### $p < 0.001$ # used for comparison between isoDIPG-H3WT and isoDIPG-H3.3K27M cells.

In conclusion, whereas knockdown of CBP and p300 resulted in comparable effects in isoDIPG-H3WT and isoDIPG-H3.3K27M cells, BRD2 and BRD4, but not BRD3, appear to play a role in cell viability and proliferation exclusively in isoDIPG-H3.3K27M cells, but might be dispensable in isoDIPG-H3WT cells.

4.2.4.2 CBP/p300 and BET proteins are crucial for clonogenicity of isoDIPG cells

To assess clonogenicity under stem cell-like spheroid and differentiating monolayer culture conditions after siRNA-mediated knockdown as well as after inhibition of CBP/p300 and BET proteins, sphere formation and colony formation assays were performed. Additionally, expression of common stemness markers was evaluated using qPCR (**Figure 26**).

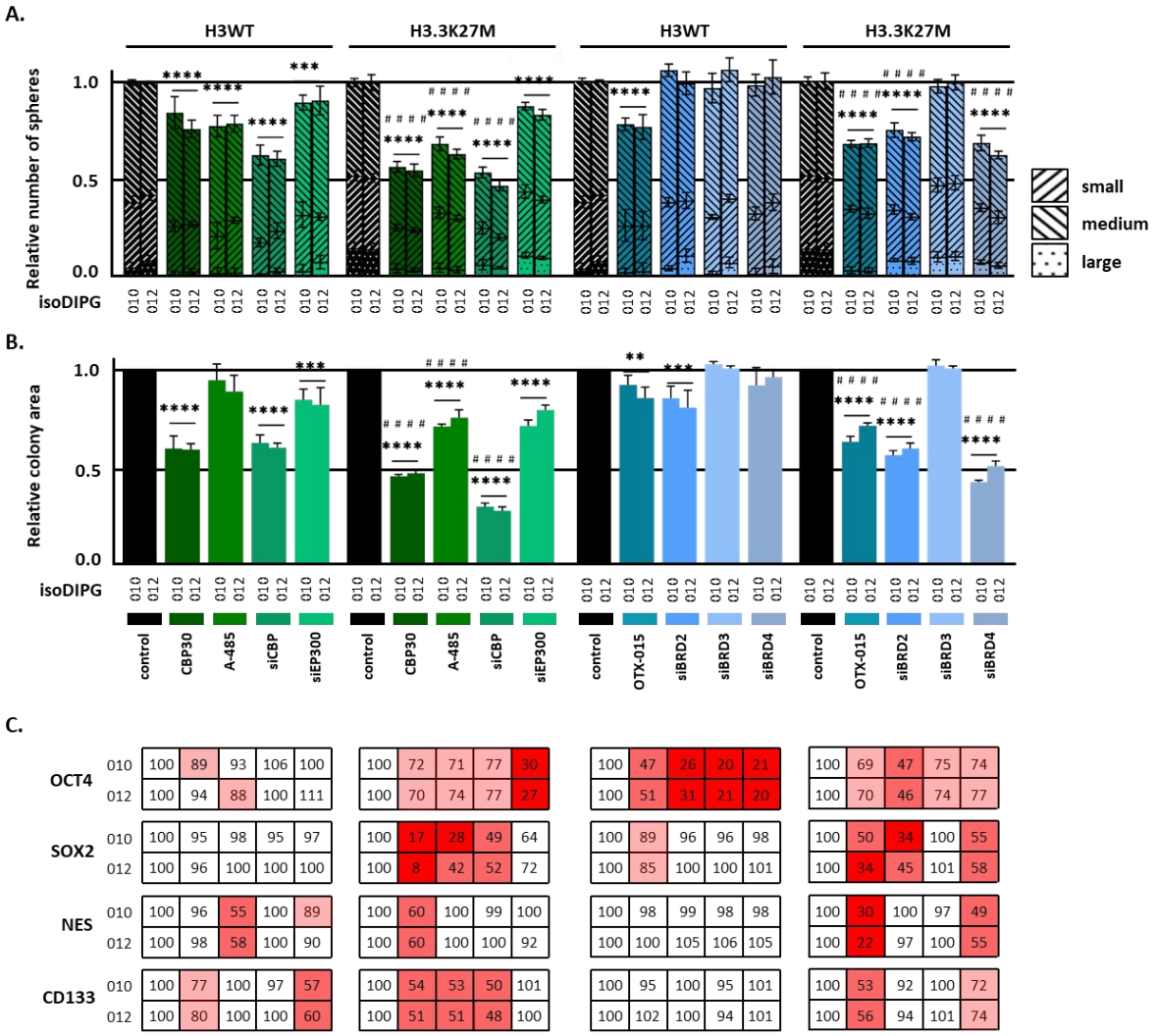

Figure 26 | CBP/p300 and BET proteins are essential for stemness features of isoDIPG-H3.3K27M cells.
isoDIPG-H3WT and isoDIPG-H3.3K27M cell lines were subjected to (A) sphere and (B) colony formation assays. (C) mRNA expression of stemness markers *POU5F1* (OCT4), *SOX2*, *NES* (Nestin) and *PROM1* (CD133) was investigated using qPCR and normalized to ß-actin after knockdown and inhibition of CBP/p300 and BET proteins, as indicated. Percentage of the remained expression was summarized and a color code was used to highlight different gene expression levels in dependence on the respective knockdown and inhibition effects. */# $p < 0.05$; **/## $p < 0.01$; ***/### $p < 0.005$; ****/#### $p < 0.001$ # used for comparison between isoDIPG-H3WT and isoDIPG-H3.3K27M cells.

CBP/p300

Knockdown of CBP and inhibition of BD and HAT activity of CBP/p300 using CBP30 and A-485, respectively, resulted in a strong decrease of sphere formation ability in both tested cell lines, to a significantly higher extent in isoDIPG-H3.3K27M cells of approximately 50%, while in isoDIPG-H3WT with only approximately 20% reduction compared to untreated control cells (**Figure 26A**). However, knockdown of p300 was less efficient and caused only slight sphere reduction of 10%, irrespectively of H3-mutation status (**Figure 26A**).

Colony forming capacity was evaluated under differentiating culture conditions. As already shown in sphere formation assay, BD inhibition with CBP30 as well as CBP knockdown resulted in pronounced reduction of colony formation to a significantly higher extent in isoDIPG-H3.3K27M cells with 50% inhibition for CBP30 treatment and 70% for CBP knockdown, while in isoDIPG-H3WT with approximately 45% reduction compared to untreated control cells (**Figure 26B**). In comparison, inhibition of CBP/p300 HAT activity by A-485 and p300 knockdown resulted in less severe effects, but still significant in isoDIPG-H3WT and isoDIPG-H3.3K27M cells of approximately 20%, irrespectively of H3-mutation status (**Figure 26B**).

Additionally, the overall stronger effect of inhibition and siRNA-mediated knockdown of CBP/p300 on clonogenicity in isoDIPG-H3.3K27M cells had been reflected by strong regulation of common stemness markers on mRNA level. OCT4 *(POU5F1*), SOX2, Nestin and CD133 (*PROM1*) expression were evaluated and remained overall mainly unchanged in isoDIPG-H3WT cells, whereas inhibition and knockdown of CBP/p300 in isoDIPG-H3.3K27M cells showed strong effects especially on expression of OCT4, SOX2 and CD133 (**Figure 26**). Interestingly, differential effects were found after knock down of p300 which resulted in strongest reduction of OCT4 (**Figure 26C**), but not of the glioma stemness marker CD133 (**Figure 26C**), whereas CBP knockdown showed opposite effects pointing to the differential function of CBP and p300 in isoDIPG-H3.3K27M cells.

BET proteins

In isoDIPG-H3WT cells, sphere as well as colony formation abilities were decreased only upon BET bromodomain inhibition by OTX-015 of approximately 20% in isoDIPG-H3WT and 40% in isoDIPG-H3.3K27M cells compared to untreated control cells (**Figure 26A and 26B**). Additionally, in isoDIPG-H3.3K27M cells clonogenicity was diminished not only after OTX-015 treatment, but also upon knockdown of BRD2 and BRD4 of approximately 60% compared to untreated control cells. Only BRD3 knockdown had no effect on stemness potential (**Figure 26A and 26B**).

In addition, the overall stronger effect of BET inhibition and knockdown on clonogenicity in isoDIPG-H3.3K27M cells was reflected by stronger regulation of selected stemness markers on mRNA level. OCT4 *(POU5F1*), Nestin and CD133 (*PROM1*) expression had been evaluated and remained overall mainly unchanged in isoDIPG-H3WT cells, whereas inhibition and knockdown of BET proteins in isoDIPG-H3.3K27M cells showed stronger effects on Nestin, SOX2 and CD133 expression (**Figure 26C**). Interestingly, expression of OCT4 was the only marker that turned out to be more affected in isoDIPG-H3WT cells compared to isoDIPG-H3.3K27M cells upon BET proteins inhibition and knockdown, suggesting different mechanism behind maintaining stem cell-like characteristics in dependence on H3-mutation status in DIPG cells (**Figure 26C**).

Moreover, in isoDIPG-H3.3K27M cells knockdown of BRD2 affected OCT4 expression more profoundly (**Figure 26C**), while knockdown of BRD4 had a stronger effect on Nestin and CD133 expression (**Figure 26C**), pointing out to the differential function of BRD2 and BRD4 in isoDIPG-H3.3K2M cells.

4.2.4.3 CBP, BRD2 and BRD4 are essential for invasive properties especially in isoDIPG-H3.3K27M cells

The ability of tumor cells to invade into surrounding tissue is an important characteristic of the malignant phenotype observed in DIPG tumors. To investigate if CBP/p300 and BET proteins are essential for migration and invasion ability of DIPG cells migration and invasion assays were performed. Additionally, qPCR analyses were carried out to investigate expression of common mesenchymal markers on mRNA level which are usually associated with the migratory and invasive potential of glioma cells (**Figure 27**).

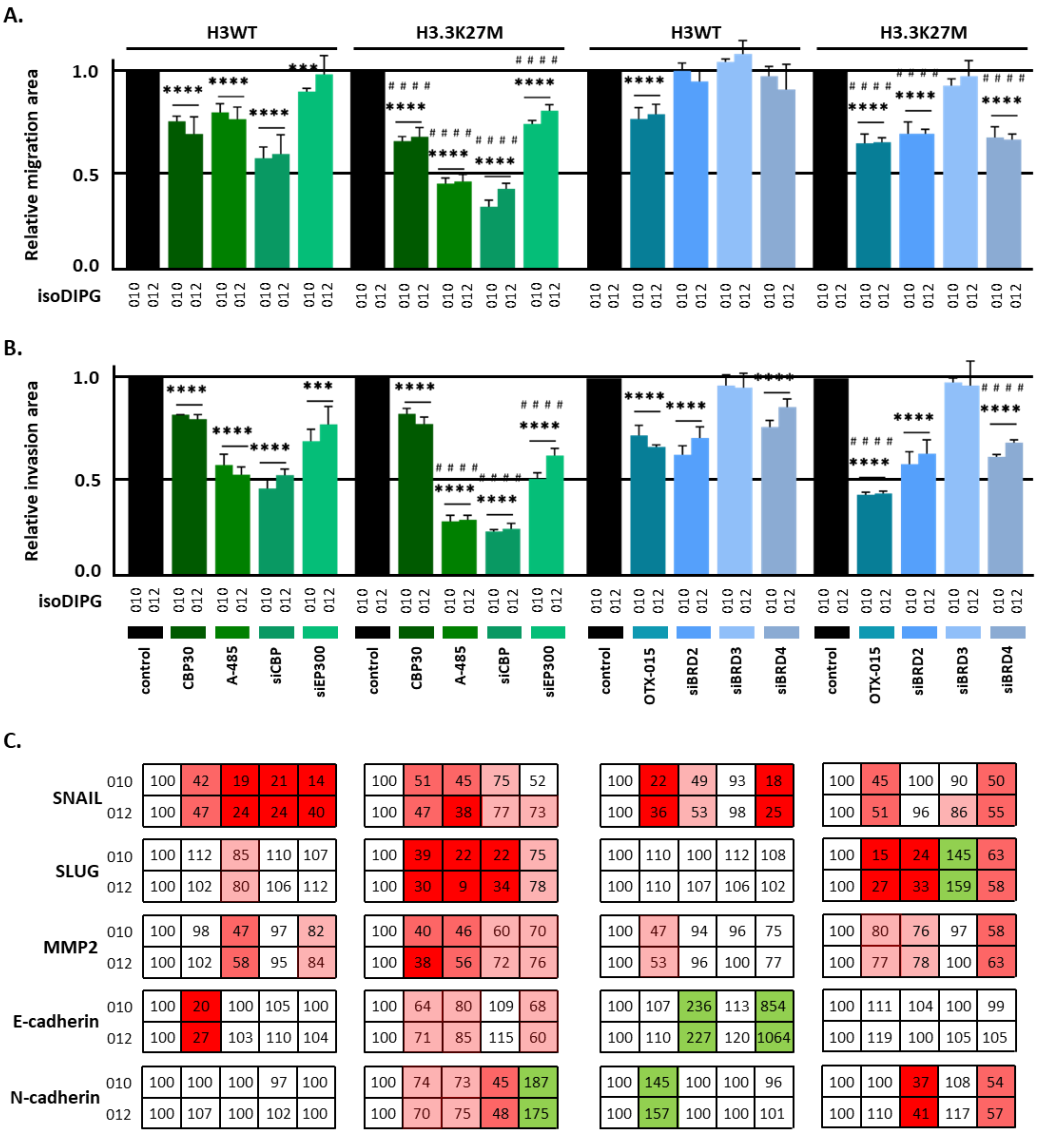

Figure 27 | CBP/p300 and BET proteins are essential for malignant phenotype of isoDIPG-H3.3K27M cells.
isoDIPG-H3WT and isoDIPG-H3.3K27M cell lines were subjected to (A) migration and (B) invasion assays (C) mRNA expression of mesenchymal markers *SNAI1* (SNAIL), *SNAI2* (SLUG), *MMP2*, *CDH1* (E-cadherin) and *CDH2* (N-cadherin) was investigated using qPCR and normalized to ß-actin after knockdown and inhibition of CBP/p300 and BET proteins, as indicated. Percentage of the remained expression was summarized and a color code was used to highlight different gene expression levels in dependence on the respective knockdown and inhibition effects. */# $p < 0.05$; **/## $p < 0.01$; ***/### $p < 0.005$; ****/#### $p < 0.001$ # used for comparison between isoDIPG-H3WT and isoDIPG-H3.3K27M cells.

CBP/p300

Knockdown of CBP and p300 as well as inhibition of bromodomain and HAT activity of CBP and p300 strongly reduced migration and invasion abilities in both tested cell lines, to a significantly higher extent in isoDIPG-H3.3K27M cells. CBP30 treatment resulted in reduction of migration and invasion abilities of approximately 40% in isoDIPG-H3.3K27M cells, while in isoDIPG-H3WT cells with only approximately 25% reduction compared to untreated control cells (**Figure 27A and 27B**). Whereas A-485 treatment as well as CBP knockdown caused reduction of mesenchymal phenotype of approximately 60% in isoDIPG-H3.3K27M cells and in isoDIPG-H3WT cells with only approximately 40% reduction compared to untreated control cells (**Figure 27A and 27B**). Knockdown of p300, however, resulted in reduction of migration ability of 40% in isoDIPG-H3.3K27M cells, whereas in isoDIPG-H3WT cells only in a slight decrease of 10% compared to untreated control cells (**Figure 27A**). Moreover, invasion ability of isoDIPG-H3.3K27M after p300 knockdown was reduced to approximately 50%, while in isoDIPG-H3WT only to 30% (**Figure 27B**).

In addition, the overall stronger effects of inhibition and siRNA-mediated knockdown of CBP/p300 on malignant phenotype in isoDIPG-H3.3K27M cells were reflected by strong regulation of common mesenchymal markers on mRNA level. SNAIL (*SNAI1*), SLUG (*SNAI2*), MMP2, E-cadherin (*CDH1*) and N-cadherin (*CDH2*) expression were evaluated and remained overall mainly unchanged in isoDIPG-H3WT cells, whereas inhibition and knockdown of CBP/p300 in isoDIPG-H3.3K27M cells showed strong reduction of SNAIL, SLUG, MMP2, E-cadherin and N-cadherin expression (**Figure 27C**). Interestingly, expression of SNAIL was found to be strongly influenced by inhibition and knockdown of CBP/p300 in isoDIPG-H3WT cells (**Figure 27C**). Furthermore, in isoDIPG-H3.3K27M cells expression of E-cadherin was reduced by p300 knockdown, but not affected by knockdown of CBP, while N-cadherin expression was decreased upon CBP and increased upon p300 knockdown, respectively (**Figure 27C**). This finding points to an important function of CBP in mesenchymal, while p300 in epithelial characteristics in isoDIPG-H3.3K27M cells.

BET proteins

Inhibition of BET proteins and siRNA-mediated knockdown of BRD2 and BRD4 resulted in a strong reduction of migration and invasion in isoDIPG-H3.3K27M cells of approximately 40% and 50%, respectively, while in isoDIPG-H3WT cells migration ability was reduced of approximately 20% compared to control cells (**Figure 27A and 27B**). In addition, in isoDIPG-H3WT cells level of migration was found to be slightly reduced upon BET proteins inhibition of approximately 15% compared to control cells (**Figure 27A**). Knockdown of BRD3 had no significant effect on migration and invasion, irrespectively of H3-mutation status (**Figure 27A**).

Additionally, the overall stronger effects of inhibition and siRNA-mediated knockdown of BET proteins on the malignant phenotype of isoDIPG-H3.3K27M cells were reflected by strong regulation of common mesenchymal markers on mRNA level: SNAIL (*SNAI1*), SLUG (*SNAI2*), MMP2, E-cadherin (*CDH1*) and N-cadherin (*CDH2*) expression were evaluated and remained overall mainly unchanged in isoDIPG-H3WT cells, whereas inhibition or/and knockdown of BET proteins in isoDIPG-H3.3K27M cells resulted in a strong reduction of SNAIL, SLUG, MMP2, E-cadherin and N-cadherin expression (**Figure 27C**). Similar to CBP/p300 inhibition and siRNA-mediated knockdown, expression of SNAIL has been found to be strongly influenced by inhibition and knockdown of BET proteins in isoDIPG-H3WT cells compared to isoDIPG-H3.3K27M cells (**Figure 27C**). Moreover, expression of E-cadherin was found to be significantly upregulated upon BRD4 knockdown exclusively in isoDIPG-H3WT cells (**Figure 27C**).

In conclusion, CBP, p300, BRD2 and BRD4 seem to play a different role in mediating certain tumor-associated characteristics in dependence on H3-mutation status reflected by proliferation assays, sphere and colony formation as well as migration and invasion assays. These findings were also supported by the differential regulation of common genes contributing to stemness or mesenchymal phenotype by CBP/p300 and BET proteins. Overall, CBP, p300, BRD2 and BRD4 appear to play a more profound role in the expression of tumor-associated characteristic in isoDIPG-H3.3K27M cells compared to isoDIPG-H3WT cells.

4.2.5 CBP and p300 influence global gene expression pattern to a significantly higher extent in isoDIPG-H3.3K27M cells compared to isoDIPG-H3WT cells

In order to discover CBP and p300-dependent differentially regulated subsets of genes in isoDIPG-H3WT and isoDIPG-H3.3K27M cells mRNA sequencing was performed. To identify global differences in gene expression after CBP and p300 knockdown and inhibition in isoDIPG-

H3WT (**Figure 28A**) and isoDIPG-H3.3K27M cells (**Figure 28B**) principal component analysis (PCA) plot was used.

The effect of knockdown of CBP and p300 on global gene expression pattern was stronger in isoDIPG-H3.3K27M cells compared to isoDIPG-H3WT cells. In addition, inhibition of CBP/p300 bromodomain led to more profound mRNA expressional changes in isoDIPG-H3.3K27M cells (**Figure 28B**). In contrast HAT inhibition of CBP/p300 resulted in stronger changes in gene expression in isoDIPG-H3WT cells (**Figure 28A**).

Additionally, in isoDIPG-H3.3 K27M cells CBP/p300 BD inhibition had similar effects on gene expression as knockdown of CBP, while CBP/p300 HAT activity inhibition shared differentially expressed genes with p300 knockdown indicating a role of CBP associated with BD and p300 with HAT function in H3.3 K27M-mutated DIPG cells (**Figure 28B**).

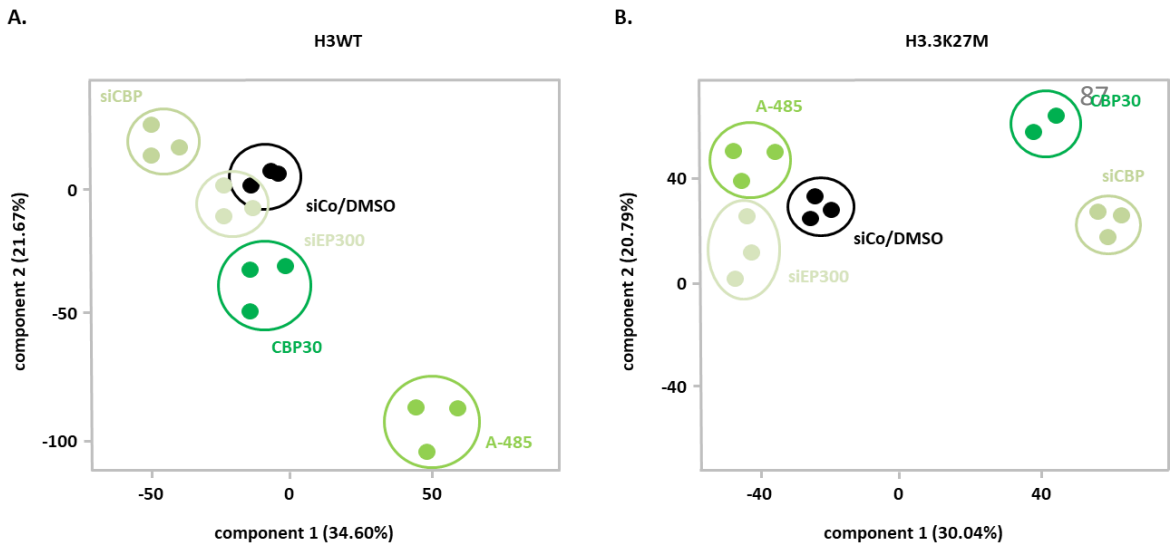

Figure 28 | CBP and p300 differently affect gene expression in isoDIPG-012-H3WT and isoDIPG-012-H3.3K27M cells.
Principal component analysis (PCA) of global gene expression in isoDIPG-012- (A) H3WT and (B) H3.3K27M cells after inhibition and knockdown of CBP and p300.

4.2.5.1 CBP and p300 play a more profound role in isoDIPG-H3.3K27M cells

To investigate transcriptional regulatory function of CBP and p300 in dependence on H3-mutation status, venn diagram and gene set enrichment analyses were performed using 2-fold enriched and 0.5-fold reduced genes upon inhibiton and knockdown of CBP and p300.

818 genes in isoDIPG-H3WT cells and 950 in isoDIPG-H3.3K27M cells were differentially regulated after inhibition of BD of CBP/p300 by CBP30 (**Figure 29A**). Although the expression of only 87 genes were found to be commonly changed in isoDIPG-H3WT and isoDIPG-H3.3K27M

cells after CBP30 treatment, these genes revealed an enrichment of biological processes such as nervous system development, cell locomotion, motility and migration (**Appendix J**).

Inhibition of HAT activity of CBP/p300 by A-485 revealed 1189 differentially regulated genes in isoDIPG-H3WT cells that are involved in cell morphogenesis as well as neurogenesis and Wnt signaling pathway. While in isoDIPG-H3.3K27M cells 923 genes were differentially regulated upon A-485 treatment and associated with processes like cell proliferation and migration, but also angiogenesis, cell death and apoptotic processes (**Figure 29B; Appendix J**).

Knockdown of CBP revealed only 7 differentially expressed genes in isoDIPG-H3WT cells, while in isoDIPG-H3.3K27M cells 2054 genes were found to be associated with important tumor-associated mechanisms such as cell migration and cell proliferation, as well as regulation of apoptosis, already indicating a more profound role of CBP in isoDIPG-H3.3K27M cells (**Figure 29C; Appendix J**).

In contrast p300 knockdown was less effective in isoDIPG-H3.3K27M cells than knockdown of CBP resulting in 439 differentially regulated genes associated with processes such as cell migration, proliferation and adhesion, but also in blood vessel development (**Figure 29D; Appendix J**). Only 42 genes were differentially regulated in isoDIPG-H3WT cells.

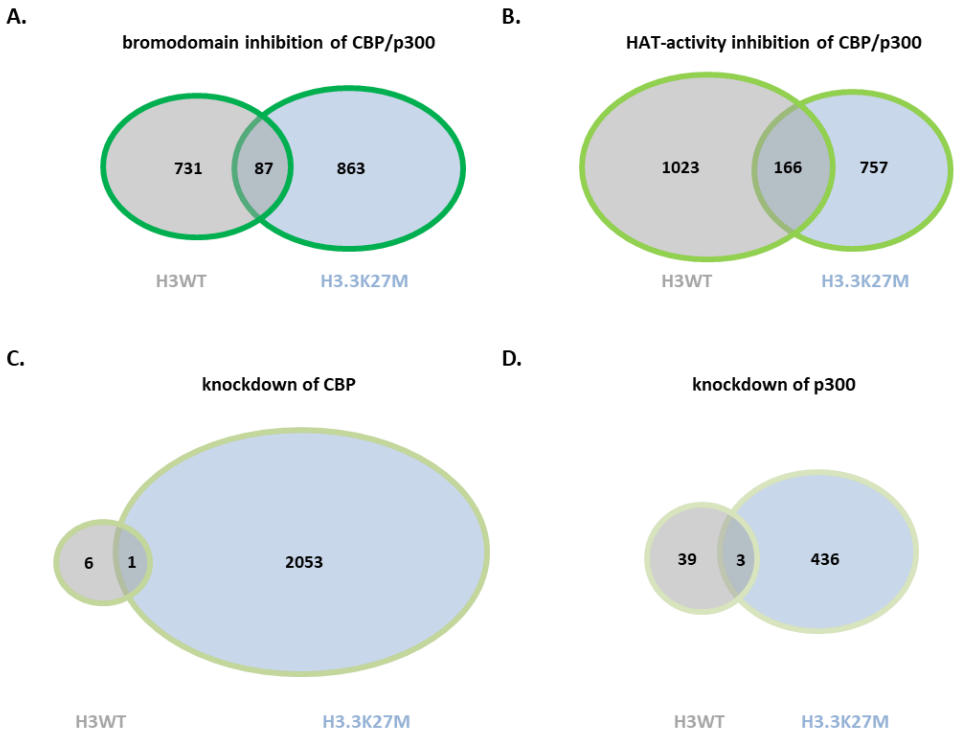

Figure 29 | CBP and p300 display a more profound function in isoDIPG-012-H3.3K27M cells. Venn diagram analyses showed commonly regulated 0.75-fold downregulated and 1.5-fold upregulated (adjusted p-value ≤0.05) genes in isoDIPG-H3WT and isoDIPG-H3.3K27M cells after (A) CBP/p300 HAT activity inhibition by A-485, (B) CBP/p300 bromodomain inhibition by CBP30, (C) CBP knockdown and (D) p300 knockdown in isoDIPG-012 cells**.**

In summary, CBP and p300 appear to play a more profound role in isoDIPG-H3.3K27M cells compared to isoDIPG-H3WT cells. Moreover, gene set enrichment analysis pointed out to a specific function of CBP and p300 in cell proliferation and migration in isoDIPG-H3.3 K27M cells. Additionally, CBP was found to be involved in cell cycle and apoptosis, while p300 was associated with angiogenesis.

4.2.5.2 CBP and p300 fulfill epigenetic writer and reader functions in isoDIPG-H3.3K27M cells

To dissect specific bromodomain- and HAT-dependent function of CBP and p300, commonly expressed genes after BD/HAT inhibition of CBP/p300 and knockdown of CBP and p300 were assesed and subjected to GO-annotation analysis.

In isoDIPG-H3WT cells almost no genes were found to be regulated by CBP or p300 knockdown (**Appendix K**). In consequence, no GO-annotation analysis of potential overlapping genes in isoDIPG-H3WT cells after BD or HAT inhibiton of CBP/p300 and upon CBP and p300 knockdown was carried out.

In contrast, in isoDIPG-H3.3K27M cells approximately 25% of all CBP target genes were changed after BD inhibition of CBP/p300 (**Figure 30A**). These genes were mainly involved in cell differentiation and neurogenesis (**Figure 30C**). On the other hand, more than 11% of all CBP target genes were changed after HAT activity inhibition of CBP/p300 (**Figure 30B**) and associated with angiogenesis processes and programmed cell death (**Figure 30D**). Furthermore, commonly enriched CBP-dependend pathways after BD and HAT activity inhibition of CBP/p300 were also discovered including cell proliferation and migration.

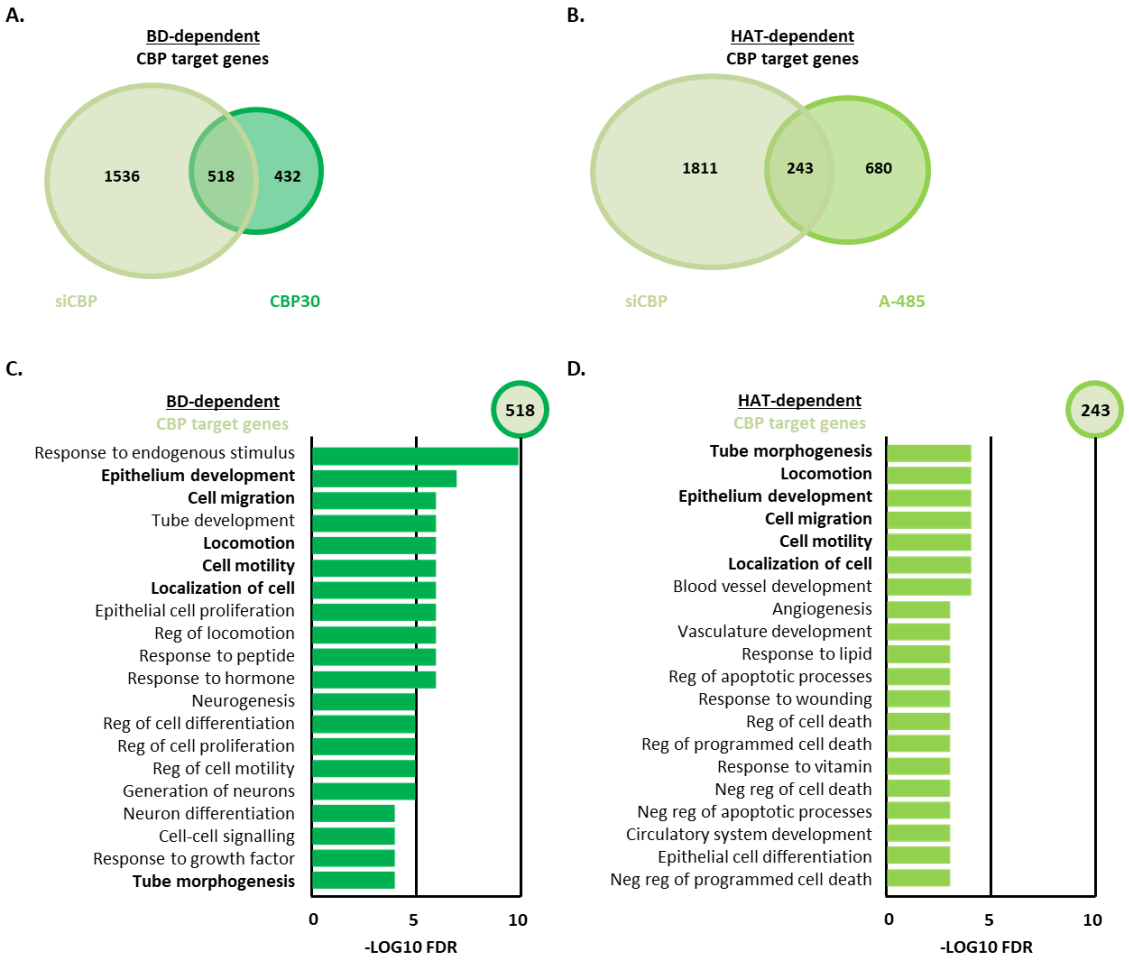

Figure 30 | CBP fulfills epigenetic writer and reader function in isoDIPG-012-H3.3K27M cells. Venn diagram analyses showed commonly regulated 0.75-fold downregulated and 1.5-fold upregulated (adjusted p-value ≤0.05) genes after (A) HAT activity or (B) BD inhibition of CBP/p300 and knockdown of CBP in H3.3K27M-mutated isoDIPG-012 cells, as indicated. Gene set enrichment analyses revealed (C) BD and (D) HAT CBP-dependent biological processes in isoDIPG-H3.3K27M cells**.** Highlighted in bold common processes were found after CBP knockdown and CBP/p300 HAT and BD inhibition**.**

In order to discover specific CBP/p300 BD and HAT-activity associated p300-dependent processes in isoDIPG-H3.3K27M cells, commonly expressed genes after BD or HAT inhibition and knockdown of p300 were investigated.

144 commonly regulated genes upon BD inhibition and knockdown of p300 were identified (**Figure 31A**). Those genes were found to regulate biological processes such as regulation of signaling and locomotion (**Figure 31C**). Whereas upon HAT activity inhibition and knockdown of p300, 149 genes were found to be commonly regulated in isoDIPG-H3.3K27M cells (**Figure 31B**) which were found to be associated with regulation of MAPK cascade and apoptosis (**Figure 31D**). Commonly enriched p300-dependend pathways after HAT and BD inhibition were discovered including cell proliferation, motility and migration (**Figure 31C and 31D**).

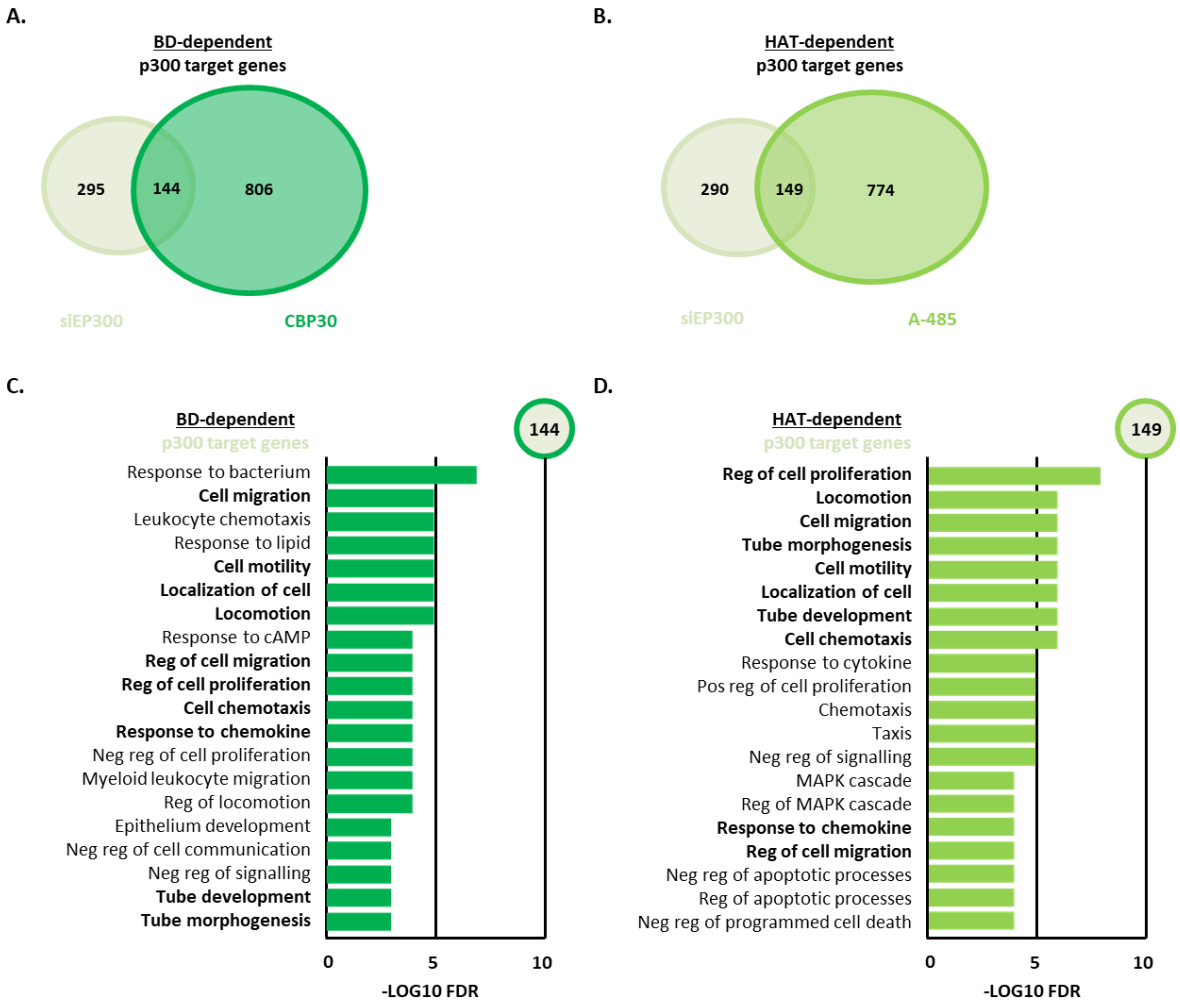

Figure 31 | p300 fulfills epigenetic writer and reader function in isoDIPG-012-H3.3K27M cells. Venn diagram analyses showed commonly regulated 0.75-fold downregulated and 1.5-fold upregulated (adjusted p-value ≤0.05) genes after (A) HAT activity or (B) BD inhibition and knockdown of p300 in isoDIPG-012-H3.3K27M cells. Gene set enrichment analyses revealed (C) BD and (D) HAT p300-dependent biological processes in isoDIPG-012-H3.3K27M cells. Highlighted in bold common processes had been found after p300 knockdown and p300 HAT and bromodomain inhibition.

To conclude, CBP and p300 fulfil epigenetic writer and reader function regulating specific biological processes in isoDIPG-H3.3K27M cells. BD-dependent CBP target genes exclusively regulate neurogenesis, whereas HAT-dependent CBP target genes are involved in regulation of programmed cell death. p300 target genes are associated with MAPK cascade and apoptotic processes in HAT-dependent manner.

4.2.5.3 HAT activity of CBP/p300 regulates apoptosis in isoDIPG-012-H3.3K27M cells

Since gene set enrichment analysis revealed that HAT-dependent CBP and p300 target genes play a role in regulation of programmed cell death **(Figure 30D)**, induction of apoptosis was investigated in isoDIPG-H3.3K27M cells. To this end, expression of three different apoptosis

protein markers was investigated using western blot analyses. In line with previous results, cleaved poly(ADP-Ribose) polymerase 1 (PARP), cleaved Caspase 3 and Bcl-2 associated X-protein (Bax) were found to be upregulated upon HAT activity inhibition of CBP/p300 in isoDIPG-H3.3K27M cells **(Figure 32A and 32B)**.

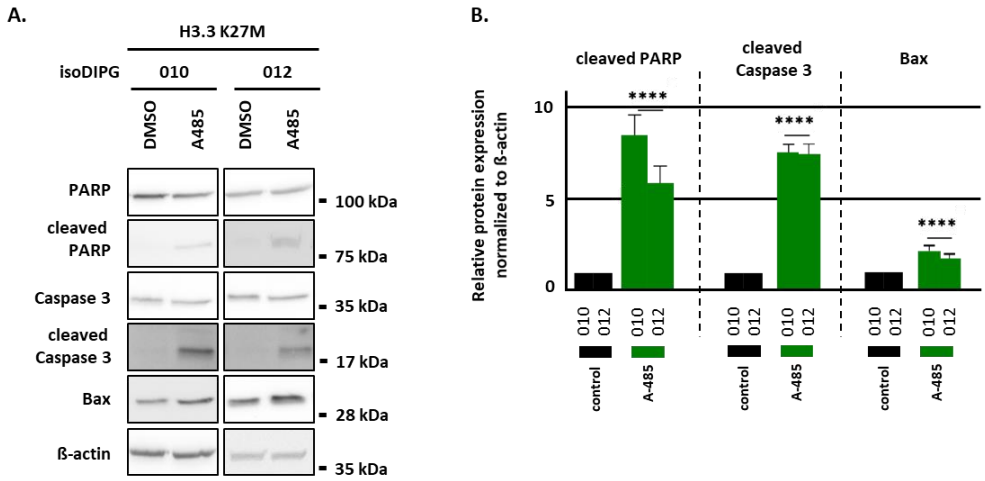

Figure 32 | HAT activity of CBP/p300 is involved in apoptosis regulation in H3.3K27M-mutated DIPG cells.
(A) Expression of cleaved PARP, cleaved Caspase 3 and Bax was investigated using western blot analyses after HAT activity inhibition of CBP/p300 by A-485 in isoDIPG-H3.3K27M cells. ß-actin served as loading control. (B) Densitometry analysis of performed western blots**.** * $p < 0.05$; ** $p < 0.01$; *** $p < 0.005$; **** $p < 0.001$.

To illustrate the effect of CBP/p300 HAT activity on apoptosis-related processes, KEGG pathway illustration was used showing upregulated (in green) and downregulated (in red) genes upon siRNA-mediated knockdown of CBP and p300 and A-485 treatment (**Appendix L**).

4.2.6 BET proteins influence global gene expression pattern to a significantly higher extent in isoDIPG-H3.3K27M cells

Principal component analysis (PCA) plot revealed differences in global gene expression after BET knockdown and inhibition in isoDIPG-H3WT (**Figure 33A**) and isoDIPG-H3.3K27M cells (**Figure 33B**). Distance of investigated control samples after knockdown of BET proteins turned out to be greater in isoDIPG-H3.3K27M than in isoDIPG-H3WT cells which suggests a more important function of BET proteins in isoDIPG-H3.3K27M cells. Combined BET proteins inhibition by OTX-015 had a strong effect on gene expression in isoDIPG-H3WT and isoDIPG-H3.3K27M cells (**Figure 33A and 33B**).

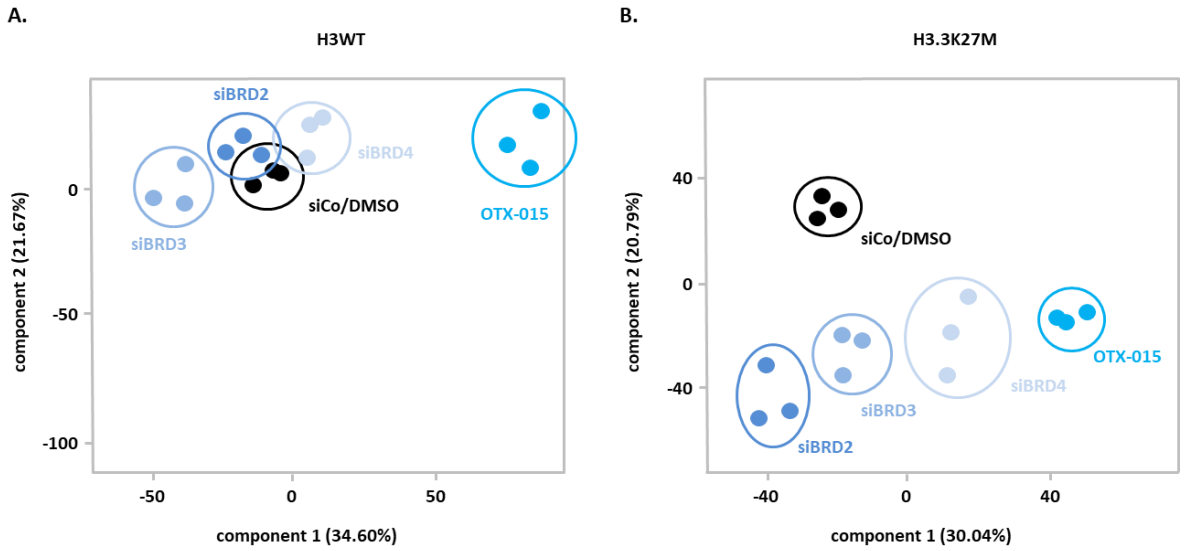

Figure 33 | BET proteins differentially affect gene expression in isoDIPG-012-H3WT and isoDIPG-012-H3.3K27M cells.
Principal component analysis (PCA) of global gene expression in of (A) isoDIPG-012-H3WT and (B) isoDIPG-012-H3.3K27M cells after inhibition and knockdown of BET proteins, as indicated**.**

To dissect distinct function of BRD2, BRD3 and BRD4 in dependence on H3-mutation status in isoDIPG cells venn diagram and gene set enrichment analyses were performed upon BET proteins inhibition and siRNA-mediated knockdown.

In isoDIPG-H3WT cells, 1802 differentially regulated genes were identified after OTX-015 treatment (**Figure 34A**). Those genes are mainly involved in cell adhesion (**Appendix M**). Whereas in isoDIPG-H3.3K27M cells inhibition of BET proteins by OTX-015 revealed 2126 differentially regulated genes (**Figure 34A**) that play a role in blood vessel development (**Appendix M**). In addition, commonly enriched pathways after BET inhibition in isoDIPG-H3WT and isoDIPG-H3.3K27M cells were discovered including cell differentiation, migration and motility as well as neurogenesis (**Appendix M**).

BRD2 knockdown had a minimal effect on global gene expression in isoDIPG-H3WT cells with only 9 differentially regulated genes (**Figure 34B**). Whereas in isoDIPG-H3.3K27M cells knockdown of BRD2 had a much more profound effect on gene expression resulting in 843 differentially regulated genes (**Figure 34B**) that were found to be involved in many processes contributing to cell motility, proliferation, migration, locomotion and neurogenesis (**Appendix M**).

Investigation of BRD3 function by siRNA mediated knockdown in dependence on H3-mutation status unveiled 6 differentially regulated genes in isoDIPG-H3WT DIPG cells (**Figure 34C**) (**Appendix M**). While in isoDIPG-H3.3K27M cells knockdown of BRD3 caused 85 genes to be differentially regulated with no significantly regulated biological processes (**Figure 34C**).

Knockdown of BRD4 in isoDIPG-H3WT cells revealed 131 differentially regulated genes (**Figure 34D**). Whereas in isoDIPG-H3.3K27M cells knockdown of BRD4 resulted in 704 diffferentially regulated genes (**Figure 34D**) that contribute to processes including cell differentiation, migration and motility as well as neurogenesis and cell death (**Appendix M**).

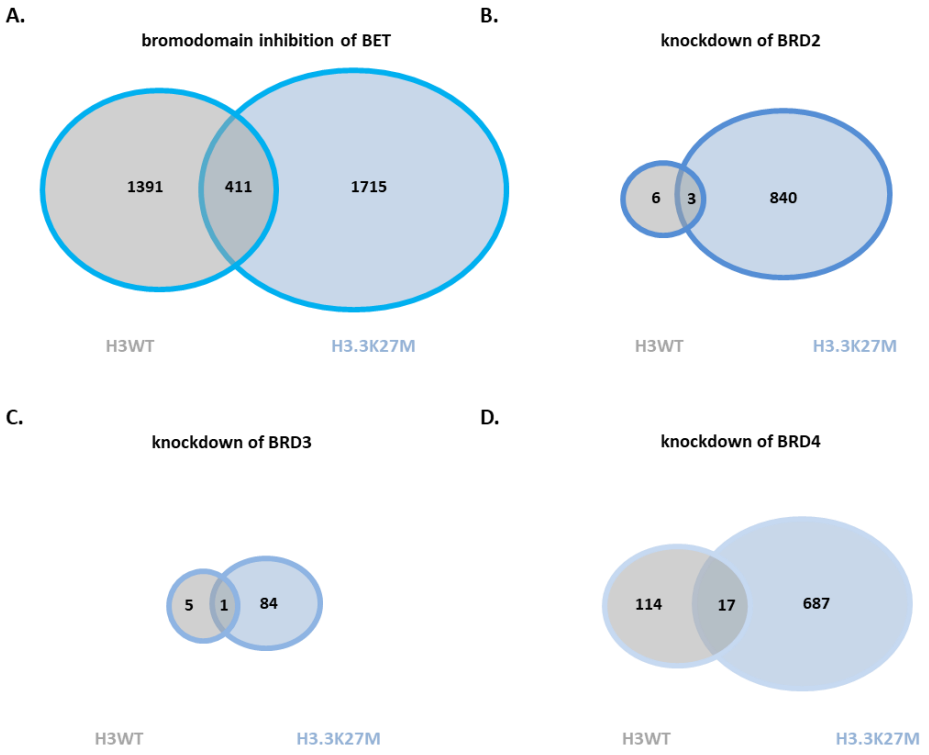

Figure 34 | BET proteins play a more crucial role in gene expression in isoDIPG-012-H3.3K27M cells.
Venn diagram analyses showed commonly regulated 0.75-fold downregulated and 1.5-fold upregulated (adjusted p-value ≤0.05) genes in isoDIPG-H3WT and isoDIPG-H3.3K27M cells after (A) BET proteins inhibition by OTX-015, (B) BRD2, (C) BRD3 and (D) BRD4 knockdown in isoDIPG-012 cells**.**

In summary, venn diagram analysis revealed a more important function of BET proteins in isoDIPG-H3.3 K27M cells compared to isoDIPG-H3WT cells. Furthermore, gene set enrichment analysis pointed out to a specific role of BET proteins in isoDIPG-H3.3K27M cells being involved, among others, in cancer-related processes such as cell proliferation, motility and migration.

4.2.6.1 BRD4 plays the most prominent role out of all BET proteins in isoDIPG-H3.3K27M cells

In order to dissect specific bromodomain-dependent function of each member of BET protein family in isoDIPG-H3.3K27M cells, venn diagram analyses were used.

Genes regulated by knockdown of BRD2, BRD3 and BRD4 did not share high similarity among each other (**Appendix N**). However, 487 commonly regulated genes were found upon OTX-015 treatment and siBRD2 transfection in isoDIPG-H3.3K27M cells (**Figure 35A**), whereas knockdown of BRD3 and inhibition of BET proteins revealed 33 commonly regulated genes (**Figure 35B**). However, these genes did not reveal any pathway enrichment. In contrast, 359 commonly regulated genes were found after OTX-015 treatment and BRD4 knockdown in isoDIPG-H3.3K27M cells (**Figure 35C**) being involved in processes such as DNA methylation, HDAC deacetylation of histones, DNA damage and Wnt signaling (**Figure 35C and 35D**).

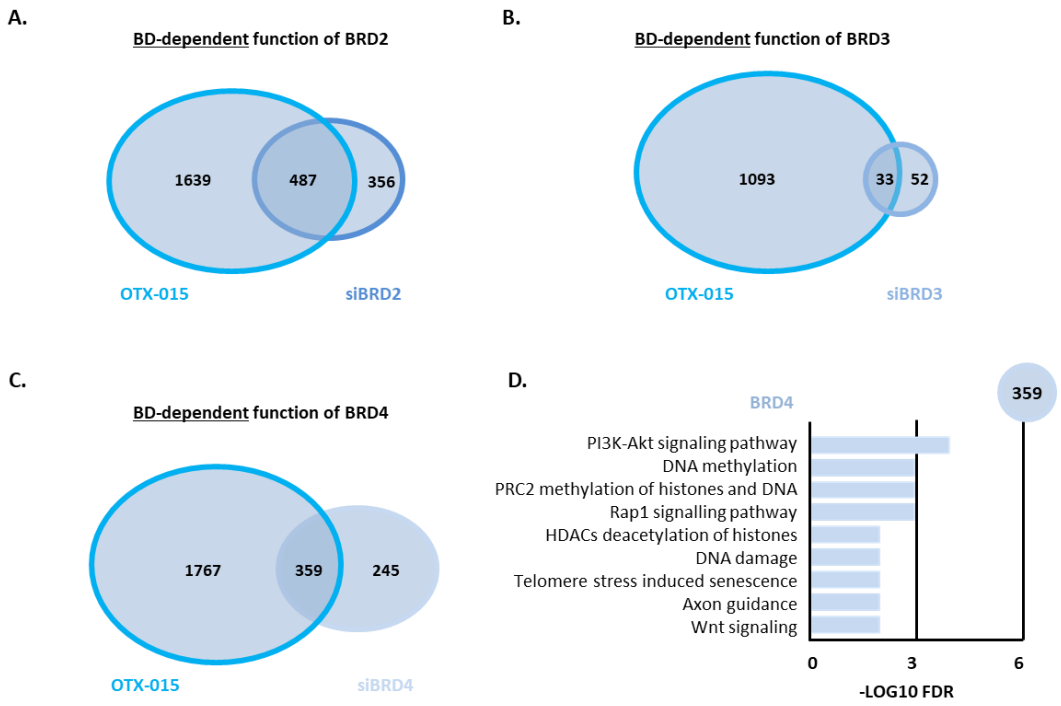

Figure 35 | Bromodomain function of BRD4 plays a crucial role in isoDIPG-012-H3.3K27M cells. Venn diagram analyses showed commonly regulated 0.75-fold downregulated and 1.5-fold upregulated (adjusted p-value ≤0.05) genes after BET inhibition by OTX-015 and knockdown of (A) BRD2, (B) BRD3 and (C) BRD4 in isoDIPG-H3.3K27M cells. (D) Gene set enrichment analyses revealed bromodomain-dependent BRD4-relevant biological processes in isoDIPG-012-H3.3 K27M cells.

In summary, out of BET protein family members, BRD4 seems to be the most epigenetically-relevant protein in isoDIPG-H3.3 K27M cells.

4.2.6.2 Inhibition of BRD4 induces cell cycle arrest in isoDIPG-H3.3K27M cells

Whole genome mRNA sequencing indicated a profound role of BRD4 in isoDIPG-H3.3K27M cells. To study H3.3K27M-mutation-dependent function of BRD4 in cell cycle progression, fluorescence activated cell sorting (FACS) analysis was performed after bromodomain inhibition of BET proteins (**Figure 36A**) which revealed that majority of OTX-015 treated isoDIPG-

H3.3K27M cells gathered in G1 phase (**Figure 36B**). In order to investigate different cell cycle-related key players on protein and mRNA level after inhibition of BET proteins western blot and qPCR analyses were performed. In line with the results obtained by FACS analysis, expression of cell cycle driver c-myc and cyclin-dependent kinase 2 (CDK2) were reduced after OTX-015 treatment on protein level (**Figure 36C; Appendix O**) and after knockdown of BRD4 on mRNA level (**Figure 36D**). In contrast, cell cycle inhibitors, cyclin-dependent kinase 4 (CDK4) and p38 mitogen-activated protein kinases, were upregulated upon BET protein inhibition (**Figure 36C; Appendix O**). Additionally, tumor suppressor proteins, p21 and p16, were found to be significantly elevated after OTX-015 treatment on protein level (**Figure 36C; Appendix O**) and also after knockdown of BRD4 on mRNA level (**Figure 36D**).

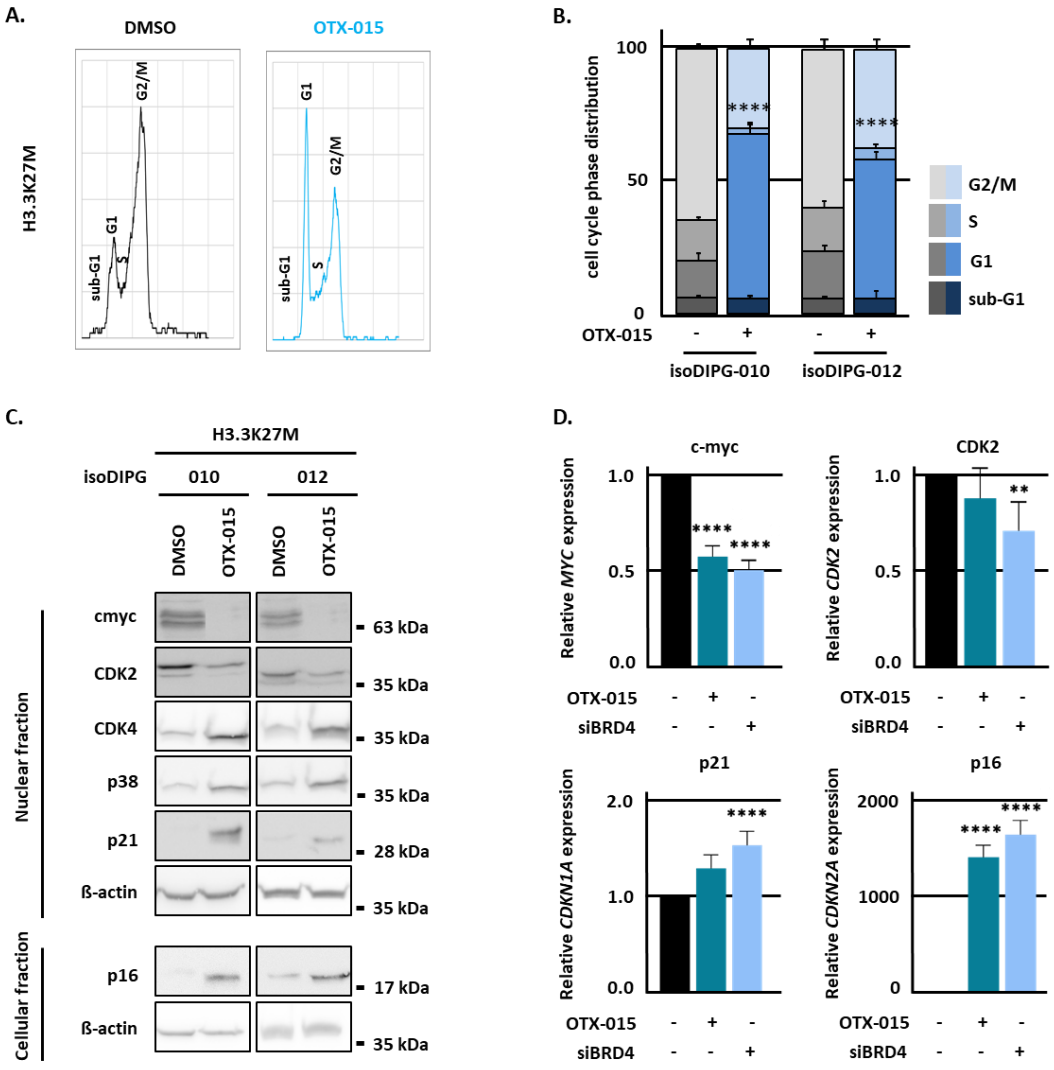

Figure 36 | Inhibition of BRD4 induces cell cycle arrest in isoDIPG-H3.3K27M cells.
(A) Fluorescence activated cell sorting (FACS) analysis was performed 24 h after OTX-015 treatment in isoDIPG-010-H3.3K27M and isoDIPG-012-H3.3K27M cells. (B) Quantification of FACS analysis revealed cell cycle phase distribution in isoDIPG-H3.3K27M cells. (C) Expression of c-myc, CDK2, CDK4, p38, p21 and p16 was investigated using western blot analyses after BET proteins inhibition in H3.3K27M-mutated isoDIPG-010 and isoDIPG-012 cells line. ß-actin served as loading control. (D) mRNA expression of cell

cycle-associated genes was investigated using qPCR and normalized to ß-actin**.** * p < 0.05; ** p < 0.01; *** p < 0.005; **** p < 0.001.

Furthermore, KEGG pathway analysis revealed several either upregulated (in green) or downregulated (in red) genes associated with cell cycle after BRD4 inhibition in isoDIPG-H3.3 K27M cells (**Appendix P**).

4.2.6.3 BRD4 regulates canonical Wnt signaling pathway in isoDIPG-H3.3K27M cells

Wnt signaling is associated with an increased cell proliferation and stemness characteristics, as well as oncogenesis of different tumor entities (Komiya and Habas 2008). Since gene set enrichment analysis revealed that BRD4 is involved in Wnt signaling pathway in isoDIPG-H3.3K27M cells (**Figure 37D**) expression of selected Wnt-related genes was investigated using mRNA sequencing. Inhibition and knockdown of BRD4 had a strong effect on expression of Wnt signaling-associated genes. Primarly, genes associated with activation of canonical Wnt signaling pathway were found to be downregulated upon BRD4 inhibition and knockdown in H3.3K27M-mutated DIPG cells, including *WNT10B*, *FZD4* and *WNT3A*. Moreover, expression of Wnt-components and target genes, *AXIN2* and *BAMBI*, was decreased upon BRD4 inhibition in isoDIPG-H3.3K27M cells. Additionally, another Wnt target gene, *CCN4*, was also found to be reduced upon BRD4 inhibition in isoDIPG-H3.3K27M cells (**Figure 37**).

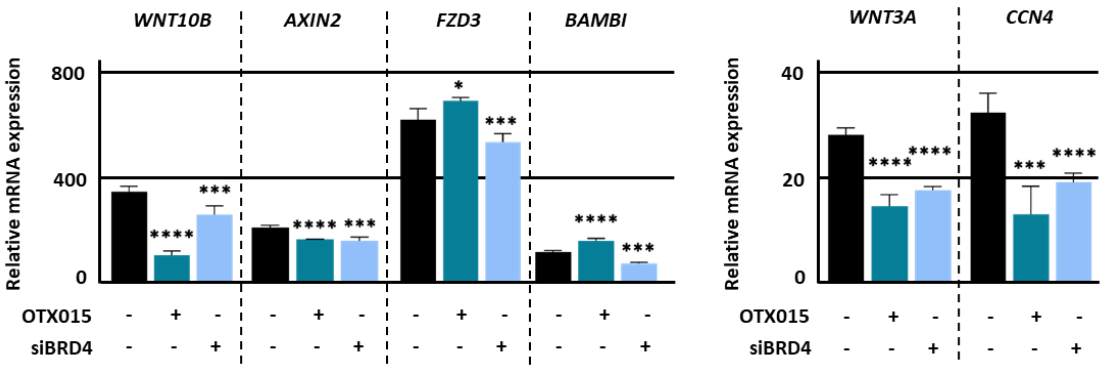

Figure 37 | BRD4 regulates canonical Wnt signaling pathway in isoDIPG-012-H3.3K27M cells. mRNA expression of Wnt signaling-associated genes was investigated using mRNA-sequencing in isoDIPG-012-H3.3 K27M cells. * p < 0.05; ** p < 0.01; *** p < 0.005; **** p < 0.001.

In summary, inhibition of BRD4 affects expression of several Wnt signaling-related genes which results in dysregulation of canonical Wnt signaling pathway in isoDIPG-H3.3K27M cells.

4.2.7 CBP/p300 and BET proteins inhibition reduce tumor growth *in vivo*

As previously shown (**Figure 23**), CAM assay is a suitable *in vivo* model to study H3.3K27M-dependent effects of chosen putative therapeutics. In order to investigate the impact of inhibition of CBP/p300 BD and HAT activity using CBP30 and A-485, respectively, as well as BET proteins inhibition by OTX-015 treatment in isoDIPG-H3WT and isoDIPG-H3.3K27M cells, CAM assay was used (**3.2.5.1**). Treatment with CBP/p300 and BET proteins inhibitors resulted in significant decrease of tumor size **(Figure 40B)** and volume (**Appendix R**), irrespectively of H3-mutation status. The strongest effects were observed after inhibition of BET proteins by OTX-015 treatment.

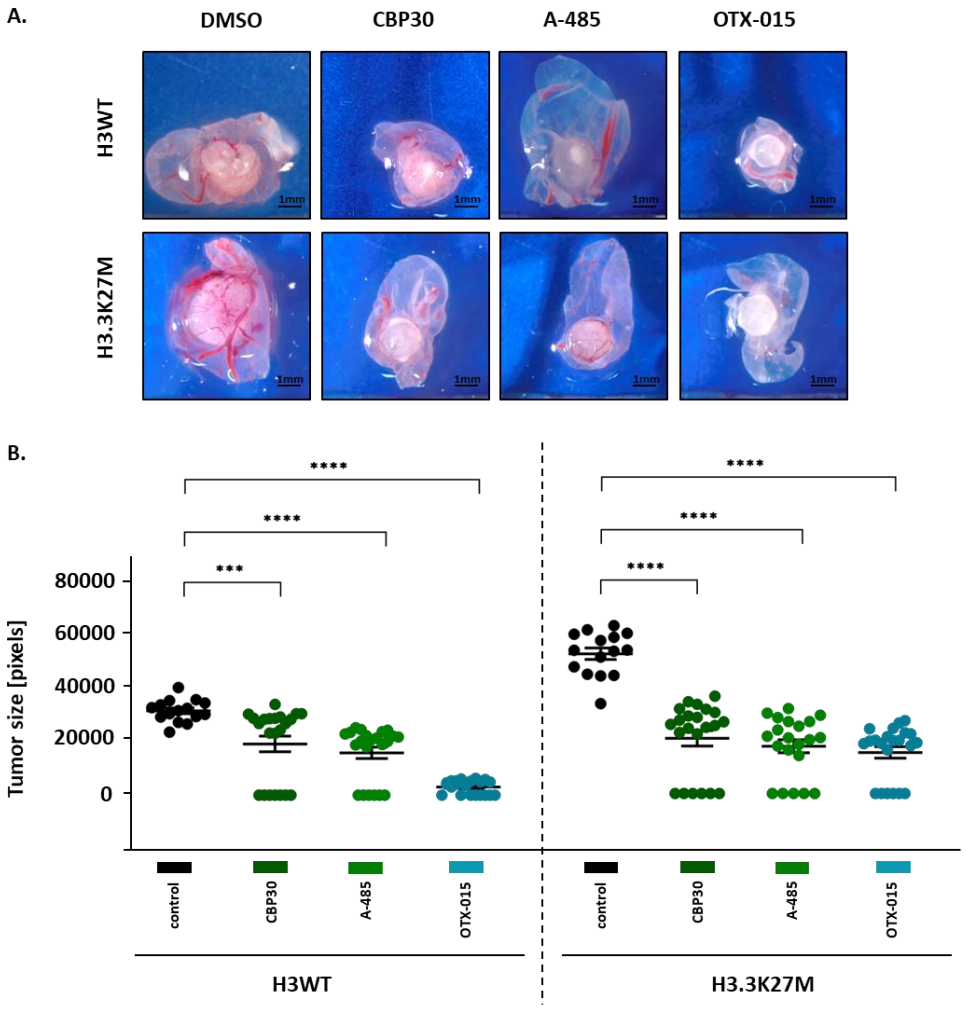

Figure 38 | Inhibition of CBP/p300 and BET proteins reduce size of isoDIPG-H3WT and isoDIPG-H3.3K27M derived tumors in CAM assay.
(A) Respective microscope photos of freshly harvested tumors and (B) quantification of tumor size after CBP30, A-485 and OTX-015 treatment in isoDIPG-012 cell line. * $p < 0.05$; ** $p < 0.01$; *** $p < 0.005$; **** $p < 0.001$.

To investigate effects of CBP30, A-485 and OTX-015 treatment in H3-wildtype and H3.3K27M-mutated DIPG tumors *in vivo*, expression of stemness markers OCT4 and CD133, oncogene c-myc, tumor suppressor gene p16 and vascular growth factor V (VEGFA) was analyzed on mRNA level using qPCR. In addition, previous *in vitro* results had been compared with the mRNA expression results obtained *in vivo* to find out if the *in vivo* data are reflected by the data obtained *in vitro*.

Expression of the stemness marker OCT4 was decreased after inhibition of CBP/p300 BD by CBP30 in isoDIPG-H3WT and isoDIPG-H3.3K27M cells *in vivo* and *in vitro*. Inhibition of CBP/p300 HAT activity by A-485 had no significant effect *in vitro* or *in vivo*, with the exception of isoDIPG-H3WT cells, where the expression of OCT4 was slightly reduced. BET proteins inhibition resulted in significantly increased expression of OCT4 in H3-wildtype tumors and remained unchanged in isoDIPG-H3WT cells. Whereas in isoDIPG-H3.3K27M cells, OCT4 expression was significantly decreased *in vivo* and *in vitro* (**Figure 39A**).

Expression of CD133 was significantly reduced upon all treatments in both, H3-wildtype and H3.3K27M-mutated DIPG tumors and cells with the exception of CBP/p300 HAT activity inhibition in isoDIPG-H3WT cells, where CD133 expression remained unchanged (**Figure 39B**).

Expression of oncogene, c-myc, was found to be downregulated after CBP30 treatment in H3-wildtype tumors and cells, while c-myc expression remained unchanged in H3.3K27M-mutated DIPG tumors and was reduced in isoDIPG-H3.3K27M cells. HAT activity of CBP/p300 inhibition also resulted in decreased c-myc expression *in vitro*, irrespective of H3-mutation status. Whereas, *in vivo*, in H3-wildtype DIPG tumors c-myc expression was significantly elevated, while in H3.3K27M-mutated DIPG tumors c-myc level was reduced. Surprisingly, upon OTX-015 treatment c-myc expression was found to be significantly increased in H3-wildtype tumors, while *in vitro* it remained unchanged. In isoDIPG-H3.3K27M cells and tumors c-myc expression was significantly reduced (**Figure 39C**).

Expression of tumor suppressor gene, p16, was found to be increased only in DIPG cells and tumors carrying H3.3K27M-mutation after CBP30 and OTX-015 treatment, to a significantly higher extent *in vitro*. Furthermore, p16 was significantly higher expressed *in vitro* than *in vivo* (**Figure 39D**).

Additionally, vascular growth factor gene expression, VEGFA, was investigated. The analysis revealed reduced levels of VEGFA in isoDIPG-H3WT and isoDIPG-H3.3K27M cells and tumors upon all performed treatments, with the significant distinction of HAT activity inhibition of CBP/p300 in H3.3K27M-mutated tumors (**Figure 39E**).

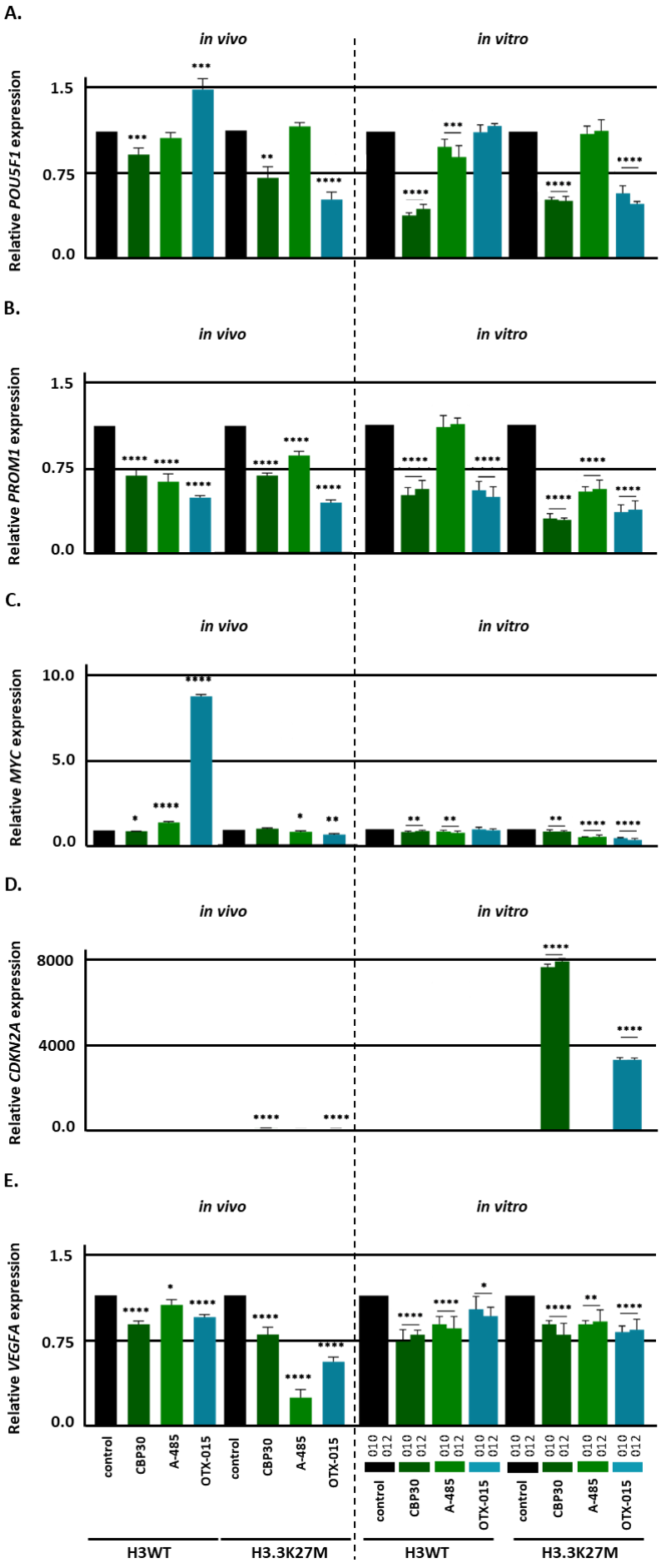
A.
in vivo
in vitro
Relative POU5F1 expression
1.5
0.75
0.0
B.
in vivo
in vitro
Relative PROM1 expression
1.5
0.75
0.0
C.
in vivo
in vitro
Relative MYC expression
10.0
5.0
0.0
D.
in vivo
in vitro
Relative CDKN2A expression
8000
4000
0.0
E.
in vivo
in vitro
Relative VEGFA expression
1.5
0.75
0.0
control
CBP30
A-485
OTX-015
H3WT
H3.3K27M
H3WT
H3.3K27M

Figure 39 | ***In vivo* CAM analysis reflects inhibiting effects of CBP/p300 and BET proteins inhibition in DIPG cells on tumor-related gene expression.**
mRNA expression of (A) *POU5F1*, (B) *PROM1*, (C) *MYC*, (D) *CDKN2A* and (E) *VEGFA* was investigated using mRNA sequencing. * $p < 0.05$; ** $p < 0.01$; *** $p < 0.005$; **** $p < 0.001$.

In conclusion, impact of investigated inhibitors found *in vitro* was also to some extent reflected in the CAM-DIPG tumor model *in vivo*. CBP/p300 and BET proteins inhibition reduced cell proliferation *in vitro* and tumor size *in vivo* of isoDIPG cells independently of H3-mutation status. Moreover, expression of stemness markers, oncogene c-myc and tumor suppressor p16 was similarly affected by CBP/p300 and BET proteins inhibition *in vitro* and *in vivo*.

4.3 Combined treatment with EZH2 and CBP/p300 inhibitors has no additive effect on cell proliferation and expression of H3K27me3 and H3K27ac in isoDIPG cells

CBP, p300 and EZH2 are epigenetically relevant proteins (Piunti et al. 2017; Greer and Shi 2012). The present study has already proven that CBP and p300 play a significant role in isoDIPG-H3.3K27M cells compared to isoDIPG-H3WT cells. In addition, impairment of EZH2 function might be responsible for the epigenetic imbalance observed in isoDIPG-H3.3K27M cells. Thus, combined treatment using CBP/p300 inhibitors (CBP30 and A-485) and EZH2 inhibitor (EPZ-6438) was investigated to find out if additive effects might be observed and if combined treatment could serve as novel therapeutic option.

In order to investigate the effect of combined treatment using two CBP/p300 inhibitors, inhibiting different function of CBP/p300, on cell viability, MTT cell viability assay was carried out. No additive effect of combinatory treatment on cell viability in isoDIPG-H3WT and isoDIPG-H3.3K27M cells was found (**Figure 40A**). To study the impact of EZH2 and CBP/p300 inhibition on cell viability in isoDIPG cells, CBP30 or A-485 treatment, respectively, was combined with EPZ/6438 treatment. No significant additive effect of the combined treatment approaches could be demonstrated for either CBP30/EPZ-6438 (**Figure 40B**) or A-485/EPZ-6438 (**Figure 40C**) in isoDIPG-H3WT and isoDIPG-H3.3K27M cells.

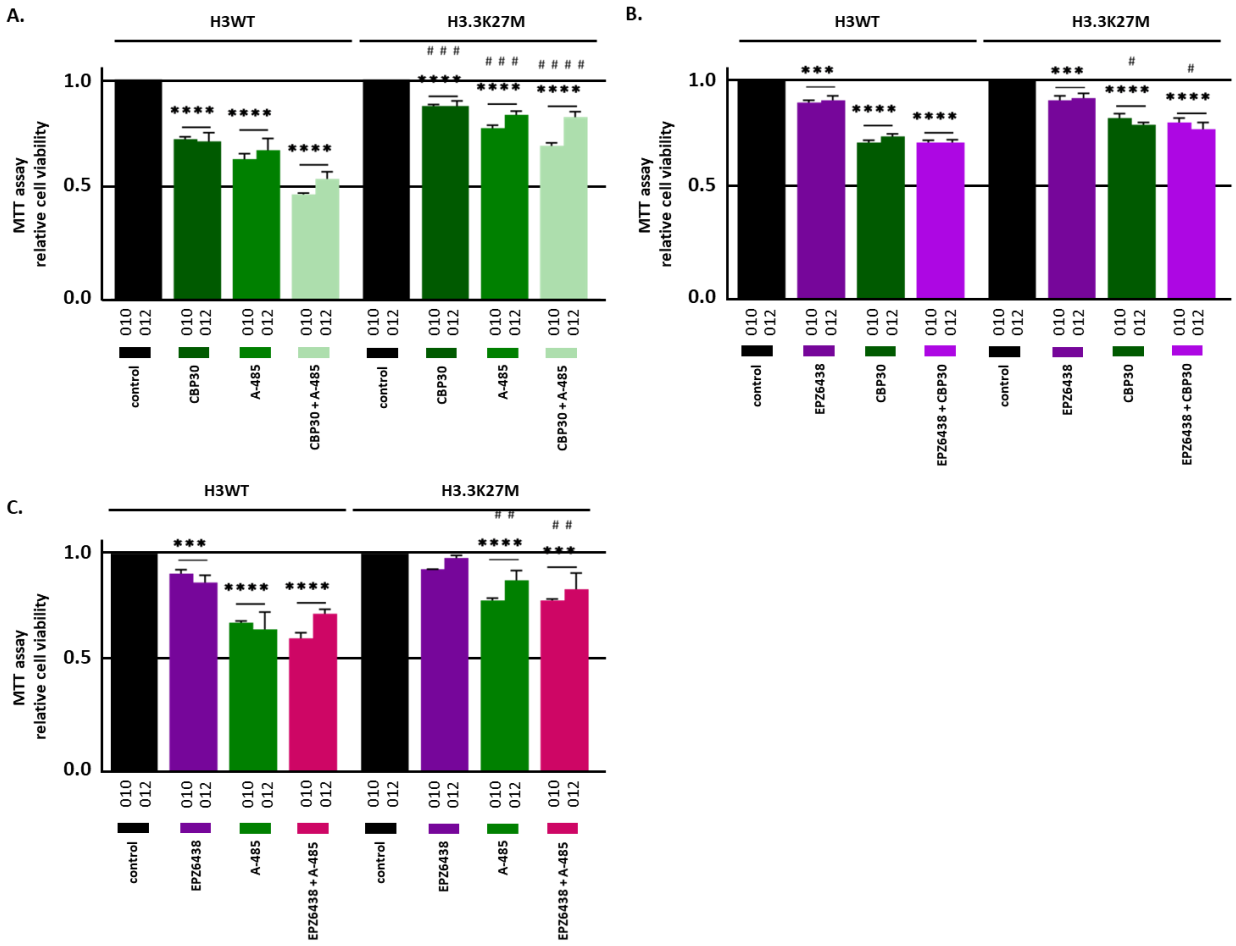

Figure 40 | Combined treatment approaches have no additive effect on cell viability in isoDIPG cell lines.
MTT cell viability assay was used to assess cell viability after single and combined treatment using (A) CBP30 and A-485, (B) EPZ-6438 and CBP30, (C) EPZ-6438 and A-485 in isoDIPG-H3WT and isoDIPG-H3.3K27M cell lines. */# $p < 0.05$; **/## $p < 0.01$; ***/### $p < 0.005$; ****/#### $p < 0.001$ # used for comparison between isoDIPG-H3WT and isoDIPG-H3.3K27M cells.

To investigate expression of H3K27me3 and H3K27ac after combined treatment of EZH2 (EPZ-6438) and CBP/p300 (CBP30 or A-485) inhibitors, western blot analyses were performed. Reduction of H3K27me3 after single treatment with EPZ-6438 in isoDIPG-H3WT and isoDIPG-H3.3K27M cells, but no additional decrease or a compensatory effect was present after combined treatment with either CBP30 (**Figure 41A**) or A-485 (**Figure 41B**)**.** H3K27ac levels were found to be significantly decreased upon CBP/p300 inhibition single treatment, but again, no compensatory nor additive effect was observed when combined treatment with EZH2 inhibitor was performed (**Figure 41A and 41B**).

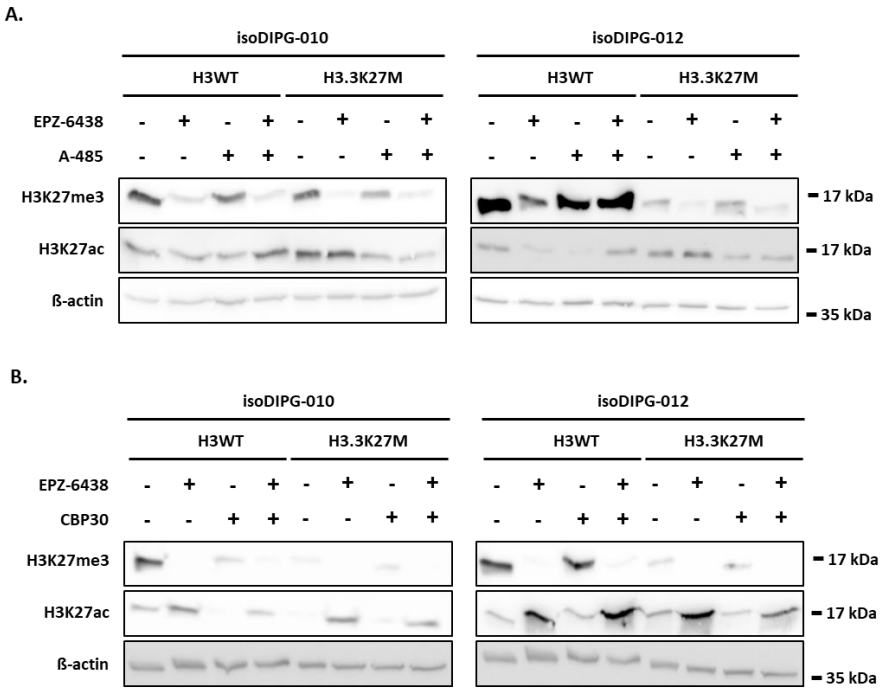

Figure 41 | Combined treatment with EZH2 and CBP/p300 inhibitors do not affect expression of H3K27me3 and H3K27ac in isoDIPG cells.
To investigate expression of H3K27me3 and H3K27ac level, western blot was performed 72 h after treatment with EPZ-6438 and (A) A-485 or (B) CBP30 in isoDIPG-010 and isoDIPG-012 cell lines. ß-actin served as loading control.

In conclusion, combinatory treatment using EZH2 and CBP/p300 inhibitors had no additive effect on cell viability nor expression of H3K27me3 and H3K27ac levels in isoDIPG cells, making the combined treatment not suitable for DIPG patients as a therapeutic approach.

5 Discussion

Diffuse intrinsic pontine gliomas (DIPG) are the most devastating pediatric tumors type with around 85% occurrence of a heterozygous mutation either in *H3F3A* gene encoding for H3.3 or in *HIST1H3B/C* gene encoding for H3.1 (Hoffman et al. 2018; Castel et al. 2015). Lysine (K) to methionine (M) substitution in histone 3 (H3K27M) changes the epigenetic landscape resulting in impaired EZH2 function and subsequently global loss of H3K27me3 mark which is associated with repression of transcription (Lewis et al. 2013; Wang et al. 2009). At the same time global gain of H3K27ac is observed which loosens the chromatin state and allows transcription factors to start transcription (Piunti et al. 2017; Hashizume 2017). It has already been shown that DIPG cells carrying H3.3K27M-mutation display an elevated proliferative activity when compared to H3-wildtype DIPG cells and are characterized by increased stem cell-like characteristics (Wiese et al. 2020).

Since in H3.3K27M-DIPG cells hyperacetylation is observed, proteins that are associated with H3K27ac mark might demonstrate a distinct function in dependence on H3-mutation status. Epigenetic writer and reader, CREB-binding protein (CBP and p300), does not only mediate H3K27ac, but also interacts with transcription associated proteins subsequently promoting gene transcription (Bedford and Brindle 2012; Stauffer et al. 2007). Whereas members of bromodomain and extra-terminal domain (BET) protein family (BRD2, BRD3 and BRD4) act as epigenetic readers and bind acetylated histone residues recruiting certain proteins to start transcription (Belkina and Denis 2012; Conery et al. 2016).

Thus, the present study aimed to identify genetic and tumor-biological effects in DIPG cells which may be atributed to presence of H3.3K27M-mutation. To ensure that the observed effects are indeed due to presence of H3.3K27M-mutation in DIPG, the study was conducted using isogenic DIPG cells lines providing the same cellular and genetic background, but differing in their H3-mutation status. To this end, CRISPR/Cas9 system was used to either introduce H3.3K27M-mutation to originally H3-wildtype DIPG cells or remove it from originally H3.3K27M-mutated DIPG cells. Additionally, the role of CBP/p300 and BET proteins in dependence on H3-mutation status was investigated using small molecules inhibiting either the epigenetic writing or reading functions of CBP/p300 and BET proteins. Moreover, siRNA-mediated knockdown was performed in order to dissect the specific functions of CBP and p300 as well as BRD2, BRD3 and BRD4 in dependence on H3-mutation status in DIPG cells.

5.1 Impact of H3.3K27M-mutation in DIPG cells

Using CRISPR/Cas9 system, H3.3K27M-mutation was introduced to originally H3-wildtype VUMC-DIPG-010 cell line and removed from originally H3.3K27M-mutated HSJD-DIPG-012 cells. Successful introduction or removal of H3.3K27M-mutation was confirmed by Sanger sequencing and western blot analyses. After genetic modification, effects of H3.3K27M-mutation on tumor biological properties of isoDIPG cells were investigated and summarized in **Table 22**. Worth noticing is the fact that originally H3-wildtype DIPG cells reacted almost identically as originally H3.3K27M-mutated DIPG cells in which the mutation was removed from, and H3.3K27M-mutated DIPG in which the mutation was introduced to showed similar features as originally H3.3K27M-mutated DIPG cells.

Table 22 | Summary of the effects observed upon introduction and removal of H3.3K27M-mutation in isogenic DIPG cells

Single, double or triple "-" and "+" as well as the intensities of the colour green and red semiquantitatively indicate different extents of the investigated features oberserved in the presence or absence of H3.3K27M-mutation in isoDIPG cells.

H3-status	CRISPR clone	Tumor-associated characteristics			Response to standard treatment		Tumor growth *in vivo*
	isoDIPG-	Cell proliferation	Stemness characteristics	Invasiveness	Temozolomide	Irradiation	
H3WT	010	+	+	+	---	--	+
	012	+	+	+	---	--	+
H3.3K27M	010	+++	+++	+++	-	--	+++
	012	+++	+++	+++	-	--	+++

H3-status	CRISPR clone	Activating histone marks				Repressive histone marks				Dual histone marks	
	isoDIPG-	H3K27ac	H3K4me3	H3K236me2	H4ac	H3K27me3	H3.3S31p	H3K9me3	H2AK119ub	H3K236me3	H4K16ac
H3WT	010	+	+	+	+	+	+	+	+	+	+
	012	+	+	+	+	+	+	+	+	+	+
H3.3K27M	010	+++	+++	+++	+++	---	---	---	---	+	---
	012	+++	+++	+++	+++	---	---	---	---	+	---

H3-status	CRISPR clone	Epigenetic writers/readers		Epigenetic readers			Epigenetic writer
	isoDIPG-	CBP	p300	BRD2	BRD3	BRD4	EZH2
H3WT	010	+	+	+	+	+	+
	012	+	+	+	+	+	+
H3.3K27M	010	++	++	++	++	++	--
	012	++	++	++	++	++	--

5.1.1 H3.3K27M-mutation globally changes the epigenetic landscape in DIPG cells

As expected, introduction of H3.3K27M-mutation resulted in strong reduction of H3K27me3 accompanied by an increase of H3K27ac levels. Removal of H3.3K27M-mutation, on the other hand, restored H3K27me3 and decreased H3K27ac levels in isoDIPG cells.

In line with this result, Harutyunyan *et al.* removed H3.3K27M-mutaton from H3.3K27M-mutated DIPG cells using CRISPR/Cas9 system and found out a significant upregulation of H3K27me3 levels (Harutyunyan et al. 2019). Moreover, they also overexpressed H3.3K27M-mutation in H3-wildtype pedHGG cells which led to reduction of H3K27me3 mark, proving that presence of H3.3K27M-mutation directly affects H3K27me3 levels (Harutyunyan et al. 2019).

Previous studies showed that, although H3.3K27M-mutant histones comprise only 3-17% of the whole H3 pool, H3.3K27M-mutation inhibits the polycomb repressive complex 2 (PRC2) which results in global loss of H3K27me3 and increased levels of H3K27ac (Bender et al. 2013; Lewis et al. 2013; Bechet et al. 2014). While it is well known that H3K27me3 is being retained at certain unmethylated CpG islands and mostly lost everywhere else in the genome (Harutyunyan et al. 2020), the mechanisms behind those changes are still unclear. Different theories were proposed trying to explain this phenomenon including preferential recruitment of PRC2 complex to nucleosomes containing H3K27M-mutation (Chan et al. 2013; Diehl et al. 2019; Lewis et al. 2013) or maintenance of genes that are targets of PRC2 by H3K27me3 mark in H3K27M-mutated DIPG cells (Mohammad et al. 2017). Furthermore, Harutyunyan *et al.* argued that presence of H3K27M-mutation allows deposition of H3K27me3 mark at unmethylated CpG islands, but may deny further spread of this histone mark, which indicates that propagation of PRC2 on chromatin does not seem not to be affected by the presence of H3K27M-mutation and supports the H3K27M-induced defective spread of H3K27me3 (Harutyunyan et al. 2019). In contrast, Stafford *et al.* found out that interaction between H3K27M-mutation and PRC2 is only temporary and even after PRC2 dissociation from chromatin inhibition is still present which suggests a long lasting effect of PRC2 on H3K27M-containing chromatin and only partial inhibition of PRC2 complex by presence of H3K27M-mutation (Stafford et al. 2018). Remarkably, recent studies showed that glioma cases lacking H3K27M-mutation, but exhibiting EZH inhibitor protein (EZHIP) overexpression, are also affected by reduction of H3K27me3, suggesting that both oncoproteins can drive the same subtype of diffuse midline gliomas (Castel et al. 2020; Pratt et al. 2020).

It is worth mentioning that most studies have been focusing on H3K27me3 as a main target of H3K27M-mutation, whereas only few investigations have been carried out studying the role of

hyperacetylation at H3K27 in tumorigenesis (Krug et al. 2019; Lewis et al. 2013; Mohammad et al. 2017; Piunti et al. 2017). Considering increased levels of CBP/p300 and BET proteins in isoDIPG-H3.3K27M cells, elevated levels of H3K27ac could be explained by increased functions of these acetylation-associated epigenetic key players in isoDIPG-H3.3K27M cells with subsequent profound impact on regulation of transcription (Sur and Taipale 2016).

Presence of H3.3K27M-mutation is associated with hypotrimethylation at H3K27 which is probably at least partly due to lower expression of the associated methyltransferase EZH2. As a compensatory effect, increased levels of H3K27ac as well as elevated expression of acetyltransferase CBP/p300 and readers of H3K27ac mark, BET proteins, are demonstrated in isoDIPG-H3.3K27M cells. Therefore, it could be assumed that H3.3K27M-mutation disproportionately blocks spreading of PRC2 because of the hyperacetylation that PRC2 does not overcome, resulting in an epigenetic imbalance in isoDIPG-H3.3K27M cells. In line with these results, siRNA-mediated knockdown of CBP indeed resulted in reduction of H3K27ac and at the same time restored H3K27me3 levels, suggesting that the epigenetic imbalance observed in isoDIPG-H3.3K27M cells can be reversed by modifying expression of certain epigenetic key players affected by H3.3K27M-mutation. These results point to a direct regulatory interaction between PRC2 and CBP/p300 by most probably inhibition of CBP/p300 transcription by PRC2 resulting in modification of H3K27ac and H3K27me3 levels in isoDIPG-H3.3K27M cells.

Taken altogether, it can be concluded that removal of H3.3K27M-mutation from primary H3.3K27M-mutated DIPG cells leads to ‘phenotype rescue’ characterized by reduction of H3K27ac and restored H3K27me3 levels.

Notably, most of the studies so far have focused either on H3K27me3 or H3K27ac mark as a primary target of H3.3K27M-mutation in DIPG cells. But other histone marks which might also contribute to H3.3K27M-mediated DIPG pathogenesis have not received the same degree of attention.

Mono-ubiquitination of histone H2A at lysine 119 (H2AK119ub) is being catalyzed by polycomb repressive complex 1 (PRC1) (Blackledge et al. 2014; Wang et al. 2004), tightly associated with H3K27me3 and specifically enriched at repressed CpG islands-containing promoters, thereby playing a major role in establishing transcriptional repression (Tamburri et al. 2020). Similarly to H3K27me3, H2AK119ub was shown in the present study to be significantly reduced in isoDIPG-H3.3K27M cells compared to isoDIPG-H3WT cells. We also conducted inhibition of B cell-specific Moloney murine leukemia virus integration site 1 (BMI1) as one main component of PRC1 to mediate H2AK119ub, using PTC209. BMI1 inhinbition resulted in a stronger response of isoDIPG-H3WT cells than of isoDIPG-H3.3K27M cells in regard to cell viability and proliferation (data not

shown). In contrast, H2AK119ub histone mark and BMI1 were found to be elevated in H3.3K27M-DIPG cells in comparison to H3WT-DIPG cells, but this comparison was limited due to the low number of H3WT-DIPG samples (Balakrishnan et al. 2020). Inhibition of BMI1 also significantly decreased cell proliferation in H3.3K27M-mutated DIPG cells (Kumar et al. 2017). Additionally, BMI1 inhibition impaired stem cell renewal in H3K27M-DIPG cells and induced senescence with upregulation of tumor suppressor genes, encoding for p16 and p21 (Balakrishnan et al. 2020). Nevertheless, these previous findings are not contradictory to the present study since the reported therapeutic responses upon BMI1 inhibition in H3.3K27M-DIPG cells may be different to the ones our group found being stronger in isoDIPG-H3WT cells than in isoDIPG-H3.3K27M cells. In isoDIPG-H3.3K27M cells, there is a reduction of H2AK119ub and PRC1 expression, suggesting that any effects of BMI1 inhibition might be possibly due to PRC1-independent effects, whereas in isoDIPG-H3WT cells, higher expression of H2AK119ub with a strong response of cell viability and proliferation might direct towards a strong PRC1-dependent function of BMI1. Future studies will have to dissect how PRC1-dependent and independent functions of BMI1, which is already explored in clinical DIPG trials, contribute to potential therapeutic responses in dependence of the H3-mutation status.

Another repressive histone mark, H3K9me3, is often associated with heterochromatin and was reported to interact with H3K27me3 (Nicetto and Zaret 2019). Western blot analysis revealed upregulation of H3K9me3 in isoDIPG-H3.3K27M in comparison to isoDIPG-H3WT cells. In line with this result, it was previously reported that H3K9me3 is elevated in the regions where H3K27me3 is lost (Harutyunyan et al. 2020), suggesting possible compensation for losing one repressive mark by relying on another. In order to identify genes regulated by H3K9me3 in isoDIPG-H3WT and isoDIPG-H3.3K27M cells, ChIP sequencing using H3K9me3 antibody could be performed.

Elevated expression of H3K4me3 was observed in isoDIPG-H3.3K27M cells compared to isoDIPG-H3WT cells. H3K4me3 is often seen to interact with H3K27me3 (Meissner et al. 2008). Since H3K4me3 leads to activation of genes involved in essential cancer related functions, reduction of H3K4me3 may indeed decrease the metastatic potential of cancer cells (Santos-Rosa et al. 2003; Beacon et al. 2021).

Dimethylation (me2) of H3K36 was recently suggested as a novel epigenetic signature of H3.3K27M-DIPG (An et al. 2020). This is also reflected by the present study where H3K36me2 was found to be elevated in isoDIPG-H3.3K27M cells. Other studies also reported similar results (Krug et al. 2019; Stafford et al. 2018) suggesting an antagonistic role of the transcription activating H3K36me2 mark to the H3K27me3. However, it is still unclear whether upregulated

levels of H3K36me2 observed in isoDIPG-H3.3K27M cells occurred because of general transcriptional activation in those cells or because of any antagonistic effect in response to loss of H3K27me3. Unlike H3K36me2, distribution of trimethylation of histone H3 at lysine 36 (H3K36me3) is more restricted and associated with transcribed gene bodies (Bhattacharya and Workman 2020). However, the present study showed no changes in expression of H3K36me3 in dependence on H3-mutation status.

H3.3 specific serine 31 mitotic phosphorylation (H3.3S31p) mark is found in close proximity to H3K27M and was shown in the present study to be reduced in isoDIPG-H3.3K27M cells compared to isoDIPG-H3WT cells. H3.3S31 is phosphorylated by checkpoint kinase 1 (Chk1) (Chang et al. 2015) which leads to transcriptional repression and activation (Martire et al. 2019). Several studies showed that downregulation of Chk1 in pedHGG leads to cell cycle dysregulation and sensitization to irradiation which might also open a new therapeutic window for DIPG (Qin et al. 2022; Kumar et al. 2017; Werbrouck et al. 2019) In a yet unpublished study by our group, a stronger impact of Chk1 inhibition by SB-218078 on cell viability was found in isoDIPG-H3WT compared to isoDIPG-H3.3K27M cells which is in line with the elevated expression of H3.3S31p found in isoDIPG-H3WT cells.

H3.3K27M-mutation appears to not only affect expression of different histone marks at H3, but also H4, including acetylation of histone H4 (K5 + K8 + K12 + K16) and H4K16. H4ac is widely associated with competence for transcription (Clayton et al. 2006; Koch et al. 2007) and was found in the present study to be significantly upregulated in isoDIPG-H3.3 K27M cells. H4ac and BRD4 had been shown before as regulators of stem cell pluripotency (Gonzales-Cope et al. 2016), highlighting their impact on cell differentiation. In isoDIPG-H3.3K27M cells expression of both, BRD4 and H4ac, was also elevated when compared to isoDIPG-H3WT cells, suggesting a more prominent role in the presence of H3.3K27M-mutation. Moreover, inhibition and siRNA-mediated knockdown of BRD4 led in the present study to a stronger reduction of stem cell-like properties in isoDIPG-H3.3K27M compared to isoDIPG-H3WT cells. In order to further elucidate the connection between H4ac and BRD4, expression of H4ac could be investigated using western blot analysis after knockdown of BRD4. Furthermore, ChIP sequencing after BRD4 inhibition could be performed using an H4ac antibody to identify potential interactions between BRD4 and H4ac.

H4K16ac displays both, transcriptional activating and repressive functions, and reduced H4K16ac expression has been strongly associated with cancer (Wang et al. 2009; Sen et al. 2016). In accordance, the present study demonstrated reduced levels of H4K16ac in isoDIPG-H3.3K27M compared to isoDIPG-H3WT cells. Contradictory to these results, An *et al.* found H4K16ac to be

the most acetylated residue in DIPG cells carrying H3.3K27M-mutation (An et al. 2020). A possible explanation to solve this apparent contradiction may be that the primary cell lines studied by An *et al.* may contain other genetic alterations besides H3.3K27M-mutation which might affect expression of H4K16ac. Our studies using isogenic cell lines would not support a direct association of elevated H4K16ac and H3.3K27M, in contrary, thus the contribution of additional genetic alterations as main drivers for elevated H4K16ac levels would be the first conclusion.

To summarize, the present study showed that several histone marks, other than H3K27ac and H3K27me3, are affected by presence of H3.3K27M-mutation in isoDIPG cells. In order to identify DNA binding sites of those marks in dependence on H3-mutation status in DIPG cells, ChIP sequencing with specific antibodies recognizing different histone marks could be performed. In addition, to further understand the impact of these histone marks in DIPG cells, mass spectrometry could reveal potential functional interaction partners and if their binding to chromatin might be affected by presence of the H3.3K27M-mutation. Thus, novel potential therapeutic targets for DIPG could be possibly identified. Since H3K27me3 and H3K27ac change state of chromatin and therefore accessibility of DNA to different transcription factors, it could also be assumed that there might be a shift of closed and open chromatin regions in isoDIPG-H3.3K27M cells compared to H3-wildtype equivalents. In order to study the impact of H3.3K27M-mutation on accessibility of chromatin in DIPG cells, an assay for transposase accessible chromatin (ATAC) sequencing could be performed.

5.1.2 H3.3K27M-mutation induces the expression of tumor-associated characteristics in DIPG cells

In the present study, introduction of H3.3K27M-mutation followed by global loss of H3K27me3 and gain of H3K27ac resulted in a more aggressive tumor phenotype as reflected by increased cell viability and proliferation, stem cell-like properties as well as migration and invasion abilities similar to originally H3.3K27M-mutated HSJD-DIPG-012 cells.

Cell proliferation investigated using three different proliferation assays and time-dependent brightfield microscopy was found to be significantly upregulated upon introduction of H3.3K27M-mutation and reduced after removal of H3.3K27M-mutation from primary DIPG cells originally carrying this mutation. These results were confirmed by gene set enrichment analysis of commonly regulated genes in isoDIPG-H3.3K27M compared to isoDIPG-H3WT cells revealing processes such as cell motility, locomotion and proliferation to be significantly affected. These

findings correspond to a previous study that reported reduced cell viability upon shRNA-mediated knockdown of H3.3K27M-mutation (Welby et al. 2019). Moreover, Kfoury-Beaumont *et al.* used CRISPR/Cas genome editing system to introduce H3.3K27M-mutation into human embryonic stem cells and found out that presence of H3.3K27M-mutation led to increased stem cell proliferation (Kfoury-Beaumont et al. 2022).

DIPG tumor cells often evade radiochemotherapy by exhibiting stem cell-like properties (Pedersen et al. 2020). Interestingly, the present study showed increased sphere and colony formation abilities upon introduction of H3.3K27M-mutation and reduction of these properties after removal of H3.3K27M-mutation. These findings were supported by elevated expression of common stemness markers on mRNA and protein level in isoDIPG-H3.3K27M cells compared to their H3-wildtype equivalents, including OCT4, SOX2, Nanog and Nestin. In line with these results, Rakotomalala *et al.* found that presence of H3.3K27M-mutation controls cell proliferation and self-renewal potential of DIPG cells (Rakotomalala et al. 2021). Interestingly, ability to form spheres under stemness conditions, as well as colonies under differentiating conditions was significantly increased in isoDIPG-H3.3K27M compared to isoDIPG-H3WT cells pointing to a strong potential of isoDIPG-H3.3K27M cells to evade radiotherapy under certain conditions. Taken altogether, observed radiochemoresistance of isoDIPG-H3.3K27M cells could possibly be explained by elevated stemness potential of these cells. Therefore, targeting factors responsible for self-renewal might possibly result in better response of DIPG-H3.3K27M cells to standard treatment.

Moreover, presence of H3.3K27M-mutation may result in increased resistance to single treatment with temozolomide (TMZ), while single dose of irradiation had no differential H3-mutation dependent effect in isoDIPG cells. This finding points out to a specific mechanism behind chemo-, but not radioresistance in dependence on H3-mutation status in DIPG cells. This interesting observation could be investigated further using mRNA sequencing after irradiation or temozolomide in order to identify differentially regulated genes upon treatment with TMZ that could be knocked down to study if radio- and chemotherapy would then have the same effect on cell viability independently of the H3-mutation status of DIPG cells. However, chemoresistance of pedHGG cell lines had been shown before to either depend on promoter methylation and repression of O6-methylguanin-DNA-methyltransferase (MGMT) DNA repair enzyme expression or an increased expression of homebox (HOX) genes (Gaspar et al. 2010). EZH2 within the PRC2 complex is well-known for regulation and inhibition of HOX genes (Kanduri et al. 2013). In consequence, in DIPG cells harboring H3.3K27M-mutation malfunctioning EZH2 and loss of H3K27me3 (Lewis et al. 2013) might lead to elevated expression of HOX genes. Indeed, mRNA-sequencing revealed upregulation of the majority of HOX genes, including

HOXA9, *HOXA10*, *HOXB13*, *HOXC10*, *HOXC11* and *HOXD1* in isoDIPG-H3.3K27M cells compared to isoDIPG-H3WT cells (data not shown) that had been described before to be associated with chemoresistance, suggesting that chemoresistance observed in isoDIPG-H3.3K27M cells might also depend on increased HOX genes expression. Gaspar *et al*. also reported that CD133 (*PROM1*) expression in different pedHGG cell lines was associated with temozolomide resistance (Gaspar et al. 2010). However, the present study can contribute to this finding in that way that isoDIPG-H3WT cells exhibited higher expression of CD133 compared to isoDIPG-H3.3K27M cells; this may suggest a particular importance of CD133 in chemoresistance of isoDIPG-H3WT cells in lack of other stemness markers and increased HOX genes expression.

Considering the fact that tumor cells are able to migrate into the surrounding brain tissue, thereby contributing to their malignant phenotype, migration and invasion abilities of isoDIPG cells were also investigated. Introduction of H3.3K27M-mutation into originally H3-wildtype DIPG cells resulted in increased migration and invasion, while reduction of these properties was observed when H3.3K27M-mutation had been removed from originally H3.3K27M-mutated DIPG cells.

These findings were also supported by elevated levels of mesenchymal markers ZEB1, MMP9 and Vimentin on mRNA and protein level in isoDIPG-H3.3K27M cells since these markers are associated with a highly migratory and invasive tumor phenotype. Additionally, elevated expression of another mesenchymal marker, SNAIL, which is associated with epithelial-mesenchymal transition, was found in H3.3K27M-mutated human embryonic stem cells compared to H3-wildtype human embryonic stem cells (Kfoury-Beaumont et al. 2022). Furthermore, gene set enrichment analysis of commonly expressed genes revealed upregulation of migration processes in isoDIPG-H3.3K27M cells, while cell differentiation processes such as axonogenesis and neuron differentiation were found to be significantly enriched in isoDIPG-H3WT cells. In line with these resulta, a recent study by Qi *et al.* also pointed to an increased expression of several genes involved in cell invasion in H3K27M-mutated DIPG cells (Qi et al. 2019). Several previous studies have confirmed that presence of H3.3K27M-mutation blocks normal cell differentiation (Kfoury-Beaumont et al. 2022; Haag et al. 2021). In conclusion, the present data suggest that presence of H3.3K27M-mutation do not only promote cell proliferation, clonogencity and invasiveness, but also derails differentiation in isoDIPG cells which also contributes to the malignant phenotype observed in isoDIPG-H3.3K27M cells.

Furthermore, EZH2 has been reported to be overexpressed in several cancer types (Breuer et al. 2004; Bachmann et al. 2006; Sudo et al. 2005; Beke et al. 2007) and has been shown to be important for regulation of tumor cells invasion. Different studies reported that EZH2 indeed

acts as an oncogene and promotes tumor invasiveness (Bryant et al. 2007; Liu et al. 2017). Moreover, Liu *et al.* showed that EZH2 is responsible for mediating silencing of E-cadherin which is responsible for cell adhesion and is disrupted in many aggressive tumors, promoting invasion (Liu et al. 2008). In contrast, the present study revealed that presence of H3.3K27M-mutation in isoDIPG cells disrupts function of EZH2 and reduces its expression. These observations do not correlate with increased expression of E-cadherin or an EZH2-mediated effect on migration and invasion in isoDIPG-H3.3K27M cells, suggesting EZH2-independent mechanisms of the malignant phenotype observed in isoDIPG-H3.3K27M cells.

Interestingly, two independent studies have suggested that presence of H3.3K27M-mutation in DIPG cells may provide unique accessible chromatin at regions involved in NOTCH signaling and neurogenesis with an impact for DIPG maintenance (Lewis et al. 2022; Chen et al. 2020). In contrast, the present study showed strong reduction of NOTCH-related genes (*NOTCH1*, *NOTCH3, DLL1*) in isoDIPG-H3.3K27M cells compared to isoDIPG-H3WT cells (data not shown). This could be explained by dual function of NOTCH signaling in dependence on cellular context, acting either as tumor promoter or suppressor, since Lewis *et al.* used monolayers and the present study focused on tumorspheres. These findings could be further investigated in our isogenic DIPG cell model using ATAC sequencing.

Another study revealed biological relevance of signal transducer and activator of transcription 3 (STAT3) as a therapeutic target in H3.3K27M-DIPG cells, since DIPG cells carrying H3.3K27M-mutation were shown to express elevated levels of activated STAT3 compared to H3WT-DIPG cells (Zhang et al. 2022). This result could be confirmed by investigating impact of STAT3 inhibitor on tumor-related characteristics in dependence on H3-mutation status in isoDIPG cells.

Furthermore, Chung *et al.* showed that DIPG cells harboring H3.3K27M-mutation may display upregulated metabolic processes including glycolysis, glutaminolysis and tricarboxylic acid (TCA) cycle and that interruption of these processes may mediate potent therapeutic efficacy *in vitro* and *in vivo* (Chung et al. 2020). The present study also showed upregulation of several glycolysis-related genes such as *HIF1A*, *SLC2A1*, *HK1*, *PKM* and *ALDH1A3*, as well as genes involved in TCA cycle including *IDH1*, IDH2 and *ACO1* in isoDIPG-H3.3K27M cells compared to isoDIPG-H3WT cells (data not shown). These findings also suggest that selected metabolic pathways might be indeed potential therapeutic targets in DIPG.

In order to evaluate the *in vitro* findings of the present study *in vivo*, chorioallantoic membrane (CAM) assay demonstrated that presence of H3.3K27M-mutation significantly increased size and volume of tumor grown on the CAM. This result reflects previous findings *in vitro* showing elevated cell proliferation in isoDIPG-H3.3K27M compared to isoDIPG-H3WT cells. Moreover,

investigation of H3.3K27M-dependent expression of common stemness markers, such as *POU5F1* (OCT4) and *PROM1* (CD133) on mRNA level also corresponded with findings *in vitro* (data not shown). Furthermore, expression of *CDKN2A* (p16) was found to be decreased and *MYC* (c-myc) expression elevated in isoDIPG-H3.3K2M tumors compared to isoDIPG-H3WT tumors, respectively (data not shown), also reflecting more aggressive behavior of isoDIPG-H3.3K27M cells *in vitro*. To this date only one study used CAM assays to study DIPG tumor growth thereby reporting that CAM grown tumors do not only maintain the genetic and epigenetic phenotype of DIPG cells, but are also a suitable *in vivo* model to study anti-angiogenic effects and perform drug screenings (Power et al. 2022). To confirm that CAM tumors in the present study also show certain characteristics of isoDIPG cells obtained *in vitro*, immunohistochemistry using antibodies against H3K27M-mutation, H3K27ac and H3K27me3 will have to be performed. Additionally, expression of specific glioma markers such as GFAP should be investigated on mRNA and protein level. The CAM isogenic DIPG model could be used for studying the effect of certain inhibitors in DIPG *in vivo*.

In conclusion, presence of H3.3K27M-mutation hints to a crucial role of H3.3K27M-mutation in induction of malignant phenotype observed in isoDIPG-H3.3K27M cells. Expression of increased tumor phenotype-associated characteristics in isoDIPG-H3.3K27M cells was also reflected *in vivo*.

5.2 H3.3K27M-dependent function of CBP and p300 in DIPG cells

Presence of H3.3K27M-mutation in DIPG cells is accompanied by global loss of H3K27me3 and gain of H3K27ac (Bender et al. 2013; Piunti et al. 2017). In consequence, histone acetyltransferases responsible for acetylating H3K27 might play a major role in H3.3 K27M-mutated DIPG cells. CBP and p300 were shown to mediate as well as interact with histone residues (Bedford and Brindle 2012; Conery et al. 2016; Zheng et al. 2004). They consist of a bromodomain, recognizing and interacting with acetylated histones (epigenetic reader function), and an acetyltransferase domain, acetylating histones (epigenetic writer function) (Xu et al. 2006; Spiegelman and Heinrich 2004; Stauffer et al. 2007). Generally, CBP and p300 are thought to be functionally redundant proteins, since their domains share a high percentage of identity (Zeng et al. 2008; Liu et al. 2008).

In order to study the impact of H3.3K27M-mutation on CBP and p300 function in DIPG cells, isogenic DIPG cell lines were used. To dissect and functions of CBP/p300, suitable inhibitors that disable specific CBP/p300 functions were investigated: two small molecules inhibiting CBP/p300

HAT activity (A-485, C646), two inhibiting BD (CBP30, CBP112) and one inhibiting binding of other N-terminal cofactors (ICG-001).

MTT cell viability assays were subsequently used as a read out to investigate the concentration-dependent cell toxicity effects of the CBP/p300 inhibitors in isoDIPG-H3WT and isoDIPG-H3.3K27M cells.

A-485 and C646 inhibit HAT activity of CBP/p300 (Mastracchio et al. 2021; van den Bosch et al. 2016). Treatment with C646 revealed significant reduction in cell viability of isoDIPG cells, irrespectively of H3-mutation status. C646 was not further studied because of the many described off-target effects of C646, including modulation of cys-rich proteins at very low concentrations (Shrimp et al. 2015), which made C646 not a very promising inhibitor to study function of CBP/p300 in isoDIPG cells.

In contrast, A-485 decreased cell viability to a significantly higher extent in isoDIPG-H3WT cells compared to isoDIPG-H3.3K27M cells. As discussed above, isoDIPG-H3.3K27M cells display increased chemoresistance and an elevated stemness potential, both might contribute to a lower susceptibility of isoDIPG-H3.3K27M cells to A-485 treatment. However, compared to other cancer types, including non-small-cell lung carcinoma with IC_{80} of 6.25 µM (Zhang et al. 2020) and growth hormone pituitary adenoma with IC_{50} of 500 nM (Ji et al. 2022), DIPG cells responded much stronger to A-485 with IC_{80} of 50 nM.

CBP30 and CBP112 inhibit the BD function of CBP/p300, which results in an impairment of acetylation of different further histone residues (Hammitzsch et al. 2015; Hay et al. 2014). Cell viability assay revealed that isoDIPG-H3WT cells were more sensitive towards CBP30 treatment compared to isoDIPG-H3.3K27M cells which again might be explained by increased chemoresistance and stemness potential of DIPG cells carrying H3.3K27M-mutation. CBP112 treatment resulted in slight reduction of cell viability. CBP112 was in the end excluded from further analysis because of its limited efficiency, and the fact that it also activates p300 (Zucconi et al. 2016), which would not allow to draw correct conclusions about potential different roles of CBP and p300.

Treatment with ICG-001, an inhibitor of CBP/p300-ß-catenin interaction and therefore canonical Wnt-signaling (Emami et al. 2004), resulted in a significant reduction of cell viability in isoDIPG cells, independently of H3-mutation status. Previous study carried out by Wiese *et al.* showed that ICG-001 was very potent to decrease cell proliferation, migration and clonogenicity in different pedHGG cell lines (Wiese et al. 2017). However, the present study aimed to investigate

HAT and BD function of CBP and p300. Thus, ICG-001 was also excluded from further investigations.

In summary, two small molecules were finally chosen for further experiments: CBP30 inhibiting BD function and A-485 inhibiting HAT activity of CBP/p300. In addition, this project aimed to dissect potentially different functions of CBP and p300. To this end, siRNA-mediated knockdown of CBP and p300 was performed, which was validated on mRNA and protein level.

5.2.1 H3K27 is acetylated by CBP in isoDIPG-H3.3K27M cells and by p300 in isoDIPG-H3WT cells

Presence of H3.3K27M-mutation, which frequently occurs in DIPG, results in an epigenetic imbalance characterized by loss of H3K27me3 and hyperacetylation at H3K27 (Piunti et al. 2017).

H3K27ac, which is associated with activation of tumor-promoting genes (Bedford et al. 2010; Zheng et al. 2004), was found to be diminished after BD and HAT inhibition of CBP/p300 in both, isoDIPG-H3WT and isoDIPG-H3.3K27M cells. These results were expected after HAT inhibition, since H3K27 is mainly acetylated by CPB/p300 (Bedford and Brindle 2012). Interestingly, as no one showed this before, knockdown of CBP reduced level of H3K27ac exclusively in isoDIPG-H3.3K27M cells, while knockdown of p300 decreased H3K27ac exclusively in isoDIPG-H3WT cells. In line with these results, it was shown that expression of CBP and p300 influence distinct changes in levels of histone acetylation, with CBP selectively acetylating H3 and H4K12 and p300 H4K8 (McManus and Hendzel 2003). Moreover, in developing muscle plasticity CBP and p300 were suggested to play more non-redundant roles in regulating modifications of chromatin, with CBP acetylating genes involved in dedifferentiation, while p300 in differentiation processes (Chakraborty et al. 2022). In summary, the present study may indeed indicate specific function of CBP and p300 in acetylating H3K27 in dependence on H3-mutation status in isoDIPG cells.

In the present study, H3K27me3 levels, associated with repression of transcription (Hashizume 2017), were mainly unaffected by inhibition of HAT activity and BD function of CBP/p300 in isoDIPG-H3WT and isoDIPG-H3.3K27M cells. In contrast, knockdown of CBP, but not p300, resulted in upregulation of H3K27me3 levels, to a significantly higher extent in isoDIPG-H3.3K27M cells. These findings may point to a compensatory H3K27me3 upregulating effect, exclusive for isoDIPG cells harboring H3.3K27M-mutation, suggesting again a potentially different function of CBP in dependence on H3-mutation status in DIPG cells.

In conclusion, this study points to a specific functions of CBP and p300 in mediating H3K27ac in isoDIPG-H3.3K27M and isoDIPG-H3WT cells, respectively. In order to investigate the direct impact of CBP- or p300-dependent H3K27ac on transcription, ChIP sequencing with antibodies detecting H3K27ac, CBP and p300 after CBP/p300 HAT inhibition would have to be performed in comparison with untreated DIPG cells. Thus, specific H3K27ac-CBP and -p300 bound target genes may be identified and further validated using mRNA sequencing to show that H3K27ac by CBP or/and p300 contribute to gene transcription.

5.2.2 HAT activity of CBP is crucial for mediating cancer-related biological processes in isoDIPG-H3.3K27M cells

Since it was shown that isoDIPG-H3.3K27M cells are characterized by hypotrimethylation and hyperacetylation at H3K27, and associated with enhanced tumor characteristics, several tumor-biological cell assays were performed in order to investigate the impact of CBP and p300 on tumor behavior. To find out whether HAT activity or BD function of CBP/p300 is more important in maintaining tumor-associated characteristics of isoDIPG-H3WT and isoDIPG-H3.3K27M cells, BD inhibitor (CBP30) and HAT activity inhibitor (A-485) were used. In order to investigate potentially specific function of CBP and p300 in dependence on H3-mutation status in isoDIPG cells, siRNA-mediated knockdown of CBP and p300 was performed. To characterize CBP/p300-dependent changes in tumor cell behavior, cell proliferation and viability, clonogenicitiy and invasiveness of isoDIPG cells were examined.

MTT cell viability assay, crystal violet staining and BrdU cell proliferation assay showed comparable results: CBP30 and A-485 treatment resulted in a higher reduction of cell proliferation in isoDIPG-H3WT than isoDIPG-H3K27M cells. These results were also reflected *in vivo*, resulting in a comparable reduction of tumor size of isoDIPG cell derived tumors grown on CAM, irrespectively of H3-mutation status. In agreement, gene set enrichment analysis revealed cell proliferation to be strongly regulated by CBP/p300 in both, isoDIPG-H3WT and isoDIPG-H3.3K27M cells. Additionally, PI-FACS analysis showed that CBP30 and A-485 treatment led to cell cycle arrest in G1 phase (data not shown). Moreover, mRNA sequencing revealed a specific function of CBP HAT activity in regulating programmed cell death in isoDIPG-H3.3K27M cells. In agreement, loss of CBP HAT activity has already been demonstrated to induce apoptosis in different cancers (Santer et al. 2011; Gu et al. 2016; Inagaki et al. 2016). Reduction of CBP/p300 expression, and subsequently global hypoacetylation, were shown to accompany apoptosis (Rouaux et al. 2003). In accordance, inhibition of HAT activity of CBP resulted in upregulation of pro-apoptotic genes involved in both, intrinsic and extrinsic signaling cascade, and

downregulation of anti-apoptotic genes in isoDIPG-H3.3K27M cells, highlighting the importance of CBP in cell cycle regulation. Additionally, western blot analyses also confirmed upregulation of pro-apoptotic proteins such as cleaved Caspase 3 and cleaved PARP upon inhibition of CBP/p300 HAT activity in isoDIPG-H3.3 K27M cells. To investigate if loss of CBP/p300 HAT activity induces apoptosis in isoDIPG-H3.3K27M cells, FACS analysis should be repeated with prolongation of inhibitor incubation time to validate the present results. In addition, annexin V counterstaining could be performed to specifically stain apoptotic cells.

In summary, reduced cell proliferation after inhibition of CBP/p300 HAT activity and BD function in isoDIPG-H3.3K27M cells is due to not only cell cycle arrest, but also apoptosis of these cells.

Interestingly, knockdown of CBP and p300 led to decreased cell proliferation in isoDIPG cells, irrespectively of H3-mutation status. It is well-known that CBP and p300 regulate cell cycle progression (Kawasaki et al. 1998). Fauquier *et al.* reported specific function of CBP and p300 in mediating cell cycle with CBP controlling E2F transcription factor 1 (*E2F1*) and cyclin-dependent kinase 4 (*CDK4*) expression and p300 regulating retinoblastoma protein (*Rb1*) and cyclin D (*CCND1*), which results in cycle arrest in G1 phase (Fauquier et al. 2018). In line with this result, mRNA sequencing revealed that knockdown of CBP indeed downregulated *E2F1* and *CDK4* and knockdown of p300 reduced expression of *Rb1*, having no effect on *CCND1* expression (data not shown). Interestingly, expression of cyclin dependent kinase inhibitor 1A (*CDKN1A*), p21, which promotes cell cycle arrest (Karimian et al. 2016), was found to be elevated upon p300, but not CBP knockdown in isoDIPG-H3.3K27M cells, while expression of cyclin dependent kinase inhibitor 2A (*CDKN2A*), p16, was not affected (data not shown). These findings are in line with the study carried out by Snowden and Perkins which showed that p300 is negatively regulated by G1/S phase transition checkpoint proteins, cyclin E/CDK2 which is inhibited by p21, while p300 has no effect on p16 in cell cycle regulation (Snowden and Perkins 1998). The described effects were observed exclusively in isoDIPG-H3.3K27M cells and not in isoDIPG-H3WT cells, suggesting specific H3.3K27M-dependent functions of CBP and p300 in regulating cell cycle. The observed impact of CBP and p300 on cell cycle progression in isoDIPG-H3.3K27M cells could be further validated using FACS analysis upon knockdown of CBP and p300.

In conclusion, HAT activity of CBP/p300 has a profound function in regulating programmed cell death in isoDIPG-H3.3K27M cells. Furthermore, CBP and p300 have been shown to affect cell proliferation by regulating cell cycle progression to a higher extent in isoDIPG-H3.3K27M cells compared to isoDIPG-H3WT cells.

Stemness is often associated with tumor cells evading radiochemotherapy (Schulz et al. 2019) and increased mesenchymal characteristics (Zhou et al. 2020) which makes stemness associated parameters attractive therapeutic targets. HAT and BD inhibition of CBP/p300 resulted in reduction of sphere and colony formation abilities, to a significantly higher extent in isoDIPG-H3.3K27M compare to isoDIPG-H3WT cells. These results were also reflected by reduced expression of several different stemness markers on mRNA level: expression of *SOX2*, *OCT4* and *PROM1* (CD133) was affected by interfering with CBP/p300 HAT activity and BD function exclusively in isoDIPG-H3.3K27M cells. These results suggest that HAT and BD function of CBP/p300 contribute equally to maintaining stemness potential of isoDIPG-H3.3K27M cells. Interestingly, knockdown of CBP significantly decreased sphere and colony formation abilities to a higher extent in isoDIPG-H3.3K27M compare to isoDIPG-H3WT cells, whereas p300 knockdown had slight reducing effect, irrespectively of H3-mutation status. The observed results were also supported by differential effects of CBP and p300 knockdown on the expression of stemness markers *SOX2*, *POU5F1* (OCT4) and *PROM1* (CD133) in isoDIPG-H3.3K27M cells. Interestingly, upon knockdown of p300, but not CBP, reduction of OCT4 expression was observed in isoDIPG-H3.3K27M cells, indicating a role of p300 in regulating OCT4 activity. In opposite, CD133 was found to be significantly reduced upon knockdown of CBP, but unchanged upon p300 knockdown, suggesting that CBP might regulate expression of CD133 in isoDIPG-H3.3K27M cells. In line with this result, it was published that inhibition and knockdown of CBP in liver cancer cells significantly reduced CD133 expression (Tang et al. 2018). Moreover, p300 was shown to promote activation of OCT4 genes in embryonic stem cells (ESCs) (Hu et al. 2014). Additionally, Gonzalez-Martinez *et al.* showed that under neurosphere-induced differentiation conditions NSC cells upon CBP knockout differentiated into oligodendrocytes instead of astrocytes, while upon p300 knockout neural stem cells (NSCs) were maintained at the pluripotent stage (Gonzalez-Martinez et al. 2022). Altogether, these results highlight the differential functions of CBP and p300 in isoDIPG-H3.3K27M cells in maintaining stemness characteristics by regulation of partially different genes.

In summary, CBP and p300 may play distinct roles in maintaining self-renewal ability of H3.3K27M-mutated DIPG cells. CBP/CD133 and p300/OCT4 interactions may mediate stemness potential of isoDIPG-H3.3K27M. Moreover, HAT activity and BD function of CBP/p300 seem to contribute equally to the level of stemness potential observed in isoDIPG-H3.3K27M cells. Whereas in isoDIPG-H3WT cells, CBP and p300 may play a moderate role in maintaining stem cell-like properties. In order to validate those results on protein level, western blot analyses using antibodies against CD133 and OCT4 upon knockdown of CBP and p300 in isoDIPG-H3.3K27M cells would need to be performed.

Mesenchymal phenotype of tumor cells contributes to maintenance of tumor cells migration and invasion abilities (Raggi et al. 2016). BD inhibition of CBP/p300 resulted in reduction of migration and invasion of isoDIPG cells, irrespectively of the H3-mutation status. Interestingly, inhibition of CBP/p300 HAT activity decreased migration and invasion to a significantly higher extent compared to bromodomain inhibition of CBP/p300, independently on H3-mutation status.

Knockdown of CBP and p300 reduced migration and invasion abilities of isoDIPG cells, to a higher extent in isoDIPG-H3.3K27M compared to isoDIPG-H3WT cells. These results are in line with the finding that isoDIPG cells carrying H3.3K27M-mutation exhibit much higher basal levels of mesenchymal markers compared to isoDIPG-H3WT cells. These mesenchymal transcription factors induce cell migration and are associated with maintenance of stem cell-like properties (Batlle et al. 2000; Dong et al. 2014; Ghahhari and Babashah 2015). Consequently, *SNAI2* (SLUG), *MMP2*, and *CDH2* (N-cadherin) were strongly affected by reduced CBP/p300 expression, to a significantly higher extent in isoDIPG-H3.3K27M compared to isoDIPG-H3WT cells. Contrastingly, *SNAI1* (SNAIL) expression was found to be reduced to a higher extent in isoDIPG-H3WT than in isoDIPG-H3.3K27M cells. Interestingly, knockdown of p300, but not CBP, reduced expression of *CDH1* (E-cadherin) in isoDIPG-H3.3K27M cells, indicating a role of p300 in regulating E-cadherin expression which is a marker of more epithelial cells – in contrast to a mesenchymal cell phenotype. On the other hand, mesenchymal marker, N-cadherin, was found to be significantly reduced upon knockdown of CBP, and even increased after p300 knockdown, suggesting that expression of N-cadherin may be regulated by CBP in isoDIPG-H3.3K27M cells. These findings indicate that CBP and p300 not only regulate different target genes, but also contribute to different phenotypes of isoDIPG-H3.3K27M cells. To further investigate this hypothesis, western blot analyses investigating the expression of N-cadherin and E-cadherin after CBP and p300 knockdown in isoDIPG-H3.3K27M cells should be performed. In addition, time-dependent phenotype of isoDIPG cells should be monitored after knockdown of CBP in comparison to p300 knockdown.

In conclusion, migration and invasion seem to be highly dependent on HAT-mediated CBP function in isoDIPG cells. Moreover, CBP seems to exclusively regulate expression of N-cadherin, while p300 may control E-cadherin expression in isoDIPG-H3.3K27M cells. These results suggest a distinctive role of CBP and p300 in the malignant phenotypes of DIPG in dependence on H3-mutation status.

Taken together, the observed effects suggest diverse roles of CBP and p300 in regulating tumor-associated characteristics in isoDIPG-H3.3K27M cells. CBP/p300 HAT activity seems to have a

major function over CBP/p300 BD function in maintainting the malignant phenotype commonly observed in isoDIPG-H3.3K27M cells. Interestingly, knockdown of CBP, but not p300, had more profound effect on cell proliferation, stem cell-like characteristics and migration/invasion abilities, irrespectively of H3-mutation status in isoDIPG cells.

Overall, CBP appeared to be one of the key players for acetylation of H3K27 in isoDIPG-H3.3K27M cells, while p300 played a crucial role for H3K27ac in isoDIPG-H3WT cells. Moreover, mostly HAT function of CBP and, to a lesser extent, of p300 appeared to be crucial for maintaining tumor-associated characteristics, especially in isoDIPG-H3.3K27M cells. Furthermore, impaired function of CBP/p300 HAT activity was shown to induce programmed cell death and contributed to cell cycle inhibition in isoDIPG-H3.3K27M cells. Overall, CBP might be a promising target to treat DIPG patients, especially since isoDIPG cells carrying H3.3K27M-mutation seem to highly depend on CBP/p300 to maintain their aggressive tumor phenotype.

5.3 H3.3K27M-dependent function of BET proteins in DIPG cells

BET proteins BRD2, BRD3 and BRD4 play a major role in mediating histone acetylation, remodeling chromatin and recruiting other factors crucial for transcription (Bedford and Brindle 2012). BET proteins were found to be highly expressed in isoDIPG-H3.3K27M cells compared to isoDIPG-H3WT cells. Given the observed hyperacetylation at H3K27 in isoDIPG-H3.3K27M cells, BET proteins might be also strongly involved in maintenance of tumor-associated properties.

To study functions of BET protein members in dependence on H3-mutation status, OTX-015 was used to impair BET proteins binding to acetylated chromatin in isogenic DIPG cell lines. MTT cell viability assay was applied as a readout to select the most potent BET proteins inhibitor and to study the concentration-dependent cell toxicity of MS346, OTX-015 and JQ1 in isoDIPG-H3WT and isoDIPG-H3.3K27M cells.

OTX-015 and JQ1 inhibit function of BRD2, BRD3 and BRD4 (Filippakopoulos et al. 2010; Berthon et al. 2016). Treatment with JQ1 demonstrated significant reduction of cell viability, irrespectively of H3-mutation status in isoDIPG cells. Whereas OTX-015 treatment resulted in decreased cell viability, to a significantly higher extent in isoDIPG-H3WT compared to isoDIPG-H3.3K27M cells. These observations reflect the results obtained after CBP/p300 inhibition by A-485, suggesting possible functional dependence of BET proteins and CBP/p300 in isoDIPG cells. JQ1 was reported to have a very short half-life *in vitro* (Filippakopoulos et al. 2010) and therefore was not further investigated in the present study.

Treatment with MS436, which exclusively inhibits BRD4, resulted in significant reduction of cell viability, irrespectively of H3-mutation status in isoDIPG cells. Since it was shown that not only BRD4, but also BRD2 may be essential in mediating transcription (Cribbs et al. 2021), MS346 was excluded from further investigations.

Finally, OTX-015 has been a subject in many clinical trials, such as in NUT carcinoma (Stathis et al. 2016), acute leukemia (Berthon et al. 2016) or lymphoma (Amorim et al. 2016), thus, OTX-015 represents an already well-studied molecule and was chosen for further investigation in the present study.

In addition, siRNA-mediated knockdown was performed in isoDIPG cells in order to dissect specific function of BRD2, BRD3 and BRD4, which was validated on both, protein and mRNA levels before continuing with further investigations.

5.3.1 BET proteins modulate levels of H3K27ac and H3K27me3 in isoDIPG cells

Since H3.3K27M-mutation is associated with loss of H3K27me3 and gain of H3K27ac (Piunti et al. 2017), acetylating proteins such as CBP/p300 and proteins that recognize this acetylation mark, including BET proteins, might play a more profound role in isoDIPG-H3.3K27M cells.

H3K27ac is associated with transcriptional activation (Bedford et al. 2010; Zheng et al. 2004) and was found to be decreased after BET inhibition, irrespectively of H3-mutation status. Whereas, siRNA-mediated knockdown of BRD2, BRD3 and BRD4 resulted in reduction of H3K27ac exclusively in isoDIPG-H3.3K27M cells. Surprisingly, in isoDIPG-H3WT cells, H3K27ac levels were found to be elevated after knockdown of BRD2, BRD3 and BRD4, suggesting a distinctive role of BET proteins in DIPG cells in dependence on H3-mutation status.

In the present study expression of H3K27me3, a histone mark associated with repression of transcription (Piunti et al. 2017), was mainly not affected by BET proteins inhibition nor BRD4 knockdown, irrespectively of H3-mutation status. Interestingly, H3K27me3 was found to be significantly upregulated upon knockdown of BRD3 in both, isoDIPG-H3WT and isoDIPG-H3.3K27M cells and after BRD2 knockdown exclusively in isoDIPG-H3.3K27M cells. Increased levels of H3K27me3 could be explained by compensatory effects following H3K27ac reduction in isoDIPG-H3.3K27M cells.

In conclusion, this study suggests BET proteins may indirectly modulate expression of H3K27ac, but in a completely different way in dependence on H3-mutation status in isoDIPG cells. Moreover, these results highlight a distinct function of BRD3 in regulating H3K27me3 mark in isoDIPG cells in dependence on H3-mutation status. To further investigate the impact of

H3K27me3 and H3K27ac on transcription after BET proteins inhibition in isoDIPG cells, ChIP sequencing using H3K27me3 and H3K27ac antibody should be performed.

5.3.2 BRD2 and BRD4 play a crucial role in the expression of tumor-associated characteristics in isoDIPG-H3.3K27M cells

BET proteins are essential regulators of transcription and were shown to be involved in maintenance of tumor associated characteristics in many tumor entities (Cheung et al. 2021). In addition, H3K27me3 and H3K27ac levels were dependent on BET proteins in isoDIPG cells as shown in the present study. In order to investigate if the observed epigenetic changes contribute to the reduction of malignant phenotype in isoDIPG cells, cell proliferation and viability, clonogenicity and invasiveness of isoDIPG cells were examined after BET proteins inhibition and knockdown.

MTT cell viability assay, crystal violet staining and BrdU proliferation assay showed comparable results upon knockdown and inhibition of BET proteins. OTX-015 treatment as well as knockdown of BRD2 and BRD4 decreased cell proliferation exclusively in isoDIPG-H3.3K27M cells, suggesting a more profound function of BRD2 and BRD4 in isoDIPG-H3.3K27M cells compared to isoDIPG-H3WT cells. These results were in line with mRNA sequencing data and subsequent gene set enrichment analysis revealing cell motility and cell proliferation to be affected by BRD2 and BRD4, but not BRD3, in isoDIPG-H3.3K27M cells. These findings were also reflected by the results of CAM assays showing reduced tumor size upon BET protein inhibition *in vivo*. In line with this result, several studies showed that BET proteins inhibition resulted in reduction of tumor growth *in vivo* including JQ1 in acute myeloid leukemia (Zuber et al. 2011), breast (Shu et al. 2016) and lung cancer (Klingbeil et al. 2016) and OTX-015 in B-cell lymphoma (Boi et al. 2015) and mesothelioma (Vazquez et al. 2017).

Furthermore, it was shown that BRD4 impairment inhibits cell cycle progression and induces cell death mechanisms in various tumor entities (Mochizuki et al. 2008; Patel et al. 2013; Hussong et al. 2017). Indeed, OTX-015 treatment also led to G1/S phase cell cycle arrest in the present study. In line with these results, expression of cyclin-dependent kinase 2 (CDK2), responsible for G1/S transition, was found to be downregulated upon BRD4 inhibition. Moreover, cell cycle regulators, p21 and p16 (*CDKN1A* and *CDKN2A*) were shown to be elevated upon BRD4 knockdown. It was reported that, although p16 as well as p21 are both thought to be crucial regulators of cell senescence (Sharpless and Sherr 2015; Bracken et al. 2007), BRD4 inhibition-induced senescence in gastric cancer seemed to be dependent more on p21 (Dong et al. 2018). p21 is reported to be regulated by p53 (Abbas and Dutta 2009), but in the present study p53

expression remained unchanged, suggesting a p53-independent, but BRD4-dependent regulation of p21. Furthermore, Jang et al. indicated that regulation of MYC, proto-oncogene, positively regulates BRD4 expression (Jang et al. 2005). In accordance, expression of MYC was found to be indeed downregulated upon BRD4 inhibition in isoDIPG-H3.3K27M cells, suggesting that BRD4 may be indeed crucial for MYC expression in DIPG cells carrying H3.3K27M-mutation.

In tumor cells, autophagy can induce cell death, but may also facilitate tumorigenesis (Lin et al. 2021; Marsh and Debnath 2020). In isoDIPG-H3.3K27M cells, BET inhibition induced autophagy, which was supported by elevated levels of autophagy markers, LC3B and ATG7 (data not shown). Although several recent studies reported BRD4 to be transcription repressor of autophagy (Sakamaki et al. 2017; Kim et al. 2022; Wakita et al. 2020), the present study suggested BRD2 to regulate autophagy in isoDIPG-H3.3K27M cells, which was reflected by elevated expression of autophagy markers such as ATG5, PIK3CA, LAMP2 and ATG2B upon knockdown of BRD2. Autophagy is often thought to act as protective and even resistance mechanism against radio- and chemotherapy. Interestingly, the effectiveness of autophagy inhibition by chloroquine as therapeutic option for DIPG patients in combination with temozolomide was recently investigated in a clinical trial (Kramm et al. unpublished), which showed that patients treated with chloroquine exhibited a significantly better overall survival (OS) with a median of 16.1 months as compared to a median OS of only 9 to 12 months without chloroquine treatment. Thus, inhibition of autophagy in combination with BET proteins inhibition appears to be a potentially promising novel therapeutic strategy for DIPG patients. In order to investigate if autophagy inhibition may indeed increase the therapeutic effect of BET proteins inhibition, chloroquine could be added to OTX-015 treatment and tumor-associated characteristcs could be investigated.

In conclusion, BRD2 and BRD4 seem to play a more crucial role over BRD3 in regulating cell proliferation in isoDIPG-H3.3K27M cells, with BRD4 regulating cell cycle progression amd BRD2 controling autophagy. These findings highlight distinct functions of BRD2 and BRD4 in isoDIPG-H3.3K27M cells.

Tumor cells evading chemotherapy usually exhibit elevated levels of stemness characteristics. Inhibition and knockdown of BRD2 and BRD4 resulted in reduction of sphere and colony formation abilities exclusively in isoDIPG-H3.3K27M cells. These results were also reflected by reduction of expression of several stemness markers on mRNA level: *SOX2*, *POU5F1* (OCT4) and *PROM1* (CD133). Surprisingly, OCT4 expression was found to be significantly reduced upon BRD2 and BRD4 knockdown in isoDIPG-H3WT cells compared to isoDIPG-H3.3K27M cells, suggesting that BRD2 and BRD4 regulate OCT4 expression in isoDIPG-H3WT cells. Interestingly, knockdown

of BRD4 was found to be the most effective for self-renewal ability in isoDIPG-H3.3K27M cells. In line with these data, previous results from our group showed reduction of malignant phenotype of H3.3K27M-DIPG cells upon inhibition of BRD4 (by JQ1) (Wiese et al. 2020). Wu et al. found that indeed BRD4 is responsible for maintaining pluripotency of stem cells (Wu et al. 2015). Additionally, Tsume-Kajioka *et al.* reported that not only BRD4, but also BRD2, is essential for stem cell-like characteristics (Tsume-Kajioka et al. 2022) which supports findings from the present study. In addition, gene set enrichment analysis revealed processes such as stem cell differentiation to be regulated by target genes of BRD2 in isoDIPG-H3.3K27M cells, highlighting a potential BRD2 function in maintaining stemness-associated characteristics in DIPG cells carrying H3.3K27M-mutation. Interestingly, mRNA sequencing revealed several genes involved in canonical Wnt signaling pathway to be affected by BRD4 in isoDIPG-H3.3K27M cells. Wnt signaling pathway is associated with an increased cell proliferation and maintenance of stemness characteristics (Wang et al. 2013). Observed restoration of *DKK1* function is associated with reduced cell proliferation and invasiveness of glioma cells (Wang et al. 2013). This aspect could explain why stronger anti-proliferative effects are observed in isoDIPG-H3.3K27M cells upon OTX-015 treatment, since those cells grow faster (Wiese et al. 2020) and may therefore be more susceptible to Wnt signaling inhibition by OTX-015 treatment. In accordance, several studies indicated function of BRD4 in promoting stemness characteristics through mediating Wnt signaling pathway in different types of cancer (Song et al. 2019; Wang et al. 2021).

In conclusion, not only BRD4, but also BRD2 exhibits a crucial function in maintaining stem cell-like characteristics, with BRD4 regulating Wnt signaling in isoDIPG-H3.3K27M cells.

Mesenchymal phenotype of tumor cells is associated with cell migration and invasion. Knockdown of BRD2 and BRD4 reduced migration and invasion abilities, to a significantly higher extent in isoDIPG-H3.3K27M compared to isoDIPG-H3WT cells. These results were nicely reflected by reduced expression of mesenchymal markers: *SNAI1* (SNAIL), *SNAI2* (SLUG), *MMP2* and *CDH2* (N-cadherin). In line with these results, gene set enrichment analysis revealed cell migration as a process strongly regulated by BRD2 and BRD4 exclusively in isoDIPG-H3.3K27M cells, highlighting a possible function of BRD2 and BRD4 in maintaining mesenchymal phenotype.

In summary, migration and invasion depend strongly on BRD2 and BRD4 function in isoDIPG-H3.3K27M cells.

Overall, the effects observed in the present study suggest distinct functions of BET proteins in maintaining tumor-associated characteristics in isoDIPG-H3.3K27M cells compared to isoDIPG-H3WT cells. This indicates that higher H3K27ac levels indeed lead to increased functions of BET

proteins in isoDIPG cells. Furthermore, BRD2 and BRD4 seem to play a major role over BRD3 in tumor malignant phenotype observed in isoDIPG-H3.3K27M cells, regulating Wnt signaling, cell cycle and programmed cell death. Interestingly, BRD2 and BRD4 do not fulfill the same role in isoDIPG-H3.3K27M cells, for example BRD2 appears to regulate autophagy and BRD4 may mediate Wnt signaling in isoDIPG-H3.3K27M cells.

5.4 Conclusion

DIPG are a very rare subtype of pediatric brain tumors with an overall survival median of 11 months after diagnosis (Hoffman et al. 2018). In 2012, a novel mutation was discovered in DIPG: lysine (K) to methionine (M) substitution at position K27 in a histone H3 gene variant (H3K27M), which results in global loss of H3K27me3 and global gain of H3K27ac (Lewis et al. 2013; Bender et al. 2013). Because of hyperacetylation observed in isoDIPG-H3.3K27M cells, epigenetically active proteins involved in the regulation and translation of acetylation at H3K27 into gene transcription, including CBP/p300 and BET proteins, might have a major function in H3.3K27M-mutated DIPG cells.

The present study revealed successfully generated isogenic DIPG cell lines using CRISPR/Cas9 system, which differ from each other only in H3-mutation status, that were used to investigate the impact of H3.3K27M-mutation on tumor-associated characteristics and the function of different epigenetically relevant proteins, such as CBP and p300, as well as BRD2, BRD3 and BRD4.

H3.3K27M-mutation was introduced to originally H3-wildtype DIPG cells and consequently removed from originally H3.3K27M-mutated DIPG cells. In conclusion, this isogenic cell model helped to reveal that presence of H3.3K27M-mutation is indeed responsible for the malignant phenotype observed in DIPG cells.

Furthermore, isoDIPG-H3.3K27M cells seem to be more profoundly dependent on acetyltransferases, CBP and p300, and BET proteins function. Inhibition and knockdown of CBP, BRD2 and BRD4 resulted in reduction of cell proliferation, stem cell-like characteristics and invasion, as well as changes in expression of H3K27me3 and H3K27ac levels in isoDIPG-H3.3K27M cells. Interestingly, HAT function of p300 seems to be more crucial in isoDIPG-H3WT cells, whereas CBP HAT activity plays a major role for H3K27ac in isoDIPG-H3.3K27M cells.

The present study hints to a specific function of CBP in regulation of apoptosis, BRD2 in regulation of autophagy and BRD4 in cell cycle progression and Wnt signaling in isoDIPG-H3.3K27M cells.

Overall, this study reveals that presence of H3.3K27M-mutation is a key player important for the malignant phenotype observed in DIPG cells carrying H3.3K27M-mutation. Moreover, CBP as a main acetyltransferase of H3K27, and BRD2 and BRD4 as important translators of H3K27ac appeared to be promising therapeutic targets for treatment of DIPG and require further investigation.

References

Abbas, T.; Dutta, A. (2009): p21 in cancer: intricate networks and multiple activities. In *Nature reviews. Cancer* 9 (6), pp. 400–414. Available online at DOI: 10.1038/nrc2657.

Ameyar, M.; Wisniewska, M.; Weitzman, J. (2003): A role for AP-1 in apoptosis: the case for and against. In *Biochimie* 85 (8), pp. 747–752. Available online at DOI: 10.1016/j.biochi.2003.09.006.

Amorim, S.; Stathis, A.; Gleeson, M.; Iyengar, S.; Magarotto, V.; Leleu, X. et al. (2016): Bromodomain inhibitor OTX015 in patients with lymphoma or multiple myeloma: a dose-escalation, open-label, pharmacokinetic, phase 1 study. In *The Lancet. Haematology* 3 (4), pp. 196–204. Available online at DOI: 10.1016/S2352-3026(16)00021-1.

An, S.; Camarillo, J.; Huang, T.; Li, D.; Morris, J. (2020a): Histone tail analysis reveals H3K36me2 and H4K16ac as epigenetic signatures of diffuse intrinsic pontine glioma. Available online at doi: 10.1186/s13046-020-01773-x.

An, S.; Camarillo, J.; Huang, T.; Li, D.; Morris, J.; Zoltek, M. et al. (2020b): Histone tail analysis reveals H3K36me2 and H4K16ac as epigenetic signatures of diffuse intrinsic pontine glioma. In *Journal of experimental and clinical cancer research* 39 (1), p. 261. Available online at DOI: 10.1186/s13046-020-01773-x.

Ansari, M.; Stagni, V.; Iuzzolino, A.; Rotili, D.; Mai, A.; Bufalo, D. et al. (2023): Pharmacological targeting of CBP/p300 drives a redox/autophagy axis leading to senescence-induced growth arrest in non-small cell lung cancer cells. In *Cancer gene therapy* 30 (1), pp. 124–136. Available online at DOI: 10.1038/s41417-022-00524-8.

Avantaggiati, M.; Ogryzko, V.; Gardner, K.; Giordano, A.; Levine, A.; Kelly, K. (1997): Recruitment of p300/CBP in p53-dependent signal pathways. In *Cell* 89 (7), pp. 1175–1184. Available online at DOI: 10.1016/s0092-8674(00)80304-9.

Babelova, A.; Burckhardt, B.; Salinas-Riester, G.; Pommerenke, C.; Burckhardt, G.; Henjakovic, M. (2015): Next generation sequencing of sex-specific genes in the livers of obese ZSF1 rats. In *Genomics* 106 (4), pp. 204–213. Available online at DOI: 10.1016/j.ygeno.2015.07.006.

Bachmann, I.; Halvorsen, O.; Collett, K.; Stefansson, I.; Straume, O.; Haukaas, S. et al. (2006): EZH2 expression is associated with high proliferation rate and aggressive tumor subgroups in cutaneous melanoma and cancers of the endometrium, prostate, and breast. In *Journal of Clinical Oncology* 24 (2), pp. 268–273. Available online at DOI: 10.1200/JCO.2005.01.5180.

Bailey, P.; Figueroa, M.; Mohiuddin, S.; Zaky, W.; Chandra, J. (2018): Cutting Edge Therapeutic Insights Derived from Molecular Biology of Pediatric High-Grade Glioma and Diffuse Intrinsic Pontine Glioma (DIPG). In *Bioengineering* 5 (4), p. 88. Available online at DOI: 10.3390/bioengineering5040088.

Balakrishnan, I.; Danis, E.; Pierce, A.; Madhavan, K.; Wang, D.; Dahl, N. et al. (2020): Senescence Induced by BMI1 Inhibition Is a Therapeutic Vulnerability in H3K27M-Mutant DIPG. In *Cell reports* 33 (3), p. 108286. Available online at DOI: 10.1016/j.celrep.2020.108286.

Barrows, J.; Lin, B.; Quaas, C.; Fullbright, G.; Wallace, E.; Long, D. (2022): BRD4 promotes resection and homology-directed repair of DNA double-strand breaks. In *Nature communications* 13 (1), p. 3016. Available online at DOI: 10.1038/s41467-022-30787-6.

Batlle, E.; Sancho, E.; Franci, C.; Dominguez, D.; Monfar, M.; Baulida, J.; Garcia De Herreros, A. (2000): The transcription factor snail is a repressor of E-cadherin gene expression in epithelial tumour cells. In *Nature cell biology* 2 (2), pp. 84–89. Available online at DOI: 10.1038/35000034.

Beacon, T.; Delcuve, G.; Lopez, C.; Nardocci, G.; Kovalchuk, I.; van Wijnen, A.; Davie, J. (2021): The dynamic broad epigenetic (H3K4me3, H3K27ac) domain as a mark of essential genes. In *Clinical epigenetics* 13 (1), p. 138. Available online at DOI: 10.1186/s13148-021-01126-1.

Bechet, D.; Gielen, G.; Korshunov, A.; Pfister, S.; Rousso, C.; Faury, D. et al. (2014): Specific detection of methionine 27 mutation in histone 3 variants (H3K27M) in fixed tissue from high-grade astrocytomas. In *Acta neuropathologica* 128 (5), pp. 733–741. Available online at DOI: 10.1007/s00401-014-1337-4.

Bedford, CD.; Kasper, HL.; Fukuyama, T.; Brindle, K. P. (2010): Target gene context influences the transcriptional requirement for the KAT3 family of CBP and p300 histone acetyltransferases. In *Epigenetics* 5 (1), pp. 9–15. Available online at DOI: 10.4161/epi.5.1.10449.

Bedford, D.; Brindle, P. (2012): Is histone acetylation the most important physiological function for CBP and p300? In *Aging* 4 (4), pp. 247–255. Available online at DOI: 10.18632/aging.100453.

Beke, L.; Nuytten, M.; van Eynde, A.; Beullens, M.; Bollen, M. (2007): The gene encoding the prostatic tumor suppressor PSP94 is a target for repression by the Polycomb group protein EZH2. In *Oncogene* 26 (31), pp. 4590–4595. Available online at DOI: 10.1038/sj.onc.1210248.

Belkina, A. C.; Denis, G. V. (2012a): BET domain co-regulators in obesity, inflammation and cancer. In *Nature reviews. Cancer* 12 (7), pp. 465–477. Available online at DOI: 10.1038/nrc3256.

Belkina, Anna C.; Denis, Gerald V. (2012b): BET domain co-regulators in obesity, inflammation and cancer. In *Nature reviews. Cancer* 12 (7), pp. 465–477. Available online at doi: 10.1038/nrc3256.

Benayoun, Bérénice A.; Pollina, Elizabeth A.; Ucar, Duygu; Mahmoudi, Salah; Karra, Kalpana; Wong, Edith D. et al. (2014): H3K4me3 breadth is linked to cell identity and transcriptional consistency. In *Cell* 158 (3), pp. 673–688. Available online at doi: 10.1016/j.cell.2014.06.027.

Bender, S.; Tang, Y.; Lindroth, MA.; Hovestadt, V.; Jones, TDW.; Kool, M. (2013a): Reduced H3K27me3 and DNA hypomethylation are major drivers of gene expression in K27M mutant pediatric high-grade gliomas. In *Cancer Cell* 24 (5), pp. 660–672. Available online at DOI: 10.1016/j.ccr.2013.10.006.

Bender, Sebastian; Tang, Yujie; Lindroth, Anders M.; Hovestadt, Volker; Jones, David T. W.; Kool, Marcel (2013b): Reduced H3K27me3 and DNA hypomethylation are major drivers of

gene expression in K27M mutant pediatric high-grade gliomas. In *Cancer Cell* 24 (5), pp. 660–672. Available online at doi: 10.1016/j.ccr.2013.10.006.

Berger, S. L. (2007): The complex language of chromatin regulation during transcription. In *Nature* 447 (7143), pp. 407–412. Available online at DOI: 10.1038/nature05915.

Berthon; Raffoux; Thomas; Vey (2016a): Bromodomain inhibitor OTX015 in patients with acute leukaemia: a dose-escalation, phase 1 study. In *The Lancet. Haematology*. Available online at DOI: 10.1016/S2352-3026(15)00247-1.

Berthon, C.; Raffoux, E.; Thomas, X.; Vey, N.; Gomez-Roca, C.; Yee, K. et al. (2016b): Bromodomain inhibitor OTX015 in patients with acute leukaemia: a dose-escalation, phase 1 study. In *The Lancet. Haematology* 3 (4), pp. 186–195. Available online at DOI: 10.1016/S2352-3026(15)00247-1.

Bhattacharya, S.; Workman, J. (2020): Regulation of SETD2 stability is important for the fidelity of H3K36me3 deposition. In *Epigenetics and chromatin* 13 (1), p. 40. Available online at DOI: 10.1186/s13072-020-00362-8.

Bhattacharyya, S.; Pradhan, K.; Campbell, N.; Mazdo, J.; Vasantkumar, A.; Bhagat, T. et al. (2017): Altered hydroxymethylation is seen at regulatory regions in pancreatic cancer and regulates oncogenic pathways. In *Genome research* 27 (11), pp. 1830–1842. Available online at DOI: 10.1101/gr.222794.117.

Blackledge, N.; Farcas, A.; Kondo, T.; King, H.; McGouran, J.; Hanssen, L. et al. (2014): Variant PRC1 complex-dependent H2A ubiquitylation drives PRC2 recruitment and polycomb domain formation. In *Cell* 157 (6), pp. 1445–1459. Available online at DOI: 10.1016/j.cell.2014.05.004.

Boi, M.; Zucca, E.; Inghirami, G.; Bertoni, F. (2015): PRDM1/BLIMP1: a tumor suppressor gene in B and T cell lymphomas. In *Leukemia and lymphoma* 56 (5), pp. 1223–1228. Available online at DOI: 10.3109/10428194.2014.953155.

Boland, MJ.; Nazor, KL.; Loring, J. F. (2014): Epigenetic regulation of pluripotency and differentiation. In *Circulation research* 115 (2), pp. 311–324. Available online at DOI: 10.1161/CIRCRESAHA.115.301517.

Bowers, E.; Yan, G.; Mukherjee, Ch; Orry, A.; Wang, L.; Holbert, M. et al. (2010): Virtual ligand screening of the p300/CBP histone acetyltransferase: identification of a selective small molecule inhibitor. In *Chemistry and biology* 17 (5), pp. 471–482. Available online at DOI: 10.1016/j.chembiol.2010.03.006.

Bracken, A.; Kleine-Kohlbrecher, D.; Dietrich, N.; Pasini, D.; Gargiulo, G.; Beekman, Ch et al. (2007): The Polycomb group proteins bind throughout the INK4A-ARF locus and are disassociated in senescent cells. In *Genes & development* 21 (5), pp. 525–530. Available online at DOI: 10.1101/gad.415507.

Breuer, R.; Snijders, P.; Smit, E.; Sutedja, T.; Sewalt, R.; Otte, A. et al. (2004): Increased expression of the EZH2 polycomb group gene in BMI-1-positive neoplastic cells during bronchial carcinogenesis. In *Neoplasia* 6 (6), pp. 736–743. Available online at DOI: 10.1593/neo.04160.

Bryant, R.; Cross, N.; Eaton, C.; Hamdy, F.; Cunliffe, V. (2007): EZH2 promotes proliferation and invasiveness of prostate cancer cells. In *The Prostate* 67 (5), pp. 547–556. Available online at DOI: 10.1002/pros.20550.

Bueren, A.; Wiese, M.; Gielen, G.; Kramm, C. (2017): Maligne Gliome: Therapieoptionen bei Kindern und Jugendlichen. In *TumorDiagnostik & Therapie* 38 (03), pp. 172–177. Available online at DOI: 10.1055/s-0043-101185.

Canoll, P.; Goldman, J. (2008): The interface between glial progenitors and gliomas. In *Acta neuropathologica* 116 (5), pp. 465–477. Available online at doi: 10.1007/s00401-008-0432-9.

Caslini, C.; Hong, S.; Ban, Y.; Chen, X.; Ince, T. (2019): HDAC7 regulates histone 3 lysine 27 acetylation and transcriptional activity at super-enhancer-associated genes in breast cancer stem cells. In *Oncogene* 38 (39), pp. 6599–6614. Available online at DOI: 10.1038/s41388-019-0897-0.

Castel, D.; Kergrohen, T.; Tauziede-Espariat, A.; Mackay, A.; Ghermaoui, S.; Lechapt, E. et al. (2020): Histone H3 wild-type DIPG/DMG overexpressing EZHIP extend the spectrum diffuse midline gliomas with PRC2 inhibition beyond H3-K27M mutation. In *Acta neuropathologica* 139 (6), Article DOI: 10.1007/s00401-020-02142-w, pp. 1109–1113.

Castel, D.; Philippe, C.; Calmon, R.; Le Dret, L.; Truffaux, N.; Boddaert, N. (2015a): Histone H3F3A and HIST1H3B K27M mutations define two subgroups of diffuse intrinsic pontine gliomas with different prognosis and phenotypes. In *Acta neuropathologica* 130 (6), pp. 815–827. Available online at DOI: 10.1007/s00401-015-1478-0.

Castel, D.; Philippe, C.; Kergrohen, T.; Sill, M.; Merlevede, J.; Barret, E. (2018a): Transcriptomic and epigenetic profiling of 'diffuse midline gliomas, H3 K27M-mutant' discriminate two subgroups based on the type of histone H3 mutated and not supratentorial or infratentorial location. In *Acta neuropathologica communications* 6 (1). Available online at DOI: 10.1186/s40478-018-0614-1.

Castel, David; Philippe, Cathy; Calmon, Raphaël; Le Dret, Ludivine; Truffaux, Nathalène; Boddaert, Nathalie (2015b): Histone H3F3A and HIST1H3B K27M mutations define two subgroups of diffuse intrinsic pontine gliomas with different prognosis and phenotypes. In *Acta neuropathologica* 130 (6), pp. 815–827. Available online at doi: 10.1007/s00401-015-1478-0.

Castel, David; Philippe, Cathy; Kergrohen, Thomas; Sill, Martin; Merlevede, Jane; Barret, Emilie (2018b): Transcriptomic and epigenetic profiling of 'diffuse midline gliomas, H3 K27M-mutant' discriminate two subgroups based on the type of histone H3 mutated and not supratentorial or infratentorial location. In *Acta neuropathologica communications* 6. Available online at doi: 10.1186/s40478-018-0614-1.

Chakraborty, R.; Ostriker, A.; Xie, Y.; Dave, J.; Gamez-Mendez, A.; Abu, Y. et al. (2022): Histone Acetyltransferases p300 and CBP Coordinate Distinct Chromatin Remodeling Programs in Vascular Smooth Muscle Plasticity. In *Circulation research* 145 (23), pp. 1720–1737. Available online at https://doi.org/10.1161/CIRCULATIONAHA.121.057599.

Chan, Y-S; Goeke, J.; Venkatesan, N.; Feng, B.; Su, I-H; Ng, H-H (2013): A PRC2-dependent repressive role of PRDM14 in human embryonic stem cells and induced pluripotent stem cell reprogramming. In *Stem cells* 31 (4), pp. 682–692. Available online at DOI: 10.1002/stem.1307.

Chang, F.; Chan, L.; McGhie, J.; Udugama, M.; Mayne, L.; Collas, P. et al. (2015): CHK1-driven histone H3.3 serine 31 phosphorylation is important for chromatin maintenance and cell survival in human ALT cancer cells. In *Nucleic acids research* 43 (5), pp. 2603–2614. Available online at DOI: 10.1093/nar/gkv104.

Chawla, S.; Hardingham, G.; Quinn, D.; Bading, H. (1998): CBP: a signal-regulated transcriptional coactivator controlled by nuclear calcium and CaM kinase IV. In *Science* 281 (5382), pp. 1505–1509. Available online at DOI: 10.1126/science.281.5382.1505.

Chekler, E. L.P.; Pellegrino, J. A.; Lanz, T. A.; Denny, R. A.; Flick, A. C.; Coe, J. et al. (2015): Transcriptional Profiling of a Selective CREB Binding Protein Bromodomain Inhibitor Highlights Therapeutic Opportunities. In *Chemistry and biology* 22 (12), pp. 1588–1596. Available online at DOI: 10.1016/j.chembiol.2015.10.013.

Chen, J.; Xue, Y. (2016): Emerging roles of non-coding RNAs in epigenetic regulation. In *Science china. Life sciences* 59 (3), pp. 227–235. Available online at DOI: 10.1007/s11427-016-5010-0.

Chen, K-Y; Bush, K.; Klein, R.; Cervantes, V.; Lewis, N.; Naqvi, A. et al. (2020): Reciprocal H3.3 gene editing identifies K27M and G34R mechanisms in pediatric glioma including NOTCH signaling. In *Communications biology* 3 (1), p. 363. Available online at DOI: 10.1038/s42003-020-1076-0.

Cheung, K.; Kim, Ch; Zhou, M-M (2021): The Functions of BET Proteins in Gene Transcription of Biology and Diseases. In *Frontiers in molecular biosciences* 8, p. 728777. Available online at DOI: 10.3389/fmolb.2021.728777.

Cheung, K.; Lu, G.; Sharma, R.; Vincek, A.; Zhang, R.; Plotnikov, A. et al. (2007): BET N-terminal bromodomain inhibition selectively blocks Th17 cell differentiation and ameliorates colitis in mice. In *Proceedings of the National Academy of Sciences of the United States of America* 114 (11), pp. 2952–2957. Available online at DOI: 10.1073/pnas.1615601114.

Cheung, K. L.; Zhang, F.; Jaganathan, A.; Sharma, R.; Zhang, Q.; Konuma, T. et al. (2017): Distinct Roles of Brd2 and Brd4 in Potentiating the Transcriptional Program for Th17 Cell Differentiation. In *Molecular cell* 65 (6), pp. 1068–1080. Available online at DOI: 10.1016/j.molcel.2016.12.022.

Choe, J.; Lin, S.; Zhang, W.; Liu, Q.; Wang, L.; Ramirez-Moya, J. et al. (2018): mRNA circularization by METTL3-eIF3h enhances translation and promotes oncogenesis. In *Nature* 561 (7724), pp. 556–560. Available online at DOI: 10.1038/s41586-018-0538-8.

Chrivia, J.; Kwok, R.; Lamb, N.; Hagiwara, M.; Montminy, M.; Goodman, R. (1993): Phosphorylated CREB binds specifically to the nuclear protein CBP. In *Nature* 365 (6449), pp. 855–859. Available online at DOI: 10.1038/365855a0.

Chung, Ch; Sweha, S.; Pratt, D.; Tamrazi, B.; Panwalkar, P.; Banda, A. et al. (2020): Integrated Metabolic and Epigenomic Reprograming by H3K27M Mutations in Diffuse Intrinsic Pontine

Gliomas. In *Cancer Cell* 38 (3), pp. 334–349. Available online at DOI: 10.1016/j.ccell.2020.07.008.

Clayton, A.; Hazzalin, C.; Mahadevan, L. (2006): Enhanced histone acetylation and transcription: a dynamic perspective. In *Molecular cell* 23 (3), pp. 289–296. Available online at DOI: 10.1016/j.molcel.2006.06.017.

Cockle, J. V.; Picton, S.; Levesley, J.; Ilett, E.; Carcaboso, A.; Short, S. et al. (2015): Cell migration in paediatric glioma; characterisation and potential therapeutic targeting. In *British Journal of Cancer*. Available online at doi: 10.1038/bjc.2015.16.

Cohen, K. J.; Heideman, R. L.; Zhou, T.; Holmes, E. J.; Lavey, R. S.; Bouffet, E.; Pollack, I. F. (2011): Temozolomide in the treatment of children with newly diagnosed diffuse intrinsic pontine gliomas: a report from the Children's Oncology Group. In *Neurooncology* 13 (4), pp. 410–416. Available online at DOI: 10.1093/neuonc/noq205.

Conery, A.; Centore, R.; Spillane, K.; Follmer, N.; Bommi-Reddy, A.; Hatton, Ch et al. (2016): Preclinical Anticancer Efficacy of BET Bromodomain Inhibitors Is Determined by the Apoptotic Response. In *Cancer research* 76 (6), pp. 1313–1319. Available online at DOI: 10.1158/0008-5472.CAN-15-1458.

Cribbs, A.; Filippakopoulos, P.; Philpott, M.; Wells, G.; Penn, H.; Oerum, H. et al. (2021): Dissecting the Role of BET Bromodomain Proteins BRD2 and BRD4 in Human NK Cell Function. In *Frontiers in immunology* 12, p. 626255. Available online at DOI: 10.3389/fimmu.2021.626255.

Da Costa, D.; Agathanggelou, A.; Weston, T. P.; Petermann, E.; Zlatanou, A.; Oldreive, C. et al. (2013): BET inhibition as a single or combined therapeutic approach in primary paediatric B-precursor acute lymphoblastic leukaemia. In *Blood cancer journal* 3 (7), p. 126. Available online at DOI: 10.1038/bcj.2013.24.

Dancy, B. M.; Cole, P. A. (2015): Protein lysine acetylation by p300/CBP. In *Chemical reviews* 115 (6), pp. 2419–2452. Available online at DOI: 10.1021/cr500452k.

Daneshvar, K.; Ardehali, M. B.; Klein, I. A.; Hsieh, F-K; Kratkiewicz, A. J.; Mahpour, A. et al. (2020): lncRNA DIGIT and BRD3 protein form phase-separated condensates to regulate endoderm differentiation. In *Nature cell biology* 22 (10), pp. 1211–1222. Available online at DOI: 10.1038/s41556-020-0572-2.

Danieau, G.; Morice, S.; Renault, S.; Brion, R.; Biteau, K.; Amiaud, J. et al. (2021): ICG-001, an Inhibitor of the β-Catenin and cAMP Response Element-Binding Protein Dependent Gene Transcription, Decreases Proliferation but Enhances Migration of Osteosarcoma Cells. In *Pharmaceuticals* 14 (5), p. 421. Available online at DOI: 10.3390/ph14050421.

Delmore, J.; Issa, G.; Lemieux, M.; Rahl, P.; Shi, J.; Jacobs, H. et al. (2011): BET bromodomain inhibition as a therapeutic strategy to target c-Myc. In *Cell* 146 (6), pp. 904–917. Available online at DOI: 10.1016/j.cell.2011.08.017.

Denis, G.; McComb, M.; Faller, D.; Sinha, A.; Romesser, P.; Costello, C. (2006): Identification of transcription complexes that contain the double bromodomain protein Brd2 and chromatin

remodeling machines. In *Journal of proteosome research* 5 (3), pp. 502–511. Available online at DOI: 10.1021/pr050430u.

Devaiah, B.; Mu, J.; Akman, B.; Uppal, S.; Weissman, J.; Cheng, D. et al. (2020): MYC protein stability is negatively regulated by BRD4. In *Proceedings of the National Academy of Sciences of the United States of America* 117 (24), pp. 13457–13467. Available online at DOI: 10.1073/pnas.1919507117.

Dhar, S.; Gursoy-Yuzugullu, O.; Parasuram, R.; Price, B. (2017): The tale of a tail: histone H4 acetylation and the repair of DNA breaks. In *Philosophical transactions of the Royal Society of London. Series B, Biological sciences* 372 (1731), p. 20160284. Available online at DOI: 10.1098/rstb.2016.0284.

Diehl, J. A. (2002): Cycling to cancer with cyclin D1. In *Cancer biology and therapy* 1 (3), pp. 226–231. Available online at DOI: 10.4161/cbt.72.

Diehl, K.; Ge, E.; Weinberg, D.; Jani, K.; Allis, D.; Muir, T. (2019): PRC2 engages a bivalent H3K27M-H3K27me3 dinucleosome inhibitor. In *Proceedings of the National Academy of Sciences of the United States of America* 116 (44), pp. 22152–22157. Available online at DOI: 10.1073/pnas.1911775116.

Dong, P.; Kaneuchi, M.; Watari, H.; Sudo, S.; Sakuragi, N. (2014): MicroRNA-106b modulates epithelial-mesenchymal transition by targeting TWIST1 in invasive endometrial cancer cell lines. In *Molecular carcinogenesis* 53 (5), 349-359. Available online at DOI: 10.1002/mc.21983.

Dong, X.; Hu, X.; Chen, J.; Hu, D.; Chen, L. (2018): BRD4 regulates cellular senescence in gastric cancer cells via E2F/miR-106b/p21 axis. In *Cell death and disease* 9 (2), p. 203. Available online at DOI: 10.1038/s41419-017-0181-6.

Eckner, R.; Oldread, T.; Livingston, D. (1996): Interaction and functional collaboration of p300/CBP and bHLH proteins in muscle and B-cell differentiation. In *Genes & development* 10 (19), pp. 2478–2490. Available online at DOI: 10.1101/gad.10.19.2478.

Emami, K.; Nguyen, C.; Ma, H.; Kim, D.; Jeong, K.; Eguchi, M. et al. (2004): A small molecule inhibitor of beta-catenin/CREB-binding protein transcription. In *Proceedings of the National Academy of Sciences of the United States of America* 101 (34), pp. 12682–12687. Available online at DOI: 10.1073/pnas.0404875101.

Ernst, T.; Chase, A. J.; Score, J.; Hidalgo-Curtis, C. E.; Bryant, C.; Jones, A. V. et al. (2010): Inactivating mutations of the histone methyltransferase gene EZH2 in myeloid disorders. In *Nature genetics* 42 (8), pp. 722–726. Available online at DOI: 10.1038/ng.621.

Facompre, N.; Harmeyer, K.; Sahu, V.; Gimotty, P.; Rustgi, A.; Nakagawa, H.; Basu, D. (2017): Targeting JARID1B's demethylase activity blocks a subset of its functions in oral cancer. In *Oncotarget* 9 (10), pp. 8985–8998. Available online at DOI: 10.18632/oncotarget.23739.

Fang, F.; Xu, Y.; Chew, K.; Chen, X.; Ng, H.; Matsudaira, P. (2014): Coactivators p300 and CBP maintain the identity of mouse embryonic stem cells by mediating long-range chromatin structure. In *Stem cells* 32 (7), pp. 1805–1816. Available online at DOI: 10.1002/stem.1705.

Fangusaro, J. (2012): Pediatric high grade glioma: a review and update on tumor clinical characteristics and biology. In *Frontiers in oncology* 2, p. 105. Available online at DOI: 10.3389/fonc.2012.00105.

Fauquier, L.; Azzag, K.; PArra, M. A.M.; Quillien, A.; Boulet, M.; Diouf, S. et al. (2018): CBP and P300 regulate distinct gene networks required for human primary myoblast differentiation and muscle integrity. In *Scientific reports* 8 (1), p. 12629. Available online at DOI: 10.1038/s41598-018-31102-4.

Filippakopoulos, P.; Knapp, S. (2014): Targeting bromodomains: epigenetic readers of lysine acetylation. In *Nature reviews. Drug discovery* 13 (5), pp. 337–356. Available online at DOI: 10.1038/nrd4286.

Filippakopoulos, P.; Picaud, S.; Mangos, M.; Keates, T.; Lambert, J-P; Felletar, I. et al. (2012): Histone recognition and large-scale structural analysis of the human bromodomain family. In *Cell* 149 (1), pp. 214–231. Available online at DOI: 10.1016/j.cell.2012.02.013.

Filippakopoulos, P.; Qi, J.; Picaud, S.; Shen, Y.; Smith, W.; Fedorov, O. et al. (2010): Selective inhibition of BET bromodomains. In *Nature* 468 (7327), 1967-1073. Available online at DOI: 10.1038/nature09504.

Fleige, S.; Pfaffl, M. W. (2006): RNA integrity and the effect on the real-time qRT-PCR performance. In *Molecular aspects of medicine* 27 (2-3), pp. 126–139. Available online at DOI: 10.1016/j.mam.2005.12.003.

Foglizzo, M.; Middleton, A.; Burgess, A.; Crowther, J.; Dobson, R.; Murphy, J. et al. (2018): A bidentate Polycomb Repressive-Deubiquitinase complex is required for efficient activity on nucleosomes. In *Nature communications*. Available online at doi: 10.1038/s41467-018-06186-1.

Fontanals-Cirera, B.; Hasson, D.; Vardabasso, Ch; Di Micco, R.; Agrawal, P.; Chowdhury, A. et al. (2017): Harnessing BET Inhibitor Sensitivity Reveals AMIGO2 as a Melanoma Survival Gene. In *Molecular cell* 68 (4), pp. 731–744. Available online at DOI: 10.1016/j.molcel.2017.11.004.

French, C. A. (2010): NUT midline carcinoma. In *Cancer genetics and cytogenetics* 203 (1), pp. 16–20. Available online at DOI: 10.1016/j.cancergencyto.2010.06.007.

Fu; Phillips (1991): Biologic rationale of combined radiotherapy and chemotherapy. In *Hematology/oncology clinics of north america*.

Gang; Hsieh; Pham; Zhao (2014): Small-molecule inhibition of CBP/catenin interactions eliminates drug-resistant clones in acute lymphoblastic leukemia. In *Oncogene*. Available online at DOI: 10.1038/onc.2013.169.

Gao, X.; Lin, J.; Ning, Q.; Gao, L.; Yao, Y.; Zhou, J. et al. (2013): A histone acetyltransferase p300 inhibitor C646 induces cell cycle arrest and apoptosis selectively in AML1-ETO-positive AML cells. In *PloS one* 8 (2). Available online at DOI: 10.1371/journal.pone.0055481.

Garcia-Carpizo, V.; Ruiz-Llorente, S.; Sarmentero, J.; Grana-Castro, O.; Pisano, D.; Barrero, M. (2018): CREBBP/EP300 bromodomains are critical to sustain the GATA1/MYC regulatory axis in

proliferation. In *Epigenetics and chromatin* 11 (1), p. 30. Available online at DOI: 10.1186/s13072-018-0197-x.

Gaspar, N.; Marshall, L.; Perryman, L.; Bax, D.; Little, S.; Viana-Pereira, M. et al. (2010): MGMT-independent temozolomide resistance in pediatric glioblastoma cells associated with a PI3-kinase-mediated HOX/stem cell gene signature. In *Cancer research* 70 (22), pp. 9243–9252. Available online at DOI: 10.1158/0008-5472.CAN-10-1250.

Gatchalian, J.; Malik, S.; Ho, J.; Lee, D-S; Kelso, T.; Shokhirev, M. et al. (2018): A non-canonical BRD9-containing BAF chromatin remodeling complex regulates naive pluripotency in mouse embryonic stem cells. In *Nature communications* 9 (1), p. 5139. Available online at DOI: 10.1038/s41467-018-07528-9.

Ghahhari, N.; Babashah, S. (2015): Interplay between microRNAs and WNT/β-catenin signalling pathway regulates epithelial-mesenchymal transition in cancer. In *European journal of cancer* 51 (12), pp. 1638–1649. Available online at DOI: 10.1016/j.ejca.2015.04.021.

Gielen, G.; Baugh, J. N.; van Vuurden, D. G.; van Veldhuijzen Zanten, S. E.M.; Hargrave, D.; Massimino, M. et al. (2022): Pediatric high-grade gliomas and the WHO CNS Tumor Classification-Perspectives of pediatric neuro-oncologists and neuropathologists in light of recent updates. In *Neuro-oncology advances* 4 (1). Available online at DOI: 10.1093/noajnl/vdac077.

Gonzales-Cope, M.; Sidoli, S.; Bhanu, N.; Won, K-J; Garcia, B. (2016): Histone H4 acetylation and the epigenetic reader Brd4 are critical regulators of pluripotency in embryonic stem cells. In *BMC Genomics* 17, p. 95. Available online at DOI: 10.1186/s12864-016-2414-y.

Gonzalez-Martinez, R.; Marquez-Galera, A.; Del Blanco, B.; Lopez-Atalaya, J.; Barco, A.; Herrera, E. (2022): CBP and p300 Jointly Maintain Neural Progenitor Viability but Play Unique Roles in the Differentiation of Neural Lineages. In *Cells* 11(24), p. 4118. Available online at DOI: 10.3390/cells11244118.

Goodman, R.; Smolik, S. (2000): CBP/p300 in cell growth, transformation, and development. In *Genes & development* 14 (13), pp. 1553–1577.

Greer, E. L.; Shi, Y. (2012): Histone methylation: a dynamic mark in health, disease and inheritance. In *Nature reviews. Genetics* 13 (5), pp. 343–357. Available online at DOI: 10.1038/nrg3173.

Grigsby, P. W.; Thomas, P. R.; Schwartz, H. G.; Fineberg, B. B. (1989): Inhibition of BET bromodomains as a therapeutic strategy for cancer drug discovery. In *International Journal of Radiation Oncology, Biology, Physics* 16 (3), pp. 649–655. Available online at DOI: 10.1016/0360-3016(89)90480-x.

Grossman, S.; Perez, M.; Kung, A.; Joseph, M.; MAnsur, C.; Xiao, Z. et al. (1998): p300/MDM2 complexes participate in MDM2-mediated p53 degradation. In *Molecular cell* 2 (4), pp. 405–415. Available online at DOI: 10.1016/s1097-2765(00)80140-9.

Gu, M-L; Wang, Y-M; Zhou, X-X; Yao, H-P; Zheng, S.; Xiang, Z.; Ji, F. (2016): An inhibitor of the acetyltransferases CBP/p300 exerts antineoplastic effects on gastrointestinal stromal tumor

cells. In *Oncology reports* 36 (5), pp. 2763–2770. Available online at DOI: 10.3892/or.2016.5080.

Gu, W.; Shi, X.; Roeder, R. (1997): Synergistic activation of transcription by CBP and p53. In *Nature* 387 (6635), pp. 819–823. Available online at DOI: 10.1038/42972.

Haag, D.; Mack, N.; Da Silva, P.; Statz, B.; Clark, J.; Tanabe, K. et al. (2021): H3.3-K27M drives neural stem cell-specific gliomagenesis in a human iPSC-derived model. In *Cancer Cell* 39 (3), pp. 407–422. Available online at DOI: 10.1016/j.ccell.2021.01.005.

Haar, C. P.; Hebba, r. P.; Wallace, G. C.; Das, A.; Vandergrift, A.; Smith, J. A. et al. (2012): Drug resistance in glioblastoma: a mini review. In *Neurochemical Research* 37 (6), pp. 1192–1200. Available online at DOI: 10.1007/s11064-011-0701-1.

Hajmirza, A.; Emadali, A.; Gauthier, A.; Casasnovas, O.; Gressin, R.; Callanan, M. (2018): BET Family Protein BRD4: An Emerging Actor in NFκB Signaling in Inflammation and Cancer. In *Biomedicines* 6 (1), p. 16. Available online at DOI: 10.3390/biomedicines6010016.

Hammitzsch, A.; Tallant, C.; Fedorov, O.; O'Mahony, A.; Da Hay; Martinez, F. O. et al. (2015): CBP30, a selective CBP/p300 bromodomain inhibitor, suppresses human Th17 responses. In *Proceedings of the National Academy of Sciences of the United States of America* 112 (34), pp. 10768–10773. Available online at DOI: 10.1073/pnas.1501956112.

Hammitzsch A, Tallant C, Fedorov O, O'Mahony A, Brennan PE, Hay DA, Martinez FO, Al-Mossawi MH, de Wit J, Vecellio M, Wells C, Wordsworth P, Müller S, Knapp S, Bowness P (2015): CBP30, a selective CBP/p300 bromodomain inhibitor, suppresses human Th17 responses. In *Proc Natl Acad Sci U.S.A* 112 (34), pp. 10768–10773. Available online at doi: 10.1073/pnas.1501956112.

Hardingham, G.; Chawla, S.; Cruzalegui, F.; Bading, H. (1999): Control of recruitment and transcription-activating function of CBP determines gene regulation by NMDA receptors and L-type calcium channels. In *Neuron* 22 (4), pp. 789–798. Available online at DOI: 10.1016/s0896-6273(00)80737-0.

Harutyunyan, A.; Chen, H.; Lu, T.; Horth, C.; Nikbakht, H.; Krug, B. et al. (2020): H3K27M in Gliomas Causes a One-Step Decrease in H3K27 Methylation and Reduced Spreading within the Constraints of H3K36 Methylation. In *Cell reports* 33 (7), p. 108390. Available online at DOI: 10.1016/j.celrep.2020.108390.

Harutyunyan, A. S.; Krug, B.; Chen, H.; Papillon-Cavanagh, S.; Zeinieh, M.; Jay, N. de et al. (2019): H3.3K27M induces defective chromatin spread of PRC2-mediated repressive H3.3K27me2/me3 and is essential for glioma tumorigenesis. In *Nature communications* 10 (1), p. 1262. Available online at DOI: 10.1038/s41467-019-09140-x.

Hashizume, R. (2017): Epigenetic Targeted Therapy for Diffuse Intrinsic Pontine Glioma. In *Neurologia medico.chirurgica* 57 (7), pp. 331–342. Available online at DOI: 10.2176/nmc.ra.2017-0018.

Hatoum, R.; Chen, J-S; Lavergne, P.; Shlobin, N.; Wang, A.; Elkaim, L. et al. (2022): Extent of Tumor Resection and Survival in Pediatric Patients With High-Grade Gliomas: A Systematic Review and Meta-analysis. In *JAMA network open* 5 (8), p. 2226551.

Hay, D.; Fedorov, O.; Martin, S.; Singleton, D.; Tallant, C.; Wells, Ch et al. (2014): Discovery and optimization of small-molecule ligands for the CBP/p300 bromodomains. In *Journal of the American Chemical Society* 136 (26), pp. 9308–9319. Available online at DOI: 10.1021/ja412434f.

Hayward, Robert M.; Patronas, Nicolas; Baker, Eva H.; Vézina, Gilbert; Albert, Paul S.; Warren, Katherine E. (2008): Inter-observer variability in the measurement of diffuse intrinsic pontine gliomas. In *Journal of Oncology* 90(1), pp. 57–61. Available online at DOI: 10.1007/s11060-008-9631-4.

Helin, K.; Dhanak, D. (2013): Chromatin proteins and modifications as drug targets. In *Nature* 502 (7472), pp. 480–488. Available online at DOI: 10.1038/nature12751.

Hoffman, L. M.; van Veldhuijzen Zanten, S. E.M.; Colditz, N.; Baugh, J.; Chaney, B.; Hoffmann, M. et al. (2018): Clinical, Radiologic, Pathologic, and Molecular Characteristics of Long-Term Survivors of Diffuse Intrinsic Pontine Glioma (DIPG): A Collaborative Report From the International and European Society for Pediatric Oncology DIPG Registries. In *Journal of Clinical Oncology* 36 (19), pp. 1963–1972. Available online at DOI: 10.1200/JCO.2017.75.9308.

Hsu, S.; Gilgenast, T.; Bartman, C.; Edwards, Ch; Stonestrom, A.; Huang, P. et al. (2017): The BET Protein BRD2 Cooperates with CTCF to Enforce Transcriptional and Architectural Boundaries. In *Molecular cell* 66 (1), pp. 102–116. Available online at DOI: 10.1016/j.molcel.2017.02.027.

Hu, J.; Lei, Y.; Wong, W-K; Liu, S.; Lee, K-Ch; He, X. et al. (2014): Direct activation of human and mouse Oct4 genes using engineered TALE and Cas9 transcription factors. In *Nucleic acids research* 42 (7), pp. 4375–4390. Available online at DOI: 10.1093/nar/gku109.

Hussong, M.; Kaehler, Ch; Kerick, M.; Grimm, Ch; Franz, A.; Timmermann, B. et al. (2017a): The bromodomain protein BRD4 regulates splicing during heat shock. In *Nucleic acids research* 45 (1), pp. 382–394. Available online at DOI: 10.1093/nar/gkw729.

Hussong, M.; Kaehler, Ch; Kerick, M.; Grimm, Ch; Franz, A.; Timmermann, B. et al. (2017b): The bromodomain protein BRD4 regulates splicing during heat shock. In *Nucleic acids research* 45 (1), pp. 382–394. Available online at DOI: 10.1093/nar/gkw729.

Inagaki, Y.; Shiraki, K.; Sugimoto, K.; Yada, T.; Tameda, M.; Ogura, S. et al. (2016): Epigenetic regulation of proliferation and invasion in hepatocellular carcinoma cells by CBP/p300 histone acetyltransferase activity. In *International Journal of Oncology* 48 (2), pp. 533–540. Available online at DOI: 10.3892/ijo.2015.3288.

Ionov, Y.; Matsui, S.; Cowell, J. K. (2004): A role for p300/CREB binding protein genes in promoting cancer progression in colon cancer cell lines with microsatellite instability. In *Proceedings of the National Academy of Sciences of the United States of America* 101 (5), pp. 1273–1278. Available online at DOI: 10.1073/pnas.0307276101.

Izumi, H.; Ohta, R.; Nagatani, G.; Ise, T.; Nakayama, Y.; Nomoto, M.; Kohno, K. (2003): p300/CBP-associated factor (P/CAF) interacts with nuclear respiratory factor-1 to regulate the UDP-N-acetyl-alpha-d-galactosamine: polypeptide N-acetylgalactosaminyltransferase-3 gene. In *The biochemical journal* 373, pp. 713–722. Available online at DOI: 10.1042/BJ20021902.

Jang, M. K.; Mochizuki, K.; Zhou, M.; Jeong, H-S; Brady, J. N.; Ozato, K. (2005): The bromodomain protein Brd4 is a positive regulatory component of P-TEFb and stimulates RNA polymerase II-dependent transcription. In *Molecular cell* 19 (4), pp. 523–534. Available online at DOI: 10.1016/j.molcel.2005.06.027.

Janknecht, R.; Nordheim, A. (1996): MAP kinase-dependent transcriptional coactivation by Elk-1 and its cofactor CBP. In *Biochemical and biophysical research communications* 228 (3), pp. 831–837. Available online at DOI: 10.1006/bbrc.1996.1740.

Ji, Ch; Xu, W.; Ding, H.; Chen, Z.; Shi, Ch; Han, J. et al. (2022): The p300 Inhibitor A-485 Exerts Antitumor Activity in Growth Hormone Pituitary Adenoma. In *The journal of clinical endocrinology and metabolism* 107 (6), pp. 2291–2300. Available online at DOI: 10.1210/clinem/dgac128.

Kanduri, M.; Sander, B.; Ntoufa, S.; Papakonstantinou, N.; Sutton, L-A; Stamatopoulos, K. et al. (2013): A key role for EZH2 in epigenetic silencing of HOX genes in mantle cell lymphoma. In *Epigenetics* 8 (12), pp. 1280–1288. Available online at DOI: 10.4161/epi.26546.

Kania, A.; Price, M.; George-Alexander, L.; Patterson, D.; Hicks, S.; Scharer, C.; Boss, J. (2022): H3K27me3 Demethylase UTX Restrains Plasma Cell Formation. In *Journal of immunology* 208 (8), pp. 1873–1885. Available online at DOI: 10.4049/jimmunol.2100948.

Kaochar, S.; Dong, J.; Torres, M.; Rajapakshe, K.; Nikolos, F.; Davis, Ch et al. (2018): ICG-001 Exerts Potent Anticancer Activity Against Uveal Melanoma Cells. In *Investigative ophthamology nad visual science* 59 (1), pp. 132–143. Available online at DOI: 10.1167/iovs.17-22454.

Karamouzis, M.; Konstantinopoulos, P.; Papavassiliou, A. (2007): Roles of CREB-binding protein (CBP)/p300 in respiratory epithelium tumorigenesis. In *Cell research* 17 (4), pp. 324–332. Available online at DOI: 10.1038/cr.2007.10.

Karimian, A.; Ahmadi, Y.; Yousefi, B. (2016): Multiple functions of p21 in cell cycle, apoptosis and transcriptional regulation after DNA damage. In *DNA repair* 42, pp. 63–71. Available online at DOI: 10.1016/j.dnarep.2016.04.008.

Karremann, M.; Perwein, T.; Bueren, A. von; Behrens, L.; Gielen, G.; Bison, B.; Kramm, Ch (2021): Hirntumore im Kindes- und Jugendalter. In *Kinderärztliche Praxis* 92, pp. 151–156.

Kasper, L. H.; Qu, C.; Obenauer, J. C.; McGoldrick, D. J.; Brindle, P. K. (2014): Genome-wide and single-cell analyses reveal a context dependent relationship between CBP recruitment and gene expression. In *Nucleic acids research* 42 (18), pp. 11363–11382. Available online at DOI: 10.1093/nar/gku827.

Kawasaki, H.; Eckner, R.; Yao, T.; Taira, K.; Chiu, R.; Livingston, D.; Yokoyama, K. (1998): Distinct roles of the co-activators p300 and CBP in retinoic-acid-induced F9-cell differentiation. In *Nature* 393 (6682), pp. 284–289. Available online at DOI: 10.1038/30538.

Kfoury-Beaumont, N.; Prakasam, R.; Pondugula, S.; Lagas, J.; Matkovich, S.; Hontarz, P. et al. (2022): The H3K27M mutation alters stem cell growth, epigenetic regulation, and differentiation potential. In *BMC biology* 20 (1), p. 124. Available online at DOI: 10.1186/s12915-022-01324-0.

Khuong-Quang, D-A; Buczkowicz, P.; Rakopoulos, P.; Liu, X-Y; Fontebasso, AM.; Bouffet, E. (2012): K27M mutation in histone H3.3 defines clinically and biologically distinct subgroups of pediatric diffuse intrinsic pontine gliomas. In *Acta neuropathologica* 124 (3), pp. 439–447. Available online at DOI: 10.1007/s00401-012-0998-0.

Kim, K. H.; Roberts, C. W.M. (2016): Targeting EZH2 in cancer. In *Nature medicine* 22 (2), pp. 128–134. Available online at DOI: 10.1038/nm.4036.

Kim, Y.; Jo, D.; Park, N.; Bae, J.; Kim, J.; Lee, H. et al. (2022): Inhibition of BRD4 Promotes Pexophagy by Increasing ROS and ATM Activation. In *Cells* 11 (18), p. 2839. Available online at DOI: 10.3390/cells11182839.

Klingbeil, O.; Lesche, R.; Gelato, K. A.; Haendler, B.; Lejeune, P. (2016): Inhibition of BET bromodomain-dependent XIAP and FLIP expression sensitizes KRAS-mutated NSCLC to pro-apoptotic agents. In *Cell death and disease* 7 (9), p. 2365. Available online at DOI: 10.1038/cddis.2016.271.

Kluiver, T.; Alieva, M.; van Vuurden, D. G.; Wehrens, E.; Rios, A. (2020): Invaders Exposed: Understanding and Targeting Tumor Cell Invasion in Diffuse Intrinsic Pontine Glioma. In *Frontiers in oncology*. Available online at doi: 10.3389/fonc.2020.00092.

Koch, Ch; Andrews, R.; Flicek, P.; Dillon, S.; Karaoez, U.; Clelland, G. et al. (2007): The landscape of histone modifications across 1% of the human genome in five human cell lines. In *Genome research* 17 (6), pp. 691–707. Available online at DOI: 10.1101/gr.5704207.

Komiya, Y.; Habas, R. (2008): Wnt signal transduction pathways. In *Organogenesis* 4 (2), pp. 68–75. Available online at DOI: 10.4161/org.4.2.5851.

Krug, B.; Jay, N. D.; Harutyunyan, A. S.; Deshmukh, S.; Marchione DM; Guilhamon, P. et al. (2019): Pervasive H3K27 Acetylation Leads to ERV Expression and a Therapeutic Vulnerability in H3K27M Gliomas. In *Cancer Cell* 35 (5), pp. 782–797. Available online at DOI: 10.1016/j.ccell.2019.04.004.

Kumar, S.; Satarupa, S.; Kyungwoo, L.; Nanki, S. (2017a): BMI-1 is a potential therapeutic target in diffuse intrinsic pontine glioma. In *Oncotarget*. Available online at doi: 10.18632/oncotarget.18002.

Kumar, S.; Sengupta, S.; Lee, K.; Hura, N.; Fuller, Ch; DeWire, M. et al. (2017b): BMI-1 is a potential therapeutic target in diffuse intrinsic pontine glioma. In *Oncotarget* 8 (38), pp. 62962–62975. Available online at DOI: 10.18632/oncotarget.18002.

Kundaje, J. (2015): H3K4me3 breadth is linked to cell identity and transcriptional consistency. In *Cell* 158 (3), pp. 673–688. Available online at DOI: 10.1016/j.cell.2014.06.027.

Lamonica, J.; Deng, W.; Kadauke, S.; Campbell, A.; Gamsjaeger, R.; Wang, H. et al. (2011): Bromodomain protein Brd3 associates with acetylated GATA1 to promote its chromatin occupancy at erythroid target genes. In *Proceedings of the National Academy of Sciences of the United States of America* 108 (22), pp. 159–168. Available online at DOI: 10.1073/pnas.1102140108.

Lecona, E.; Narendra, V.; Reinberg, D. (2015): USP7 cooperates with SCML2 to regulate the activity of PRC1. In *Molecular and Cellular Biology* 35 (7), pp. 1157–1168. Available online at DOI: 10.1128/MCB.01197-14.

Lee, J-K; Louzada, S.; An, Y.; Kim, S.; Youk, J.; Park, S. et al. (2017): Complex chromosomal rearrangements by single catastrophic pathogenesis in NUT midline carcinoma. In *Annals of Oncology* 28 (4), pp. 890–897. Available online at DOI: 10.1093/annonc/mdw686.

LeRoy, G.; Rickards, B.; Flint, S. J. (2008): The double bromodomain proteins Brd2 and Brd3 couple histone acetylation to transcription. In *Molecular cell* 30 (1), pp. 51–60. Available online at DOI: 10.1016/j.molcel.2008.01.018.

Lewis, N.; Klein, R.; Kelly, C.; Yee, J.; Knoepfler, P. (2022): Histone H3.3 K27M chromatin functions implicate a network of neurodevelopmental factors including ASCL1 and NEUROD1 in DIPG. In *Epigenetics and chromatin* 15 (1), Article DOI: 10.1186/s13072-022-00447-6, p. 18.

Lewis, P. L.; Müller, M. M.; Koletsky, M. S.; Cordero, F.; Lin, S.; La Banaszynski et al. (2013a): Inhibition of PRC2 activity by a gain-of-function H3 mutation found in pediatric glioblastoma. In *Nature* 340 (6134), pp. 857–861.

Li, X.; Baek, G.; Ramanand, S.; Sharp, A.; Gao, Y.; Yuan, W. et al. (2018): BRD4 Promotes DNA Repair and Mediates the Formation of TMPRSS2-ERG Gene Rearrangements in Prostate Cancer. In *Cell reports* 22 (3), pp. 796–808. Available online at DOI: 10.1016/j.celrep.2017.12.078.

Li, Y.; Reverter, D. (2021): Molecular Mechanisms of DUBs Regulation in Signaling and Disease. In *International Journal of Molecular Sciences* 22 (3), p. 986. Available online at DOI: 10.3390/ijms22030986.

Li M, Pathak RR, Lopez-Rivera E, Friedman SL, Aguirre-Ghiso JA, Sikora AG (2015): The In Ovo Chick Chorioallantoic Membrane (CAM) Assay as an Efficient Xenograft Model of Hepatocellular Carcinoma. In *Journal of Visualized Experiments*. Available online at doi: 10.3791/52411.

Lill, N.; Grossman, S.; Ginsberg, D.; DeCaprio, J.; Livingston, D. (1997): Binding and modulation of p53 by p300/CBP coactivators. In *Nature* 387 (6635), pp. 823–827. Available online at DOI: 10.1038/42981.

Lin, S.; Hanif, E.; Chin, S. (2021): Is targeting autophagy mechanism in cancer a good approach? The possible double-edge sword effect. In *Cell and bioscience* 11 (1), p. 56. Available online at DOI: 10.1186/s13578-021-00570-z.

Liu, X.; Wang, L.; Zhao, K.; Thompson, P. R.; Hwang, Y.; Marmorstein, P. A.C. (2008): The structural basis of protein acetylation by the p300/CBP transcriptional coactivator. In *Nature* 451 (7180), pp. 846–850. Available online at DOI: 10.1038/nature06546.

Liu, X.; Wu, Q.; Li, L. (2017a): Functional and therapeutic significance of EZH2 in urological cancers. In *Oncotarget* 8 (22), pp. 38044–38055. Available online at DOI: 10.18632/oncotarget.16765.

Liu, Y.; Chen, H.; Zheng, P.; Zheng, Y.; Luo, Q.; Xie, G. et al. (2017b): ICG-001 suppresses growth of gastric cancer cells and reduces chemoresistance of cancer stem cell-like population. In *Journal of experimental and clinical cancer research* 36 (1), p. 125. Available online at DOI: 10.1186/s13046-017-0595-0.

Louis, D.; Perry, A.; Reifenberger, G.; Deimling, A. von; Figarella-Branger, D.; Cavenee, W. et al. (2016): The 2016 World Health Organization Classification of Tumors of the Central Nervous System: a summary. In *Acta neuropathologica* 131 (6), pp. 803–820. Available online at DOI: 10.1007/s00401-016-1545-1.

Lu, Z.; Zou, J.; Li, S.; Topper, M.; Tao, Y.; Zhang, H. et al. (2020): Epigenetic therapy inhibits metastases by disrupting premetastatic niches. In *Nature* 579 (7798), pp. 284–290. Available online at DOI: 10.1038/s41586-020-2054-x.

Luger, K.; Mäder, AW: Richmond, RK; Sargent, D. F.; Richmond, T. J. (1997): Crystal structure of the nucleosome core particle at 2.8 Å resolution. In *Nature* 389, pp. 251–260. Available online at DOI: 10.1038/38444.

Marsh, T.; Debnath, J. (2020): Autophagy suppresses breast cancer metastasis by degrading NBR1. In *Autophagy* 16 (6), pp. 1164–1165. Available online at DOI: 10.1080/15548627.2020.1753001.

Martire, S.; Gogate, A.; Whitmill, A.; Tafessu, A.; Nguyen, J.; Teng, Y-Ch et al. (2019): Phosphorylation of histone H3.3 at serine 31 promotes p300 activity and enhancer acetylation. In *Nature genetics* 51 (6), Article DOI: 10.1038/s41588-019-0428-5, pp. 941–946.

Mastracchio, A.; Lai, Ch; Digiammarino, E.; Ready, D.; Lasko, L.; Bromberg, K. et al. (2021): Discovery of a Potent and Selective Covalent p300/CBP Inhibitor. In *ACS medicinal chemistry letters* 12 (5), 726-731. Available online at DOI: 10.1021/acsmedchemlett.0c00654.

McManus, K.; Hendzel, M. (2003): Quantitative analysis of CBP- and P300-induced histone acetylations in vivo using native chromatin. In *Molecular and Cellular Biology* 23 (21), pp. 7611–7627. Available online at DOI: 10.1128/MCB.23.21.7611-7627.2003.

Meissner, A.; Mikkelsen, T.; Gu, H.; Wernig, M.; Hanna, J.; Sivachenko, A. et al. (2008): Genome-scale DNA methylation maps of pluripotent and differentiated cells. In *Nature* 454 (7205), pp. 766–770. Available online at DOI: 10.1038/nature07107.

Merika, M.; Williams, A.; Chen, G.; Collins, T.; Thanos, D. (1998): Recruitment of CBP/p300 by the IFN beta enhanceosome is required for synergistic activation of transcription. In *Molecular cell* 1 (2), pp. 277–287. Available online at DOI: 10.1016/s1097-2765(00)80028-3.

Mertz, J.; Conery, A.; Bryant, B.; Sandy, P.; Mele, D.; Bergeron, L.; Sims, R. (2011): Targeting MYC dependence in cancer by inhibiting BET bromodomains. In *Proceedings of the National Academy of Sciences of the United States of America* 108 (40), pp. 16669–16674. Available online at DOI: 10.1073/pnas.1108190108.

Messaoudi, K.; Clavreul, A.; Lagarce, F. (2015): Toward an effective strategy in glioblastoma treatment. Part I: resistance mechanisms and strategies to overcome resistance of glioblastoma to te-mozolomide. In *Drug Discovery Today* 20 (7), pp. 899–905. Available online at DOI: 10.1016/j.drudis.2015.02.011.

Miller, T.; Simon, B.; Rybin, V.; Groetsch, H.; Curtet, S.; Khochbin, S. et al. (2016): A bromodomain-DNA interaction facilitates acetylation-dependent bivalent nucleosome recognition by the BET protein BRDT. In *Nature communications* 7, p. 13855. Available online at DOI: 10.1038/ncomms13855.

Miyai, M.; Kanayama, T.; Hyodo, F.; Kinoshita, T.; Ishihara, T.; Okada, T. et al. (2021): Glucose transporter Glut1 controls diffuse invasion phenotype with perineuronal satellitosis in diffuse glioma microenvironment. In *Neuro-oncology advances*. Available online at https://doi.org/10.1093/noajnl/vdaa150.

Mochizuki, K.; Nishiyama, A.; Jang, M.; Dey, A.; Ghosh, A.; Tamura, T. et al. (2008): The bromodomain protein Brd4 stimulates G1 gene transcription and promotes progression to S phase. In *The journal of biological chemistry* 283 (14), pp. 9040–9048. Available online at DOI: 10.1074/jbc.M707603200.

Mohammad, F.; Weissmann, S.; Leblanc, B.; Pandey, D. P.; Hojfeldt, J. W.; Comet, I. et al. (2017): EZH2 is a potential therapeutic target for H3K27M-mutant pediatric gliomas. In *Nature medicine* 23 (4), pp. 483–492. Available online at DOI: 10.1038/nm.4293.

Nicetto, D.; Zaret, K. (2019): Role of H3K9me3 heterochromatin in cell identity establishment and maintenance. In *Current opinion in genetics and development* 55, pp. 1–10. Available online at DOI: 10.1016/j.gde.2019.04.013.

Ntziachristos, P.; Tsirigos, A.; van Vlierberghe, P.; Nedjic, J.; Trimarchi, T.; Sol Flaherty, M. et al. (2012): Genetic inactivation of the polycomb repressive complex 2 in T cell acute lymphoblastic leukemia. In *Nature medicine* 18 (2), pp. 298–301. Available online at DOI: 10.1038/nm.2651.

O'Dwyer, P.; Piha-Paul, S.; French, Ch; Harward, S.; Wu, Y.; Barbash, O. et al. (2016): GSK525762, a selective bromodomain (BRD) and extra terminal protein (BET) inhibitor: results from part 1 of a phase I/II open-label single-agent study in patients with NUT midline carcinoma (NMC) and other cancers. In *Cancer research* 76. Available online at https://doi.org/10.1158/1538-7445.AM2016-CT014.

Oelgeschlaeger, M.; Janknecht, R.; Krieg, J.; Schreek, S.; Luescher, B. (1996): Interaction of the co-activator CBP with Myb proteins: effects on Myb-specific transactivation and on the cooperativity with NF-M. In *The EMBO journal* 15 (11), pp. 2771–2780.

Ogryzko, V.; Kotani, T.; Zhang, X.; Schiltz, R.; Howard, T.; Yang, X. et al. (1998): Histone-like TAFs within the PCAF histone acetylase complex. In *Cell* 94 (1), pp. 35–44. Available online at DOI: 10.1016/s0092-8674(00)81219-2.

Oike, T.; Komachi, M.; Ogiwara, H.; Amornwichet, N.; Saitoh, Y.; Torikai, K. et al. (2014): C646, a selective small molecule inhibitor of histone acetyltransferase p300, radiosensitizes lung cancer cells by enhancing mitotic catastrophe. In *Radiotherapy and oncology* 111 (2), pp. 222–227. Available online at DOI: 10.1016/j.radonc.2014.03.015.

Oike, Y.; Takakura, N.; Hata, A.; Kaname, T.; Akizuki, M.; Yamaguchi, Y. et al. (1999): Mice homozygous for a truncated form of CREB-binding protein exhibit defects in hematopoiesis and vasculo-angiogenesis. In *Blood* 93 (9), pp. 2771–2779.

Ono, H.; Kato, T.; Murase, Y.; Nakamura, Y.; Ishikawa, Y.; Watanabe, S. et al. (2021): C646 inhibits G2/M cell cycle-related proteins and potentiates anti-tumor effects in pancreatic cancer. In *Scientific reports* 11 (1), p. 10078. Available online at DOI: 10.1038/s41598-021-89530-8.

Pao, G.; Janknecht, R.; Ruffner, H.; Hunter, T.; Verma, I. (2000): CBP/p300 interact with and function as transcriptional coactivators of BRCA1. In *Proceedings of the National Academy of Sciences of the United States of America* 97 (3), pp. 1020–1025. Available online at DOI: 10.1073/pnas.97.3.1020.

Pastori, C.; Daniel, M.; Penas, C.; Volmar, C-H; Johnstone, A. L.; Brothers, S. P. et al. (2014a): BET bromodomain proteins are required for glioblastoma cell proliferation. In *Epigenetics* 9 (4), pp. 611–620. Available online at DOI: 10.4161/epi.27906.

Pastori, Chiara; Daniel, Mark; Penas, Clara; Volmar, Claude-Henry; Johnstone, Andrea L.; Brothers, Shaun P. (2014b): BET bromodomain proteins are required for glioblastoma cell proliferation. In *Epigenetics* 9 (4), pp. 611–620. Available online at doi: 10.4161/epi.27906.

Patel, M.; Debrosse, M.; Smith, M.; Dey, A.; Huynh, W.; Sarai, N. et al. (2013): BRD4 coordinates recruitment of pause release factor P-TEFb and the pausing complex NELF/DSIF to regulate transcription elongation of interferon-stimulated genes. In *Molecular and Cellular Biology* 33 (12), pp. 2497–2507. Available online at DOI: 10.1128/MCB.01180-12.

Paugh, B. S.; Qu, C.; Jones, C.; Liu, Z.; Adamovicz-Brice, M.; Zhang, J. et al. (2010): Integrated molecular genetic profiling of pediatric high-grade gliomas reveals key differences with the adult disease. In *Journal of Clinical Oncology* 28 (18), pp. 3061–3068. Available online at DOI: 10.1200/JCO.2009.26.7252.

Pearson, G.; Robinson, F.; Gibson, T.; Xu, B.; Karandikar, M.; Berman, K.; Cobb, M. (2001): Mitogen-activated protein (MAP) kinase pathways: regulation and physiological functions. In *Endocrine reviews* 22 (2), pp. 152–183. Available online at DOI: 10.1210/edrv.22.2.0428.

Pedersen, H.; Schmiegelow, K.; Hamerlik, P. (2020): Radio-Resistance and DNA Repair in Pediatric Diffuse Midline Gliomas. In *Cancers* 12 (10), p. 2813. Available online at DOI: 10.3390/cancers12102813.

Perkins, N.; Felzien, L.; Betts, J.; Leung, K.; Beach, D.; Nabel, G. (1997): Regulation of NF-kappaB by cyclin-dependent kinases associated with the p300 coactivator. In *Science* 275 (5299), pp. 523–527. Available online at DOI: 10.1126/science.275.5299.523.

Perwein, T.; Karremann, M.; Bueren, A. von; Behrens, L.; Gielen, G.; Bison, B.; Kramm, Ch (2021): Hirntumore im Kindes- und Jugendalter. In *Kinderärztliche Praxis* 92, pp. 384–392.

Picaud; Fedorov; Leonards; Jones (2015a): Generation of a Selective Small Molecule Inhibitor of the CBP/p300 Bromodomain for Leukemia Therapy. In *Cancer research*. Available online at DOI: 10.1158/0008-5472.CAN-15-0236.

Picaud, S.; Fedorov, O.; Thanasopoulou, A.; Leonards, K.; Jones, K.; Meier, J. et al. (2015b): Generation of a Selective Small Molecule Inhibitor of the CBP/p300 Bromodomain for Leukemia Therapy. In *Cancer research* 75 (23), pp. 5106–5119. Available online at DOI: 10.1158/0008-5472.CAN-15-0236.

Piunti, A.; Hashizume, R.; Morgan, M. A.; Bartom, E. T.; Horbinski, C. M.; Marshall, S. A. et al. (2017a): Therapeutic targeting of polycomb and BET bromodomain proteins in diffuse intrinsic pontine gliomas. In *Nature medicine* 23 (4), pp. 493–500. Available online at DOI: 10.1038/nm.4296.

Piunti, Andrea; Hashizume, Rintaro; Morgan, Marc A.; Bartom, Elizabeth T.; Horbinski, Craig M.; Marshall, Stacy A. (2017b): Therapeutic targeting of polycomb and BET bromodomain proteins in diffuse intrinsic pontine gliomas. In *Nature medicine* 23 (4), pp. 493–500. Available online at doi: 10.1038/nm.4296.

Power, E.; Fernandez-Torres, J.; Zhang, L.; Yaun, R.; Lucien, F.; Daniels, D. (2022): Chorioallantoic membrane (CAM) assay to study treatment effects in diffuse intrinsic pontine glioma. In *PloS one* 17 (2), p. 263822. Available online at DOI: 10.1371/journal.pone.0263822.

Pratt, D.; Quezado, M.; Abdullaev, Z.; Hawes, D.; Yang, F.; Garton, H. et al. (2020): Diffuse intrinsic pontine glioma-like tumor with EZHIP expression and molecular features of PFA ependymoma. In *Acta neuropathologica communications* 8 (1), p. 37. Available online at DOI: 10.1186/s40478-020-00905-w.

Qi, J.; Esfahani, D.; Huang, T.; Ozark, P.; Bartom, E.; Hashizume, R. et al. (2019): Tenascin-C expression contributes to pediatric brainstem glioma tumor phenotype and represents a novel biomarker of disease. In *Acta neuropathologica communications* 7 (1), p. 75. Available online at DOI: 10.1186/s40478-019-0727-1.

Qin, T.; Mullan, B.; Ravindran, R.; Messinger, D.; Siada, R.; Cummings, J. et al. (2022): ATRX loss in glioma results in dysregulation of cell-cycle phase transition and ATM inhibitor radio-sensitization. In *Cell reports* 38 (2), p. 110216. Available online at DOI: 10.1016/j.celrep.2021.110216.

Raggi, C.; Mousa, H. S.; Correnti, M.; Sica, A.; Invernizzi, P. (2016): Cancer stem cells and tumor-associated macrophages: a roadmap for multitargeting strategies. In *Oncogene* 35 (6), pp. 671–682. Available online at DOI: 10.1038/onc.2015.132.

Rahman, S.; Sowa, M.; Ottinger, M.; Smith, J.; Shi, Y.; Harper, J.; Howley, P. (2011): The Brd4 extraterminal domain confers transcription activation independent of pTEFb by recruiting multiple proteins, including NSD3. In *Molecular and Cellular Biology* 31 (13), pp. 2641–2652. Available online at DOI: 10.1128/MCB.01341-10.

Rahnamoun, H.; Lee, J.; Sun, Z.; Lu, H.; Ramsey, K.; Komives, E.; Lauberth, S. (2018): RNAs interact with BRD4 to promote enhanced chromatin engagement and transcription activation. In *Nature structural and molecular biology* 25 (8), pp. 687–697. Available online at DOI: 10.1038/s41594-018-0102-0.

Rakotomalala, A.; Bailleul, Q.; Savary, C.; Arcicasa, M.; Hamadou, M.; Huchede, P. et al. (2021): H3.3K27M Mutation Controls Cell Growth and Resistance to Therapies in Pediatric Glioma Cell Lines. In *Cancers* 13 (21), p. 5551. Available online at DOI: 10.3390/cancers13215551.

Ramos, Y. F.M.; Hestand, M. S.; Verlaan, M.; Krabbendam, E.; Ariyurek, V.; van Galen, M. et al. (2010): Genome-wide assessment of differential roles for p300 and CBP in transcription regulation. In *Nucleic acids research* 38 (16), pp. 5396–5408. Available online at DOI: 10.1093/nar/gkq184.

Ren, W.; Fan, H.; Grimm, S.; Guo, Y.; Kim, J.; Yin, J. et al. (2020): Direct readout of heterochromatic H3K9me3 regulates DNMT1-mediated maintenance DNA methylation. In *Proceedings of the National Academy of Sciences of the United States of America* 117 (31), pp. 18439–18447. Available online at DOI: 10.1073/pnas.2009316117.

Roberts, T.; Etxaniz, U.; Dallagnese, A.; Wu, S-Y; Chiang, Ch-M; Brennan, P. et al. (2017): BRD3 and BRD4 BET Bromodomain Proteins Differentially Regulate Skeletal Myogenesis. In *Scientific reports* 7 (1), p. 6153. Available online at DOI: 10.1038/s41598-017-06483-7.

Rouaux, C.; Jokic, N.; Mbebi, C.; Boutillier, S.; Loeffler, J-P; Boutillier, A-L (2003): Critical loss of CBP/p300 histone acetylase activity by caspase-6 during neurodegeneration. In *The EMBO journal* 22 (24), pp. 6537–6549. Available online at DOI: 10.1093/emboj/cdg615.

Sakamaki, J.; Wilkinson, S.; Hahn, M.; Tasdemir, N.; Clark, W.; Hedley, A. et al. (2017): Bromodomain Protein BRD4 Is a Transcriptional Repressor of Autophagy and Lysosomal Function. In *Molecular cell* 66 (4), 517-532. Available online at DOI: 10.1016/j.molcel.2017.04.027.

Sansam, C.; Pietrzak, K.; Majchrzycka, B.; Kerlin, M.; Chen, J.; Rankin, S.; Sansam, Ch (2018): A mechanism for epigenetic control of DNA replication. In *Genes and development* 32 (3-4), pp. 224–229. Available online at DOI: 10.1101/gad.306464.117.

Santer, F.; Hoeschele, P.; Oh, S.; Erb, H.; Bouchal, J.; Cavaretta, I. et al. (2011): Inhibition of the acetyltransferases p300 and CBP reveals a targetable function for p300 in the survival and invasion pathways of prostate cancer cell lines. In *Molecular cancer therapeutics* 10 (9), pp. 1644–1655. Available online at DOI: 10.1158/1535-7163.MCT-11-0182.

Santos-Rosa, H.; Schneider, R.; Bernstein, B.; Karabetsou, N.; Morillon, A.; Weise, Ch et al. (2003): Methylation of histone H3 K4 mediates association of the Isw1p ATPase with

chromatin. In *Molecular cell* 12 (5), pp. 1325–2332. Available online at DOI: 10.1016/s1097-2765(03)00438-6.

Sartorelli, V.; Huang, J.; Hamamori, Y.; Kedes, L. (1997): Molecular mechanisms of myogenic coactivation by p300: direct interaction with the activation domain of MyoD and with the MADS box of MEF2C. In *Molecular and Cellular Biology* 17 (2), pp. 1010–1026. Available online at DOI: 10.1128/MCB.17.2.1010.

Satoru, O.; van Meir, E. G. (2017): Overcoming therapeutic resistance in glioblastoma: the way forward. In *Journal of Clinical Investigation* 127 (2), pp. 415–426. Available online at DOI: 10.1172/JCI89587.

Schneider, C.; Rasband, W.; Eliceiri, K. (2012a): NIH Image to ImageJ: 25 years of image analysis. In *Nature methods*. Available online at doi: 10.1038/nmeth.2089.

Schneider, C. A.; Rasband, W. S.; Eliceiri, K. W. (2012b): NIH Image to ImageJ: 25 years of image analysis. In *Nature methods* 9 (7), pp. 671–675. Available online at DOI: 10.1038/nmeth.2089.

Schulz, A.; Meyer, F.; Dubrovska, A.; Borgmann, K. (2019): Cancer Stem Cells and Radioresistance: DNA Repair and Beyond. In *Cancers* 11(6), p. 862. Available online at DOI: 10.3390/cancers11060862.

Schwartzentruber, J.; Korshunov, A.; Liu, X-Y; Jones, D. T.W.; Pfaff, E.; Jacob, K.; Sturm, D. (2012): Driver mutations in histone H3.3 and chromatin remodelling genes in paediatric glioblastoma. In *Nature* 482, pp. 226–231. Available online at DOI: 10.1038/nature10833.

Sen, P.; Shah, P.; Nativio, R.; Berger, S. (2016): Epigenetic Mechanisms of Longevity and Aging. In *Cell* 166 (4), pp. 822–839. Available online at DOI: 10.1016/j.cell.2016.07.050.

Shapiro, G.; Dowlati, A.; LoRusso, P.; Eder, J.; Anderson, A.; Do, K. et al. (2015): Clinically efficacy of the BET bromodomain inhibitor TEN-010 in an open-label substudy with patients with documented NUT-midline carcinoma (NMC). In *Molecular cancer therapy* 14. Available online at https://doi.org/10.1158/1535-7163.TARG-15-A49.

Sharma, S.; Free, A.; Mei, Y.; Peiper, S. C.; Wang, Z.; Cowell, J. K. (2010): Distinct molecular signatures in pediatric infratentorial glioblastomas defined by aCGH. In *Experimental and Molecular Pathology* 89 (2) (169-174). Available online at DOI: 10.1016/j.yexmp.2010.06.009.

Sharpless, N.; Sherr, Ch (2015): Forging a signature of in vivo senescence. In *Nature reviews. Cancer* 15 (7), pp. 397–408. Available online at DOI: 10.1038/nrc3960.

Shi, W.; Zhang, Ch; Ning, Z.; Hua, Y.; Li, Y.; Chen, L. et al. (2019): Long non-coding RNA LINC00346 promotes pancreatic cancer growth and gemcitabine resistance by sponging miR-188-3p to derepress BRD4 expression. In *Journal of experimental and clinical cancer research* 38 (1), p. 60. Available online at DOI: 10.1186/s13046-019-1055-9.

Shikama, N.; Lee, C.; France, S.; Delavaine, L.; Lyon, J.; Krstic-Demonacos, M.; La Thangue, N. (1999): A novel cofactor for p300 that regulates the p53 response. In *Molecular cell* 4 (3), pp. 365–376. Available online at DOI: 10.1016/s1097-2765(00)80338-x.

Shintani, M.; Okazaki, A.; Masuda, T.; Kawada, M.; Ishizuka, M.; Doki, Y. et al. (2002): Overexpression of cyclin DI contributes to malignant properties of esophageal tumor cells by increasing VEGF production and decreasing Fas expression. In *Anticancer research* 22 (2A), pp. 639–647.

Shrimp; Sorum; Garlick; Guasch (2015a): Characterizing the Covalent Targets of a Small Molecule Inhibitor of the Lysine Acetyltransferase P300. In *ACS medicinal chemistry letters*. Available online at DOI: 10.1021/acsmedchemlett.5b00385.

Shrimp, J.; Sorum, A.; Garlick, J.; Guasch, L.; Nicklaus, M.; Meier, J. (2015b): Characterizing the Covalent Targets of a Small Molecule Inhibitor of the Lysine Acetyltransferase P300. In *ACS medicinal chemistry letters* 7 (2), pp. 151–155. Available online at DOI: 10.1021/acsmedchemlett.5b00385.

Shu; S; Lin, Ch; He, H.; Witwicki, R.; Tabassum, D. et al. (2016a): Response and resistance to BET bromodomain inhibitors in triple-negative breast cancer. In *Nature* 529 (7586), pp. 413–417. Available online at DOI: 10.1038/nature16508.

Shu, S.; Lin, Ch; He, H.; Witwicki, R.; Tabassum, D.; Roberts, J. et al. (2016b): Response and resistance to BET bromodomain inhibitors in triple-negative breast cancer. In *Nature* 529 (7586), pp. 413–417. Available online at DOI: 10.1038/nature16508.

Sinha, A.; Faller, D.; Denis, G. (2005): Bromodomain analysis of Brd2-dependent transcriptional activation of cyclin A. In *The biochemical journal* 87 (1), pp. 257–269. Available online at DOI: 10.1042/BJ20041793.

Skowron MA; Sathe A; Romano A; Hoffmann MJ; Schulz WA; van Koeveringe GA (2017): Applying the chicken embryo chorioallantoic membrane assay to study treatment approaches in urothelial carcinoma. In *Urological Oncology*. Available online at doi: 10.1016/j.urolonc.2017.05.003.

Snowden, A.; Perkins, N. (1998): Cell Cycle Regulation of the Transcriptional Coactivators p300 and CREB Binding Protein. In *Biochemical pharmacology* 55 (12), pp. 1947–1954. Available online at DOI: 10.1016/s0006-2952(98)00020-3.

Song, H.; Shi, L.; Xu, Y.; Xu, T.; Fan, R.; Cao, M. et al. (2019): BRD4 promotes the stemness of gastric cancer cells via attenuating miR-216a-3p-mediated inhibition of Wnt/β-catenin signaling. In *European journal of pharmacology* 8, pp. 189–197. Available online at DOI: 10.1016/j.ejphar.2019.03.018.

Spiegelman, B. M.; Heinrich, R. (2004): Biological control through regulated transcriptional coactivators. In *Cell* 119 (2), pp. 157–167. Available online at DOI: 10.1016/j.cell.2004.09.037.

Stafford, J.; Lee, Ch-H; Voigt, P.; Descostes, N.; Saldana-Meyer, R.; Yu, J-R et al. (2018): Multiple modes of PRC2 inhibition elicit global chromatin alterations in H3K27M pediatric glioma. In *Science advances* 4 (10), p. 5935. Available online at DOI: 10.1126/sciadv.aau5935.

Stathis, A.; Zucca, E.; Bekradda, M.; Gomez-Roca, C.; Delord, J-P; La Motte Rouge, T. de et al. (2016): Clinical Response of Carcinomas Harboring the BRD4-NUT Oncoprotein to the Targeted

Bromodomain Inhibitor OTX015/MK-8628. In *Cancer discovery* 6 (5), pp. 492–500. Available online at DOI: 10.1158/2159-8290.CD-15-1335.

Stauffer, D.; Chang, B.; Huang, J.; Dunn, A.; Thayer, M. (2007): p300/CREB-binding protein interacts with ATR and is required for the DNA replication checkpoint. In *The journal of biological chemistry* 282 (13), pp. 8678–9687. Available online at DOI: 10.1074/jbc.M609261200.

Stonestrom, A. J.; Hsu, S. C.; Jahn, K. S.; Huang, P.; Keller, C. A.; Giardine, B. M. et al. (2015): Functions of BET proteins in erythroid gene expression. In *Blood* 125 (18), pp. 2825–2834. Available online at DOI: 10.1182/blood-2014-10-607309.

Strachowska, M.; Gronkowska, K.; Michlewska, S.; Robaszkiewicz, A. (2021): CBP/p300 Bromodomain Inhibitor-I-CBP112 Declines Transcription of the Key ABC Transporters and Sensitizes Cancer Cells to Chemotherapy Drugs. In *Cancers* 13 (18), p. 4614. Available online at DOI: 10.3390/cancers13184614.

Stupp, R.; Brada, M.; van den Bent, M. J.; Tonn, J-C; Pentheroudakis, G. (2014): High-grade glioma: ESMO Clinical Practice Guidelines for diagnosis, treatment and follow-up. In *Annals of Oncology*, pp. 93–101. Available online at DOI: 10.1093/annonc/mdu050.

Stupp, R.; Mason, W. P.; van den Bent, M. J.; Weller, M.; Fisher, B.; Taphoorn, M. J. (2005): Radiotherapy plus concomitant and adjuvant temozolomide for glioblastoma. In *The New England Journal of Medicine* 352 (10), pp. 987–996. Available online at DOI: 10.1056/NEJMoa043330.

Sturm, D.; Witt, H.; Hovestadt, V.; Khuong-Quang, D-A; Jones, D. T.W.; Konermann, C.; Pfaff, E. (2012): Hotspot mutations in H3F3A and IDH1 define distinct epigenetic and biological subgroups of glioblastoma. In *Cancer Cell* 22 (4), pp. 425–437. Available online at DOI: 10.1016/j.ccr.2012.08.024.

Su, Z.; Zhang, Y.; Jia, J.; Fang, Y.; Tang, Y.; Wu, H.; Fang, D. (2020): H3K36me3, message from chromatin to DNA damage repair. In *Cell and bioscience* 10, DOI: 10.1186/s13578-020-0374-z.

Sudo, T.; Utsunomiya, T.; Mimori, K.; Nagahara, H.; Ogawa, K.; Inoue, H. et al. (2005): Clinicopathological significance of EZH2 mRNA expression in patients with hepatocellular carcinoma. In *British Journal of Cancer* 92 (9), pp. 1754–1758. Available online at DOI: 10.1038/sj.bjc.6602531.

Sur, I.; Taipale, J. (2016): The role of enhancers in cancer. In *Nature reviews. Cancer* 16 (8), pp. 483–493. Available online at DOI: 10.1038/nrc.2016.62.

Takahashi, T.; Suwabe, N.; Dai, P.; Yamamoto, M.; Ishii, S.; Nakano, T. (2000): Inhibitory interaction of c-Myb and GATA-1 via transcriptional co-activator CBP. In *Oncogene* 19 (1), pp. 134–140. Available online at DOI: 10.1038/sj.onc.1203228.

Tamburri, S.; Lavarone, E.; Fernandez-Perez, D.; Conway, E.; Zanotti, M.; Manganaro, D.; Pasini, D. (2020a): Histone H2AK119 Mono-Ubiquitination Is Essential for Polycomb-Mediated Transcriptional Repression. In *Molecular cell* 77 (4), pp. 840–856. Available online at DOI: 10.1016/j.molcel.2019.11.021.

Tamburri, S.; Lavarone, E.; Fernández-Pérez, D.; Conway, E.; Zanotti, M.; Manganaro, D.; Pasini, D. (2020b): Histone H2AK119 Mono-Ubiquitination Is Essential for Polycomb-Mediated Transcriptional Repression. In *Molecular cell*. Available online at doi: 10.1016/j.molcel.2019.11.021: 10.1016/j.molcel.2019.11.021.

Tanaka, Y.; Naruse, I.; Maekawa, T.; Masuya, H.; Shiroishi, T.; Ishii, S. (1997): Abnormal skeletal patterning in embryos lacking a single Cbp allele: a partial similarity with Rubinstein-Taybi syndrome. In *Proceedings of the National Academy of Sciences of the United States of America* 94 (19), pp. 10215–10220. Available online at DOI: 10.1073/pnas.94.19.10215.

Tang, Y.; Berlind, J.; Mavila, N. (2018): Inhibition of CREB binding protein-beta-catenin signaling down regulates CD133 expression and activates PP2A-PTEN signaling in tumor initiating liver cancer cells. In *Cell communication and signaling* 16 (1), p. 9. Available online at DOI: 10.1186/s12964-018-0222-5.

Taylor, G.; Eskeland, R.; Hekimoglu-Balkan, B.; Pradeepa, M.; Bickmore, W. (2013): H4K16 acetylation marks active genes and enhancers of embryonic stem cells, but does not alter chromatin compaction. In *Genome research* 23 (12), pp. 2053–2065. Available online at DOI: 10.1101/gr.155028.113.

Tonouchi, E.; Gen, Y.; Muramatsu, T.; Hiramoto, H.; Tanimoto, K.; Inoue, J.; Inazawa, J. (2018): miR-3140 suppresses tumor cell growth by targeting BRD4 via its coding sequence and downregulates the BRD4-NUT fusion oncoprotein. In *Scientific reports* 8 (1), p. 4482. Available online at DOI: 10.1038/s41598-018-22767-y.

Trouche, D.; Cook, A.; Kouzarides, T. (1996): The CBP co-activator stimulates E2F1/DP1 activity. In *Nucleic acids research* 24 (21), pp. 4139–4145. Available online at DOI: 10.1093/nar/24.21.4139.

Tsume-Kajioka, M.; Kimura-Yoshida, Ch; Mochida, K.; Ueda, Y.; Matsuo, I. (2022): BET proteins are essential for the specification and maintenance of the epiblast lineage in mouse preimplantation embryos. In *BMC biology* 20 (1), p. 64. Available online at DOI: 10.1186/s12915-022-01251-0.

van den Bosch, T.; Boichenko, A.; Leus, N.; Ourailidou, M.; Wapenaar, H.; Rotili, D. et al. (2016): The histone acetyltransferase p300 inhibitor C646 reduces pro-inflammatory gene expression and inhibits histone deacetylases. In *Biochemical pharmacology* 102, pp. 130–140. Available online at DOI: 10.1016/j.bcp.2015.12.010.

Vandel, L.; Trouche, D. (2001): Physical association between the histone acetyl transferase CBP and a histone methyl transferase. In *EMBO Reports* 2 (1), pp. 21–26. Available online at DOI: 10.1093/embo-reports/kve002.

Vazquez, R.; Licandro, S.; Astorgues-Xerri, L.; Lettera, E.; Panini, N.; Romano, M. et al. (2017): Promising in vivo efficacy of the BET bromodomain inhibitor OTX015/MK-8628 in malignant pleural mesothelioma xenografts. In *International Journal of Cancer* 140 (1), pp. 197–207. Available online at DOI: 10.1002/ijc.30412.

Vethantham, V.; Yang, V.; Bowman, C.; Asp, P.; Lee, J. H. (2012): Dynamic loss of H2B ubiquitylation without corresponding changes in H3K4 trimethylation during myogenic differentiation. In *Molecular and Cellular Biology*. Available online at doi: 10.1128/MCB.06026-11.

Waddel, A.; Mahmud, I.; Ding, H.; Huo, Z.; Liao, D. (2021): Pharmacological Inhibition of CBP/p300 Blocks Estrogen Receptor Alpha (ERα) Function through Suppressing Enhancer H3K27 Acetylation in Luminal Breast Cancer. In *Cancers* 13 (11), p. 2799. Available online at DOI: 10.3390/cancers13112799.

Wai, D.; Szyszka, T.; Campbell, A.; Kwong, Ch; Wilkinson-White, L.; Silva, A. et al. (2018): The BRD3 ET domain recognizes a short peptide motif through a mechanism that is conserved across chromatin remodelers and transcriptional regulators. In *The journal of biological chemistry* 293 (19), pp. 7160–7175. Available online at DOI: 10.1074/jbc.RA117.000678.

Wakita, M.; Takahashi, A.; Sano, O.; Loo, T.; Imai, Y.; Narukawa, M. et al. (2020): A BET family protein degrader provokes senolysis by targeting NHEJ and autophagy in senescent cells. In *Nature communications* 11 (1), p. 1935. Available online at DOI: 10.1038/s41467-020-15719-6.

Wang, F.; Marshall, CB.; Ikura, M. (2013a): Transcriptional/epigenetic regulator CBP/p300 in tumorigenesis: structural and functional versatility in target recognition. In *Cellular and molecular life sciences* 70 (21), pp. 3989–4008. Available online at DOI: 10.1007/s00018-012-1254-4.

Wang, H.; Wang, L.; Erdjument-Bromage, H.; Vidal, M.; Tempst, P.; Jones, R.; Zhang, Y. (2004): Role of histone H2A ubiquitination in Polycomb silencing. In *Nature* 431 (7010), pp. 873–878. Available online at DOI: 10.1038/nature02985.

Wang, K.; Li, N.; Yeung, C.; Li, J.; Wang, H.; Cooper, T. (2013b): Oncogenic Wnt/β-catenin signalling pathways in the cancer-resistant epididymis have implications for cancer research. In *Molecular human reproduction* 19 (2), 57-71. Available online at DOI: 10.1093/molehr/gas051.

Wang, K.; Zhao, Z.; Wang, X.; Zhang, Y. (2021): BRD4 induces osteogenic differentiation of BMSCs via the Wnt/β-catenin signaling pathway. In *Tissue and cell* 72, p. 101555. Available online at DOI: 10.1016/j.tice.2021.101555.

Wang, R.; Cao, X-J; Kulej, K.; Liu, W.; Ma, T.; MAcDonald, M. et al. (2017): Uncovering BRD4 hyperphosphorylation associated with cellular transformation in NUT midline carcinoma. In *Proceedings of the National Academy of Sciences of the United States of America* 114 (27), pp. 5352–5361. Available online at DOI: 10.1073/pnas.1703071114.

Wang, Z.; Zang, C.; Cui, K.; Schones, E. D.; Barski, A.; Peng, W.; Zhao, K. (2009): Genome-wide mapping of HATs and HDACs reveals distinct functions in active and inactive genes. In *Cell* 138 (5), pp. 1019–1031. Available online at DOI: 10.1016/j.cell.2009.06.049.

Wang F; Marshall C; Ikura M (2013): Transcriptional/epigenetic regulator CBP/p300 in tumorigenesis: structural and functional versatility in target recognition. In *Cellular and molecular life sciences*, pp. 3989–4008. Available online at doi: 10.1007/s00018-012-1254-4.

Ward, R.; Johnson, M.; Shridhar, V.; van Deursen, J.; Couch, F. (2005): CBP truncating mutations in ovarian cancer. In *Journal of medical genetics* 42 (6), pp. 514–518. Available online at DOI: 10.1136/jmg.2004.025080.

Watt, F.; Molloy, P. L. (1988): Cytosine methylation prevents binding to DNA of a HeLa cell transcription factor required for optimal expression of the adenovirus major late promoter. In *Genes and development* 2 (9), pp. 1136–1143. Available online at DOI: 10.1101/gad.2.9.1136.

Weinberg, D.; Allis, D.; Lu, Ch (2017): Oncogenic Mechanisms of Histone H3 Mutations. In *Cold Spring Harbor perspectives in medicine* 7 (1), p. 26443. Available online at DOI: 10.1101/cshperspect.a026443.

Welby, J.; Kaptzan, T.; Wohl, A.; Peterson, T.; Raghunathan, A.; Brown, D. et al. (2019): Current Murine Models and New Developments in H3K27M Diffuse Midline Gliomas. In *Frontiers in oncology* 9, p. 92. Available online at DOI: 10.3389/fonc.2019.00092.

Welti, J.; Sharp, A.; Brooks, N.; Yuan, W.; McNair, Ch; Chand, S. et al. (2021): Targeting the p300/CBP Axis in Lethal Prostate Cancer. In *Cancer discovery* 11 (5), pp. 1118–1137. Available online at DOI: 10.1158/2159-8290.CD-20-0751.

Werbrouck, C.; Evangelista, C.; Lobon-Iglesias, M-J; Barret, E.; Le Teuff, G.; Merlevede, J. et al. (2019): TP53 Pathway Alterations Drive Radioresistance in Diffuse Intrinsic Pontine Gliomas (DIPG). In *Clinical cancer research* 25 (22), pp. 6788–6800. Available online at DOI: 10.1158/1078-0432.CCR-19-0126.

Wiese, M.; Hamdan, F. H.; Kubiak, K.; Diederichs, C.; Gielen, G. H.; Nussbaumer, G. et al. (2020): Combined treatment with CBP and BET inhibitors reverses inadvertent activation of detrimental super enhancer programs in DIPG cells. In *Cell death and disease* 11 (8), p. 673. Available online at DOI: 10.1038/s41419-020-02800-7.

Wiese, M.; Walther, N.; Diederichs, C.; Schill, F.; Monecke, S.; Salinas, G. et al. (2017a): The β-catenin/CBP-antagonist ICG-001 inhibits pediatric glioma tumorigenicity in a Wnt-independent manner. In *Oncotarget*. Available online at doi: 10.18632/oncotarget.15934.

Wiese, M.; Walther, N.; Diederichs, C.; Schill, F.; Monecke, S.; Salinas, G. et al. (2017b): The β-catenin/CBP-antagonist ICG-001 inhibits pediatric glioma tumorigenicity in a Wnt-independent manner. In *Oncotarget* 8 (16), pp. 27300–27313. Available online at DOI: 10.18632/oncotarget.15934.

Wiese M; Hamdan F; Kubiak K; Diederichs C; Gielen G; Nussbaumer G et al. (2020): Combined treatment with CBP and BET inhibitors reverses inadvertent activation of detrimental super enhancer programs in DIPG cells. In *Cell death and disease*, p. 673. Available online at doi: 10.1038/s41419-020-02800-7.

Wu, S-Y; Lee, A-Y; Lai, H-S; Zhang, H.; Chiang, Ch-M (2013): Phospho switch triggers Brd4 chromatin binding and activator recruitment for gene-specific targeting. In *Molecular cell* 49 (5), pp. 843–857. Available online at DOI: 10.1016/j.molcel.2012.12.006.

Wu, T.; Kamikawa, Y.; Donohoe, M. (2018): Brd4's Bromodomains Mediate Histone H3 Acetylation and Chromatin Remodeling in Pluripotent Cells through P300 and Brg1. In *Cell reports* 25 (7), pp. 1756–1771. Available online at DOI: 10.1016/j.celrep.2018.10.003.

Wu, T.; Pinto, H.; Kamikawa, Y.; Donohoe, M. (2015): The BET family member BRD4 interacts with OCT4 and regulates pluripotency gene expression. In *Stem cell reports* 4 (3), pp. 390–403. Available online at DOI: 10.1016/j.stemcr.2015.01.012.

Xu, S.; Fan, L.; Jeon, H-Y; Zhang, F.; Cui, X.; Mickle, M. et al. (2020): p300-Mediated Acetylation of Histone Demethylase JMJD1A Prevents Its Degradation by Ubiquitin Ligase STUB1 and Enhances Its Activity in Prostate Cancer. In *Cancer research* 80 (15), 3074-2087. Available online at DOI: 10.1158/0008-5472.CAN-20-0233.

Xu, Wu; Fukuyama, T.; Ney, P. A.; Wang, D.; Rehg, J.; Boyd, K. et al. (2006): Global transcriptional coactivators CREB-binding protein and p300 are highly essential collectively but not individually in peripheral B cells. In *Blood* 107 (11), pp. 4407–4416. Available online at DOI: 10.1182/blood-2005-08-3263.

Yan, Y.; Ma, J.; Wang, D.; Lin, D.; Pang, X.; Wang, S. et al. (2019): The novel BET-CBP/p300 dual inhibitor NEO2734 is active in SPOP mutant and wild-type prostate cancer. In *EMBO molecular medicine* 11 (11), p. 10659. Available online at DOI: 10.15252/emmm.201910659.

Yao, T.; Oh, S.; Fuchs, M.; Zhou, N.; Newsome, D.; Bronson, R. et al. (1998): Gene dosage-dependent embryonic development and proliferation defects in mice lacking the transcriptional integrator p300. In *Cell* 93 (3), pp. 361–372. Available online at DOI: 10.1016/s0092-8674(00)81165-4.

Ye, J.; Coulouris, G.; Zaretskaya, I.; Cutcutache, I.; Rozen, S.; Madden, T. (2012): Primer-BLAST: A tool to design target-specific primers for polymerase chain reaction. In *BMC bioinformatics* 13, p. 134. Available online at DOI: 10.1186/1471-2105-13-134.

Yu, J.; LeRoy, G.; Bready, D.; Frenster, J.; Saldaña-Meyer, R. (2021): The H3K36me2 writer-reader dependency in H3K27M-DIPG. In *Science advances*. Available online at doi: 10.1126/sciadv.abg7444.

Zaware, N.; Zhou, M-M (2019): Bromodomain biology and drug discovery. In *Nature structural and molecular biology* 26 (10), pp. 870–879. Available online at DOI: 10.1038/s41594-019-0309-8.

Zeng, L.; Zhang, Q.; Gerona-Navarro, G.; Moshkina, N.; Zhou, M-M (2008): Structural basis of site-specific histone recognition by the bromodomains of human coactivators PCAF and CBP/p300. In *Structure* 16 (4), Article DOI: 10.1016/j.str.2008.01.010, pp. 643–652.

Zhang; Plotnikov; Rusinova; Shen (2013): Structure-guided design of potent diazobenzene inhibitors for the BET bromodomains. In *Journal of medicinal chemistry*. Available online at DOI: 10.1021/jm401334s.

Zhang, B.; Chen, D.; Liu, B.; Dekker, F. J.; Quax, W. J. (2020): A novel histone acetyltransferase inhibitor A485 improves sensitivity of non-small-cell lung carcinoma cells to TRAIL. In

Biochemical pharmacology 175, p. 113914. Available online at DOI: 10.1016/j.bcp.2020.113914.

Zhang, L.; Nesvick, C.; Day, Ch; Choi, J.; Lu, V.; Peterson, T. et al. (2022): STAT3 is a biologically relevant therapeutic target in H3K27M-mutant diffuse midline glioma. In *Neurooncology* 24 (10), pp. 1700–1711. Available online at DOI: 10.1093/neuonc/noac093.

Zhang, T.; Cooper, S.; Brockdorff, N. (2015): The interplay of histone modifications—Writers that read. In *EMBO Reports* 16 (11), pp. 1467–1481. Available online at DOI: 10.15252/embr.201540945.

Zhao, F.; Ming, J.; Zhou, Y.; Fan, L. (2016): Inhibition of Glut1 by WZB117 sensitizes radioresistant breast cancer cells to irradiation. In *Cancer chemotherapy and pharmacology*. Available online at DOI: 10.1007/s00280-016-3007-9.

Zheng, W.; Jefcoate, C. (2004): Steroidogenic factor-1 interacts with cAMP response element-binding protein to mediate cAMP stimulation of CYP1B1 via a far upstream enhancer. In *Molecular pharmacology*. Available online at doi: 10.1124/mol.104.005504.

Zheng, Y.; Huang, G.; Silva, T. C.; Yang, Q.; Jiang, Y-Y; Koeffler, P. H. et al. (2021): A pan-cancer analysis of CpG Island gene regulation reveals extensive plasticity within Polycomb target genes. In *Nature communications* 12 (1), p. 2485. Available online at DOI: 10.1038/s41467-021-22720-0.

Zheng, Y.; Thompson, PR.; Cebrat, M.; Wang, L.; Devlin, MK.; Alani, RM.; Cole, P. A. (2004): Selective HAT Inhibitors as Mechanistic Tools for Protein Acetylation. In *Methods in enzymology* 376, pp. 188–199. Available online at DOI: 10.1016/S0076-6879(03)76012-1.

Zhou, S.; Zhang, M.; Zhou, Ch; Wang, W.; Yang, H.; Wenguang, Y. (2020): The role of epithelial-mesenchymal transition in regulating radioresistance. In *Critical reviews in oncology/hematology* 150, p. 102961. Available online at DOI: 10.1016/j.critrevonc.2020.102961.

Zuber, J.; Shi, J.; Wang, E.; Rappaport, A.; Herrmann, H.; Sison, E. et al. (2011): RNAi screen identifies Brd4 as a therapeutic target in acute myeloid leukaemia. In *Nature* 478 (7370), pp. 524–528. Available online at DOI: 10.1038/nature10334.

Zucconi, B.; Luef, B.; Xu, W.; Henry, R.; Nodelman, I.; Bowman, G. et al. (2016): Modulation of p300/CBP Acetylation of Nucleosomes by Bromodomain Ligand I-CBP112. In *Biochemistry* 55 (27), pp. 3727–3734. Available online at DOI: 10.1021/acs.biochem.6b00480.

Zucconi, B.; Makofske, J.; Meyers, D.; Hwang, Y.; Wu, M.; Kuroda, M.; Cole, P. (2019): Combination Targeting of the Bromodomain and Acetyltransferase Active Site of p300/CBP. In *Biochemistry* 58 (16), pp. 2133–2143. Available online at DOI: 10.1021/acs.biochem.9b00160.

Supplementary material

Appendix A | Quantification of western blot analyses of H3.3 K27M, H3K27me3 and H3K27ac expression in isoDIPG-H3WT and isoDIPG-H3.3K27M cells.

Densitometry analyses for quantification of H3.3K27M-mutation, H3K27me3 and H3K27ac levels in isoDIPG-010 and isoDIPG-012 was carried out using ImageJ. ß-actin was used for normalization. * $p < 0.05$; ** $p < 0.01$; *** $p < 0.005$; **** $p < 0.001$.

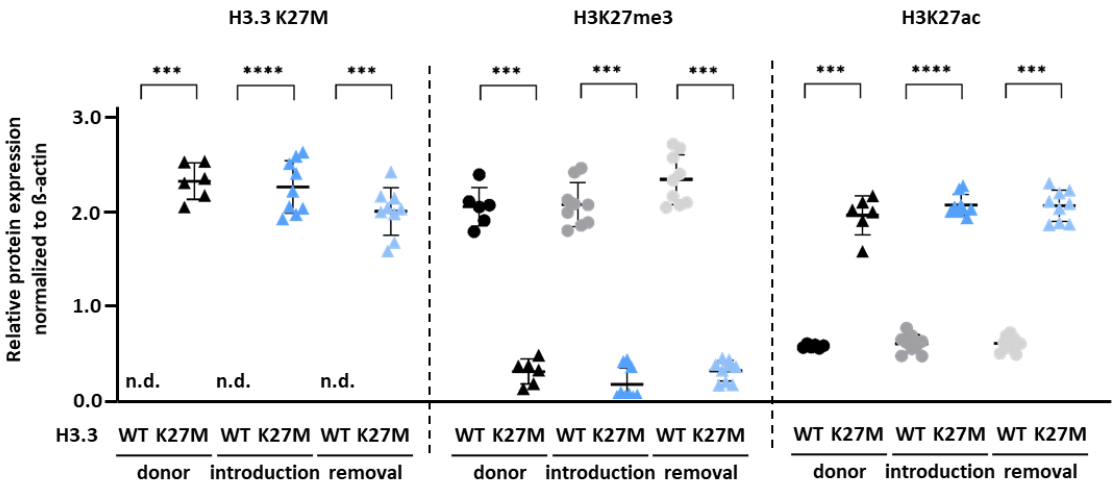

Appendix B | Quantification of western blot analyses of common stemness markers expression in isoDIPG-H3WT and isoDIPG-H3.3K27M cells.

Densitometry analyses for quantification of PAX6, OCT4, SOX2, Nanog, Nestin, CD133 and GFAP levels in isoDIPG-010 and isoDIPG-012 was carried out using ImageJ. ß-actin was used for normalization. * $p < 0.05$; ** $p < 0.01$; *** $p < 0.005$; **** $p < 0.001$.

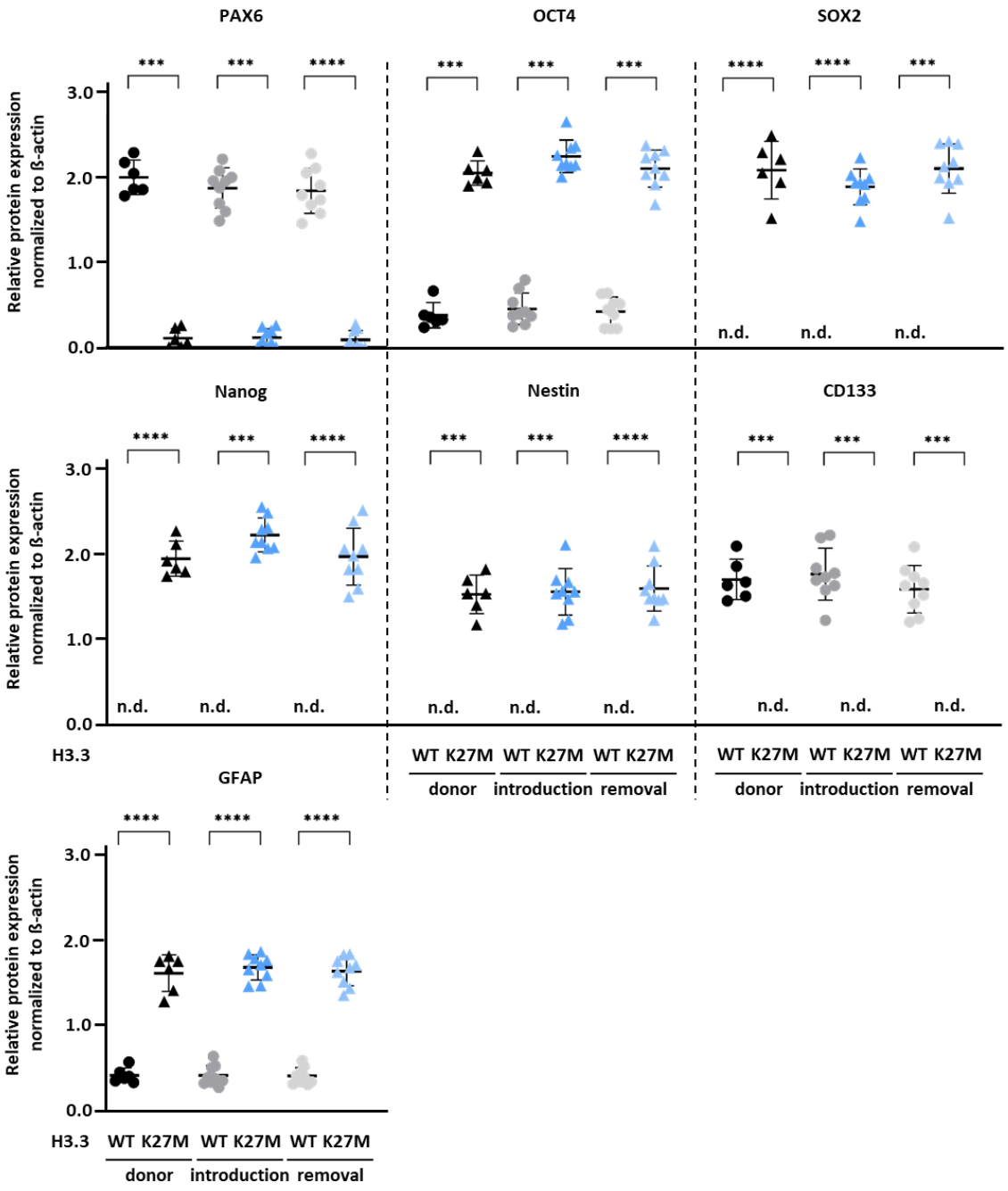

Appendix C | Quantification of western blot analyses of common mesenchymal markers expression in isoDIPG-H3WT and isoDIPG-H3.3K27M cells.

Densitometry analyses for quantification of N-cadherin, E-cadherin, MMP9, ZEB1 and Vimentin levels in isoDIPG-010 and isoDIPG-012 was carried out using ImageJ. ß-actin was used for normalization. * p < 0.05; ** p < 0.01; *** p < 0.005; **** p < 0.001.

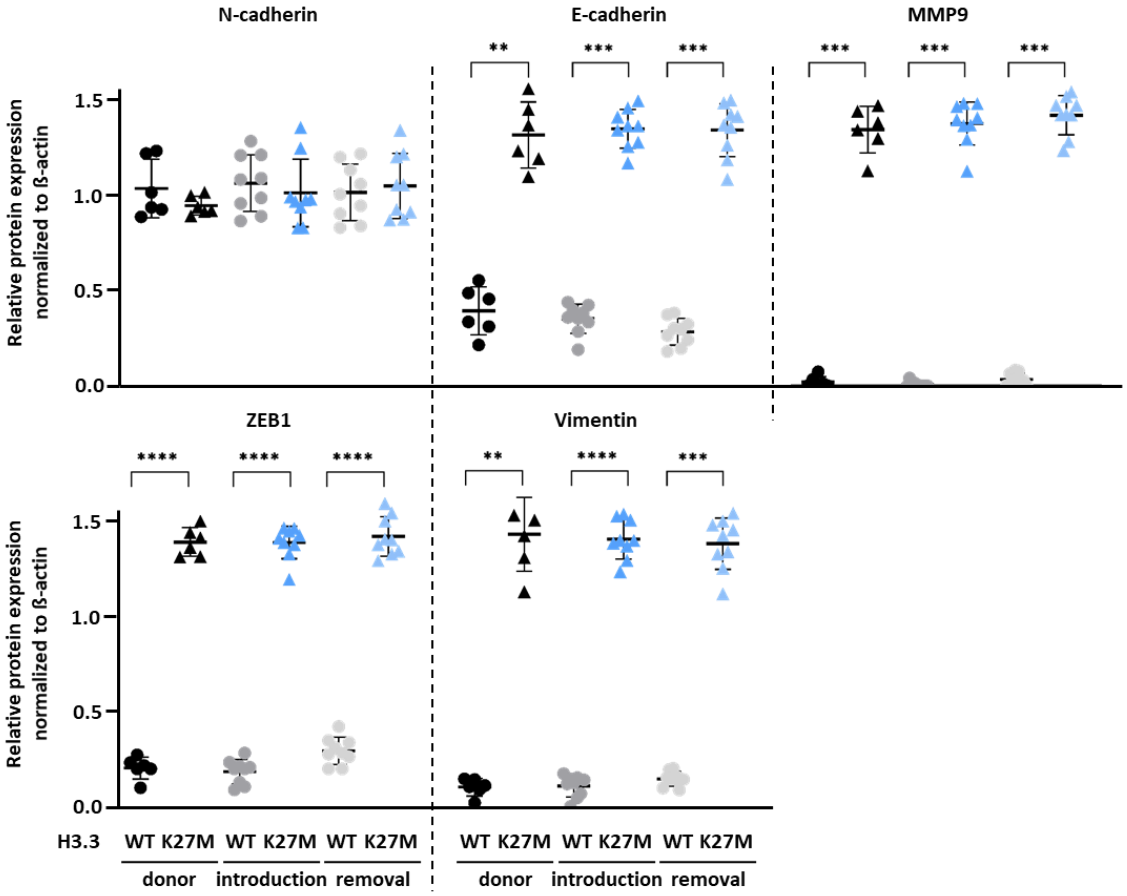

Appendix D | Quantification of western blot analyses of different histone marks expression in isoDIPG-H3WT and isoDIPG-H3.3K27M cells.

Densitometry analyses for quantification of N-cadherin, E-cadherin, MMP9, ZEB1 and Vimentin levels in isoDIPG-010 and isoDIPG-012 was carried out using ImageJ. ß-actin was used for normalization. * p < 0.05; ** p < 0.01; *** p < 0.005; **** p < 0.001.

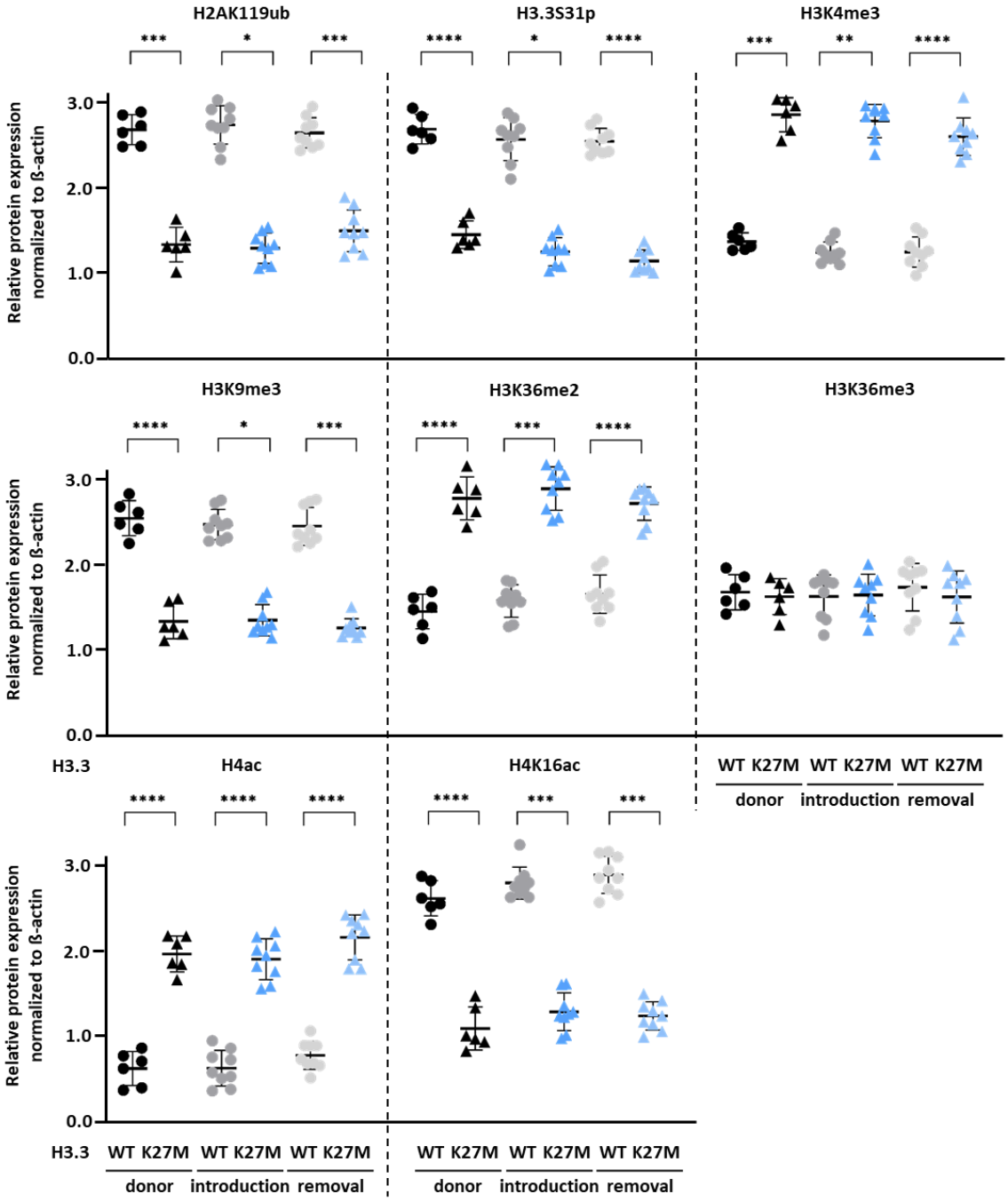

Appendix E | Quantification of western blot analyses of epigenetic key player expression in isoDIPG-H3WT and isoDIPG-H3.3K27M cells.

Densitometry analyses for quantification CBP, p300, BRD2, BRD3, BRD4 and EZH2 levels in isoDIPG-010 and isoDIPG-012 was carried out using ImageJ. ß-actin was used for normalization. * $p < 0.05$; ** $p < 0.01$; *** $p < 0.005$; **** $p < 0.001$.

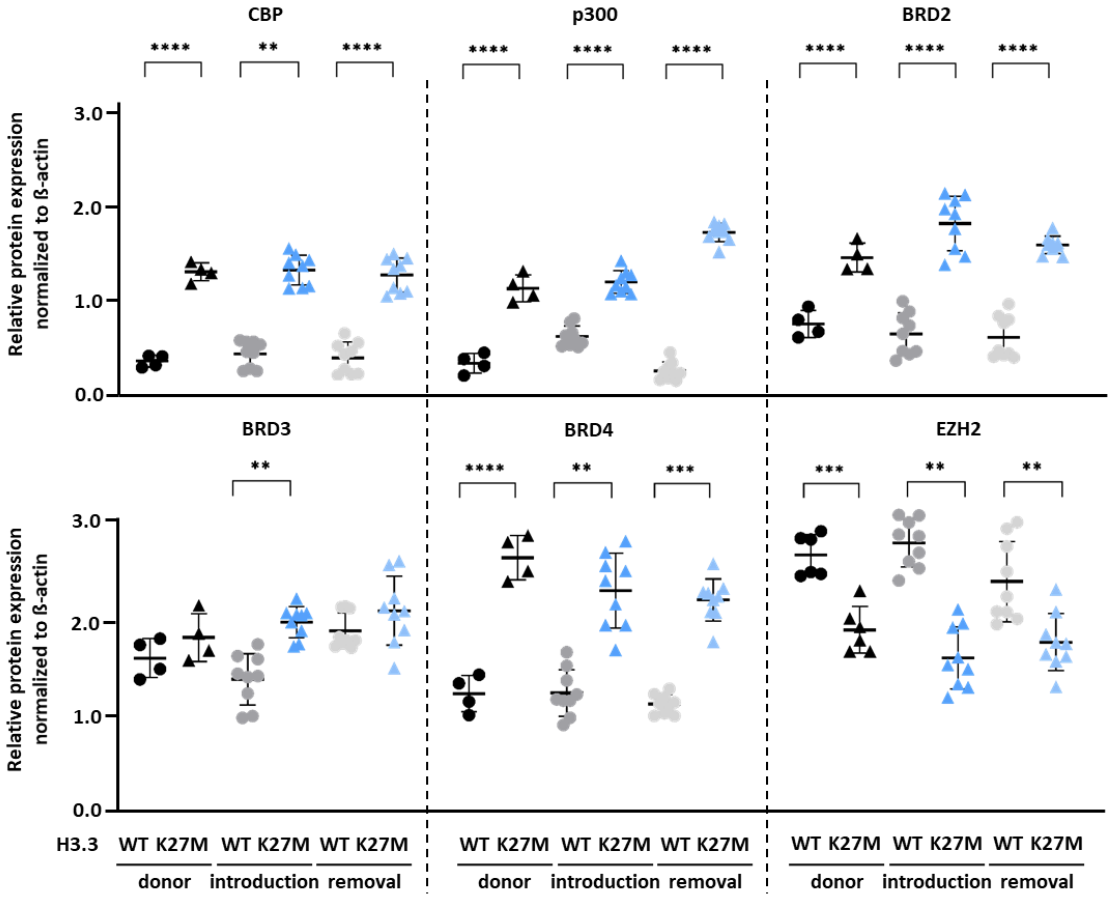

Appendix F | Quantification of western blot analyses of Glut1 and cleaved Caspase 3 expression in isoDIPG-H3WT and isoDIPG-H3.3K27M cells.

Densitometry analyses for quantification of Glut1 and cleaved Caspase 3 levels in isoDIPG-010 and isoDIPG-012 was carried out using ImageJ. ß-actin was used for normalization. * $p < 0.05$; ** $p < 0.01$; *** $p < 0.005$; **** $p < 0.001$.

SUPPLEMENTARY MATERIAL

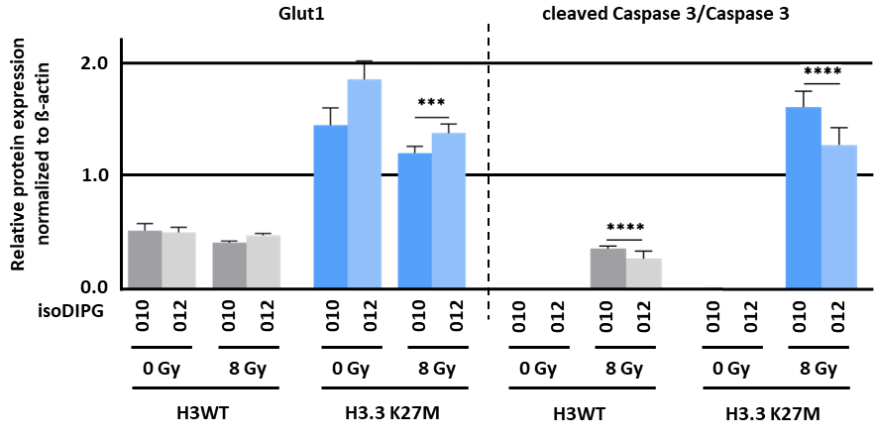

Appendix G | Illustration of cancer-related processes dependent on H3.3K27M-mutation in isoDIPG cells.

KEGG pathway analysis revealed H3.3K27M-dependent tumor-related pathways in isoDIPG cells (log2FC ≤1.0, adjusted p-value ≤0.05).

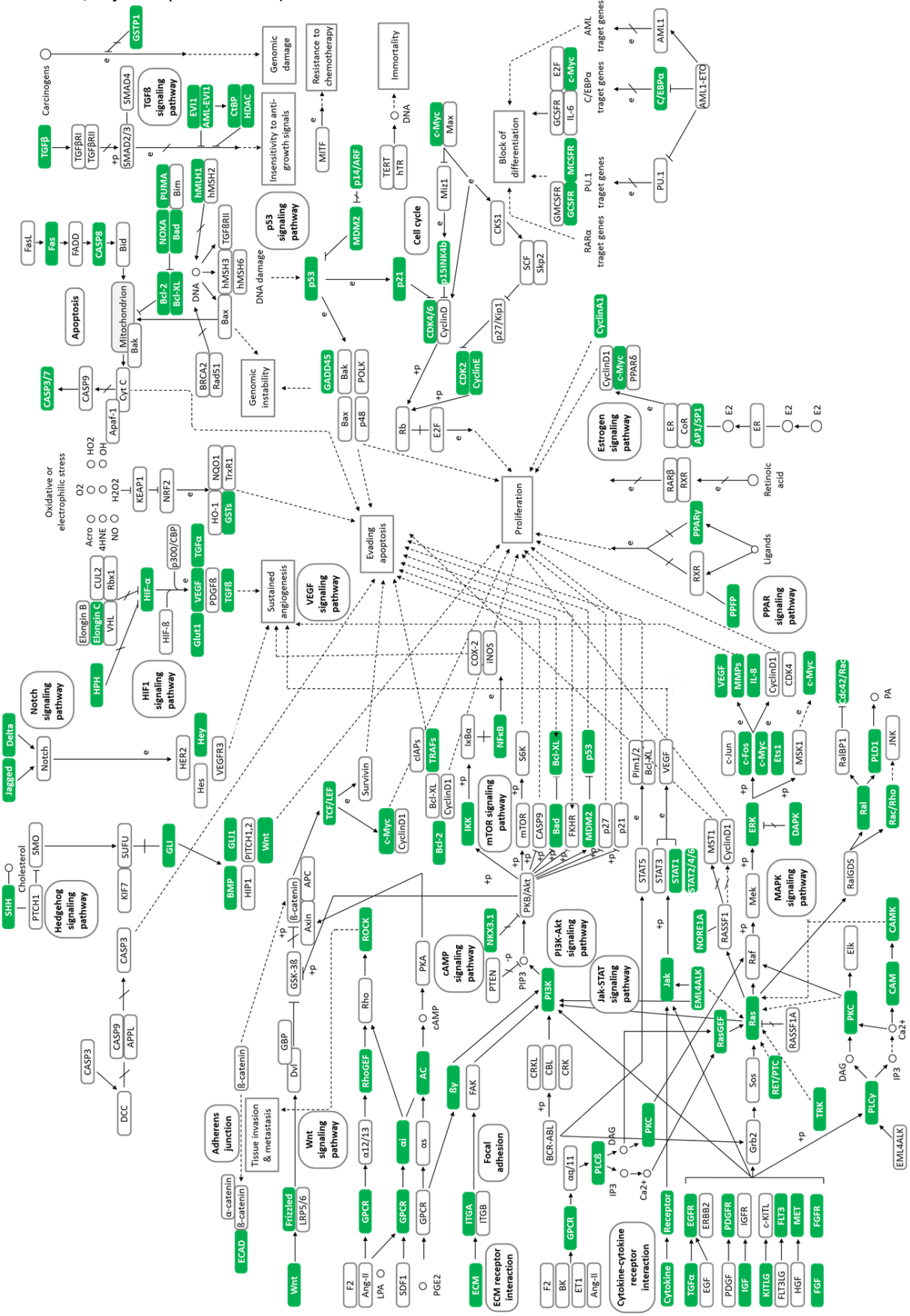

Appendix H | Western blot quantification of H3K27me3 and H3K27ac expression in isoDIPG-H3WT and isoDIPG-H3.3K27M cells.

Densitometry analyses for quantification of H3K27me3 and H3K27ac levels after inhibition and knockdown of CBP/p300 and BET proteins in isoDIPG-010 and isoDIPG-012 was carried out using ImageJ. ß-actin was used for normalization. * $p < 0.05$; ** $p < 0.01$; *** $p < 0.005$; **** $p < 0.001$.

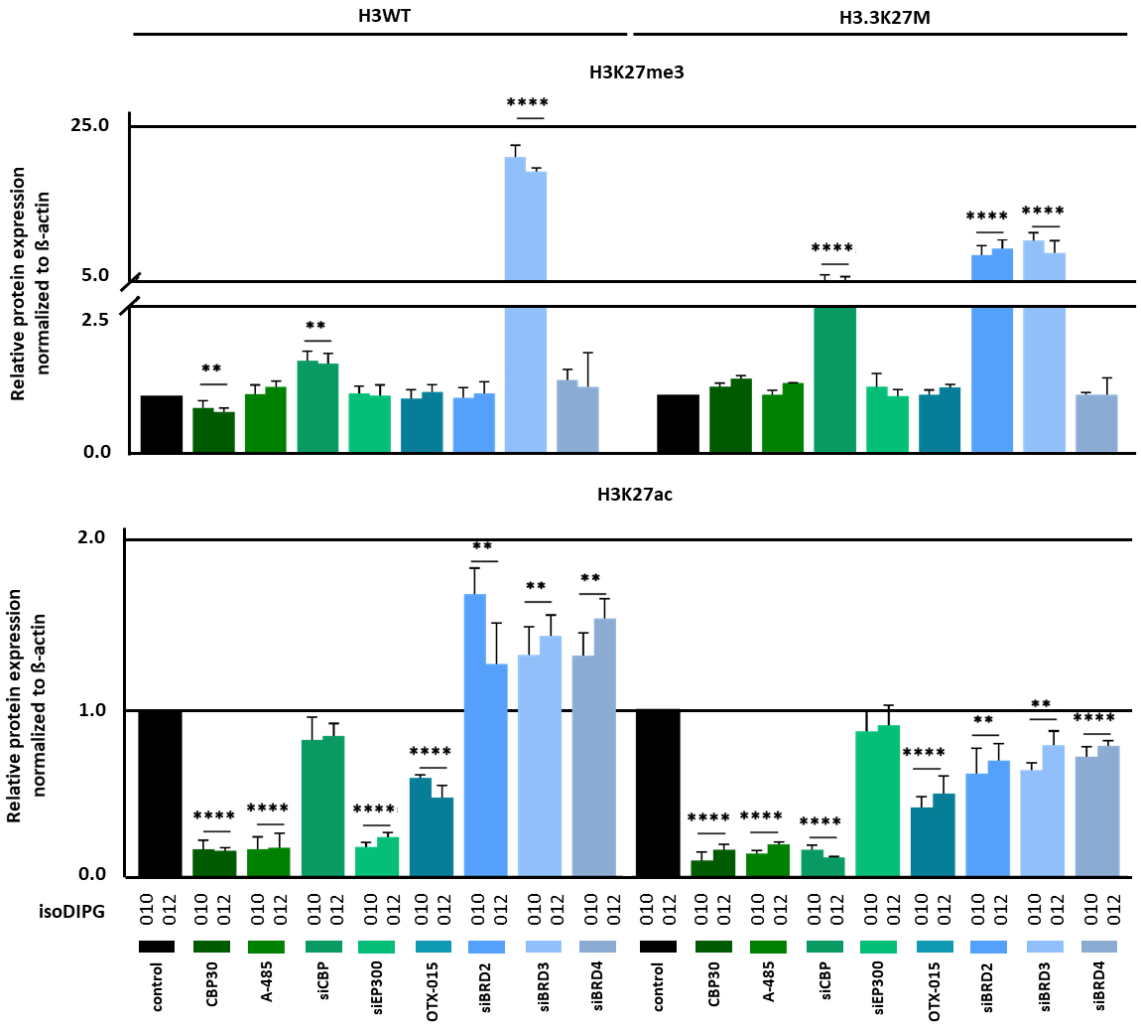

Appendix I | Cell viability assays upon CBP and BET proteins inhibition and knockdown in isoDIPG-H3WT and isoDIPG-H3.3K27M cells.

(A) MTT cell viability assay and (B) crystal violet assay were used to investigate cell viability in isoDIPG-H3WT and isoDIPG-H3. K27M cells after inhibition and knockdown of CBP/p300 and BET proteins. */# p < 0.05; **/## p < 0.01; ***/### p < 0.005; ****/#### p < 0.001 # used for comparison between isoDIPG-H3WT and isoDIPG-H3.3K27M cells.

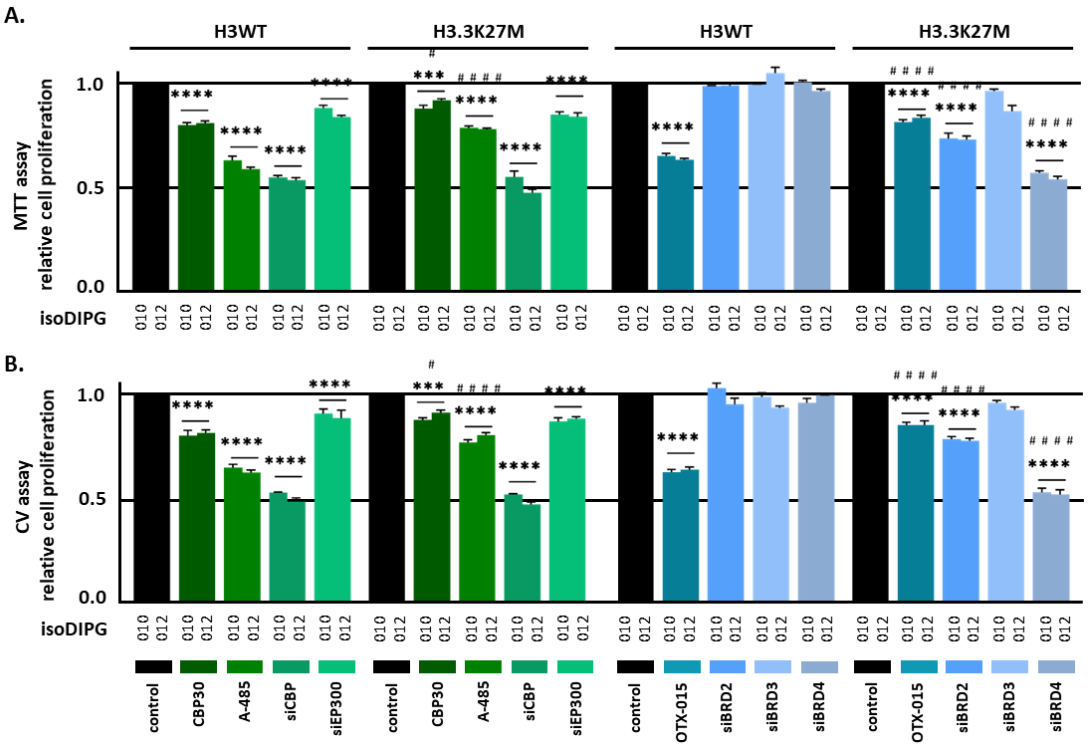

Appendix J | Gene set enrichment analyses after inhibition or knockdown of CBP/p300 in isoDIPG-012-H3WT and isoDIPG-012-H3.3K27M cells.

Gene set enrichment analyses were performed after (A and B) CBP30 treatment, (C and D) A-485 treatment, (E) CBP and (F) p300 knockdown in isoDIPG-012-H3WT and isoDIPG-H3.3K27M cells (log2FC ≤1.0, adjusted p-value ≤0.05). Highlighted in bold common processes had been found in isoDIPG-H3WT and isoDIPG-H3.3K27M cells.

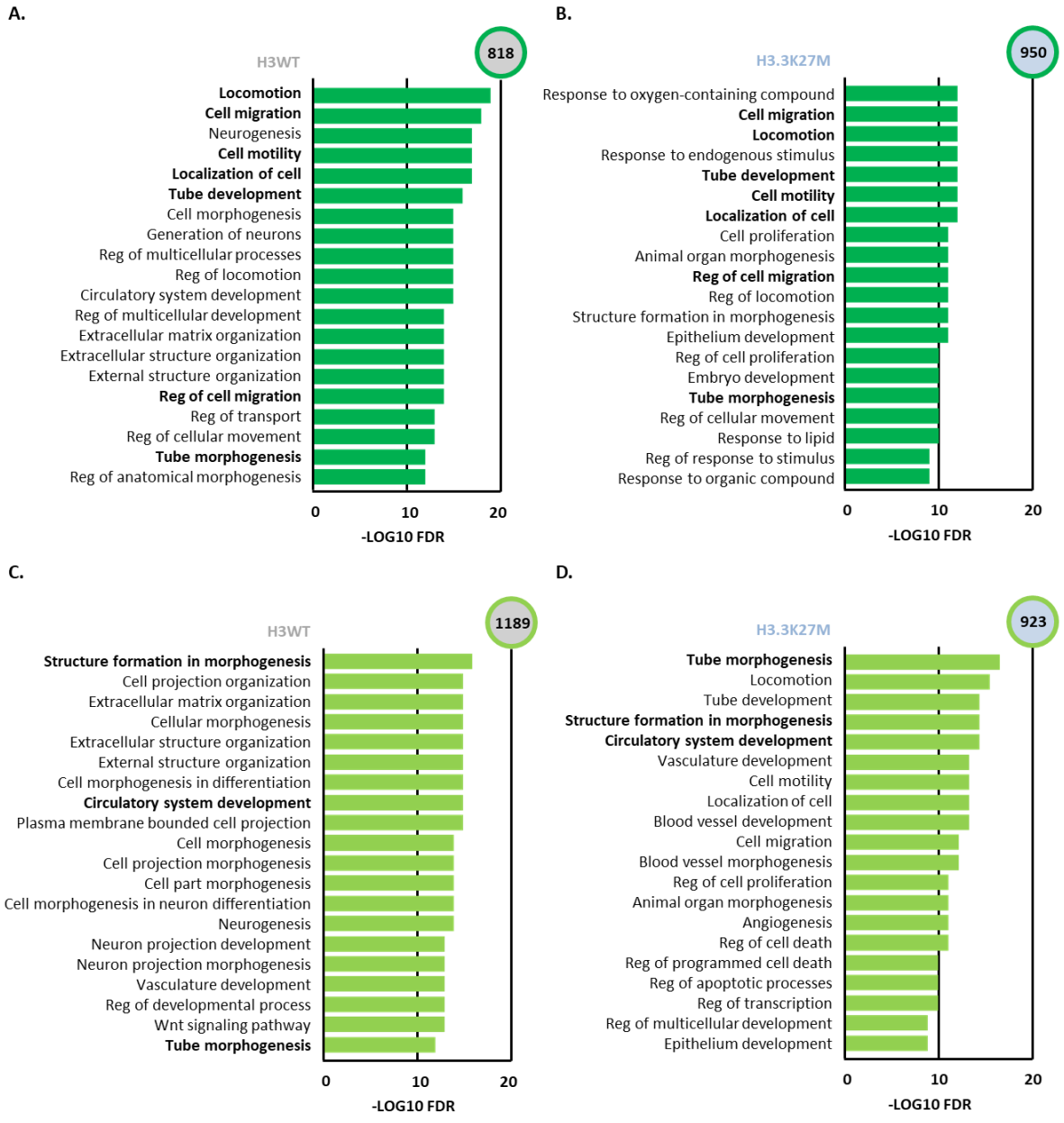

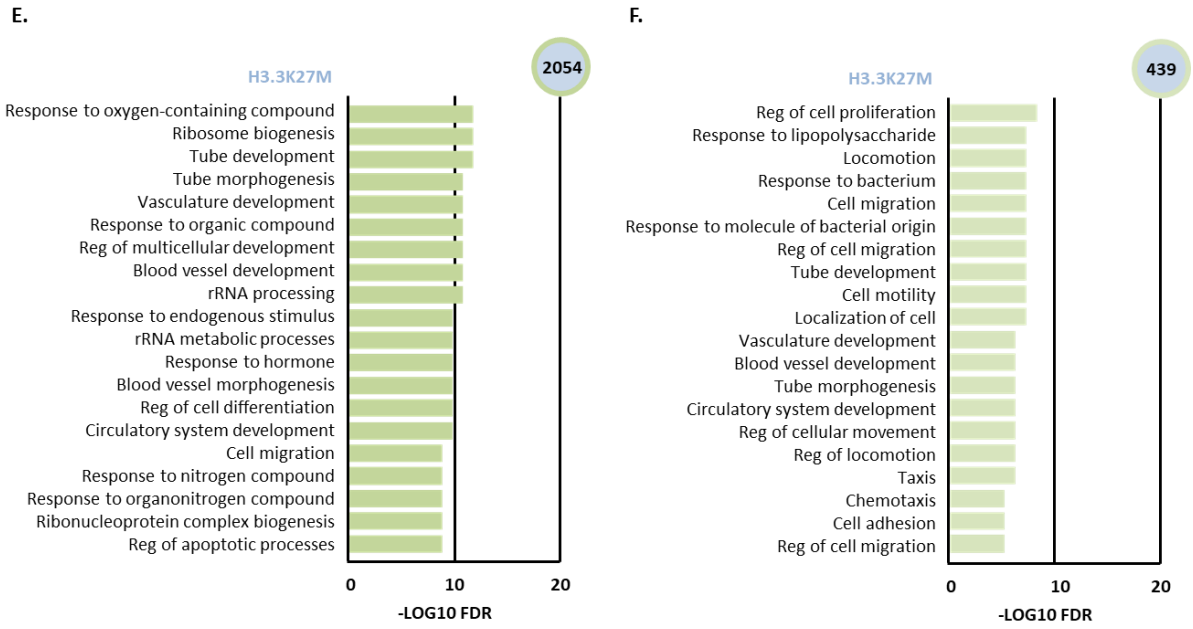
E.
H3.3K27M
2054
Response to oxygen-containing compound
Ribosome biogenesis
Tube development
Tube morphogenesis
Vasculature development
Response to organic compound
Reg of multicellular development
Blood vessel development
rRNA processing
Response to endogenous stimulus
rRNA metabolic processes
Response to hormone
Blood vessel morphogenesis
Reg of cell differentiation
Circulatory system development
Cell migration
Response to nitrogen compound
Response to organonitrogen compound
Ribonucleoprotein complex biogenesis
Reg of apoptotic processes
0
10
20
-LOG10 FDR
F.
H3.3K27M
439
Reg of cell proliferation
Response to lipopolysaccharide
Locomotion
Response to bacterium
Cell migration
Response to molecule of bacterial origin
Reg of cell migration
Tube development
Cell motility
Localization of cell
Vasculature development
Blood vessel development
Tube morphogenesis
Circulatory system development
Reg of cellular movement
Reg of locomotion
Taxis
Chemotaxis
Cell adhesion
Reg of cell migration
0
10
20
-LOG10 FDR

Appendix K | Venn diagram analyses after inhibition or knockdown of CBP/p300 in isoDIPG-012-H3WT cells.

Venn diagram analyses showed commonly regulated 0.75-fold downregulated and 1.5-fold upregulated (adjusted p-value ≤0.05) genes after CBP/p300 inhibition using CBP30 and A-485, as well as knockdown of CBP and p300 in isoDIPG-012-H3WT cells.

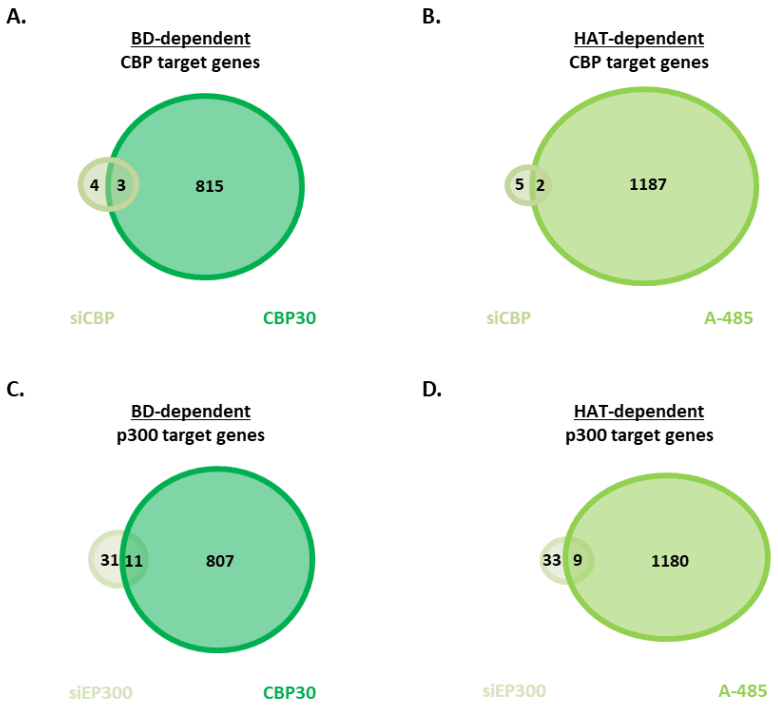

Appendix L| Illustration of apoptosis and cell cycle genes regulated by HAT CBP in isoDIPG-012-H3.3K27M cells.

KEGG pathway analysis revealed HAT CBP-dependent apoptosis-dependent genes in isoDIPG-012-H3.3K27M cells (upregulated indicated in green, downregulated in red) (log2FC ≤1.0, adjusted p-value ≤0.05).

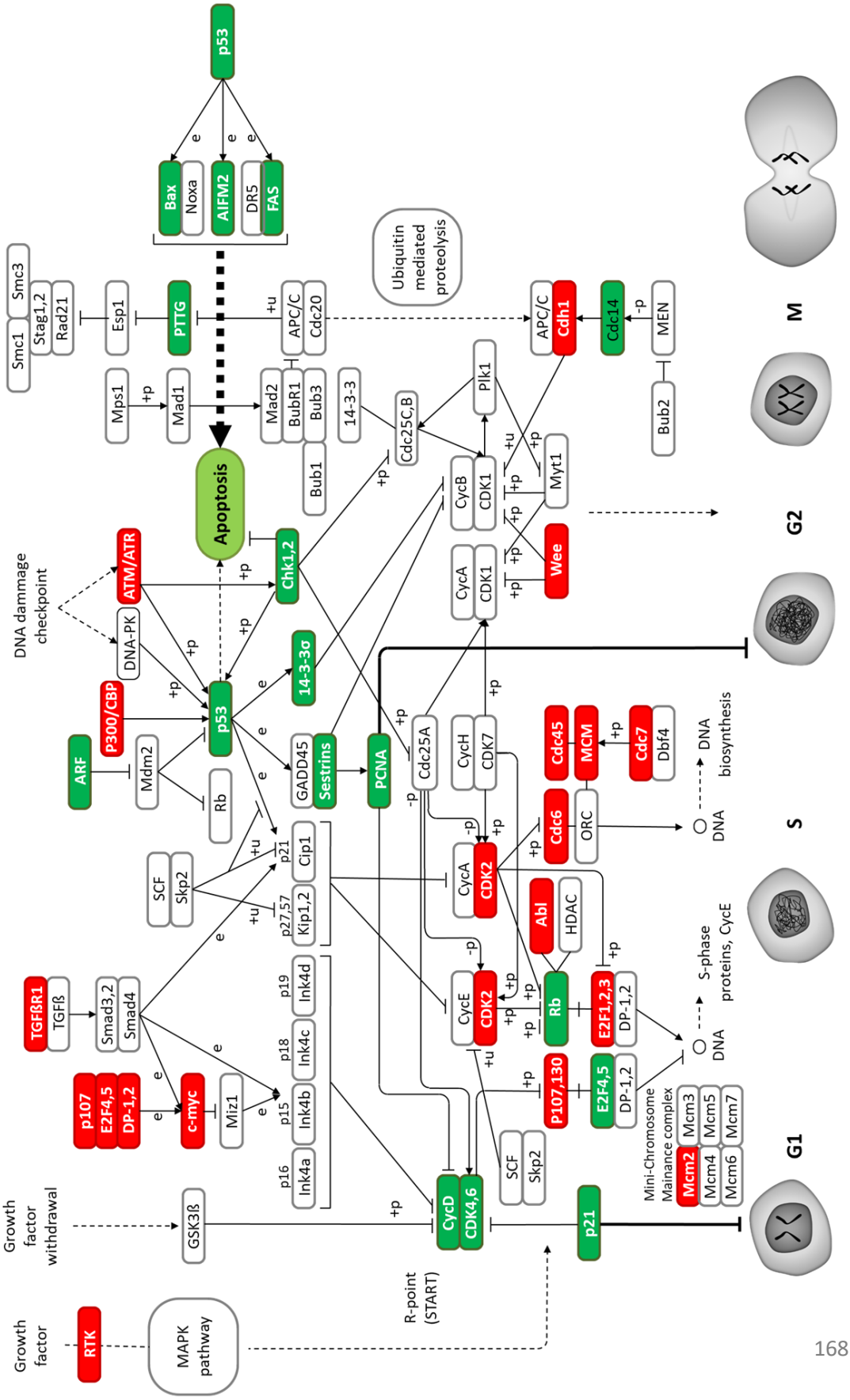

Appendix M | Gene set enrichment analyses after inhibition or knockdown of BET proteins in isoDIPG-012-H3WT and isoDIPG-012-H3.3K27M cells.

Gene set enrichment analyses were performed after (A and B) OTX-015 treatment, (C) BRD2 and (D) BRD4 knockdown in isoDIPG-012-H3WT and isoDIPG-H3.3K27M cells (log2FC ≤1.0, adjusted p-value ≤0.05). Highlighted in bold common processes had been found in isoDIPG-H3WT and isoDIPG-H3.3K27M cells.

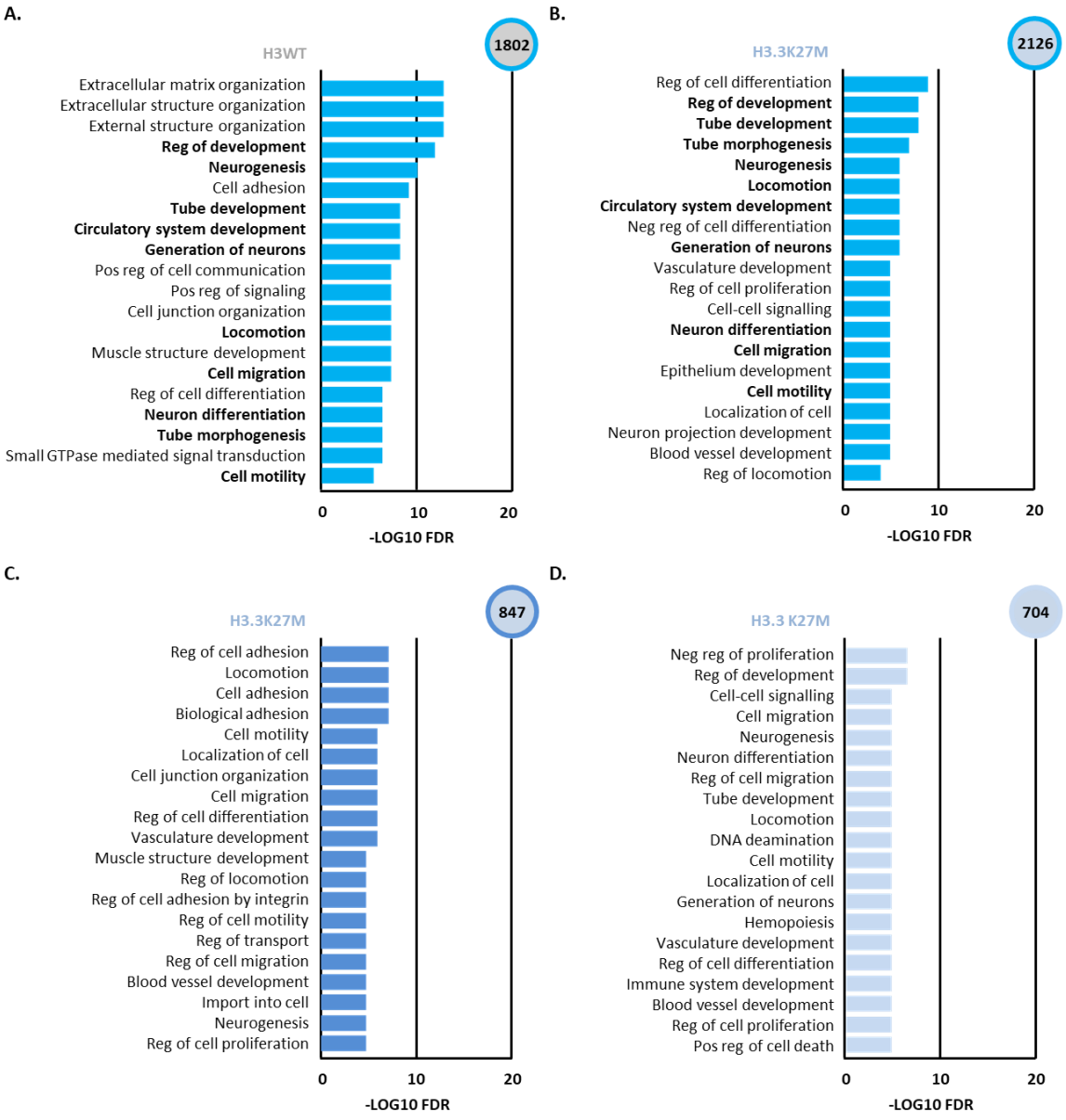

Appendix N | Venn diagram analysis after knockdown of BET proteins in isoDIPG-012-H3.3K27M cells.

Venn diagram analysis showed commonly regulated 0.75-fold downregulated and 1.5-fold upregulated (adjusted p-value ≤0.05) genes after knockdown of BRD2, BRD3 and BRD4 in isoDIPG-012-H3.3K27M cells.

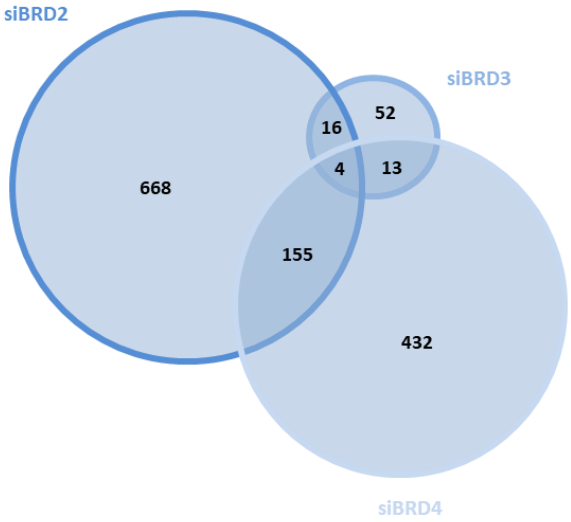

Appendix O | Quantification of western blot analyses of cell cycle regulators expression in isoDIPG-H3WT and isoDIPG-H3.3 K27M cells.

Densitometry analyses for quantification of CDK4, p21, p16, cmyc, CDK2 and p38 levels after inhibition ofBET proteins in isoDIPG-010 and isoDIPG-012 was carried out using ImageJ. ß-actin was used for normalization. * $p < 0.05$; ** $p < 0.01$; *** $p < 0.005$; **** $p < 0.001$.

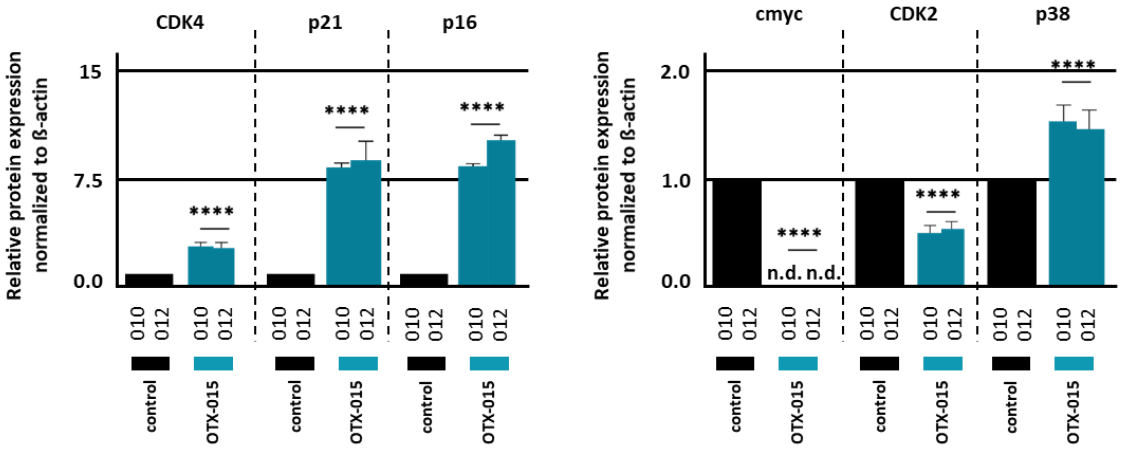

Appendix P | Illustration of cell cycle genes regulated by BRD4 in isoDIPG-012-H3.3K27M cells.

KEGG pathway analysis revealed BRD4-dependent cell cycle-dependent genes in isoDIPG-012-H3.3K27M cells (upregulated indicated in green, downregulated in red) (log2FC ≤1.0, adjusted p-value ≤0.05).

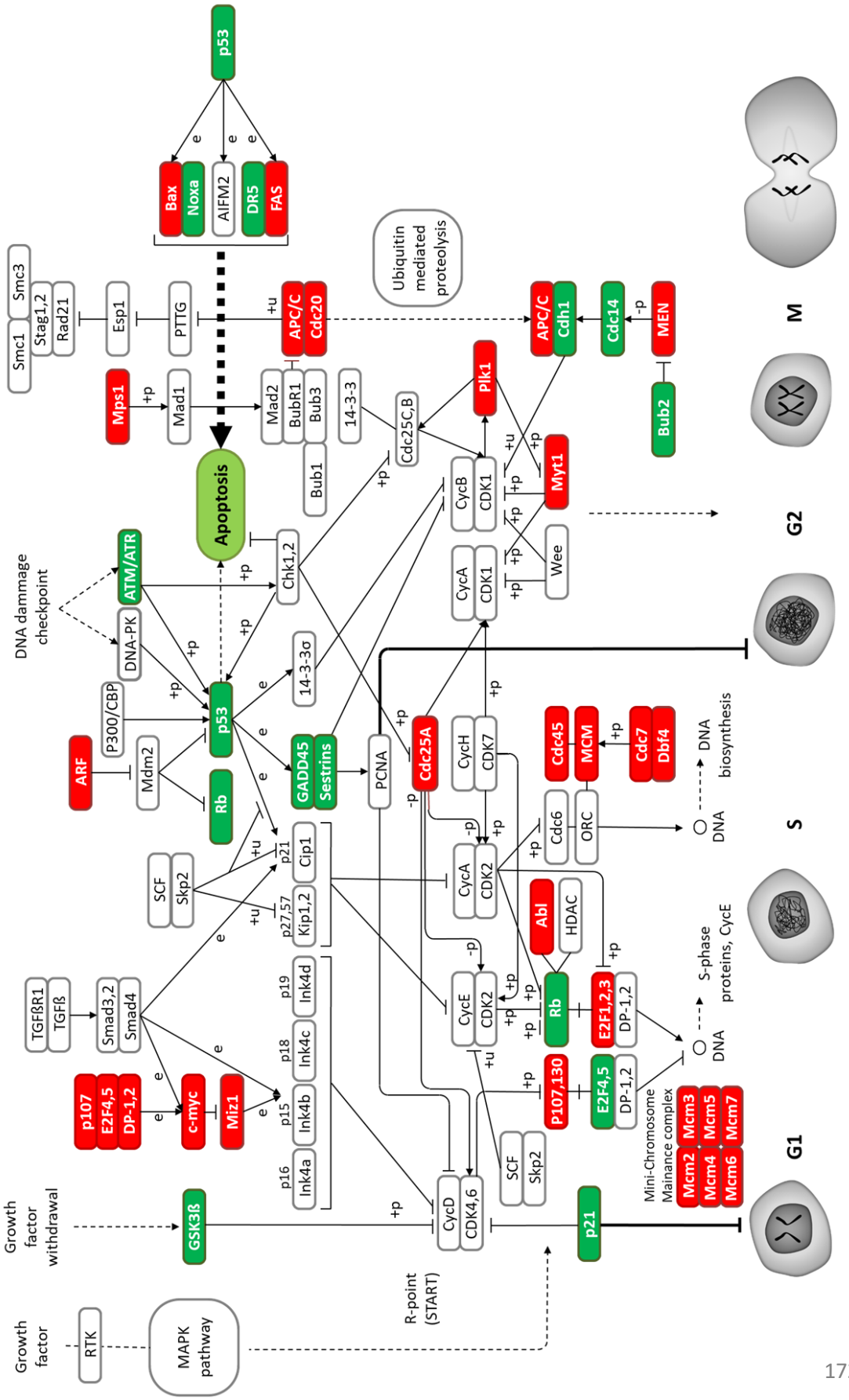

Appendix R | Computer tomography pictures of paraffin embedded tumors after treatment with CBP/p300 and BET proteins inhibitors using isoDIPG-H3WT and isoDIPG-H3.3K27M cells.
Representative computer tomography photos were taken of paraffin embedded tumors after treatment with CBP30, A-485 and OTX-015. Tumor volume was quantified using ImageJ.

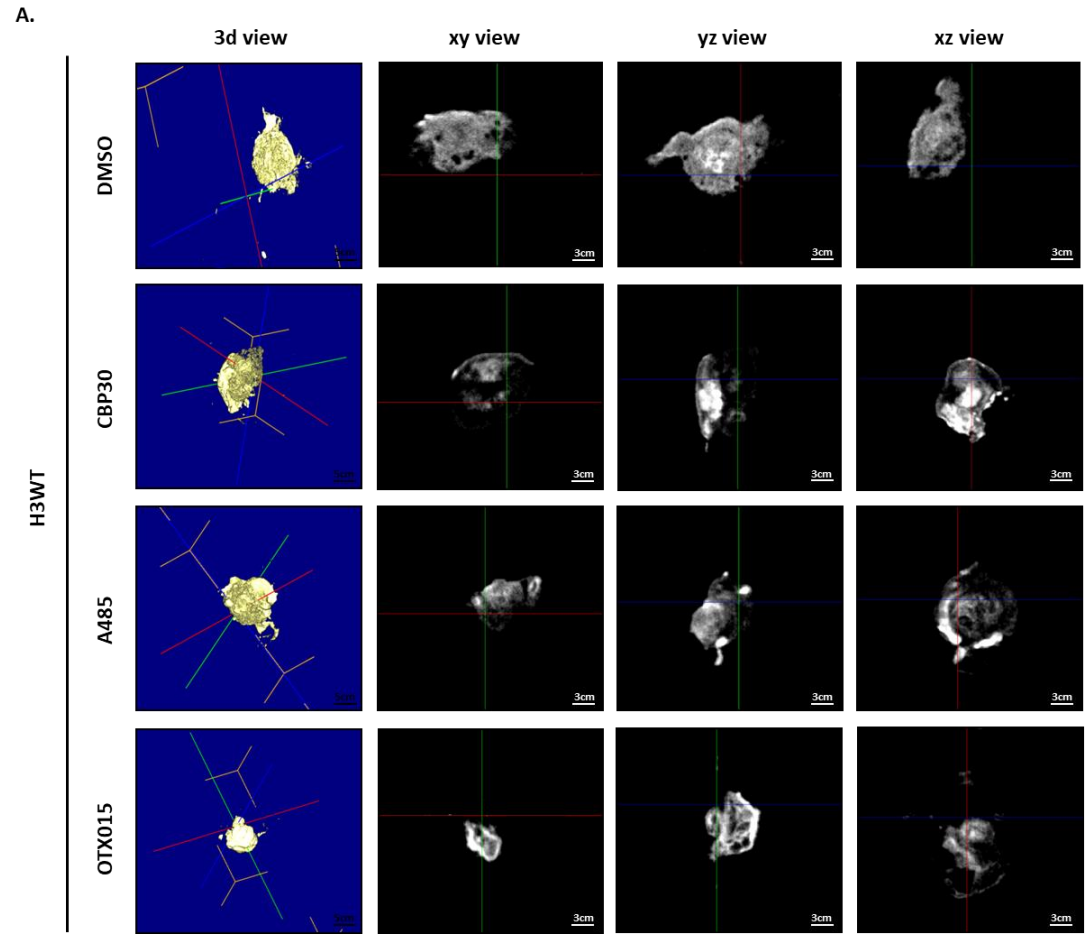

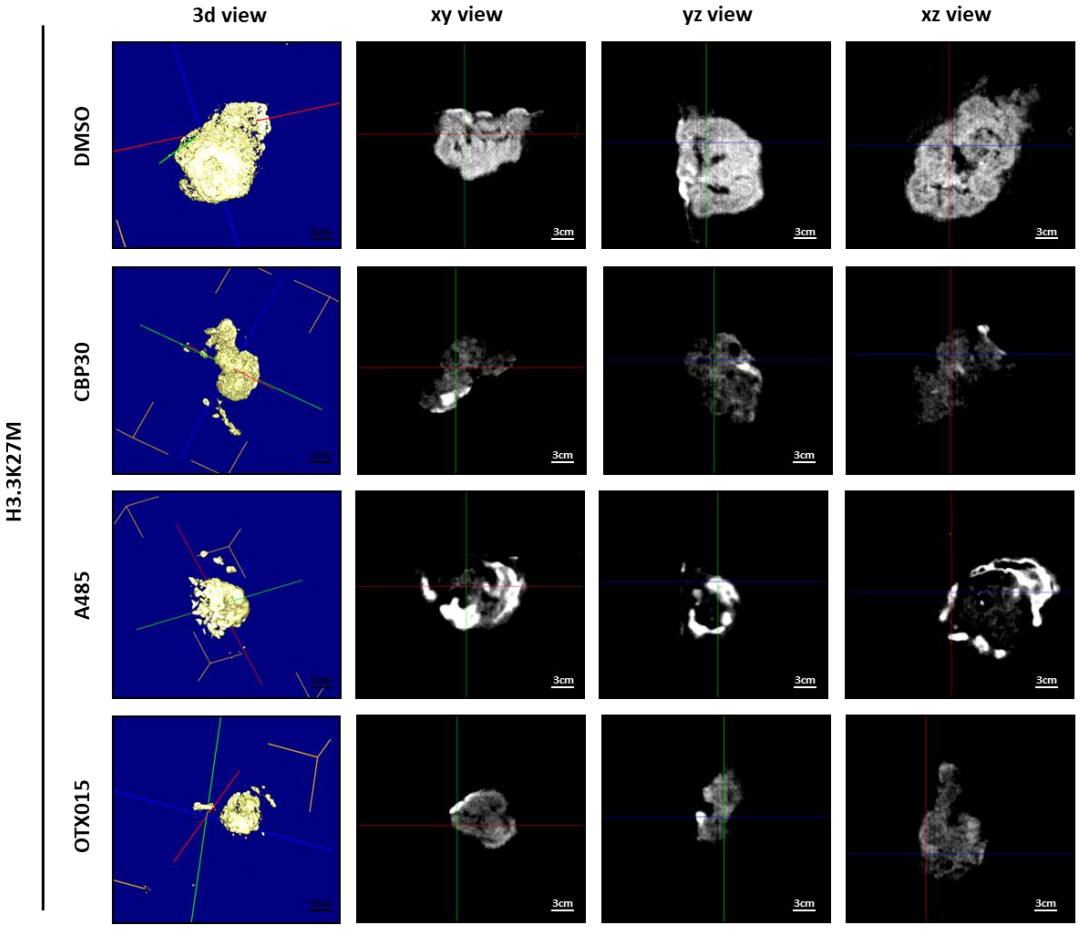
3d view
xy view
yz view
xz view
H3.3K27M
DMSO
CBP30
A485
OTX015
3cm

B.

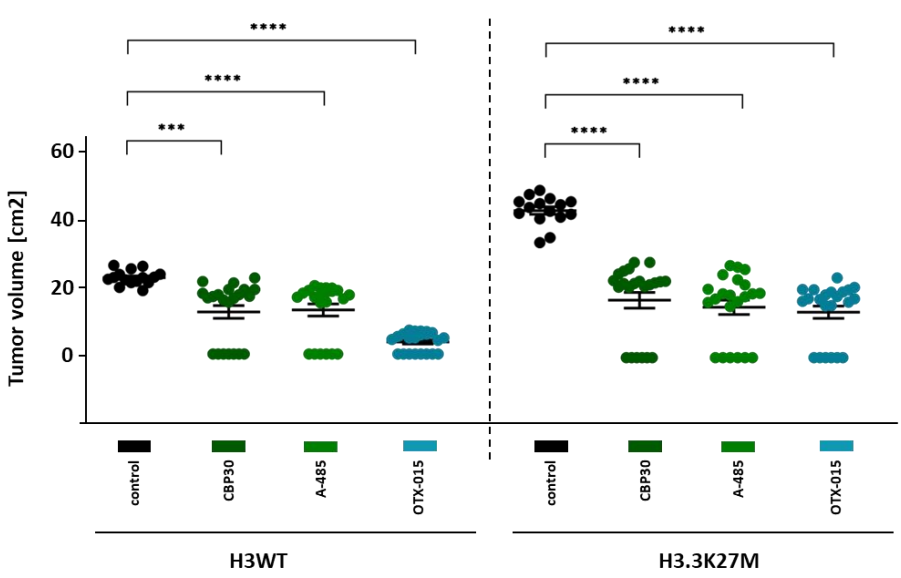
Tumor volume [cm2]
60
40
20
0
****
****
***
****
****
****
control
CBP30
A-485
OTX-015
control
CBP30
A-485
OTX-015
H3WT
H3.3K27M